TAXONOMY, PHYLOGENY, AND GENOMICS OF THE LICHEN-FORMING FUNGAL GENUS *BACIDIA*

Dissertation zur Erlangung des Doktorgrades der Naturwissenschaften
(Dr. rer. nat.) an der Fakultät für Biologie
der Ludwig-Maximilians-Universität München

Iuliia (Julia) V. Gerasimova

München

März 2022

To my parents and Margaret

PREFACE

Statutory declaration

Diese Dissertation wurde im Sinne von §12 der Promotionsordnung von Prof. Dr. Silke Werth betreut. Ich erkläre hiermit, dass die Dissertation nicht einer anderen Prüfungskommission vorgelegt worden ist und dass ich mich nicht anderweitig einer Doktorprüfung ohne Erfolg unterzogen habe.

Eidesstattliche Erklärung

Ich versichere hiermit an Eides statt, dass die vorgelegte Dissertation von mir selbstständig und ohne unerlaubte Hilfe angefertigt wurde.

Iuliia V. Gerasimova   31. May 2022
(Unterschrift)

1. Gutachter: Prof. Dr. Silke Werth
2. Gutachter: Prof. Dr. Gerhard Haszprunar

Tag der Abgabe: 8. März 2022
Tag der mündlichen Prüfung: 25. May 2022

Declaration of contribution

In this dissertation, I present the results from my doctoral research carried out in Munich from 2018 to 2022 under the guidance of Prof. Dr. Silke Werth. My dissertation resulted in four publications, presented in Chapters 2 to 5, of which all have been published. I generated all data and conducted analyses myself, involving input from all co-authors involved in the publications as detailed therein. Specimens from Kunashir and Sakhalin were collected by Aleksandr K. Ezhkin, one specimen by Evgeny A. Davydov, and specimens of *Toniniopsis* from the North Caucasus were collected by Irina N. Urbanavichene and Gennady P. Urbanavichus. All contributions by the authors are indicated in addition at the end of Chapters 2 to 5.

Iuliia V. Gerasimova   Prof. Dr. Silke Werth

(Signature)   (Signature)

List of publications

Peer-reviewed journal articles

Gerasimova JV, Ezhkin AK & Beck A (2018) Four new species of *Bacidia* s. str. (Ramalinaceae, Lecanorales) in Russian Far East. *The Lichenologist* 50: 603–625.

Gerasimova JV, Urbanavichene IN, Urbanavichus GP & Beck A (2021) Morphological and phylogenetic analyses of *Toniniopsis subincompta* s. lat. (Ramalinaceae, Lecanorales) in Eurasia. *The Lichenologist* 53: 1–13.

Gerasimova JV, Ezhkin AK, Davydov EA & Beck A (2021) Multilocus-phylogeny of the lichen-forming genus *Bacidia* s. s. (Ramalinaceae, Lecanorales) with special emphasis on the Russian Far East. *The Lichenologist* 53: 441–455.

Gerasimova JV, Beck A, Werth S & Resl P (2022) High diversity of type I polyketide genes in *Bacidia rubella* as revealed by the comparative analysis of 23 lichen genomes. *Journal of Fungi*, 8(5): 449.

Funding

Table of Contents

List of Figures

List of Tables

Summary

My dissertation deals with the taxonomy, molecular phylogeny, and genomics of the crustose lichen genus *Bacidia* De Not., with a special focus on the Russian members of group. *Bacidia* is distributed worldwide with the highest diversity found in warm and cold temperate regions, mostly growing on the bark of different broad-leafed and coniferous trees in mature forest habitats with high humidity and moderate irradiance. It cannot be found in restored forests and is thus frequently used as an indicator of stable forest communities. *Bacidia* belongs to the fungal Class Lecanoromycetes O.E. Erikss. & Winka, the largest radiation of lichen-forming Ascomycetes, and is part of the family Ramalinaceae C. Agardh, which is comprised of 40 additional genera of various growth forms and habitat preferences (Wijayawardene *et al.*, 2022).

Estimates of *Bacidia's* diversity range from 60 (Ekman, 1996) to 230 (Lücking *et al.*, 2017; Wijayawardene *et al.*, 2020) species worldwide. This number will likely increase with appropriate sampling in neglected regions. Diversity of *Bacidia* in Europe and North America is comparatively well investigated, while for the Russian territory, it was still largely understudied. Moreover, inconspicuous fruiting bodies (less than 1 mm in size) and frequently overlapping morphological and anatomical traits of species complexes, make species delimitation in *Bacidia* challenging. Although work is underway to circumscribe monophyletic entities, many names in *Bacidia* remain unresolved, thus further research within this group is needed.

My research aimed to provide a taxonomic (i) and phylogenetic (ii) revision of *Bacidia* from different areas of Europe and Russia and to conduct a genomic (iii) investigation of its biosynthetic potential. To reach these goals, my dissertation was divided into three main parts, respectively.

For the first part of my dissertation, I conducted an extensive herbarium revision of more than one thousand specimens of *Bacidia* in a large sense (i.e., including phenotypically similar species), using microscopic examinations of morphological and anatomical characters. To confirm taxon identification, I examined the type material located in different herbaria in Eurasia and North America. This work helped to settle the important characters necessary for species delimitation in *Bacidia* in a strict (s. str.) and a large (s. lat.) sense, evaluate the variation within and among species, and thus confirm or revise species IDs.

For the second part of my dissertation, I generated molecular data for phylogenetic analyses. The main criterion for specimen selection was to include species with a broad phenotypic variation collected in different localities. Thus, we used material from Asia (Russian Far East and the North Caucasus) and from various localities from the European part of Russia, which host a high diversity of *Bacidia* species. To generate data for phylogenetic analyses, I conducted DNA sequencing of the following loci within ribosomal DNA operons: the internal transcribed spacer region (nrITS), nuclear small subunit (nrSSU), nuclear large subunit (nrLSU), mitochondrial small subunit (mtSSU). In addition, the two genes encoding the largest and the second-largest subunit of RNA polymerase II were sequenced (RPB1 and RPB2, respectively).

By using multiple lines of evidence (i.e., morphology, anatomy, and phylogeny), 19 species were transferred to other genera, six species were synonymized, three species were found new to Russia, and five species were described as new to science. Thus, the final list count of *Bacidia* in Russia included 19 species, which is about 33% of the known worldwide diversity of *Bacidia* s. str. according to estimate of Ekman (1996). Thereby, my taxonomic studies contributed substantially to the species delimitation and to the understanding of species diversity in this understudied genus of lichen-forming fungi, which is a prerequisite for ecological and detailed genetic studies of individual taxa.

The final part of my dissertation includes a comparative analysis of the *Bacidia rubella* (Hoffm.) A. Massal. fungal symbiont genome. *Bacidia rubella* is a relatively widespread species confined to habitats with a high humidity and fair amount of sunlight similar to other *Bacidia* species. However, *B. rubella* can also grow in forest edges and even in some sun-exposed habitats, only rarely occupied by species of this genus. In addition, the characteristic compound of *Bacidia*, atranorin, has a wide application in the pharmaceutical industry. Given *B. rubella's* habitat range and unknown chemical composition, this species was selected for detailed genomic studies. To explore gene sets potentially involved in the adaptation to various abiotic conditions, a nearly complete genome of *B. rubella* was assembled using short and long read sequencing data from the Illumina NovaSeq and Oxford Nanopore (MinION) platforms, respectively. The genome of *B. rubella* was annotated and analyzed, focusing on the genes encoding enzymes that are involved in the production of characteristic secondary lichen metabolites, which are in turn involved in lichen defense and, at the same time, are promising candidates for pharmaceutical products.

2

Aims

The overall aims of this dissertation are to conduct a taxonomic revision of the genus *Bacidia* with a special focus on the Russian territory, investigate the relationships between species using a phylogenetic approach, and carry out a phylogenomic analysis of *Bacidia rubella* polyketide synthase genes. To this end, first, extensive herbarium revision was conducted to analyze morphological characters of different *Bacidia* species and relatives (**Q1**). Second, the phylogenetic relationships of the *Bacidia* species occurring in Russia was investigated (**Q2**). As a final step, genomic data from an axenic culture of the *B. rubella* fungal symbiont was produced (**Q3**).

(**Q1**) How many species of *Basidia* are there in Russia, based on the microscopical examination of collected specimens as well as type material and specimens deposited in various herbaria?

I have conducted extensive herbarium work and studied more than one thousand specimens of *Bacidia* s. lat., using microscopical examination of morphological and anatomical traits. To confirm taxon identifications, I examined the type material located in different herbaria in Eurasia and North America, and particularly the type material known from the *loci classici* in Russia. The results of the study are summarized in the Chapters 2, 3, and 4, where particularly the new species to science were described.

(**Q2**) Does a multilocus phylogeny and a large sampling effort support the morphological species delimitations obtained in Q1?

DNA sequence data for phylogenetic analyses was generated. For this, six different markers were sequenced, the more commonly used nrITS, nrSSU, nrLSU, and mtSSU regions and the two protein genes, RPB1 and RPB2. A set of specimens from Asia (Russian Far East and North Caucasus) and collections from various localities from Europe and the European part of Russia were used. The results are summarized in the Chapters 3 and 4.

(**Q3**) How large is the diversity of genes involved in the production of secondary compounds in *Bacidia rubella* and related species, and which gene cluster is involved in atranorin production in *B. rubella*?

To explore the gene sets encoding enzymes involved in the production of characteristic secondary lichen compounds, genomic data was produced from an axenic culture of the *B. rubella* fungal symbiont. Using short-read, paired-end Illumina NovaSeq and long-read sequencing data from the Oxford Nanopore (MinION) platform, a nearly

complete genome sequence was assembled. The results on the comparative analyses of biosynthetic gene diversity in *Bacidia* are summarized in Chapter 5.

Chapter 1

1.1. General Introduction

Fungi are among the most successful eukaryotes, as they have evolved diverse strategies to survive extreme environmental conditions and comprise an estimated 5.1 million species worldwide (Blackwell, 2011; Hibbett *et al.*, 2016). They have developed numerous adaptations to optimize their survival under harsh abiotic stresses, to colonize different substrates and to build mutualistic associations with organisms from other kingdoms (i.e., bacteria, plants, and animals), thus benefiting from a symbiotic lifestyle (Onofri *et al.*, 2007; Nash, 2008). Symbiotic relationships, in turn, play an important role in the growth, adaptation and evolution of many ecologically successful groups of organisms, particularly lichens (Douglas, 1994; Gadd, 2013; Divakar *et al.*, 2015).

Lichens are a fascinating example of an obligate fungal symbiosis. They are composed of a fungal partner, the mycobiont, and one or more photosynthetic partners, the photobiont, which is either a green alga or cyanobacterium (forming a new entity, the lichen thallus (Nash, 2008; Honegger, 2009). The morphology of a lichen thallus is primarily determined by the mycobiont and based on their overall habit, lichens are traditionally divided into three main morphological groups: crustose (crust-like, tightly attached to the substrate), foliose (leaf-like, flat and only partially attached to the substrate) and fruticose (hair-like, strap-shaped or shrubby, standing out from the surface of the substrate) (Büdel and Scheidegger, 2008).

The fungus hosts its photobionts and "harvests" part of their carbon products and, in return, provides water, possibly mineral nutrients, and protection from herbivores and unfavorable environmental conditions. Lichens are distributed in most terrestrial ecosystems of the world, occurring as epiphytic—growing on trees and other plants—, epilithic—growing over rock surfaces or embedded within the upper few millimeters—, epigeic—as an important component of soil composition—, and epiphyllic—colonizing leave surfaces (mostly in tropics and subtropics) (Lücking, 2008; Nash, 2008).

Many researchers refer to lichens as a classic case of mutualism, where all the partners benefit from the association. Alternatively, lichens are regarded as an example of controlled parasitism because the fungus seems to obtain most of the benefits, and the photobiont may grow more slowly in the lichenized state than when free-living (Nash, 2008). However, it has been shown that the lichen symbiosis is more complex than a two-partner association, and, for example, host a variety of bacteria and additional fungi with unclear significance

to the complex organism (Farrar, 1976; Schneider *et al.*, 2011; Cardinale *et al.*, 2012; Cernava *et al.*, 2015, 2017; Spribille *et al.*, 2016; Mark *et al.*, 2020).

The classification of lichens is based on the fungal component of the symbiosis. The largest number of lichens are Ascomycetes. In fact, almost half of the described Ascomycetes are lichenized (Nash, 2008) with estimates of around 20,000 species (Kirk *et al.*, 2008). However, because many regions of the world are still neglected for lichen diversity, many new species are constantly described and therefore, a higher number is expected (Chapman, 2006).

Fungal systematics was originally based only on morphological and anatomical characters (e.g., Smith *et al.*, 2009; Wirth *et al.*, 2013). However, it has been shown that many characters may change depending on abiotic conditions and thus proposing reliable classification may be complicated. A large diversity of lichen-forming fungi, cryptic speciation, and challenges in species recognition made necessary the use of integrative taxonomic approaches based on additional information from physiology, biochemistry, and molecular phylogenetics to come up with meaningful species concepts. In addition, omics data, i.e., genomics, metagenomics, phylogenomics, transcriptomics, metabolomics, and proteomics, have enormously advanced the way to understand fungal diversity at diverse taxonomic levels (Muggia *et al.*, 2020; Grimm *et al.*, 2021). All these different interdisciplinary approaches aim to identify monophyletic fungal lineages and provide valuable information for species delimitation.

1.2. Study objective: *Bacidia*. Why is the study of this genus important?

Ramalinaceae is the fourth largest family of lichen-forming fungi with a worldwide distribution, containing 39 genera and more than 900 species (Lücking *et al.*, 2017; Kistenich *et al.*, 2018), including genera of various growth forms. Ancestral state reconstruction showed that Ramalinaceae have likely arisen from an ancestor with long, multiseptate ascospores living in humid temperate forests (Kistenich *et al.*, 2018).

These characters particularly apply to the genus *Bacidia*, an almost exclusively epiphytic crustose lichen genus, growing on various broad-leaved and coniferous trees in mature forest habitats with a high humidity and moderate irradiance, thus frequently used as indicator of stable forest communities. *Bacidia* is characterized by tiny cup-shaped fruiting bodies, or apothecia (frequently not exceeding 1 mm in diameter), smooth or

warted to granular thalli and long, needle-shaped multicellular ascospores up to 100 μm in length and 2.0–4.0 μm in width (Fig. 1.1. A-B) (Ekman, 1996; Llop, 2007).
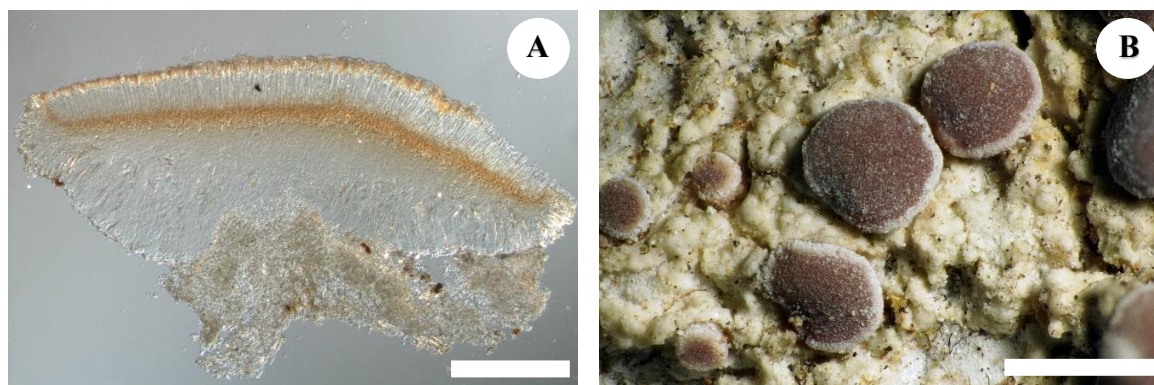
Figure 1.1. Cross-section of the apothecium and thallus structure of *Bacidia obtecta* (M-0308496, holotype). A, cross-section of apothecium. B, detailed view of apothecia and thallus structure. Thallus wrinkled, irregularly shaped. Rusty brown apothecia with scurfy surface and white pruina along the margin. Scales: A = 200 μm, B = 1 mm

Bacidia is distributed worldwide and includes up to 230 species in a large sense (Lücking *et al.*, 2017; Wijayawardene *et al.*, 2020) with almost 20 species of *Bacidia* s. str. occurring in Russia. As already indicated, this number continues to grow and there are several reasons for this: historical, morphological, and incomplete sampling.

First, historically, species boundaries in *Bacidia* were primarily based on morphological characters. When De Notaris described *Bacidia* in 1846, he placed only two species into the genus, *Bacidia rosella* (Pers.) De Not. and *Bacidia carneola* (Ach.) De Not., whose current name is *Pachyphiale carneola* (Ach.) Arnold (De Notaris, 1846). At the beginning of the 20th century, in the seminal work *Catalogus Lichenum Universalis*, the genus name has been used for all crustose lichens based on photobiont type, shape of fruiting bodies and number of cells in ascospores (Zahlbruckner, 1905). This circumscription was apparently unnatural and led to merging numerous taxa that are not closely related to the type species, *Bacidia rosella*. Therefore, more than 1300 names are currently known for *Bacidia* (MycoBank query on 06.3.2022), and thus this genus still requires a lot of effort from taxonomists to clarify the placement of species across multiple genera.

The first extensive taxonomic revision of the genus covered species from the continental United States and Canada (Ekman, 1996). As a result, twenty-seven species of *Bacidia* were distinguished, including three newly described species and two endemics for

North America. Early molecular systematic investigations narrowed down the concept of the genus (Ekman, 2001; see Phylogeny section below), showing that species with long, needle-shaped ascospores with a minimum of four cells and pronounced exciple belong to the genus in a strict sense. In the subsequent years, however, every lichen Flora was still mostly following Zahlbruckner's concept of *Bacidia*, including species with at least four cells spores into the genus, and for this reason detailed analysis of many species is still needed. Thus, in a number of subsequent publications and checklists, *Bacida* was treated in a large sense (e.g., John and Breuss, 2004 for Turkey; Santesson *et al.*, 2004 for Fennoscandia; Llop, 2007 for Spain; Smith *et al.*, 2009 for Great Britain; Wirth *et al.*, 2013 for Germany; Roux *et al.*, 2014 for France). In the recent monograph of lichens from Great Britain and Ireland, Cannon *et al.* (2021) moved towards modern morphological and phylogenetic studies on *Bacidia*. After the first extensive systematic and phylogenetic work on *Bacidia* (Ekman, 1996, 2001), more than 50 new *Bacidia* species were described, partly following Zahlbruckner's concept (e.g., Printzen and Tønsberg, 2007; Olech and Czarnota, 2009; Aptroot and da Silva Caceres, 2014; Kantivilas, 2018; Fryday, 2019). Almost half of those species, therefore, belong to *Bacidia* s. lat., characterized by rod-shaped or spindle-shaped ascospores with mainly four cells.

In addition to the complex taxonomy in *Bacidia*, species frequently have overlapping morphological and anatomical characteristics which, in some cases, make species delimitation challenging. Moreover, species are often overlooked in their natural habitat due to small and inconspicuous apothecia.

Lastly, some regions of the world are still relatively little-studied for *Bacidia* species. Although its diversity in Europe and North America was explored comparatively well, this genus was still largely understudied in the Russian territory. Thus, the first summary on *Bacidia* for the Russian territory was made at the beginning of 21st century (Golubkova, 2003) based on previous reports and literature. The checklist included 31 species, out of which, to current knowledge, only eight belonged to *Bacidia* s. str. More recently, work on a lichen checklist of Russia by Urbanavichus (2010) included 35 *Bacidia* species in the large sense, including all *Bacidia* whenever mentioned for any locality in Russia.

In summary, although some work has been done to circumscribe monophyletic entities, many names in *Bacidia* remain poorly understood, so this group is in high need of further investigation. Generally, tiny crustose lichens are less studied, given that they are less visible and more difficult to collect and identify than lichens larger in size. However, crustose lichens form the larger part of lichen diversity. Thus, much more taxonomic work

9

on these organisms is needed to improve our understanding of the diversity, ecology, and biogeographic patterns of lichen-forming fungi.

1.3. Nomenclature: *Bacidia* s. str. and *Bacidia* s. lat. – consolidating the species of *Bacidia* in Russia

1.3.1. *Morphological investigation of the type material*

To settle the taxon identification, the type material located in different herbaria in Eurasia and North America was studied, e.g., in Russia (LE), Germany (M, GLM), Finland (H, TUR), the Netherlands (L), Sweden (LD, S, UPS), Switzerland (G), Austria (GZU), Spain (MA), and Czech Republic (PRA). This work helped to understand relevant characters necessary for species delimitation in *Bacidia*, and evaluate the morphological variation within and among species.

Among these, type material of seven species known only from a single collection from the Russian territory was examined. Particularly, several species of *Bacidia* have only been known from *loci classici* where they were collected during 19th-century expeditions by Ernst Almquist during the Vega expedition 1878–1880 to the Russian Arctic, by Edvard August Vainio during the journey to western Siberia in 1880, and by Hugo Lojka, who travelled to the Caucasus in 1885 (Gerasimova and Ekman, 2017). Because of the particular historical background of the collected material, the specimens are housed in herbaria outside Russia, viz. Helsinki (H) and Turku (TUR), Finland, and Stockholm (S), Sweden. Common to all those specimens examined is that they consist of one or a few fragments and are the only material available to date. The brittleness of the specimens and their limited quantity entailed challenges in the microscopical examination. Nevertheless, the investigation of old type material was remarkable and important for evaluating morphological variation and species boundaries concerning the species presently known. The assessment of those specimens indicated that none belonged to *Bacidia* s. str.

1.3.2. *Bacidia diversity in the mountains: Altitudinal difference in the species complex*

One of the goals of this study was to investigate the *Bacidia* species found in the mountainous regions. It has been found that the former *Bacidia subincompta* (currently *Toniniopsis subincompta* (Nyl.) Kistenich, Timdal, Bendiksby & S. Ekman) is common in the North Caucasus of Russia and is the most frequent species in the Allgäu in Bavaria as well (Gerasimova *et al.*, 2021). *Toniniopsis* is morphologically similar to *Bacidia* but

10

differs in the more prominent thallus, and stronger pigmentation of the inner part of apothecia. *Toniniopsis subincompta* is a corticolous species occurring in Europe, Asia, Macaronesia, Africa, and North America in a range of woodlands from sea level to an altitude of ca. 3000 m (Ekman, 1996; Smith *et al.*, 2009). It is also used as an indicator for old-growth forests and is included in indices for assessing the conservation value of forest areas (Rücker and Wittmann, 1995; Rose and Coppins, 2002; Smith *et al.*, 2009; Brackel, 2019) (Chapter 2).

Toniniopsis subincompta can generally be recognized by its thinly granular thallus, black apothecia, green pigmentation of epithecium, red-brown colouration of hypothecium, and rod-shaped ascospores (Smith *et al.*, 2009). However, it shows considerable variation in morphology, such as ascospore shape, including both rod-shaped and needle-shaped ascospores, and in thallus structure, ranging from either irregular (discrete granules or low convex areoles) to continuous (without cracks or ± rimose, wrinkled, warted, tuberculate or distinctly granular) (Ekman 1996, studying *Bacidia subincompta*). Further detailed examination has revealed differences in colouration of the apothecia (including a pale albino morph), hypothecium and exciple, in addition to variation in thallus and ascospore morphology.

To investigate whether there is phylogenetic support for the delimitation of species in accordance with the variability of the observed characters, specimens of *T. subincompta* of mountainous regions from the North Caucasus (Russia) as well as from the Allgäuer Alpen (Germany), collected at different elevations and various substrata were selected for subsequent phylogenetic analyses. For comparison, additional specimens from European and Asian regions of Russia were included. A three-locus phylogeny and morphological investigations based on an expanded taxon sampling and detailed morphological analyses of type specimens showed that *T. subincompta* contains numerous distinct cryptic lineages under a single species name (Chapter 2). Based on these data, one new species was described, namely *Toniniopsis dissimilis,* and the new combination *T. separabilis was made.* No clear correlation between clades and geography could be observed in our limited dataset. However, the interesting case of association with cyanobacteria and presence of fruiting bodies lacking the dark pigmentation (albino morphs) were observed in *T. separabilis*. In addition, individuals in one clade (*T. dissimilis*) have so far been collected only above 1000 m or in high latitudes (Finnmark, Norway) and thus seem to be more adapted to cold than specimens in a second clade (*T. separabilis*) (see Chapter 2). This

evidence will serve for future population genomic studies and study on cold adaptation in a broader scale.

1.4. Phylogenetic investigations of *Bacidia* based on multiple gene sequences

Phylogenetic studies in the past two decades have clarified many of the relationships among fungal groups and in most cases, they have significantly narrowed generic concepts, particularly in lichen-forming fungi (e.g., Lutzoni *et al.*, 2004; James *et al.*, 2006; Miadlikowska *et al.*, 2006, 2014; McLaughlin *et al.*, 2009; Divakar *et al.*, 2015; Kistenich *et al.*, 2018). Molecular phylogenies were mostly based on single-locus trees of the nuclear ribosomal DNA (nrDNA), but in the early 21st century, more than three loci, involving protein-coding genes, were applied in most molecular studies (Lumbsch, 2000; Lutzoni *et al.*, 2004; McLaughlin *et al.*, 2009; Begerow *et al.*, 2010).

The most used region, the internal transcribed spacer region (nrITS) of the nuclear ribosomal DNA (nrDNA), was proposed as the universal fungal barcode marker (Schoch *et al.*, 2012), and eventually recommended by the International Fungal Barcoding Consortium (Xu, 2017). Among the ribosomal cistron regions, nrITS has proved to have the most clearly defined barcode gap between inter- and intraspecific variation. For this reason, it was successfully applied in barcoding of various lichen genera (e.g., Divakar *et al.*, 2016; Mark *et al.*, 2020) and lichen mycobiomes (Banchi *et al.*, 2018). However, it was shown that a combination of nrITS with other ribosomal markers results in more reliable phylogenies. Thus, nrITS together with the nuclear small subunit (nrSSU), the nuclear large subunit (nrLSU), and the mitochondrial small subunit (mtSSU) were frequently applied to construct fungal phylogenies (Lutzoni *et al.*, 2004; James *et al.*, 2006; Miadlikowska *et al.*, 2006, 2014; McLaughlin *et al.*, 2009). Several molecular studies have demonstrated that the two genes encoding the largest and the second-largest subunit of RNA polymerase II (RPB1 and RPB2, respectively) contribute significantly to resolve deep phylogenetic relationships with higher support values in lichen-forming and fungal groups (e.g., Matheny *et al.*, 2002; Reeb *et al.*, 2004; Hofstetter *et al.*, 2007; Liu *et al.*, 2015). Both genes have proven to be useful for broad-scale evolutionary studies both separately and in multilocus phylogenies, showing significant improvements in support of deep nodes (e.g., Lutzoni *et al.*, 2004; James *et al.*, 2006; Miadlikowska *et al.*, 2006, 2014; Divakar *et al.*, 2015; Kistenich *et al.*, 2018).

12

The first extensive phylogenetic study was based on nrITS sequences and resulted in the re-evaluation of the genus *Bacidia*, suggesting the transfer of several species to other genera such as *Biatora* Fr., *Toninia* A. Massal., and *Bacidina* Vězda (Ekman, 2001). In recent phylogenetic studies, several species which have been included in *Bacidia* for a long time, have been transferred to other genera such as *Bellicidia* Kistenich *et al.*, *Bibbya* J.H. Willis, *Scutula* Tul. and *Toniniopsis* Frey (Kistenich *et al.*, 2018). These phylogenetic studies narrowed the genus concept, although the relationships between species and support of the groups remained unclear. Several studies on *Bacidia* using two and three-locus data sets combined sequences from nrITS with mtSSU (Andersen and Ekman, 2005; Lendemer *et al.*, 2016; Malíček *et al.*, 2018), and nrLSU and mtSSU (Lutzoni *et al.*, 2004; Sérusiaux *et al.*, 2012), but covered only few species of *Bacidia* s. str. Additional multilocus phylogenetic studies involving RPB1 and RPB2 included only six species, namely *B. absistens* (Nyl.) Arnold, *B. arceutina* (Ach.) Arnold, *B. squamulosula* (Nyl.) Zahlbr., *B. schweinitzii* (Fr. ex Tuck.) A. Schneid., *B. rosella* (Pers.) De Not. and *B. rubella* (Hoffm.) A. Massal. (James *et al.*, 2006; Miadlikowska *et al.*, 2006, 2014; Reese Næsborg *et al.*, 2007; Ekman *et al.*, 2008; Kistenich *et al.*, 2018).

In a first molecular study on *Bacidia* s. str., the taxon sampling was expanded to include twenty-two newly obtained nrITS sequences (Gerasimova *et al.*, 2018; Chapter 3) in combination with all GenBank nrITS sequences available at that time. Even though the results revealed well-supported groups within *Bacidia* s. str., several polytomies and the basal nodes of the clades remained unresolved or received low support.

To clarify deep phylogenetic relationships among evolutionary lineages within *Bacidia* s. str., and to investigate the robustness of the deeper branches, 48 newly generated sequences and all *Bacidia* s. str. sequences from GenBank (131 sequences) were included for the subsequent analyses. The previous nrITS data was combined with two traditionally used RNA-coding genes (nrLSU and mtSSU) and with two protein-coding genes (RPB1 and RPB2), providing the most inclusive phylogeny of *Bacidia* s. str. to date (Chapter 4).

1.5. Genomics

1.5.1. *Lichen Genomics*

Detailed knowledge of habitat requirements of lichens is essential for their use as bioindicators (e.g., determining the conservation importance of forest areas) and for understanding how lichens might be affected by a changing climate. Many lichens have

13

developed numerous adaptations to optimize their persistence under various environmental stresses, e.g., by biosynthesizing unique chemical compounds, or metabolites. Production of secondary metabolites by lichens has been linked to protection from herbivory, sunscreen for photobionts, and defense from microbes (Lawrey, 1989; Torzilli *et al.*, 1999; Gauslaa and Solhaug, 2001; Färber *et al.*, 2014), and is thus important for the adaptation of lichens to their environment. Depending on the environmental context such as light levels and biotic interactions, concentrations of secondary metabolites vary (Merinero *et al.*, 2015). One way to find the genes involved in adaptation to various environmental factors, and particularly those involved in the synthesis of a certain secondary compound of adaptive relevance, is using comparative genomic analyses.

While most phylogenetic studies are based on several nuclear and mitochondrial markers (usually up to six loci), they often reveal topological incongruences resulting in poorly supported or unresolved clades. Therefore, besides obtaining information on variation in genes relevant for environmental adaptations, the phylogenomic approach involves a large number of loci studied simultaneously, resolving relationships and providing more robust phylogenetic hypotheses with improved accuracy (Rokas *et al.*, 2003).

Nevertheless, lichens are rather poorly investigated by omics approaches. The main reason is the complexity of lichen thalli, which some have described as microbial consortia or mini-ecosystems, because they harbor additional fungi, algae and bacteria in addition to the main mycobiont host (Farrar, 1976; Grube and Berg, 2009; Bates *et al.*, 2011). Genome sequences of the lichen symbionts can therefore be obtained by cultivating each individual partner axenically, or by sequencing metagenomic samples (Grube *et al.*, 2015; Parks *et al.*, 2017). However, obtaining a genome from a single symbiont is advantageous because it reduces problems with chimeric contigs where target organisms and contamination are merged in genome assemblies (Bemm *et al.*, 2016). Nevertheless, the isolation of lichen mycobiont is challenging because of a high risk of contamination, time required for a first spore discharge, and microscopical size of the spores, which makes their detection difficult (Yoshimura *et al.*, 2002). In addition, it can take several months up to one year before enough fungal mycelium can be obtained for further experiments and sequencing (Abdel-Hameed *et al.*, 2016b; Dal Grande *et al.*, 2018;).

To date, almost 5300 fungal genomes are available on National Center for Biotechnology Information (NCBI: https://www.ncbi.nlm.nih.gov/) and DOE Joint Genome Institute (JGI: https://genome.jgi.doe.gov/portal/) web-portals (date accessed: 13

January 2022), out of which only 42 genomes belong to the lichen-forming fungi. The sequenced species belonging to the latter are mostly representatives from Lecanoromycetes, which were obtained from culture isolates (e.g., Dal Grande *et al.*, 2018; Armaleo *et al.*, 2019) as well as of entire thalli by metagenome sequencing (e.g., Haridas *et al.*, 2020; Allen *et al.*, 2021).

Those genomes were used to address various questions, such as the evolution of lichen symbiosis and thus identification of genes of potential symbiotic significance (Wang *et al.*, 2014; Kono *et al.*, 2017, 2020; Armaleo *et al.*, 2019), substrate specificity (Resl *et al.*, 2018; Resl and Hahn, 2021), protein function (Junttila and Rudd, 2012; Armstrong *et al.*, 2018), and adaptation to various environmental conditions (Dal Grande *et al.*, 2017; Puvar *et al.*, 2020). One special focus of genomic studies has been to detect the genes potentially involved in the secondary metabolite production (e.g., Abdel-Hameed *et al.*, 2016a; b; Dal Grande *et al.*, 2018; Calchera *et al.*, 2019). Even though only few lichen genomes are available, a significant part of them (35.7%) were either reported as a draft-genome (nine genomes) or deposited without any following analyses (six genomes), for example, as a part of 1000 Fungal Genomes Project (Grigoriev *et al.*, 2014). Nevertheless, all these studies already provide structured data and genomic resources for further, more extensive use in phylogenomic analyses.

1.5.2. *Up-to-date sequencing approaches for genome sequencing*

The quality of a *de-novo* produced genome largely depends on the sequencing technology applied. The *de-facto* standard is short-read sequencing obtained from Illumina technology. However, the genomes may contain an abundance of repetitive sequences that are longer than the length of Illumina short reads and because of the repetitiveness of these regions, assemblies crossing the repeat will often not be possible. During genome assembly, these repeat sequences cannot be distinguished and hence are often collapsed into contigs (consensus sequence of overlapping DNA reads), leaving gaps in the genome assembly. As an alternative, longer reads might be used to span most repetitive sequences and to close the gaps in fragmented assemblies (Cao *et al.*, 2017). Therefore, in recent years, long-read sequencing technologies, e.g., using PacBio or Oxford Nanopore platforms, have been becoming increasingly popular (Cui *et al.*, 2020; Morabito *et al.*, 2020).

The MinION (Oxford Nanopore) technology allows generating longer reads (up to 30Kb), which can span most repetitive genomic regions, thus increasing assembly integrity.

Nevertheless, substantial read error correction, including bioinformatic approaches, is essential because of its high error rates (up to 30 %). A hybrid assembly that combines error-prone long reads with highly accurate short read sequence data provides an efficient method for building near to complete genome assemblies. So far, only recently a first lichen genome of *Physcia stellaris* (L.) Nyl. was sequenced and assembled from a combination of long-read Nanopore and short-read Illumina data (Wilken *et al.*, 2020). More recently, the genome of *Bacidia gigantensis* Lendemer, McCune & McMullin has been sequenced from the whole thallus using long-read sequencing on the PromethION (Oxford Nanopore) platform (Allen *et al.*, 2021), which served as a counterpart to our *Bacidia rubella* genome for subsequent comparative genomic analyses. To obtain a high-quality genome, a hybrid assembly approach using Illumina short-reads and Oxford Nanopore long reads was applied in this study as well.

1.5.3. *Importance of secondary metabolites in lichens*

Fungi synthesize a large range of natural products (secondary metabolites). Based on their biological activities and ecological roles, secondary metabolites are classified as phytotoxins, when they induce macroscopic damage to plant tissues, e.g., causing heavy diseases of important agrarian crops (Chakraborty, 2018) or therapeutical, when they possess antibiotic and pharmaceutical properties (such as penicillin) (Kolawole *et al.*, 2021 and references therein). In terms of their chemical structure, fungal secondary metabolites are structurally diverse and have been grouped into four main groups: polyketides (PK), non-ribosomal peptides (NRPS), terpenoids and tryptophan derivatives (Kolawole *et al.*, 2021). Polyketide synthases (PKSs) are a family of multi-domain enzymes or enzyme complexes that produce polyketides in bacteria, fungi, plants, and a few animal lineages with various biological activities and pharmacological properties (Punya *et al.*, 2015). They play an important role in defense from high light intensity, herbivory and as antimicrobial protectant (e.g., Demmig-Adams *et al.*, 1990; Cardarelli *et al.*, 1997; Elix and Stocker-Wörgötter, 2008; Solhaug *et al.*, 2010). Besides the benefits for the lichens, the compounds have various biological activities, resulting in a wide application in the pharmaceutical industry. A wide range of mostly foliose and fruticose lichen genera have already been used in traditional medicine all around the world, for example to treat wounds, skin disorders, respiratory, digestive, obstetric, and gynecological issues (Devkota *et al.*, 2017; Crawford,

2019; Yang *et al.*, 2021). Lichen natural products are therefore promising targets for further development of pharmaceutical applications.

1.5.4. Mining secondary metabolites in lichens

Genome mining has emerged in the past decade as a key technology to explore and exploit natural product diversity (Albarano *et al.*, 2020; Robey *et al.*, 2021). In recent years, secondary metabolites research has benefited extensively from genome mining approaches in bacteria, fungi, and plants (e.g., Nielsen, 2017; Mullins *et al.*, 2019; Lichman *et al.*, 2020). Key to this success is the fact that biosynthetic pathways of genes encoding natural product are usually clustered together on the chromosome, and thus these biosynthetic gene clusters (BGCs) can be readily identified in a genome sequence (Rokas *et al.*, 2020; Robey *et al.*, 2021).

Despite this advancement, for most secondary compounds of lichen-forming fungi, the corresponding biosynthetic genes are still unknown, complicating clear gene assignments to a particular secondary metabolite. Accordingly, earlier studies have focused only on a few well-known compounds, e.g., usnic acid, grayanic acid, and atranorin (e.g., Armaleo *et al.*, 2011; Abdel-Hameed *et al.*, 2016a; b; Elshobary *et al.*, 2018; Singh *et al.*, 2022). However, the increasing number of available lichen-forming fungal genomes provides a great resource for identifying additional PKS genes (Boustie *et al.*, 2011). We used this valuable opportunity to quantify the diversity of PKS genes in *Bacidia rubella* and compared these to other lichen-forming fungal species.

Chapter 2

Morphological and phylogenetic analyses of *Toniniopsis subincompta* s. lat. (Ramalinaceae, Lecanorales) in Eurasia

Julia V. Gerasimova, Irina N. Urbanavichene, Gennady P. Urbanavichus and Andreas Beck

CAMBRIDGE
UNIVERSITY PRESS

Standard Paper

Morphological and phylogenetic analyses of *Toniniopsis subincompta* s. lat. (*Ramalinaceae, Lecanorales*) in Eurasia

Julia V. Gerasimova[1,2] (iD), Irina N. Urbanavichene[3] (iD), Gennady P. Urbanavichus[4] (iD) and Andreas Beck[1,5] (iD)

[1]Botanische Staatssammlung München, Department of Lichenology and Bryology, SNSB-BSM, Menzinger Str. 67, 80638 Munich, Germany; [2]Ludwig-Maximilians-Universität München, Systematic Botany and Mycology, Menzinger Str. 67, 80638 Munich, Germany; [3]Laboratory of Lichenology and Bryology, Komarov Botanical Institute RAS, Professor Popov St. 2, 197376 St Petersburg, Russia; [4]Laboratory of Terrestrial Ecosystems, Institute of North Industrial Ecology Problems, Kola Science Centre, Russian Academy of Sciences, 184209 Apatity, Murmansk Region, Russia and [5]GeoBio-Center, Ludwig-Maximilians-Universität München, 80333 Munich, Germany

Abstract

In recent years, several species that have long been considered to belong in *Bacidia* s. lat. have been transferred to other genera such as *Bellicidia, Bibbya, Scutula,* and also to *Toniniopsis,* accommodating species previously placed in *Bacidia* and *Toninia.* One of its widespread species, *Toniniopsis subincompta,* can be recognized by its thinly granular thallus, dark brown to black apothecia, green epithecium, red-brown hypothecium, and bacilliform ascospores. However, it shows considerable variation in thallus structure, and coloration of apothecia, hypothecium and exciple. We sequenced 20 specimens of *T. subincompta* to investigate whether there is phylogenetic support for the delimitation of species in accordance with the variability of the observed characters. For phylogenetic analyses, we used newly generated sequence data from the nuclear internal transcribed spacer (nrITS), mitochondrial small subunit (mtSSU) and DNA-directed RNA polymerase II subunit (*RPB*2). Maximum likelihood and Bayesian inference analyses, as well as three species delimitation programs, provided consistent evidence that *T. subincompta* forms two separate lineages, to be recognized at the species level. The complex nomenclature of *T. subincompta* (basionym *Lecidea subincompta*) shows it to be a synonym of *Bellicidia incompta.* For the most common taxon previously called *Bacidia* (*Toniniopsis*) *subincompta,* the new combination *T. separabilis* is made, rather than proposing a conserved type for *Lecidea subincompta. Toniniopsis dissimilis* is newly described to accommodate the less common taxon. *Toniniopsis dissimilis* is characterized by a predominantly wrinkled to warted to subsquamulose thallus; generally grey-brown to dark brown apothecia, often with a lighter margin; a dark brown hypothecium, frequently gradually merging into the coloration of the exciple below and the lateral part of the exciple attached to the hymenium; a mostly colourless rim and lateral part of the exciple. The closely related *T. separabilis* is characterized by a thallus of mostly single or contiguous ±loose granules, often forming short, coralloid, isidium-like bulges; darker apothecia, with a margin mostly of the same colour or darker than the disc; a comparatively thinner hypothecium easily separated from the exciple below. The rim and lateral part of the exciple often contain either a blue, brown or mixed blue-brown colour in the upper part or along the whole margin. Lectotypes of *Bacidia vegeta, Lecidea bacillifera* f. *melanotica* and *Secoliga atrosanguinea* var. *affinis* (the synonyms of *T. separabilis*) are selected. Cyanotrophy and the occurrence of albino morphs in *T. separabilis* are discussed.

Keywords: albino morph, *Bacidia* s. lat, cyanotrophy, lichen, phylogeny, species delimitation, taxonomy

(Accepted 9 November 2020)

Introduction

Until recently, a large variety of lichens were accommodated in the genus *Bacidia* in the broad sense. Zahlbruckner (1905) used the genus name for crustose lichens with a chlorococcoid photobiont, biatorine apothecia, and ascospores with three or more transverse septa. This circumscription was apparently unnatural and included numerous taxa that are not closely related to the type species, *Bacidia rosella* (Pers.) De Not. (Gerasimova & Ekman 2017). In recent phylogenetic studies, several species that have been considered within *Bacidia* for a long time have

been transferred to other genera such as *Bellicidia* Kistenich *et al., Bibbya* J. H. Willis, *Scutula* Tul. and *Toniniopsis* Frey (Kistenich *et al.* 2018). Moreover, phylogenetic results showed that *Toninia* A. Massal. was paraphyletic and *Bacidia subincompta* (Nyl.) Arnold, *Toninia aromatica* (Sm.) A. Massal. and *T. coelestina* (Anzi) Vězda grouped with *Toniniopsis illudens* (Nyl.) Kistenich *et al.* (formerly *Bacidia illudens* (Nyl.) H. Olivier). *Toniniopsis* is morphologically similar to *Toninia* but differs in the stronger pigmentation of the exciple and the presence of a blue-green pigment in the hymenium and sometimes also in the proper exciple.

A widespread species of the genus, *T. subincompta* (Nyl.) Kistenich *et al.,* is a corticolous species, occurring in Europe, Asia, Macaronesia, Africa and North America. It occurs in a range of woodlands from sea level to an altitude of *c.* 3000 m (Ekman 1996; Coppins & Aptroot 2009). It is also used as an

CrossMark

indicator for old-growth forest and is included in indices for determining the conservation importance of woodland areas (Rücker & Wittmann 1995; Rose & Coppins 2002; Coppins & Aptroot 2009; Brackel 2019). *Toniniopsis subincompta* can generally be recognized by its thinly granular thallus, black apothecia, green epithecium, red-brown hypothecium, and bacilliform ascospores (Coppins & Aptroot 2009). However, it can vary in spore shape, including both bacilliform and acicular spores, and in thallus structure, ranging from either discontinuous (discrete granules or low convex areoles) to continuous (without cracks or ±rimose, wrinkled, warted, tuberculate or distinctly granular) (Ekman (1996) as *Bacidia subincompta*). Further detailed examination has revealed differences in coloration of the apothecia (including a pale albino morph (Gilbert 1996)), hypothecium and exciple, in addition to the thallus and ascospore variation.

The aim of this paper is to clarify and re-evaluate the taxonomy of the morphologically variable *T. subincompta* s. lat. using different approaches based on material collected from the mountain regions of Allgäu (Germany) and the North Caucasus (Russia), where *T. subincompta* is well represented at different elevations and on various substrata. Here we present a three-locus phylogeny of *T. subincompta* s. lat. and assess the species morphology based on an enlarged taxon sampling and detailed observation of type specimens. Furthermore, we applied several species delimitation programs in order to test for congruence of species differentiation based on different analyses of the molecular data.

Material and Methods

We included specimens from Germany (Allgäu mountain region; eight specimens), Russia (the North Caucasus as well as the Altay, Kaliningrad and Murmansk regions; ten specimens) and Estonia (Valgamaa and Harjumaa; two specimens) collected at different elevations and bark substrata, in the period 2013–2018 (Table 1). To test if dark and albino morphs belong to the same species, we selected specimens of both morph types from the bark of the same tree (JG145 and JG146). Voucher specimens are deposited in the herbaria of the Botanische Staatssammlung München (M), University of Tartu (TU) and Komarov Botanical Institute (LE). The herbarium collection of *T. subincompta* s. lat. (55 specimens) stored in the Botanical Collection of Munich (M) was also studied.

Morphology

Microscopic observations were made using a Zeiss Axioplan light microscope (Oberkochen, Germany) equipped with differential interference contrast (DIC). Cross-sections of apothecia were made on a Leica Jung Histoslide 2000 Mikrotom (Heidelberg, Germany), with a thickness of 8–10 µm. Micrographs of cross-sections were taken on a Zeiss Axioplan with an attached AxioCam 512 Color camera and processed with the Zeiss ZEN 2.3. (blue edition) image program. Macrographs of external characters were taken on a Leica Z6 Apo microscope (with a ×2.0 Planapo lens; Leica, Germany) with a Sony Alpha 6400 camera (Sony, Japan) attached and equipped with a StackShot Macro Rail (Cognisys, USA). A single image was prepared from 30–40 serial images using Helicon Focus v.7 software (Helicon, USA).

Measurements are given as (min–) average ± SD (–max) (SD = standard deviation, n_1 = number of all observations, n_2 = number of specimens observed). We provide a detailed description of specimens using standard microscopic techniques following Coppins & Aptroot (2009) and the subdivision scheme of the proper exciple according to Ekman (1996), differentiating the following structures: the rim, lateral part and medullary part. To delimit the species lineages, we discuss the following diagnostic characters in detail: 1) thallus structure; 2) colour of disc and margin of apothecium; 3) colour of hypothecium; 4) colour and structure of exciple; 5) shape and size of ascospores. Pigment characterizations follow Meyer & Printzen (2000).

DNA extraction, PCR amplification and DNA sequencing

DNA extraction was carried out using the Stratec Invisorb Spin Plant Mini Kit (Stratec Molecular GmbH, Berlin, Germany) following the manufacturer's instructions. Five to eight apothecia were used from fresh material not older than 5 years and thallus fragments were removed in order to minimize the risk of contamination by, for example, lichenicolous fungi. PCR amplification, purification and sequencing were performed as described in Gerasimova *et al.* (2018). Cycling conditions included initial denaturation at 95 °C for 2 min, 5 cycles of 95 °C for 40 s, 54 °C for 60 s and 72 °C for 90 s, 33 cycles of 95 °C for 40 s, 54 °C for 60 s and 72 °C for 90 s, and a final extension step at 72 °C for 7 min. In those cases when the PCR product was not sufficient, a second PCR with a reduced number of cycles was conducted: denaturation at 95 °C for 2 min, 5 cycles of 95 °C for 40 s, 54 °C for 60 s and 72 °C for 90 s, 22 cycles of 95 °C for 40 s, 54 °C for 60 s and 72 °C for 90 s, with a final extension step at 72 °C for 7 min. We used the primers ITS1F (White *et al.* 1990) and ITS4m (Beck & Mayr 2012), mtSSU1 and mtSSU3R (Zoller *et al.* 1999), and fRPB2-5F and fRPB2-7cR (Liu *et al.* 1999).

Alignment and phylogenetic analyses

In addition to 57 (18 nrITS, 19 mtSSU and 20 *RPB*2) newly obtained sequences of *Toniniopsis subincompta* s. lat., we included sequences of *Toniniopsis* and *Toninia* from GenBank in our alignment when at least two loci were available (published in Ekman 2001; Kistenich *et al.* 2018). In an additional analysis, we added to our alignment six further nrITS sequences of *Toniniopsis subincompta* from GenBank, collected in Switzerland (Mark *et al.* 2016) and Norway (Ekman 2001; Kistenich *et al.* 2018), in order to examine their distribution among specimens from other localities in our phylogeny (results are discussed below, and see Supplementary Material File S1, Figs S2–S4, available online).

BLAST searches in GenBank were performed to detect and exclude accessory/lichenicolous fungi and potential contaminations. Alignments were carried out using standard settings in MUSCLE v.3.8.31 (Edgar 2004) as implemented in PhyDE-1 v.0.9971 and optimized manually. Positions, where a gap had to be inserted in more than 95% of the sequences, were excluded. The alignment with nrITS, mtSSU and *RPB*2 was subjected to Bayesian inference (BI) and maximum likelihood (RAxML and IQ-TREE) analyses for the single and concatenated datasets separately.

Bayesian inference was carried out using the Markov chain Monte Carlo method (MCMC) using MrBayes v.3.2.6 (Ronquist *et al.* 2012). The GTR substitution model with gamma-distributed rate variations across sites and a proportion of invariable sites was selected by jModelTest 2.1.10 v20160303 (Darriba *et al.* 2012) based on the Akaike Information Criterion. Two parallel runs were performed (two cold chains) with a single tree saved every 10th generation for a total of 1 000 000 generations. The initial 25% was discarded as burn-in and the results are summarized as a 50% majority-rule consensus tree.

Table 1. Specimen information and DNA codes for *Toninia* and *Toniniopsis* samples used in this study, with their respective GenBank Accession numbers. New sequences are in bold.

DNA no. (JG)	Name	Country	Locality	Specimen voucher	GenBank Accession number nrITS	*RPB*2	mtSSU
	Toninia cinereovirens	Norway	no indication	*Haugan & Timdal* 7953 (O)	AF282104	AM292781	AY567724
	T. squalida	Norway	no indication	*Haugan* 4970 (O)	AF282103	MG926297	MG925940
	Toniniopsis aromatica	Norway	no indication	*Haugan & Timdal* 4819 (O)	AF282126	MG926285	MG925926
	T. coelestina	Norway	no indication	*Haugan* 5985 (O)	AF282127	MG926291	MG925933
	T. dissimilis	Norway	Finnmark, Batsfjord	O-L-170623	MG838157	–	–
148	*T. dissimilis*	Germany	Oberallgäu, Markt Oberstdorf	*Gerasimova & Beck* M-0290431 (M)	**MT169977**	**MT180447**	**MT162221**
149	*T. dissimilis*	Germany	Oberallgäu, Markt Oberstdorf	*Gerasimova & Beck* M-0290432 (M)	**MT169978**	**MT180448**	**MT162222**
150	*T. dissimilis*	Germany	Oberallgäu, Markt Oberstdorf	*Gerasimova & Beck* M-0290433 (M)	**MT169979**	**MT180449**	**MT162223**
153	*T. dissimilis*	Russia	Republic of Adygea, Caucasus Biosphere Reserve	*Urbanavichene & Urbanavichus* L-15293 (LE)	**MT169982**	**MT180452**	**MT162226**
154	*T. dissimilis*	Russia	Republic of Adygea, Caucasus Biosphere Reserve	*Urbanavichene & Urbanavichus* L-15294 (LE)	**MT169983**	**MT180453**	**MT162227**
158	*T. dissimilis*	Russia	Republic of Adygea, Caucasus Biosphere Reserve	*Urbanavichene & Urbanavichus* L-15297 (LE)	**MT169985**	**MT180455**	**MT162229**
159	*T. dissimilis*	Russia	Republic of Adygea, Caucasus Biosphere Reserve	*Urbanavichene & Urbanavichus* L-15298 (LE)	–	**MT180456**	–
161	*T. dissimilis*	Russia	Abkhazia, Ritsinsky Relic National Park	*Gerasimova* L-11665 (LE)	–	**MT180458**	**MT162231**
	T. illudens	Canada	no indication	*Westberg* TNW2182	MG926037	MG926301	MG925943
	T. separabilis	Sweden	no indication	*Ekman* 3413	AF282125	MG926236	MG925851
	T. separabilis	Norway	Ostfold, Marker	O-L-105331	MG838165	–	–
	T. separabilis	Norway	Oslo, Oppsal	O-L-200148	MG838175	–	–
	T. separabilis	Norway	Nordland, Hamaroy	O-L-206520	MG838176	–	–
	T. separabilis	Norway	Sogn og Fjordane, Laerdal	O-L-197862	MG838186	–	–
	T. separabilis	Switzerland	no indication		KX098342	–	–
053	*T. separabilis*	Russia	Murmansk Region, Pasvik Nature Reserve	*Urbanavichus* M-0182602 (M)	**MT169969**	**MT180439**	**MT162213**
073	*T. separabilis*	Russia	Kaliningrad Region, Curonian Spit	*Gerasimova* M-0182613 (M)	**MT169970**	**MT180440**	**MT162214**
110	*T. separabilis*	Russia	Altay Region, Cherginsky Range	*Davydov* M-0289891 (M)	**MT169971**	**MT180441**	**MT162215**
118	*T. separabilis*	Estonia	Valgamaa	*Lõhmus* TU81156 (TU)	**MT169972**	**MT180442**	**MT162216**
119	*T. separabilis*	Estonia	Harjumaa	*Suja* TU76769 (TU)	**MT169973**	**MT180443**	**MT162217**
145	*T. separabilis*	Germany	Oberallgäu, Bad Hindelang	*Gerasimova & Beck* M-0290425 (M)	**MT169974**	**MT180444**	**MT162218**
146	*T. separabilis*	Germany	Oberallgäu, Bad Hindelang	*Gerasimova & Beck* M-0290425 (M)	**MT169975**	**MT180445**	**MT162219**
147	*T. separabilis*	Germany	Oberallgäu, Markt Oberstdorf	*Gerasimova & Beck* M-0290430 (M)	**MT169976**	**MT180446**	**MT162220**

(*Continued*)

Table 1. (*Continued*)

| DNA no. (JG) | Name | Country | Locality | Specimen voucher | GenBank Accession number | | |
					nrITS	*RPB*2	mtSSU
151	*T. separabilis*	Germany	Oberallgäu, Markt Oberstdorf	*Gerasimova & Beck* M-0290436 (M)	**MT169980**	**MT180450**	**MT162224**
152	*T. separabilis*	Germany	Oberallgäu, Markt Oberstdorf	*Gerasimova & Beck* M-0290437 (M)	**MT169981**	**MT180451**	**MT162225**
155	*T. separabilis*	Russia	Republic of Adygea, Caucasus Biosphere Reserve	*Urbanavichene & Urbanavichus* L-15295 (LE)	**MT169984**	**MT180454**	**MT162228**
160	*T. separabilis*	Russia	Republic of Adygea, Caucasus Biosphere Reserve	*Urbanavichus & Urbanavichene* L-15299 (LE)	**MT169986**	**MT180457**	**MT162230**

Maximum likelihood (ML) analysis was performed with RAxML v.8.2.4 following a GTRGAMMA model of molecular evolution with bipartitions drawn onto the most likely tree topology using a multiple non-parametric bootstrap (Stamatakis 2014) on the CIPRES web portal (Miller *et al.* 2010).

Further tree reconstruction using ML analysis was performed in IQ-TREE v.1.6.12 with ultrafast bootstrap approximation (Nguyen *et al.* 2015; Hoang *et al.* 2017). Ultrafast bootstrap (UFBoot) was specified with 10 000 replicates, 1000 maximum iterations and 0.99 minimum correlation coefficient (Minh *et al.* 2013). Substitution models for concatenated and single-locus datasets were selected using ModelFinder (Kalyaanamoorthy *et al.* 2017). The TIM2e + I + G4 substitution model was selected for the 3-locus dataset, HKY + F + G4 for the nrITS and mtSSU datasets, and TIM2e + G4 for the *RPB*2 dataset.

The ML trees based on the different substitution models from the single and concatenated datasets were congruent and in accordance with the Bayesian tree topology. Therefore, only the RAxML tree for the concatenated dataset is shown, with bootstrap support values (BS), posterior probabilities (PP) and ultrafast bootstrap values (UFBoot) added above or below branches. The phylogenetic trees were visualized using FigTree v.1.4.2 (Rambaut 2009). Only clades with BS ≥ 70% in RAxML, PP ≥ 0.95 in BI and UFBoot ≥ 85% in IQ-TREE were considered highly supported and are indicated in bold. The concatenated and individual gene trees obtained from RAxML, MrBayes and IQ-TREE are provided in Supplementary Material File S1 (Figs S1–S13).

Species delimitation analyses

Molecular and morphological results were complemented with three widely used species delimitation computational approaches: 1) Automatic Barcode Gap Discovery (ABGD) (Puillandre *et al.* 2011); 2) Poisson Tree Processes (PTP) (Zhang *et al.* 2013); 3) the Generalized Mixed Yule coalescent approach (GMYC) (Pons *et al.* 2006). ABGD accounts for the barcoding gap (i.e., the difference between intraspecific and interspecific genetic distances) and results can be compared to morphological, geographical or ecological data (Puillandre *et al.* 2011). We carried out ABGD using the online server at https://bioinfo.mnhn.fr/abi/public/abgd/abgdweb.html, applying defaults following the recommendation of Puillandre *et al.* (2011). One of the most critical parameters of the ABGD method is the prior maximum divergence of intraspecific diversity (P). We assigned the range of Pmin and Pmax to 0.001 and 0.1 (defaults) but focused on

the result for P = 0.01 as previous analyses have demonstrated that the method works best for this value (Puillandre *et al.* 2011).

PTP was carried out on the online server (https://species.h-its.org/ptp/) using 100 000 MCMC generations (as recommended for small trees with < 50 taxa), saving every 100th generation with 10% discarded as burn-in. PTP is a model for delimiting species based on a phylogenetic tree. Thus, the fully resolved, optimal tree obtained from the 3-locus concatenated data from RAxML was used as an input file, but with the outgroup excluded because this can improve delimitation results (Zhang *et al.* 2013).

A close relative of PTP is the GMYC model but the latter requires an ultrametric rooted tree as input with no zero branch lengths (Fujisawa & Barraclough 2013). To that end, identical sequences were excluded and an ultrametric tree was generated using BEAST v.1.10.4 (https://beast.community/index.html). We used BEAUti v.1.10.4 (Drummond *et al.* 2012), an interactive graphical application included in the BEAST package, to generate an xml file using the following parameters: GTR + I + G model as selected by jModelTest; estimated base frequencies; a strict clock model (assumes that all branches on the tree have the same rate of evolution); Tree Prior (Speciation: Yule Process model; best suited to study the relationships between species) with a Random starting tree option (Yule 1925; Gernhard 2008), and adjusting the priors in accordance with parameters received after model calculation (parameters and table with details on prior distributions are given in Supplementary Material File S2, available online). A run of 1 M iterations logging every 100th iteration was conducted. The convergence of the Markov chain was checked using Tracer v.1.7.1. A consensus tree was generated with TreeAnotator v.1.8.2 after discarding the initial 10% of trees as burn-in. The output file was converted into a newick file using FigTree v.1.4.2 (Rambaut 2009). GMYC was executed with the gmyc function in the SPLITS package in R (v.2.10, www.cran.r-project.org), employing the single (GMYCs) threshold method following parameters in the SPLITS package manual (Supplementary Material File S2). We applied the single-threshold version of GMYC since it has been shown to outperform the multiple-threshold version (Fujisawa & Barraclough 2013; Talavera *et al.* 2013; Luo *et al.* 2018).

Results

Phylogenetic analyses

Eighteen new nrITS, 19 mtSSU and 20 *RPB*2 sequences of *Toniniopsis subincompta* s. lat. were obtained (Table 1). The ML and BI analyses
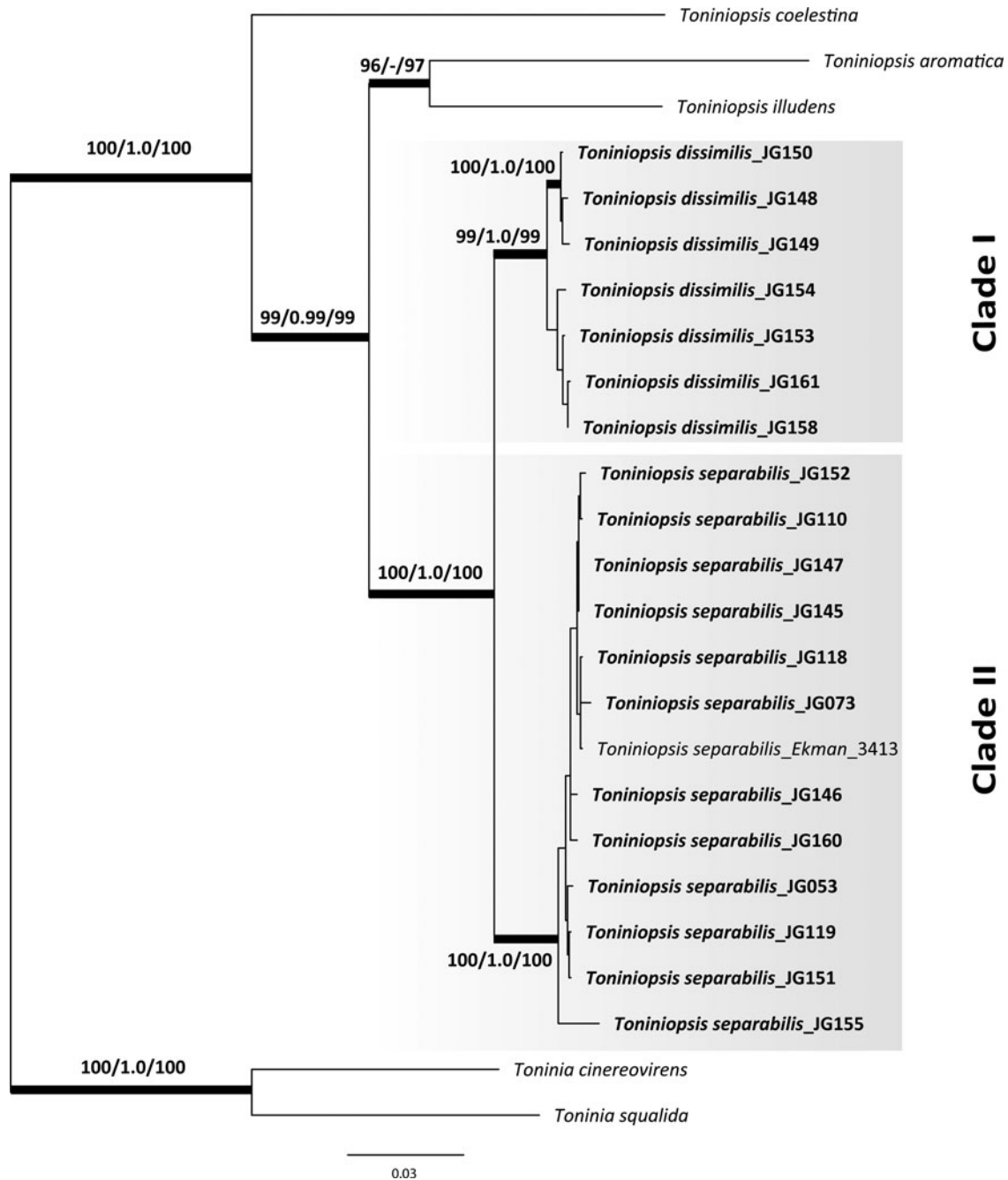
Fig. 1. Maximum likelihood (ML) tree of *Toniniopsis subincompta* s. lat. resulting from the RAxML analysis (Stamatakis 2014) of a concatenated 3-locus dataset (nrITS, mtSSU and *RPB*2). Maximum likelihood bootstrap values (BS), Bayesian posterior probabilities (PP) and ultrafast bootstrap values (UFBoot) are shown above or below branches. Branches with BS ≥ 70% in the RAxML analysis (first value), PP ≥ 0.95 (second value) and UFBoot support ≥ 85% are considered highly supported and marked in bold.

recovered highly concordant topologies in the phylogenetic trees from single genes separately and the concatenated dataset, with *Toninia cinereovirens* (Schaer.) A. Massal. and *T. squalida* (Ach.) A. Massal. used as outgroup (outgroup selection based on Kistenich *et al.* (2018)). Our phylogenetic results using three loci depict two distinct clades in *Toniniopsis subincompta* s. lat. (Fig. 1; Supplementary Material File S1 (Fig. S1), available online). Both clades were recovered with high support (BS/PP/UFBoot: 99/1.0/99 and 100/1.0/100, respectively). Clade I contains a highly supported subclade including JG148, 149 and 150 (BS/BI/UFBoot: 100/1.0/100).

Clade I (*T. dissimilis*) comprises specimens from the mountain region of Allgäu and the North Caucasus collected at elevations from 1050 to 1900 m a.s.l., and Clade II (*T. separabilis*) contains those from the Allgäu and North Caucasus in addition to those from Estonia and other parts of Russia (Altay, Murmansk and Kaliningrad regions) collected at elevations from 4 to 1800 m a.s.l. When including six nrITS sequences of *T. subincompta* from GenBank collected in Switzerland (Mark *et al.* 2016) and Norway (Ekman 2001; Kistenich *et al.* 2018), it was shown that they mostly belong to Clade II, except MG838157 in Clade I,

still with high support values for both clades (BS/BI/UFBoot: 99/1.0/100 and 98/1.0/95, respectively; see Figs S2–S4 in Supplementary Material File S1). Taken together, we observed no clear correlation between the clades and geography in our limited dataset. Nevertheless, individuals in Clade I have so far been collected only above 1000 m or in high latitudes (Finnmark, Norway) and thus seem to be more cold-adapted than specimens in Clade II.

Species delimitation

Molecular species delimitation programs belong to the methods within an integrative taxonomic framework and do not require a prior hypothesis of putative number of species. Species estimates for *T. subincompta* s. lat. using ABGD, PTP and GYMC resulted in two main species clusters in accordance with the results received from phylogenetic analyses. Thus, the first cluster included individuals from Clade I of the phylogenetic tree, and the second cluster individuals from Clade II.

Morphology

We examined the morphology and anatomy of all specimens of *T. subincompta* s. lat. included in our phylogeny, as well as relevant type specimens and herbarium material available in M (55 specimens). When comparing specimens from the two clades, we did not observe a strong difference in the size of the hymenium, exciple and ascospores (Table 2). The hymenium in Clade I is slightly thicker when compared to Clade II (72.5 ± 17 and 66.1 ± 11.1 µm, respectively). Ascospores in both clades are predominantly bacilliform, with 1 to 7 septa: 14–44 × 2–4 µm in Clade I, and 13–40 × 2–4 µm in Clade II. However, differences in thallus structure, as well as apothecia, exciple and hypothecium colour were observed (Table 2). Specimens in Clade I are characterized by having a predominantly wrinkled, warted to subsquamulose thallus whereas in Clade II the thallus mostly consists of single or contiguous ±loose granules, often forming short, coralloid, isidium-like bulges (Fig. 2). Apothecia in Clade I are generally grey-brown to dark brown, often with a lighter margin, whereas in Clade II apothecia are mainly darker, dark brown to black, with a margin mostly of the same colour or darker than the disc (pale brown in the albino morph). The hypothecium in Clade I is rather thick, often gradually merging into the coloration of the exciple downwards, whereas in Clade II the hypothecium is thinner and can easily be separated from the exciple below (Fig. 3). While in Clade I the rim of the exciple is mostly colourless with 2–3 layers of enlarged lumina cells (Figs 3A–E, 4A), in Clade II the rim and lateral part often contain either blue-green or brown or mixed blue-brown coloration in the upper part or along the whole margin (Fig. 3B, D & F), with mainly one layer of enlarged lumina cells (Fig. 4B). Two isolates collected from the same tree, representing the dark morph (JG145) and the albino morph (JG146) and confirmed to be the same species, nested in Clade II, but differed from other sequences by at least one nucleotide change in all three genes. In detail, the albino morph differs from the dark morph (JG145) by 4 nucleotides in nrITS, 2 nucleotides in mtSSU and one nucleotide in *RPB2*. Cyanotrophy, facultative or obligate association of lichens to free-living or ±lichenized cyanobacteria (Poelt & Mayrhofer 1988), and the occurrence of an albino morph were observed only in Clade II (see further details below). Based on the morphological and phylogenetic analyses,

we conclude that there are two different species within *Toniniopsis subincompta* s. lat.

Taxonomic treatment

The name *Lecidea subincompta* Nyl. was introduced as *nomen novum* for *Lecidea anomala* var. *atrosanguinea* Schaer. (Nylander 1865), because the epithet *atrosanguinea* was blocked by *Lecidea atrosanguinea* (Hoffm.) Nyl. (Nylander 1854) which was already in use. *Lecidea anomala* var. *atrosanguinea* Schaer. was based on Schaerer's *Lichenes Helvetici exs.* 212, which in fact contains specimens of *Bacidia incompta* (Borrer ex Hook) Anzi (Ekman 1996). This agrees with our observations on the type material in M (M-0308484). Hence *Toniniopsis subincompta*, based on *Lecidea subincompta*, would have to be regarded as a synonym of *Bellicidia incompta* (Borrer) Kistenich *et al.* (formerly *Bacidia incompta*). For this reason, Ekman (1996) suggested it was appropriate to select a new, conserved type specimen for *Lecidea subincompta* since the epithet *subincompta* was well known, while *Bacidia separabilis* (Nyl.) Arnold, the name to be used without a conserved type, had hardly ever been used. The necessity of conservation was also stated by Kistenich *et al.* (2018) when the taxon was transferred to *Toniniopsis*, but a formal proposal has never been made. According to the research presented here, the former *T. subincompta* consists of two species, and therefore a proposal to conserve *L. subincompta* (with a conserved type) will most likely not be approved. Consequently, *T. subincompta* is synonymized here with *Bellicidia incompta*. While working on the type material of *T. subincompta* s. lat., we did not find a matching candidate for Clade I and thus a new species must be described.

Toniniopsis dissimilis Gerasimova & A. Beck sp. nov. [Clade I]

MycoBank No.: MB 836224

This species is similar to *Toniniopsis separabilis* but differs in having a smooth to rather thick, tuberculate, warted or subsquamulose thallus and dark brown hypothecium, merging into the coloration of the exciple downwards.

Type: Germany, Bavaria, Landkreis Oberallgäu, Markt Oberstdorf, track from Oytalhaus to Käseralpe, *c.* 500 m east of Oytalhaus, mixed forest of *Picea*, *Fraxinus* and *Salix* along the River Oybach, on bark of the trunk of *Fraxinus*, *c.* 1 m above the ground, *J. Gerasimova* & *A. Beck* s. n., 27 June 2018 (M-0290432—holotype; UPS—isotype).

(Figs 2A & C, 3A, C & E, 4A)

Thallus indeterminate, thin, partly smooth to rather thick, tuberculate or warted, sometimes consisting of an appressed and continuous crust of subsquamules, granular when on twigs of mosses, consisting of single or contiguous warts or occasionally of single ±rounded granules. *Warts* ±flattened or forming subsquamules, adnate to the surface, often merged, forming a thick, wrinkled, irregularly shaped surface, light green, grey-green, green, brown-green, dirty grey-green to green-brown. *Photobiont* chlorococcoid.

Apothecia (0.2–)0.4 ± 0.15(–0.7) mm diam. (n_1 = 77, n_2 = 8), young with margin raised above the disc, mature ±flat, later becoming convex. *Disc* grey-brown, dark brown to black, sometimes with mixed colour. *Margin* of the same colour as or paler than disc, light brown, grey, brown-grey, grey-brown to dark

Table 2. Comparison of main diagnostic features between specimens from Clade I and Clade II of *Toniniopsis subincompta* s. lat.

	Clade I	Clade II
Thallus structure	Partly smooth, mostly tuberculate or warted sometimes consists of appressed and continuous crust of subsquamules or scattered or contiguous warts	Partly smooth, mostly consists of scattered ±roundish granules, often forming short, coralloid, isidium-like bulges; sometimes associates with cyanobacteria, thus forming dark green or black crust or bulges
Apothecia (colour)	Greyish brown, dark brown to black; margin brighter or concolorous, often lighter than disc	Grey-brown, dark brown to black or orange (albino morph); margin concolorous or darker (can be lighter brown); albino morph often presented
Epithecium	Colourless to brown, grey-blue, blue or blue-green	Brown to grey-blue to blue-green
Hypothecium	Often gradually merging into the coloration of the exciple downwards	Can be separated from the exciple below
Hymenium (µm)	(51–)72.5 ± 17(–122.5)	(49–)66.1 ± 11.1(–98)
Exciple (µm)	(30–)63 ± 19.3(–115)	(59–)63.5 ± 18(–122.5)
Rim of exciple	Mostly colourless or blue	Brown, blue or mixed
Lateral exciple	Brown	Brown, blue or mixed
Lumina cells along exciple rim, size (µm)	2–3 layers	1–2 layers
	(2–)4.2 ± 1.2(–7) × (5–)8.35 ± 2.9(–24)	(2.0–)3.5 ± 0.8(–6) × (5–)7.5 ± 1.8(–13)
Spores: size (µm)	(14–)26.7 ± 4.2(–44) × (2–)2.9 ± 0.4(–4)	(13–)25.2 ± 4.2(–40) × (2–)2.7 ± 0.42(–4)
Spores: septa	(1–)4 ± 2(–7)	(1–)4 ± 2(–7)
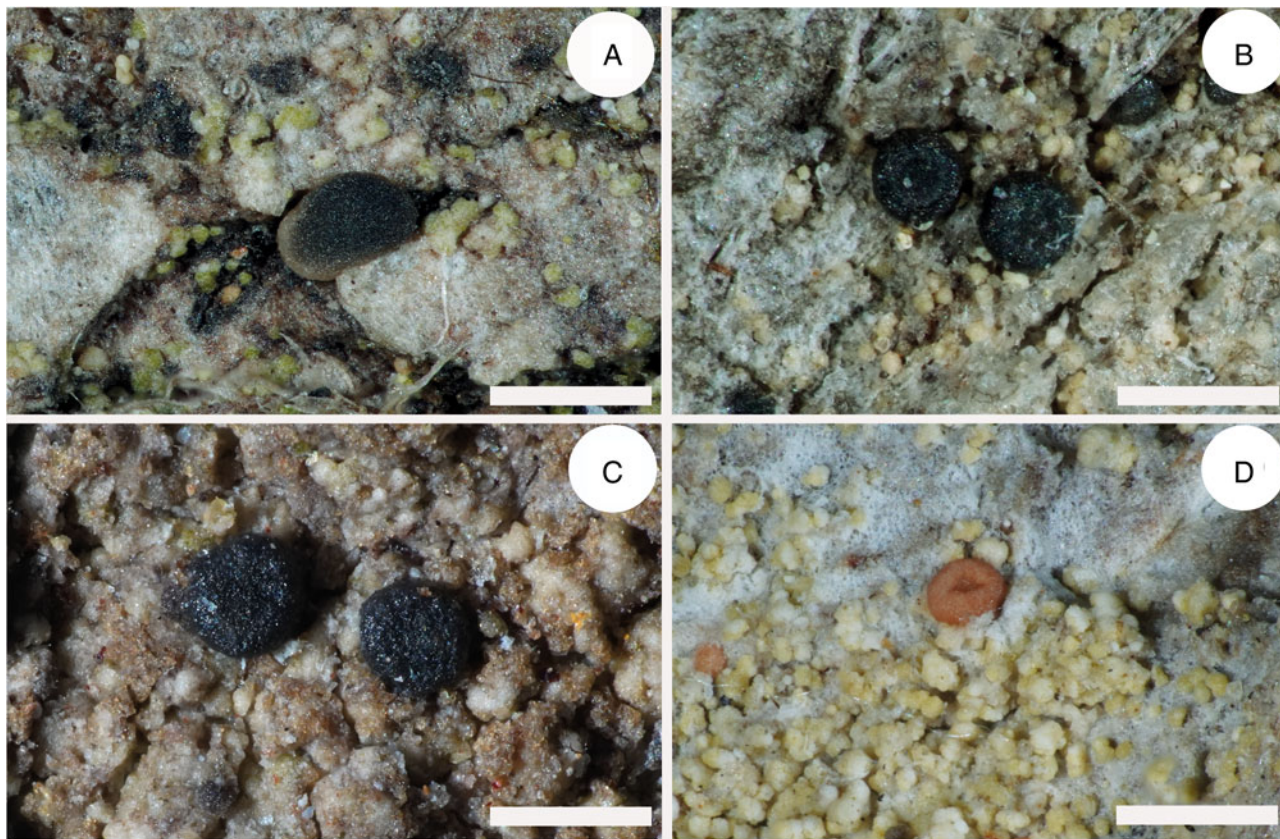
Fig. 2. Detail of *Toniniopsis dissimilis* and *T. separabilis*. A, holotype of *T. dissimilis* (M-0290432, JG149); thallus, consisting of scattered ±rounded or flattened or subsquamulose granules, and dark apothecia with light brown margin. B, *T. separabilis* (LE L-15299, JG160); thallus thin, consisting of ±rounded, loose granules. C, *T. dissimilis* (LE L-15293, JG153); thallus thick, warted to wrinkled. D, *T. separabilis* (M-0182613, JG073); thallus thick, wrinkled, forming isidium-like bulges with albino morph apothecia. Scales: A–D = 0.5 mm. In colour online.

brown. *Hymenium* $(51–)72.5 ± 17(–122.5)$ μm thick ($n_1 = 35$, $n_2 = 8$), colourless, without crystals. *Epithecium* greyish green or greyish blue, green-blue, partly almost colourless or brown. *Hypothecium* brown to dark brown, rather thick, downwards gradually merging into the coloration of the exciple. *Exciple* $(30–)63 ± 19.3(–115)$ μm wide ($n_1 = 34$, $n_2 = 8$), sometimes with minute crystals, not dissolving in K. *Rim* colourless, without or with greyish blue or blue tinge near the hymenium or along the whole margin, with 2–3 layers of cells with enlarged lumina $(2–)4.2 ± 1.2(–7)$ μm wide ($n_1 = 40$, $n_2 = 8$), and $(5–)8.3 ± 2.9(–24)$ μm long ($n_1 = 40$, $n_2 = 8$; maximum value with 24 μm was observed only once in JG149). *Lateral part* colourless or pale brown to dark brown, often coloured mainly when attached to hymenium. *Medullary part* pale brown, brown to almost colourless downwards, paler than hypothecium. *Paraphyses* simple or septate, $(1.5–)1.8 ± 0.4(–3.5)$ μm wide ($n_1 = 42$, $n_2 = 8$); apices ±clavate or not at all swollen, sometimes bifurcate, $(1.5–)2.5 ± 0.7(–4)$ μm wide ($n_1 = 42$, $n_2 = 8$), colourless or with dark blue diffuse internal pigmentation. *Ascospores* bacilliform, $(14–)26.7 ± 4.2(–44)$ μm long ($n_1 = 245$, $n_2 = 8$), and $(2–)2.9 ± 0.4(–4)$ μm wide ($n_1 = 245$, $n_2 = 8$), with $(1–)4 ± 2(–7)$ septa ($n_1 = 245$, $n_2 = 8$).

Chemistry. Hypothecium K+ intense brown to purplish; exciple K+ purplish brown.

Pigments. Bagliettoa-green in epithecium and in uppermost part and rim of exciple; Laurocerasi-brown in hypothecium and lateral part of exciple.

Etymology. Similar to *T. separabilis* but differs in some characters.

Additional specimens examined. **Turkey:** *Prov. Rize*: valley very near to the village of Ayder, 30 vii 1997, *V. John* (M-0308422). *Prov. Bursa*: Uludag, 6 ix 1976, *K. Kalb* & *G. Ploebst* (M-0308424).—**Germany:** *Bayerische Alpen*: am Taubensee ober Wessen, ix 1876, *F. Arnold* (M-0308441); *ibid.*, ix 1871, *F. Arnold* (M-0308442); Aschau, ix 1875, *F. Arnold* (M-0308443).—**Sweden:** *Södermanland*: Björkvik, 27 vi 1908, *G. O. A. Malme* (M-0308448).—**Norway:** *Troms*: Tromsø, 1868, *Th. M. Fries* (M-0308451).—**Finland:** [*South Häme*]: Luhanka, 1873, *E. Lang* (M-0308456).—**Slovakia:** *Malá Fatra*: Velký Stoh, c. 1300 m, 17 vi 1965, *I. Pišút* & *A. Vězda* (M-0308458).—**Austria:** *Steiermark*: Niedere Tauern, Wölzer Tauern, 1500 m, 15 vii 1990, *J. Hafellner* (M-0308468). *Vorarlberg*: Rätikon, Gargellen, 1300 m, 6 ix 1989, *R. Türk* (M-0308469). *Tirol*: Matrei, *F. Arnold* (M-0308476, M-0308477).

Toniniopsis separabilis (Nyl.) Gerasimova & A. Beck comb. nov. [Clade II]

MycoBank No.: MB 836225

Lecidea separabilis Nyl., *Flora (Jena)* **48**(10), 147 (1865).—*Bacidia atrosanguinea* f. *separabilis* (Nyl.) Arnold, *Flora (Jena)* **67**(30), 582 (1884); type: [Finland, South Häme], Hollola, 1863,
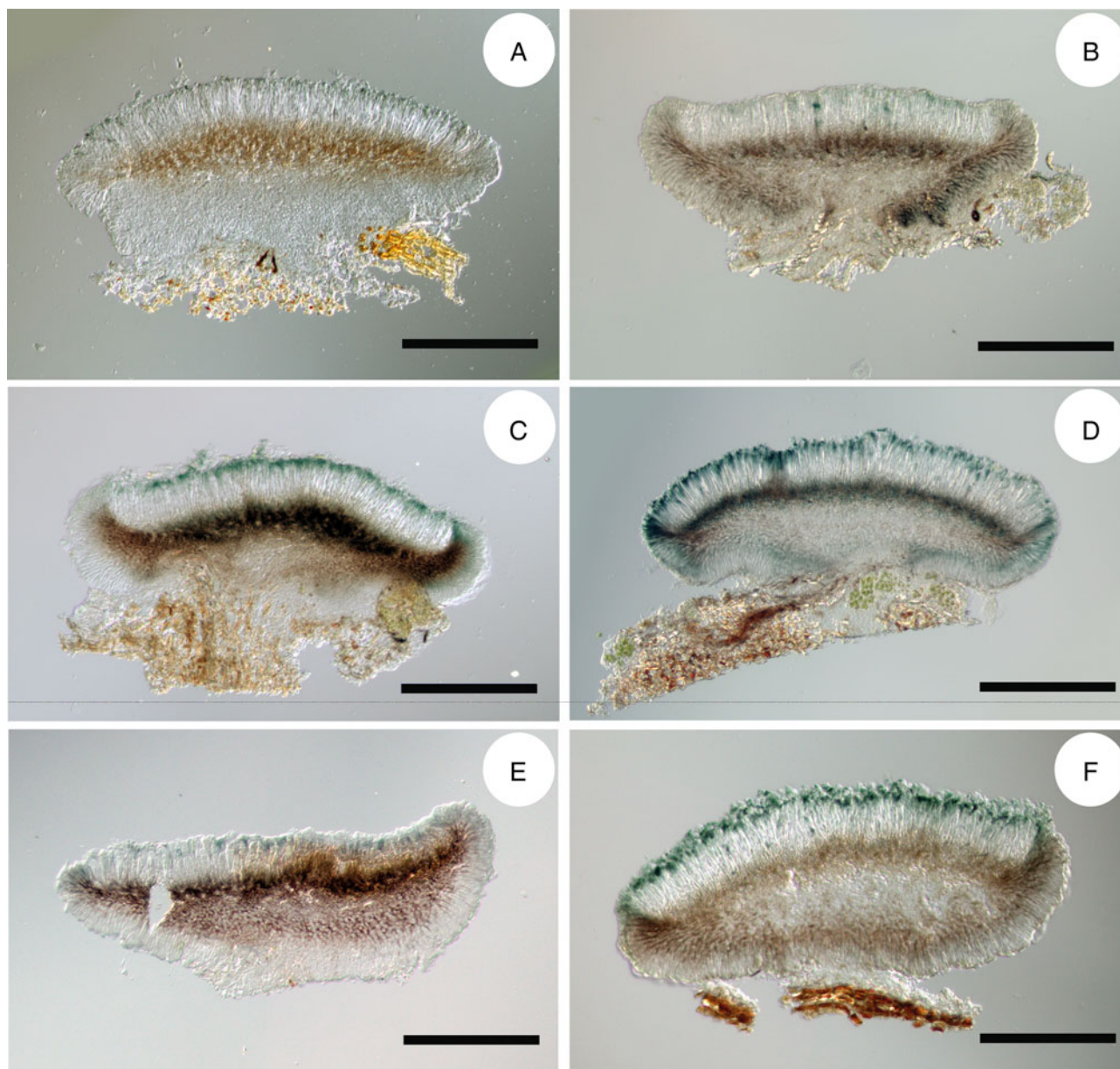
Fig. 3. Transverse sections of apothecia of *Toniniopsis dissimilis* (A, C, E) and *T. separabilis* (B, D, F). A, holotype of *T. dissimilis* (M-0290432, JG149). B, lectotype of *Lecidea separabilis* (H-NYL 17424). C, colourless rim of exciple; lateral part brown, mainly attached to hymenium, partly with blue tinge near hymenium (M-0290431, JG148). D, rim and lateral part of exciple with blue coloration along the whole margin (M-0290425, JG145; dark morph). E, dark brown hypothecium, merging into coloration of exciple below (L-15293, JG153). F, dark brown hypothecium with paler exciple below; rim and lateral part of exciple with brown coloration along the whole margin (M-0290437, JG152). Scales: A–F = 200 μm. In colour online.

J. P. Norrlin s. n. (H-NYL 17424—lectotype! selected by Ekman (1996: 105)).

Lecidea hegetschweileri Hepp [nom. nud.] in *Hepp's Systematische Sammlung*, 212 (1852).—*Biatora atrosanguinea* [unranked] *hegetschweileri* Hepp, *Die Flechten Europas* **1** (1853).—*Bacidia hegetschweileri* (Hepp) Vain. [non auct.], *Acta Soc. Fauna Flora Fenn.* **53**(1), 215 (1922); type: [Switzerland], Zürich, An der Rinde alter Eichen, *J. A. P. Hepp* s. n. [Hepp: *Flecht. Europ.*, 23] (BM00002217—lectotype! selected by Ekman (1996: 105); M-0190116, M-0154468—isolectotypes!).

Secoliga atrosanguinea var. *affinis* Stizenb., *Nova Acta Acad. Leopoldin.-Carolin.* **30**(3), 18 (1863) [non *Bacidia atrosanguinea* (Sch.) var. *affinis* Zw. in Arnold: *Lich. exs.* 505].—*Bacidia affinis* (Stizenb.) Vain., *Acta Soc. Fauna Flora Fenn.* **53**(1), 154 (1922); type: [Germany, Baden-Württemberg], Heidelberg, in der Nähe des Kohlhofs, an *Popul. tremula*, sehr selten, 1858, *Zwackh-Holzhausen* s. n. [*Lichenes exs.* 336B] (H-NYL 17397—lectotype! selected here, MBT394654).

Lecidea bacillifera f. *melanotica* Nyl., *Flora (Regensburg)* **50**, 373 (1867).—*Bacidia subincompta* var. *melanotica* (Nyl.) H. Magn., *Förteckning över Skandinaviens växter* **4**, 40 (1936); type: Finland, [South Häme], Evois (= Evo), ad corticem populi, 1866, *J. P. Norrlin* s. n. (H-NYL 17205—lectotype! selected here, MBT394655; H-NYL 17362—isolectotype!).

Bacidia vegeta Vain., *Acta Soc. Fauna Flora Fenn.* **53**(1), 153 (1922); type: [Finland, South Häme], Mustiala, 1868, *A.*
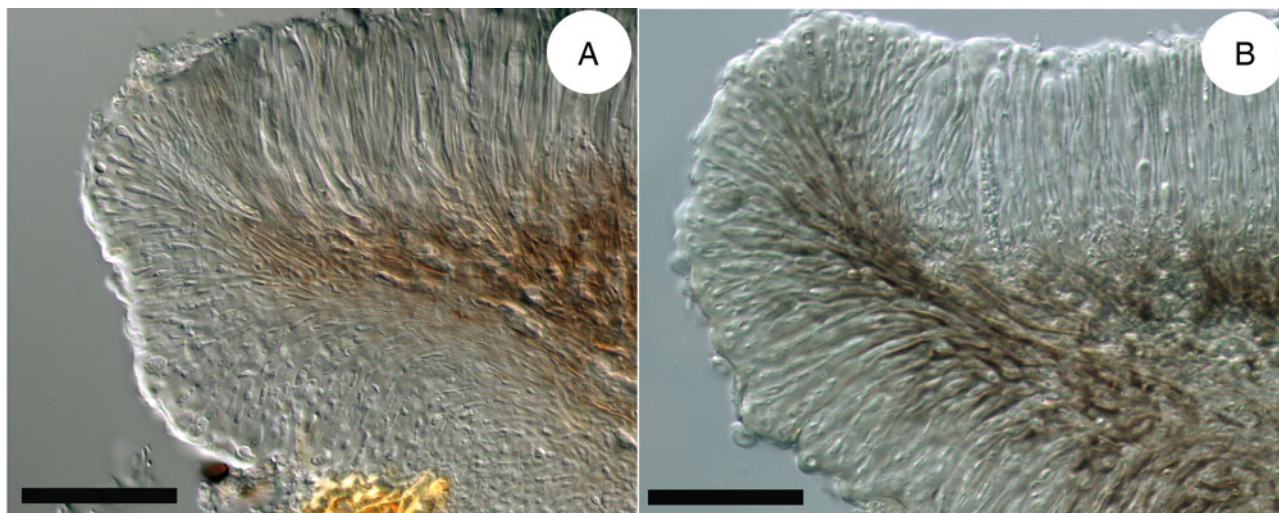
Fig. 4. Exciple structure. A, holotype of *Toniniopsis dissimilis* (M-0290432, JG149) with at least 3 layers of enlarged lumina cells. B, lectotype of *Lecidea separabilis* (H-NYL 17424) with paraplectenchymatic exciple structure and one layer of enlarged lumina cells. Scales: A & B = 50 μm. In colour online.

Kullhem s. n. (H8000177—lectotype! annotated by S. Ekman (2012), selected here, MBT394656).

(Figs 2B & D, 3B, D & F, 4B, 5)

Thallus indeterminate, thin, partly smooth, inconspicuous, discrete to rather thick, continuous, warted, thinly to coarsely granular, consisting of single or contiguous ±loose granules, especially rich in cracks of the bark, often forming short, coralloid, isidium-like bulges. *Granules* ±roundish or flattened or forming patches of irregularly shaped subsquamules, green, green-grey to green-brown, turning completely brown in the herbarium. *Photobiont* chlorococcoid, sometimes additionally associating with one or several free-living cyanobacteria: 1) *Nostoc* sp., 2) *Gloeocapsa* sp. and 3) *Scytonema* sp. (cyanotrophic association).

Apothecia (0.2–)0.4 ± 0.1(–0.8) mm diam. ($n_1 = 88$, $n_2 = 10$), young ±flat or with margin slightly above the disc, mature ±flat, later becoming convex and irregularly shaped. *Disc* grey-brown, dark brown to black or pale orange to orange-brown in albino morphs. *Margin* of the same colour as or darker than the disc, light brown, brown to dark brown to black. *Hymenium* (49–)66.1 ± 11.1(–98) μm thick ($n_1 = 43$, $n_2 = 10$), colourless, without crystals. *Epithecium* brown, greyish blue to dark blue-green or sometimes almost colourless (albino morph). *Hypothecium* thin, brown to dark brown, sometimes with green tinge, or straw-coloured, almost colourless in the albino morph, can be easily separated from exciple below. *Exciple* (59–)63.5 ± 18(–122.5) μm wide ($n_1 = 39$, $n_2 = 10$), without or with minor crystals along exciple, not dissolving in K. *Rim* pale brown, dark brown or blue, often mixed blue-brown, mostly with one layer or up to two layers of enlarged lumina cells along the rim, often inconspicuous, (2.0–)3.5 ± 0.8(–6) μm wide ($n_1 = 55$, $n_2 = 10$) and (5–)7.5 ± 1.8 (–13) μm long ($n_1 = 55$, $n_2 = 10$). *Lateral part* pale brown to brown mainly attached to hymenium, often with blue, brown or mixed blue-brown colour near hymenium or along the whole margin, or almost colourless or pale straw-coloured (albino morph). *Medullary part* under hypothecium light brown to almost colourless which downwards can eventually change to dark brown or blue. *Paraphyses* simple, (1–)1.8 ± 0.5(–3.5) μm wide ($n_1 = 60$, $n_2 = 10$); apices ±clavate or not at all swollen,

sometimes bifurcate, (1.5–)3 ± 1(–5.0) μm wide ($n_1 = 60$, $n_2 = 10$), colourless or with dark greyish blue to dark blue-green diffuse internal pigmentation. *Ascospores* bacilliform or acicular, (13–)25.2 ± 4.2(–40) μm long ($n_1 = 273$, $n_2 = 10$) and (2–)2.7 ± 0.42(–4) μm wide ($n_1 = 273$, $n_2 = 10$), with (1–)4 ± 2(–7) septa ($n_1 = 273$, $n_2 = 10$).

Chemistry. Hypothecium K+ intense brown; brown parts of exciple K+ purplish brown.

Pigments. Bagliettoa-green in epithecium and rim of exciple; Laurocerasi-brown in hypothecium and lateral part of exciple; sometimes a mixture of Bagliettoa-green and Laurocerasi-brown in exciple. Rubella-orange in epithecium, hypothecium and exciple (in the case of the albino morph).

Remarks. According to the International Code of Nomenclature, for any taxon below the rank of genus, the correct name is the combination of the final epithet of the earliest legitimate name of the taxon at the same rank (Art. 11.4, Turland *et al.* 2018). Therefore, *Lecidea separabilis* has priority at species rank from 1865, whereas the epithets *hegetschweileri* and *affinis* were validly published at the species rank only in 1922 (Vainio 1922). The complex nomenclature regarding the name *Bacidia hegetschweileri* has already been described in detail by Ekman (1996) so we do not reiterate this information here.

Additional specimens examined. **Russia:** *Republic of Adygea*: Maykop district, 1900 m, *I. Urbanavichene & G. Urbanavichus* (LE L-15296); *ibid.*, 1460 m, *I. Urbanavichene & G. Urbanavichus* (LE L-15301). *Kabardino-Balkaria*: Elbrus National Park, 1880 m, *I. Urbanavichene & G. Urbanavichus* (LE L-15302).—**Canada:** *Graham Island*: Mt Raymond, *c.* 760 m, 1988, *I. M. Brodo 26653B* (M-0308421).—**Turkey:** *Prov. Kastamonu*: Ilgaz Dağlari, 1680 m, 11 viii 1976, *K. Kalb & G. Ploebst* (M-0308423); *ibid.*, 1680 m, 31 viii 1976, *K. Kalb* (M-0308425).—**Germany:** *Landkreis Oberallgäu*: Markt Oberstdorf, 850 m, 27 vi 2018, *J. Gerasimova & A. Beck* (M-0290429); *ibid.*, 1050 m, 27 vi 2018, *J. Gerasimova & A. Beck* (M-0290434); *ibid.*, 950 m, 29 vi 2018, *J. Gerasimova & A. Beck* (M-0290439; M-0290440). *Landkreis Berchtesgadener Land*:
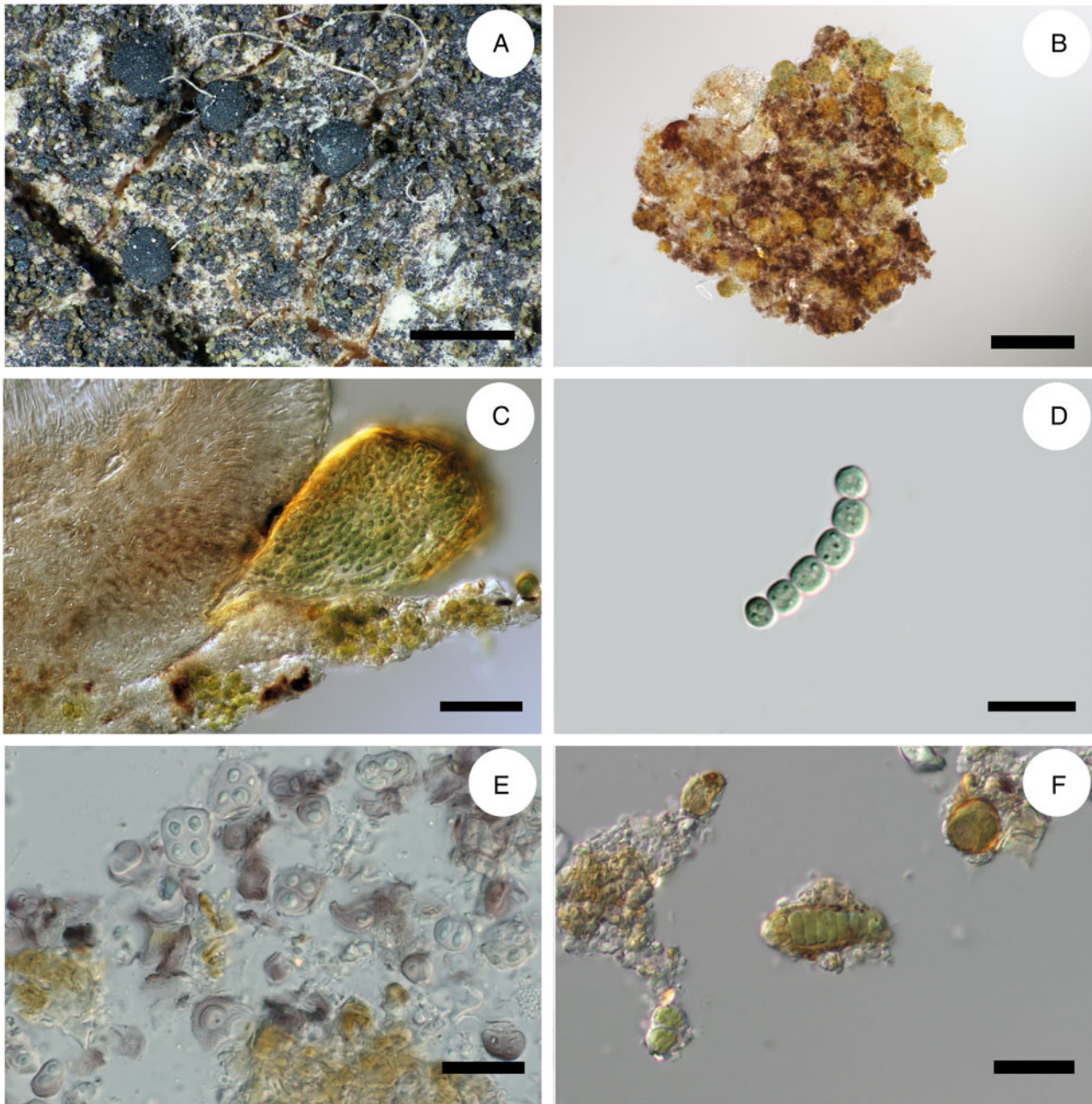
Fig. 5. Cyanotrophic association in lectotype of *Lecidea bacillifera* f. *melanotica* (A, B & E) and *T. separabilis* (C, D & F). A, thallus with cyanobacterium (dark patches) in tight association. B, composition of the thallus seen under the microscope. C, cross-section of apothecium with associated cyanobacterium cells (M-0289891, JG110). D, *Nostoc* sp. (M-0289891, JG110). E, *Gloeocapsa* sp. F, *Scytonema* sp. (M-0290436, JG151). Scales: A = 1 mm; B = 100 μm; C = 50 μm; D–F = 15 μm. In colour online.

Königssee, 605 m, 1984, *R. Türk* & *H. Wunder* 2961 (M-0308431); *ibid.*, 630 m, 1998, *R. Türk* 25704 (M-0308426); Obersalzberg, 955 m, 2011, *R. Cezanne* & *M. Eichler* 8371 (M-0308428); Ramsau, 775 m, 1988, *R. Türk* & *H. Wunder* 5988 (M-0308429*)*; Hochbahnweg, 1050 m, 1989, *R. Türk* & *H. Wunder* 6257 (M-0308430). *Landkreis Freyung-Grafenau*: National Park Bayerischer Wald, 1100–1180 m, 13 x 1999, *Ch. Printzen* (M-0308427). *Landkreis Weissenburg-Gunzenhausen*: Weissenburg, 20 v 1866, *F. Arnold* (M-0308432). *Landkreis München*: zwischen Geiselgasteig und Wörnbrunn, im Grünwalder Park, 3 x 1888, *F. Arnold* (M-0308434); zwischen Obersendling und Hesselohe, vi 1888, *F. Arnold* (M-0308436). *Landkreis Starnberg*: westlich von

Gauting, 23 iii 1896, *F. Arnold* (M-0308435). *Landkreis Coburg*: Tal W Hohe Schwemge, NW Oberwohlsbach, 1989, *L. Meinunger* 17353 (M-0308437). *Landkreis Miesbach*: Alpbach, Tegernsee, 1989, *L. Meinunger* 17135 (M-0308438). *Landkreis Eichstätt*: Eichstätt, 1858, *F. Arnold* (M-0308440); *ibid.*, v 1864, *F. Arnold* (M-0308444); *ibid.*, vii 1869, *F. Arnold* (M-0308445). *Thüringen*: Kreis Hildburghausen, 1989, *L. Meinunger* 17004 (M-0308446).— **Austria**: *Salzburg*: Brunnfeld between the villages of Pichl-Auhof and Ort, 605 m, 5 iv 2008, *R. Türk* & *S. Pfleger* (M-0308465); Hohe Tauern, Kapruner Tal, 970–1270 m, 27 x 1989, *R. Türk* (M-0308466). *Kärnten*: Rennweg N von Pörtschach, 600 m, 14 ii 1990, *R. Türk* (M-0308467). *Vorarlberg*: Lechtaler-Alpen, 1300 m,

10 vii 1986, *H. Mayerhofer, G. Grabherr & R. Türk* (M-0308470). *Steiermark*: Oberfahrenbach, 400 m, 19 iii 1995, *J. Poelt* (M-0308471). *Tirol*: Wildpark Wildbichl, vii 1895, *Schnabl* (M-0308439); Matrei, vii 1869, *F. Arnold* (M-0308472, M-0308473); *ibid.*, viii 1872, *F. Arnold* (M-0308478).—**Sweden:** *Värmland*: Ekshärad, 11 vii 1961, *S. W. Sundell* (M-0308447). *Uppland*: Värmdön, 28 vii 1908, *G. O. A. Malme* (M-0308449). *Jämtland*: Enafors, 26 vii 1910, *G. O. A. Malme* (M-0308450).—**Norway:** *Troms*: Tromsø, 1868, *Th. M. Fries* (M-0308452).—**Finland:** [*North Häme*]: Saarijärvi, Saarikylä, 6 viii 1947, *A. Koskinen* (M-0308453); Mahlu, Syväoja, 5 vii 1948, *A. Koskinen* (M-0308454); Mahlu, Lylymäki, 3 vi 1943, *A. Koskinen* (M-0308455). *South Häme*: Evo, 1874, *J. P. Norrlin* (M-0308457).—**Slovakia:** *Žilina Region*: Králova, Királyhegy hola, Teplička, *H. Lojca* (M-0308460).—**Czech Republic:** *Moravia*: Telč, 'Roštýnská obora', 550 m, 26 vi 1965, *A. Vězda* (M-0308459); Carpati, prope pagum Ostravice, 700 m, 24 viii 1964, *A. Vězda* (M-0308464).—**Romania:** *Transylvania*: ad ramulos abietum in regione Aragyes infra alpem Retyezát, c. 1500 m, 23 viii 1873, *H. Lojka* (M-0308461); *ibid.*, 9 viii 1873, *H. Lojka* (M-0308462); prope Thermas Herculis in Banatu, 16 ix 1872, *H. Lojka* (M-0308463).

Discussion

Our results clearly demonstrate the presence of two distinct species within the former *Toniniopsis subincompta*. The results obtained from phylogenetic and morphological analyses were congruent with species estimates for *T. subincompta* s. lat. using ABGD, PTP and GYMC. Based on the material examined, mainly from Eurasia, *T. separabilis* is the more common taxon (76.4%) and has the wider distribution range (Canada, Norway, Sweden, Estonia, Germany, Austria, Czech Republic, Slovakia, Romania, Turkey and Russia). *Toniniopsis dissimilis* is less frequent (23.6%) and specimens were examined from Norway, Sweden, Finland, Germany, Slovakia, Austria, Turkey and Russia. The latter species seems to be more cold-adapted as we have only seen specimens collected above 1000 m or in high latitudes.

According to the literature, the distribution of *T. subincompta* s. lat. extends to Macaronesia, Africa and North America (Ekman 1996; Llop 2007; Coppins & Aptroot 2009). Based on observations of specimens from North America by Ekman (1996), *T. subincompta* has the same variation in thallus structure as we observed in specimens from Eurasia. Apothecia are mainly dark, purple-brown to black, and the exciple rim has a single layer of enlarged globose lumina cells which correspond to Clade II but are smaller in size (5 × 8 µm). In some specimens, bacilliform ascospores were found in young apothecia, whereas acicular ascospores were found in old apothecia; a variation in spore shape may even occur within the same apothecium (Ekman 1996, loc. cit.). We found only bacilliform ascospores in all specimens except two, but looked mainly at middle-aged apothecia. The two exceptions with long acicular ascospores were JG053 (Murmansk Region) and the type specimen of *Lecidea bacillifera* f. *melanotica* (Finland). In addition, ascospores in northern American material are longer and thicker with a larger number of septa (19–64 × 1.9–6.2 µm, with 3–13 septa). Our observations correspond with those on *T. subincompta* from Great Britain and Spain (ascospores bacilliform, 20–36–40 × 2.3–3.5–4 µm, with 3–7 septa and 18–40 × 2–4 µm, with 3–9 septa, respectively (Llop 2007; Coppins & Aptroot 2009). A single herbarium specimen observed from Canada was determined to be *T. separabilis* with

characters corresponding to our description. Potentially, *T. subincompta* s. lat. from North America represents a separate entity to those from Eurasia. However, additional morphological and phylogenetic investigations are required.

In *T. subincompta* s. lat., an albino morph had already been mentioned by Coppins & Aptroot (2009). In order to test if dark and albino morphs belong to the same species, we sequenced both, a dark and an albino morph from bark of the same tree. According to our results, the two isolates belong to the same species but differ from each other in three genes. In fact, none of the sequences of dark morphs were identical to the albino morph, while identical sequences of dark morphs did occur. Further studies are required to find out if the albino morphs form a separate lineage or are formed independently by spontaneous mutation.

Cyanotrophy is defined as facultative or obligate association of lichens to free-living or ±lichenized cyanobacteria (Poelt & Mayrhofer 1988). We observed the strongest association with cyanobacteria in one of the type specimens, *Lecidea bacillifera* f. *melanotica* (*Gloeocapsa* sp. and *Nostoc* sp. (Fig. 5A, B & E)), which was assigned to *T. separabilis* in this study based on morphological observation. The strong cyanotrophic association appears to lead to a modification of the *melanotica* thallus, represented by black-coloured patches. Similarly, a strong connection was observed in two further herbarium specimens collected in Sweden (M-0308447 and M-0308450), which were associated with *Nostoc* sp. The most diverse composition of cyanobacteria was observed in JG151 (Oberallgäu), with species from three different genera: *Gloeocapsa, Nostoc* and *Scytonema*. Juvenile stages of some green-algal lichens may establish loose cyanotrophic associations with free-living cyanobacteria and/or cyanolichens (Rikkinen 2003). Such associations in *Ramalinaceae* are known in *Thalloidima* A. Massal., most species of which are parasitic on cyanolichens when young or remain parasitic (Kistenich *et al.* 2018). However, the specimens we analyzed were clearly associated with free-living cyanobacteria and were not cyanolichens. Previously, complementary associations with cyanobacteria in crustose lichens have mainly been described from saxicolous species, probably due to low nutrient levels in the substratum (Poelt & Mayrhofer 1988). However, all specimens with cyanobacteria of *T. separabilis* were collected on tree bark (*Picea* sp., *Populus* sp., *Salix* sp., *Thuja* sp. and *Ulmus* sp.). Cyanotrophy was observed only in *T. separabilis* and is considered to be facultative based on our observations that only 11 out of 68 specimens (including herbarium, type and sequenced specimens) examined were cyanotrophic (*c.* 16%). Albino morphs, which have been found in only four specimens of *T. separabilis* (*c.* 6%), were likewise not observed in specimens of *T. dissimilis*. These interesting aspects of lichen biology deserve further study.

Author ORCIDs. (ID) Julia V. Gerasimova, 0000-0002-3212-3596; Gennady P. Urbanavichus, 0000-0003-3222-5151; Irina N. Urbanavichene, 0000-0002-5492-5215; Andreas Beck, 0000-0003-2875-4464.

References

Beck A and Mayr C (2012) Nitrogen and carbon isotope variability in the green-algal lichen *Xanthoria parietina* and their implications on mycobiont-photobiont interactions. *Ecology and Evolution* **2**, 3132–3144.

Brackel W von (2019) *Rote Liste und Gesamtartenliste der Flechten (Lichenes), flechtenbewohnenden und flechtenähnlichen Pilze Bayerns. Stand 2019.* Augsburg: Bayerisches Landesamt für Umwelt.

Coppins BJ and Aptroot A (2009) *Bacidia* De Not. 1846. In Smith CW, Aptroot A, Coppins BJ, Fletcher A, Gilbert OL, James PW and Wolseley PA (eds), *Lichens of Great Britain and Ireland*. London: British Lichen Society, pp. 189–207.

Darriba D, Taboada GL, Doallo R and Posada D (2012) jModelTest 2: more models, new heuristics and parallel computing. *Nature Methods* **9**, 772.

Drummond AJ, Suchard MA, Xie D and Rambaut A (2012) Bayesian phylogenetics with BEAUti and the BEAST 1.7. *Molecular Biology and Evolution* **29**, 1969-1973.

Edgar RC (2004) MUSCLE: multiple sequence alignment with high accuracy and high throughput. *Nucleic Acids Research* **32**, 1792–1797.

Ekman S (1996) The corticolous and lignicolous species of *Bacidia* and *Bacidina* in North America. *Opera Botanica* **127**, 1–148.

Ekman S (2001) Molecular phylogeny of the *Bacidiaceae* (*Lecanorales*, lichenized Ascomycota). *Mycological Research* **105**, 783–797.

Fujisawa T and Barraclough TG (2013) Delimiting species using single-locus data and the Generalized Mixed Yule Coalescent approach: a revised method and evaluation on simulated data sets. *Systematic Biology* **62**, 707–724.

Gerasimova JV and Ekman S (2017) Taxonomy and nomenclature of seven names in *Bacidia* (*Ramalinaceae*, *Lecanorales*) described from Russia. *Phytotaxa* **316**, 292–296.

Gerasimova JV, Ezhkin AK and Beck A (2018) Four new species of *Bacidia* s.s. (*Ramalinaceae*, *Lecanorales*) in the Russian Far East. *Lichenologist* **50**, 603–625.

Gernhard T (2008) The conditioned reconstructed process. *Journal of Theoretical Biology* **253**, 769–778.

Gilbert O (1996) The occurrence of lichens with albino fruit bodies (Ascomata) and their taxonomic significance. *Lichenologist* **28**, 94–97.

Hoang DT, Chernomor O, von Haeseler A, Minh BQ and Le SV (2017 [2018]) UFBoot2: improving the ultrafast bootstrap approximation. *Molecular Biology and Evolution* **35**, 518–522.

Kalyaanamoorthy S, Minh BQ, Wong TKF, von Haeseler A and Jermiin LS (2017) ModelFinder: fast model selection for accurate phylogenetic estimates. *Nature Methods* **14**, 587–589.

Kistenich S, Timdal E, Bendiksby M and Ekman S (2018) Molecular systematics and character evolution in the lichen family *Ramalinaceae* (Ascomycota: *Lecanorales*). *Taxon* **67**, 871–904.

Liu YJ, Whelen S and Hall BD (1999) Phylogenetic relationships among ascomycetes: evidence from an RNA polymerase II subunit. *Molecular Biology and Evolution* **16**, 1799–1808.

Llop E (2007) *Lecanorales*: *Bacidiaceae*: *Bacidia* y *Bacidina*. *Flora Liquenológica Ibérica* **3**, 1–49.

Luo A, Ling C, Ho SYW and Zhu CD (2018) Comparison of methods for molecular species delimitation across a range of speciation scenarios. *Systematic Biology* **67**, 830–846.

Mark K, Cornejo C, Keller C, Flück D and Scheidegger C (2016) Barcoding lichen-forming fungi using 454 pyrosequencing is challenged by artifactual and biological sequence variation. *Genome* **59**, 685–704.

Meyer B and Printzen C (2000) Proposal for a standardized nomenclature and characterization of insoluble lichen pigments. *Lichenologist* **32**, 571–583.

Miller MA, Pfeiffer W and Schwartz T (2010) Creating the CIPRES Science Gateway for inference of large phylogenetic trees. In *Proceedings of the Gateway Computing Environments Workshop (GCE) 14 November 2010, New Orleans, Louisiana*, pp. 1–8.

Minh BQ, Nguyen MAT and von Haeseler A (2013) Ultrafast approximation for phylogenetic bootstrap. *Molecular Biology and Evolution* **30**, 1188–1195.

Nguyen LT, Schmidt HA, von Haeseler A and Minh BQ (2015) IQ-TREE: a fast and effective stochastic algorithm for estimating maximum-likelihood phylogenies. *Molecular Biology and Evolution* **32**, 268–274.

Nylander W (1854) Études sur les lichens d'Algérie. *Mémoires de la Société des Sciences Naturelles de Cherbourg* **2**, 305–344.

Nylander W (1865) Lecideae adhuc quaedam europeae novae. *Flora* (Regensburg) **48**, 145–148.

Poelt J and Mayrhofer H (1988) Uber Cyanotrophie bei Flechten. *Plant Systematics and Evolution* **158**, 265–281.

Pons J, Barraclough TG, Gómez-Zurita J, Cardoso A, Duran DP, Hazell S, Kamoun S, Sumlin WD and Vogler AP (2006) Sequence-based species delimitation for the DNA taxonomy of undescribed insects. *Systematic Biology* **55**, 595–609.

Puillandre N, Lambert A, Brouillet S and Achaz G (2011) ABGD, Automatic Barcode Gap Discovery for primary species delimitation. *Molecular Ecology* **21**, 1864–1877.

Rambaut A (2009) FigTree v.1.3.1. [WWW resource] URL http://tree.bio.ed.ac.uk/software/figtree/.

Rikkinen J (2003) Ecological and evolutionary role of photobiont-mediated guilds in lichens. *Symbiosis* **34**, 99–110.

Ronquist F, Teslenko M, van der Mark P, Ayres DL, Darling A, Höhna S, Larget B, Liu L, Suchard MA and Ronquist JP (2012) MrBayes 3.2: efficient Bayesian phylogenetic inference and model choice across a large model space. *Systematic Biology* **61**, 539–542.

Rose F and Coppins S (2002) Site assessment of epiphytic habitats using lichen indices. In Nimis PL, Scheidegger C and Wolseley PA (eds), *Monitoring with Lichens – Monitoring Lichens*. Dordrecht: Kluwer Academic Publishers, pp. 343–348.

Rücker T and Wittmann H (1995) Mykologisch-lichenologische Untersuchungen im Naturwaldreservat Kesselfall (Salzburg, Österreich) als Diskussionsbeitrag für Kryptogamenschutzkonzepte in Waldökosystemen. *Beihefte zur Sydowia* **10**, 168–191.

Stamatakis A (2014) RAxML version 8: a tool for phylogenetic analysis and post-analysis of large phylogenies. *Bioinformatics* **30**, 1312–1313.

Talavera G, Dincă V and Vila R (2013) Factors affecting species delimitations with the GMYC model: insights from a butterfly survey. *Methods in Ecology and Evolution* **4**, 1101–1110.

Turland NJ, Wiersema JH, Barrie FR, Greuter W, Hawksworth DL, Herendeen PS, Knapp S, Kusber W-H, Li D-Z, Marhold K, *et al.* (eds) (2018) *International Code of Nomenclature for Algae, Fungi, and Plants (Shenzhen Code) adopted by the Nineteenth International Botanical Congress Shenzhen, China, July 2017*. Glashütten: Koeltz Botanical Books.

Vainio EA (1922) Lichenographia fennica II. Baeomyceae et *Lecideales*. *Acta Societatis pro Fauna et Flora Fennica* **53**, 1–340.

White TJ, Bruns T, Lee S and Taylor JW (1990) Amplification and direct sequencing of fungal ribosomal RNA genes for phylogenetics. In Innis MA, Gelfand DH, Sninsky JJ and White TJ (eds), *PCR Protocols: a Guide to Methods and Applications*. New York: Academic Press, pp. 315–322.

Yule GU (1925) A Mathematical Theory of Evolution, Based on the Conclusions of Dr. J. C. Willis, F.R.S. *Philosophical Transactions of the Royal Society of London. Series B: Biological Sciences* **213**, 21–87.

Zahlbruckner A (1905) Ascolichenes. Lieferung 3. In Engler A and Prantl K (eds), *Die Natürlichen Pflanzenfamilien nebst ihren Gattungen und wichtigeren Arten insbesonderen den Nutzpflanzen 1 (1*)*. Leipzig: Engelmann, pp. 97–144.

Zhang J, Kapli P, Pavlidis P and Stamatakis A (2013) A general species delimitation method with applications to phylogenetic placements. *Bioinformatics* **29**, 2869–2876.

Zoller S, Scheidegger C and Sperisen C (1999) PCR primers for the amplification of mitochondrial small subunit ribosomal DNA of lichen-forming ascomycetes. *Lichenologist* **31**, 511–516.

Chapter 3

Four new species of *Bacidia* s.s. (Ramalinaceae, Lecanorales) in the Russian Far East

Julia V. Gerasimova, Aleksandr K. Ezhkin and Andreas Beck

Four new species of *Bacidia* s.s. (*Ramalinaceae*, *Lecanorales*) in the Russian Far East

Julia V. GERASIMOVA, Aleksandr K. EZHKIN and Andreas BECK

Abstract: The molecular phylogeny of *Bacidia* s.s. in the Russian Far East was investigated using 62 nucleotide sequences from the ITS nrDNA region, 22 of which were newly obtained. Phylogenetic reconstructions employed Bayesian inference and maximum likelihood searches using MrBayes and RAxML. In addition, ITS2 secondary structures added further support using Compensatory Base Changes. As a result of morphological and phylogenetic studies, four new species of *Bacidia* are described. *Bacidia areolata* sp. nov. belongs to the *suffusa* group. It was collected once in Khabarovskiy Krai, the Russian Far East, on the bark of *Acer tegmentosum* and is closely related to *B. suffusa* but differs in having a smooth, cracked to areolate thallus and shorter spores. *Bacidia elongata* sp. nov. is a member of the *fraxinea* group and is similar to *B. fraxinea* but differs in having a wide zone of cells with enlarged lumina along the edge of the exciple. In fact, this zone of enlarged cells, in combination with its overall habit, places it morphologically close to *B. suffusa*, *B. millegrana* and *B. campalea*. *Bacidia kurilensis* sp. nov. is a basal member of the *laurocerasi* group and closely related to *B. biatorina*, *B. heterochroa*, *B. laurocerasi* and *B. salazarensis*. However, the combination of a granular thallus, large black apothecia and a green hue in the upper part of the exciple edge as well as in the epihymenium sets it apart from the species mentioned above. *Bacidia sachalinensis* sp. nov. resolves as a strongly supported member of the *polychroa* group and is known from a single locality in Sakhalin, the Russian Far East. Its thallus structure and apothecium colour are variable, which is typical for the *polychroa* group, but it differs from *B. polychroa* by having shorter spores with fewer septa and a mainly smooth to areolate thallus.

Key words: *Bacidiaceae*, compensatory base changes, crustose lichens, diversity, ITS secondary structure, morphology, phylogenetic analysis

Introduction

The lichen flora of the Russian Far East has been investigated for more than a century (Brummitt 2001). In particular, Primorskiy Krai, the most south-eastern region of Russia, is comparatively well studied (Skirina & Moiseyevskaya 2004 and references therein). However, large areas and many lichen genera remain largely unexplored. One genus we know little about in this region is *Bacidia*. Previous reports of *Bacidia* from this area can be found in a number of lichen checklists and papers (Brotherus *et al.* 1936; Skirina 1995, 2015; Tchabanenko 2002; Galanina 2008; Kuznetsova *et al.* 2013).

Historically, *Bacidia* included crustose lichens with a chlorococcoid photobiont and biatorine apothecia producing ascospores that have at least three septa (Zahlbruckner 1921–1940). During the second half of the 20th century, *Bacidia sensu* Zahlbruckner was partially split up and numerous species were transferred to other taxa, resulting in the recognition of more than 20 genera (e.g. Santesson 1952; Vězda 1978, 1986, 1991; Hafellner 1984; Lücking 1992; Sérusiaux 1993; Ekman 1996).

The first phylogenetic study (Ekman 2001) indicated that many species referred to

J. V. Gerasimova: Komarov Botanical Institute of the Russian Academy of Sciences, Prof. Popova St. 2, 197376 St. Petersburg, Russia. Email: jgerasimova.lich@yandex.ru
J. V. Gerasimova and A. Beck: SNSB-BSM, Botanische Staatssammlung München, Menzinger Straße 67, D-80638 München, Germany.
A. K. Ezhkin: Institute of Sea Geology and Geophysics, Far East Branch of the Russian Academy of Sciences, Nauki St. 1B, 693022 Yuzhno-Sakhalinsk, Russia.
A. Beck: GeoBio-Center, Ludwigs-Maximilians-Universität München, Richard-Wagner-Str. 10, D-80333 München, Germany.

as *Bacidia*, in particular those with blue-green pigmentation in the epithecium and/or with fusiform or bacilliform spores, were more closely related to *Toninia* s.l. *Bacidia* in the strict sense is consequently characterized by acicular spores and a well-developed, prosoplectenchymatic proper exciple composed of radiating, abundantly furcate and rarely anastomosed hyphae with heavily gelatinized cell walls and cell lumina that become compressed and narrower with age. Since this first phylogenetic study, a limited set of *Bacidia* s.s. species have been investigated further (Andersen & Ekman 2005; James *et al.* 2006; Reese Næsborg *et al.* 2007; Jeon *et al.* 2009; Schmull *et al.* 2011; Sérusiaux *et al.* 2012; Miadlikowska *et al.* 2014; Mark *et al.* 2016; Lendemer *et al.* 2016).

We present here a taxonomic study of *Bacidia* s.s. using morphological and molecular data and focusing on material from the Russian Far East. In this area, members of the genus are abundant in habitats that have high humidity and moderate insolation. These include open forests, forest edges, swamps, river banks and valleys, as well as hill and mountain slopes close to the sea or near lakes or swamps. The aim of the present study was to clarify species boundaries in members of *Bacidia* s.s. from the Russian Far East.

Material and Methods

The material for this study primarily consisted of 83 fresh collections of *Bacidia* gathered in the field by the authors in the southern part of the Russian Far East (Primorskiy and Khabarovskiy Krai), as well as on Sakhalin and the Kurile Islands, from 2013 to 2015. All material was collected in old forest communities ranging from about sea level up to 1350 m. The forests were mainly in floodplains and were mixed conifer-broadleaf and spruce-fir forests in river valleys which were open with a high humidity. Herbarium material from the Pacific Institute of Geography (PIG, without acronym) and the Botanical Garden-Institute of FEB RAS (VBGI) was also studied. In order to confirm the taxonomic position of *Bacidia suffusa* (Fr.) A. Schneid. from the Russian Far East and verify the status of a specimen of that species from GenBank (AF282091), two additional specimens of *B. suffusa* and one specimen of *B. diffracta* S. Ekman that had been collected in North America were studied and sequenced. The type material of all species present in this study was analyzed. Voucher specimens were deposited in the herbaria of the Botanische

Staatssammlung München (M) and Komarov Botanical Institute RAS (LE). Detailed information of the newly obtained sequences together with their respective voucher information and GenBank Accession numbers are given in Table 1. GenBank Accession numbers additionally included in the phylogenetic analyses are given in Supplementary Table S1 (available online). Voucher information for all investigated specimens are given in Supplementary Table S2 (available online). Localities and herbarium numbers for all specimens investigated in the course of this study are given in the Supplementary Material (available online). As Japan is geographically close, we included species of *Bacidia* recorded in checklists of the lichens of Japan (Kashiwadani & Inoue 1993; Inoue 1994; Harada *et al.* 2004; see Table 2). *Bacidia arceutina* (Ach.) Arnold, *B. laurocerasi* (Delise ex Duby) Zahlbr., *B. polychroa* (Th. Fr.) Körb., *B. rosella* (Pers.) De Not., *B. rubella* (Hoffm.) A. Massal., *B. schweinitzii* (Fr.) A. Schneid. and *B. subincompta* (Nyl.) Arnold have been recorded before and not specifically from Japan and are therefore not included in Table 2.

Morphology

All specimens were examined using standard microscopic techniques following Ekman (1996). Microscopic observations were made using light microscopes and a Zeiss Axioplan microscope equipped with differential interference contrast. Micrographs of cross-sections were taken on a Zeiss Axio Imager microscope with an attached AxioCam MRc5 camera and processed with the Zeiss ZEN2012 image program. Images of the external features of the species were obtained from a Zeiss Stemi-2000 CS microscope with an attached AxioCam MRc5 camera and processed with the Zeiss AxioVision image program. The photomicrographs with detail of exciple structures in Fig. 4C were taken with a Zeiss AxioScope A1 compound microscope equipped with a Canon 60D digital camera. Spore and apothecium measurements are given as mean ($\bar{x}$) ± 1SD with outliers in parentheses. All other measurements are given as minimum, mean ($\bar{x}$) and maximum values. In those cases where not enough measurements were available for the calculation of a mean value, only minimum and maximum values are given.

DNA extraction, PCR amplification and DNA sequencing

DNA extraction was carried out using PCR Template Preparation Kit (Roche, Mannheim, Germany) following the manufacturer's instructions. 5–8 apothecia were used from fresh material not older than 3 years and thallus fragments were removed in order to minimize the risk of contamination.

PCR amplifications for the ITS1, ITS2 and 5.8S regions were performed using 5 µl 5× Green GoTaq® Flexi buffer, 1·75 µl MgCl$_2$, 2·5 µl dNTPs, 1·25 µl of each primer, 0·1 µl Taq polymerase and 1–5 µl of DNA solution in 25 µl volume. Cycling conditions included initial

TABLE 1. *Specimens used in the phylogenetic study of* Bacidia *together with their voucher information and GenBank Accession numbers.*

Specimen	Locality	Voucher	ITS GenBank Accession number
Bacidia areolata	Russia, Far East	*Gerasimova* M-0182592 (M)	MH048614
B. circumspecta	Russia, Far East	*Gerasimova* L-13006 (LE)	MH539764
B. diffracta	USA, Minnesota	*Wetmore* 46555-A (M)	MH048620
B. elongata	Russia, Far East	*Gerasimova* M-0182571 (M)	MH048626
B. elongata	Russia, Far East	*Gerasimova* M-0182625 (M)	MH048627
B. elongata	Russia, Far East	*Gerasimova* M-0182626 (M)	MH048628
B. elongata	Russia, Far East	*Gerasimova* M-0182627 (M)	MH048629
B. friesiana	Russia, Far East	*Gerasimova* L-13159 (LE)	MH539765
B. kurilensis	Russia, Far East	*Ezhkin* M-0182620 (M)	MH048610
B. kurilensis	Russia, Far East	*Ezhkin* M-0182621 (M)	MH048611
B. kurilensis	Russia, Far East	*Ezhkin* M-0182622 (M)	MH048612
B. laurocerasi	Russia, Far East	*Galanina* 424 (VBGI)	MH048609
B. rubella	Russia, Far East	*Gerasimova* M-0182581 (M)	MH048630
B. sachalinensis	Russia, Far East	*Ezhkin* M-0182619 (M)	MH048621
B. sachalinensis	Russia, Far East	*Ezhkin* M-0182623 (M)	MH048622
B. sachalinensis	Russia, Far East	*Ezhkin* SAK 147 (SAK)	MH048623
B. sachalinensis	Russia, Far East	*Ezhkin* SAK 148 (SAK)	MH048624
B. sachalinensis	Russia, Far East	*Ezhkin* M-0182624 (M)	MH048625
B. schweinitzii	Russia, Far East	*Gerasimova* M-0182580 (M)	MH048613
B. suffusa	USA, Louisiana	*Tucker* 17000 (M)	MH048618
B. suffusa	USA, Minnesota	*Wetmore* 40219 (M)	MH048619
B. suffusa	Russia, Far East	*Gerasimova* M-0182593 (M)	MH048616
B. suffusa	Russia, Far East	*Gerasimova* M-0182594 (M)	MH048617
B. suffusa	Russia, Far East	*Gerasimova* M-0182601 (M)	MH048615

denaturation at 95 °C for 2 min, 5 cycles of 95 °C for 45 s, 54 °C for 60 s and 72 °C for 60 s, 33 cycles of 95 °C for 45 s, 52 °C for 60 s and 72 °C for 60 s, with a final extension step at 72 °C for 7 min. We used the primers ITS1F (White *et al.* 1990) and ITS4m as described in Beck & Mayr (2012) or, for old herbarium specimens, primers ITS3 and ITS4 (White *et al.* 1990).

All PCR products were run on an agarose gel, cut out under UV-light and purified with the PCR Clean-Up & Gel Extraction Kit (SLG, Gauting, Germany). Purified products were labelled with the BigDye Terminator v3.1 Kit (Applied Biosystems, Darmstadt, Germany). Cycle sequencing consisted of 30 cycles of 95 °C for 10 s, 50 °C for 15 s and 60 °C for 3 min, using the PCR primers individually. Post-sequencing clean-up was performed using gel filtration with Sephadex G-50 Superfine (GE Healthcare, Uppsala, Sweden) following the manufacturer's protocol. Forward and reverse strand sequences were detected on an ABI 3730 48-capillary automatic sequencer (Applied Biosystems) and assembled using the program PhyDE (http://www.phyde.de/index.html).

Alignment and phylogenetic analyses

BLAST searches in GenBank were performed to detect and exclude accessory/lichenicolous fungi and potential contaminants. Alignments were carried out using standard settings in MUSCLE v.3.8.31 (Edgar 2004) as implemented in the program PhyDE and optimized by hand using the ITS2 secondary structures (see below) as a guide. Positions that possessed numerous indels and presented a nucleotide in less than 3% of the sequences as well as ambiguously aligned regions were excluded.

Two datasets were analyzed for this study. Using the first dataset, we aimed to ensure that the new sequences belonged to *Bacidia* s.s. and to examine the relationships of this genus within the broader context of the *Ramalinaceae*. This large dataset comprised 130 sequences that included: 1) the sequences of all representatives of former *Bacidiaceae* used in the publication by Ekman (2001); 2) all other ITS sequences of *Bacidia* as well as *Bacidina* available from GenBank (Groner & LaGreca 1997; James *et al.* 2006; Reese Næsborg *et al.* 2007; Jeon *et al.* 2009; Schmull *et al.* 2011; Czarnota & Guzow-Krzemińska 2012; Sérusiaux *et al.* 2012; Miadlikowska *et al.* 2014; Lendemer *et al.* 2016; Mark *et al.* 2016); 3) the ITS sequences of *Bacidia* s.s. generated in this study. The second dataset was restricted to *Bacidia* s.s. sequences, based on the results of the first analysis. This allowed the use of a larger part of the alignment because it did not contain ambiguous parts.

The ITS nrDNA sequence dataset was subjected to maximum likelihood (ML) and Bayesian inference (BI) analyses. To select the nucleotide substitution model and parameters for the ML searches, a statistical selection of best-fit models was carried out in jModelTest 2.1.5 (Guindon & Gascuel 2003; Darriba *et al.* 2012).

TABLE 2. Bacidia *species from Japan studied in this research for comparison with the newly described species from the Russian Far East.*

Name according to Japanese checklist*	Comments	Reference
Bacidia abducens (Nyl.) Zahlbr.	Currently: *Bacidia schweinitzii* (Fr. ex Tuck.) A. Schneid.	Ekman 1996: 99
B. akagiensis (Vain.) Yasuda	Apothecia blackish; spores fusiform-oblong, 16–24 × 4–5 μm, with 3 septa	Vainio 1921: 66
B. baculifera (Nyl.) Zahlbr.	Thallus whitish; apothecia convex, *c.* 0·5 mm diam.; spores bacilliform, 32–42 × 5–6 μm, with 1–7 septa	Nylander 1890: 67
B. beckhausii Körb.	Currently: *Biatora beckhausii* (Körb.) Tuck.	Printzen 2014: 451
B. endoleucula (Nyl.) Zahlbr.	Currently: *Bacidia laurocerasi* (Delise ex Duby) Zahlbr.	Ekman 1996: 82
B. hakkodensis Kashiw.	Apothecia pale brown to yellowish brown; spores oblong-ellipsoid, 27–35 × 5–6 μm, with 3–5(–7) septa	Kashiwadani & Sasaki 1987: 69
B. hakonensis (Müll. Arg.) Yasuda	Apothecia black; spores obovate-cylindrical, 20–35 × 7–10 μm, with 3–5 septa	Müller 1892: 198
B. invertens (Nyl.) Zahlbr.	Currently: *Bacidia laurocerasi* (Delise ex Duby) Zahlbr.	Ekman 1996: 82
B. leptoboliza (Nyl.) Zahlbr.	Belongs to *Lecanactis*	Printzen 1995: 190
B. luteorufula (Tuck.) Zahlbr.	Apothecia yellowish to orange; spores unicellular, ovoid, fusiform to ellipsoid, 5·0 × 2·5 μm	Tuckerman 1866 [1864]: 276
B. micrommata (Kremp.) R. Sant.	Currently: *Eugeniella micrommata* (Kremp.) Lücking, Sérus. & Kalb.	Lücking 2008: 716
B. myricicola (Vain.) Yasuda	Probably belongs to *Phyllopsora*	According to observation of S. Ekman [TUR-V 20326]
B. spumosula (Zahlbr. ex Yasuda) Yasuda	Apothecia black; spores unicellular, ellipsoid to oval, 11–13 μm × 7–8 μm	Yasuda 1925: 28
"*Bacidia subcontes* (Nyl.) Anzi"	Name doesn't exist; probably misspelling of *Bacidia subincompta*	
B. subdiscendens (Nyl.) Zahlbr.	Apothecia dark brown to blackish; hypothecium brown-black; spores acicular, 55–65 × 3 μm, with 7–9 septa	Nylander 1890: 67
B. subrudis (Nyl.) Zahlbr.	Apothecia blackish; epithecium yellow-brownish; spores oblong, 25–34 × 0·8–1·0 μm, with 3–7 septa	Nylander 1890: 64
B. subvermifera (Nyl.) Zahlbr.	Apothecia black; hypothecium blackish; spores vermiform, 30–40 × 3 μm, with 3–5 septa	Nylander 1900: 33
B. uvulina Zahlbr.	Apothecia black; spores vermiform, 27–36 × 1·6–3·5 μm, with uneven (up to 7) septa	Zahlbruckner 1916: 52
B. yasudae (Vain.) Yasuda	Belongs to *Micarea*	According to observation of S. Ekman [TUR-V 20783]

*Kashiwadani & Inoue 1993; Inoue 1993; Harada *et al.* 2004.

The optimal model was identical using either the corrected Akaike information criterion or the Bayesian information criterion (TIM2ef + I + G). The model provided estimations of equal nucleotide frequencies, a rate matrix with six different substitution types, assuming a heterogeneous rate of substitutions with a gamma distribution of variable sites (number of rate categories = 4, shape parameter a = 0·7160) and a proportion of invariable sites (pinvar) of 0·2781. Heuristic phylogenetic searches were conducted using 100 random addition sequence (RAS) replicates, tree bisection-reconnection branch swapping (TBR), saving all trees and collapsing branches with a maximum length equal to zero using PAUP* v4.0b10 (Swofford 2002). Due to the size of the dataset, the most likely phylogeny was calculated using PAUP* as this allows the use of a more extensive search option than for instance RAxML, which computes only an approximate log likelihood score of the alternative topology after subtree reinsertion (Stamatakis *et al.* 2008). However, support values were calculated in independent runs using RAxML and MrBayes to allow better comparability with other studies. Support values using a bootstrap search in PAUP* are indicated on the respective branches of the phylogeny.

Further ML analysis was performed using RAxML v8.2.4 on both datasets using 1000 rapid bootstrap pseudo-replicates, following a GTRGAMMA model of molecular evolution (Stamatakis 2014). Bayesian inference was carried out using the Markov chain Monte Carlo method (MCMC) using MrBayes v3.2.6 (Ronquist *et al.* 2012). As the model recommended by jModelTest (TIM2ef + I + G) is not available in MrBayes, the GTRGAMMA model was selected instead based on the recommendation of Huelsenbeck & Rannala (2004). Two parallel runs were performed (two cold chains) with a single tree saved every 100th generation for a total of 10 000 000 generations. As convergence was reached after 25% of the trees, the initial 25% was discarded as burn-in and the results summarized as a 50% majority-rule consensus tree.

The phylogenetic trees were visualized using FigTree v1.4.2 (Rambaut 2009). Only clades that received bootstrap support ≥70% in ML and PP ≥0·95 in BI were considered highly supported.

ITS secondary structures

As additional evidence, we further analyzed ITS2 secondary structure, using compensatory base changes (CBCs) and hemi-CBCs in the structurally conserved regions of helix III (Coleman 2003). CBCs are mutations that occur in a primary RNA transcript, whereby both nucleotides paired in the secondary configuration of the ITS transcript mutate so that their bond is retained (e.g. G-C mutates to A-U). A hemi-CBC (hCBC) is the mutation of one of the two nucleotides while maintaining the nucleotide bond. Most likely ITS2 secondary structures of the RNA transcript were determined by delimiting the highly conserved start and end region of the first three helices. The structure of these sequence sections was deduced using the RNAfold web server (http://rna.tbi.univie.ac.at/cgi-bin/RNAfold.cgi), folding helices I, II, III and IV individually and therefore more reliably. In all cases we used the minimum free energy (MFE) structure obtained. The depictions of ITS2 secondary structure were made for morphologically close species of *Bacidia* s.s., corresponding to the species groups as indicated on the phylogenetic tree. Comparisons among sequences from each group are shown, using the entire ITS2 structure of one species per group as a "core" and indicating nucleotide substitutions on this core. The following sequences have been used as core: *Bacidia rubella* (GenBank, AF281087) for *Bacidia fraxinea* group, *B. laurocerasi* (AF282080), *B. polychroa* (AF282089), and *B. suffusa* (MH048616) for respective groups.

Results

Morphology

Ten species of *Bacidia* s.s. were distinguished based on morphological analysis, including the previously described *Bacidia* *friesiana* (Hepp) Körb., *B. rubella* (Hoffm.) A. Massal., *B. laurocerasi* (Delise ex Duby) Zahlbr., *B. polychroa* (Th. Fr.) Körb., *B. schweinitzii* (Fr.) A. Schneid. and *B. suffusa* (Fr.) A. Schneid. As no name was available for four morphologically distinct entities, *B. areolata*, *B. elongata*, *B. kurilensis* and *B. sachalinensis* are described as new. In addition, *B. schweinitzii* is reported from Russia for the first time.

The revision of all available herbarium collections (172) resulted in a new determination for some specimens. A specimen of *B. arceutina* (Ach.) Arnold, previously reported from a single locality in Kamchatka (Neshataeva *et al.* 2004), was identified as *B. laurocerasi*. Specimens from our own collections, initially described as *B. fraxinea* Lönnr., were finally determined to be *B. elongata* sp. nov. One herbarium specimen (PIG 28798), previously labelled as *B. fraxinea* and which was old with a damaged thallus, had several apothecia with only a few spores with uneven septa. We were unable to differentiate this species from the closely related *B. rubella*, consequently its identification is uncertain. The herbarium specimens of *B. biatorina* (Körb.) Vain. (e.g. Galanina 2008; Skirina 2015) were redetermined as *B. schweinitzii*, *B. friesiana* or as belonging to *Bacidia* s.l. Therefore, the occurrence of *B. biatorina* in the Russian Far East also remains questionable. The specimen of *B. rosella* (Pers.) De Not., previously reported from a single locality (Yakovchenko *et al.* 2013), is related to *B. suffusa*. In conclusion, there are four species, *B. arceutina*, *B. biatorina*, *B. fraxinea* and *B. rosella*, which should probably not be included in the list of *Bacidia* s.s. that occur in the Russian Far East.

Detailed morphological examination was carried out for previously sequenced specimens belonging to *B. diffracta*, *B. polychroa* and *B. suffusa* (GenBank AF282090, AF282089, AF282091) and these were compared with specimens from the Russian Far East.

Based on morphological studies, it should be noted that the new species are characterized by variations in thallus structure and apothecium colour, which is characteristic of

the whole genus (Ekman 1996). Features of Far Eastern species are summarized in Table 3 including, for comparison, all morphologically similar species.

Phylogeny

The first alignment of the larger dataset comprised 130 sequences and 485 characters. *Tylothallia biformigera* was selected as outgroup. The new specimens of *Bacidia* from the Russian Far East were shown to belong to *Bacidia* s.s. However, three specimens of *Bacidia* sp. from GenBank (KX098339, KX098340 and KX098341) were found to belong to the *Bacidina* group and were therefore not included in the subsequent analyses.

The second alignment of the reduced dataset contained 62 sequences (including 22 obtained for this study) and 481 characters, with *Bacidia incompta*, *Biatora globulosa*, *B. hemipolia* and *Cliostomum griffithii* as outgroups. This dataset contained 20 Operational Taxonomic Units (OTUs) of *Bacidia* s.s.

The ML and BI analyses recovered highly concordant topologies of the phylogenetic trees. Only the phylogeny resulting from the ML search in PAUP⋆ is presented here as there were no contradictions in supported parts of the trees.

The backbone within *Bacidia* s.s. is poorly resolved; only species groups were recovered with significant support values but the relationships between these are unclear. As a result of the phylogenetic analyses, a number of well-supported clades can be recognized within the *Bacidia* s.s. clade (Fig. 1).

Bacidia polychroa, *B. diffracta* and *B. sachalinensis* belong to a highly supported *polychroa* group (ML/BI: 98/1·0) and split into two main clades, with *B. sachalinensis* as sister to the other species. Two sequences of *B. diffracta* specimens group together with GenBank sequences of *B. suffusa* from the USA (AF282091) in a supported clade (92/0·99). Given that *B. sachalinensis* is recovered as a strongly supported group, as well as its morphological differences, it is described here as a species new to science.

Sister to the *polychroa* group is a group including *B. elongata*, *B. fraxinea* and *B. rubella* (74/0·99). The last two form a clade (82/0·98), with the position of *B. rubella* remaining uncertain. In addition, as only one sequence of *B. fraxinea* was included in the analysis, we consider this group needs further work using a larger number of samples. Specimens of *B. elongata* sp. nov. form a monophyletic group with strong support (100/0·99).

Bacidia laurocerasi, *B. biatorina* and *B. kurilensis* form a strongly supported clade (100/1·0), the *laurocerasi* group (Fig. 1). Within this group, another strongly supported clade (100/1·0) includes *B. laurocerasi* sequences from the Russian Far East (MH048609) and North America (GenBank AF282078). A second clade within this group contains *B. biatorina*, and a third is composed of three sequences of *B. kurilensis* sp. nov. with high support (76/1·0). *Bacidia biatorina* was placed as sister to *B. kurilensis* in the heuristic search using PAUP⋆, but without support. In contrast, *B. biatorina* is sister to *B. laurocerasi* in RAxML and BI with strong support (95/1·0). In all analyses the relationships within the *schweinitzii* group are only weakly supported, require further investigation and are not discussed here.

Bacidia suffusa and *B. areolata* form a strongly supported group (98/1·0). Sequences of *B. suffusa* were split into two main lineages: Far Eastern populations (100/1·0) and those from North America (98/0·96). The sequence representing *B. areolata* sp. nov. was placed as sister to *B. suffusa*, forming a separate branch and described here as new to science.

There are sequences of several other species of *Bacidia* available which were included in the phylogeny but which were not found in the Russian Far East. An example is *B. absistens* (Nyl.) Arnold which is so far known from a single locality in European Russia (Gerasimova 2016). *Bacidia lutescens* Malme and *B. hostheleoides* (Nyl.) Zahlbr. belong to a well-supported clade with long branches and both of which are widely distributed in the Neotropics (Malme 1935; Ekman 1996). Species of the highly
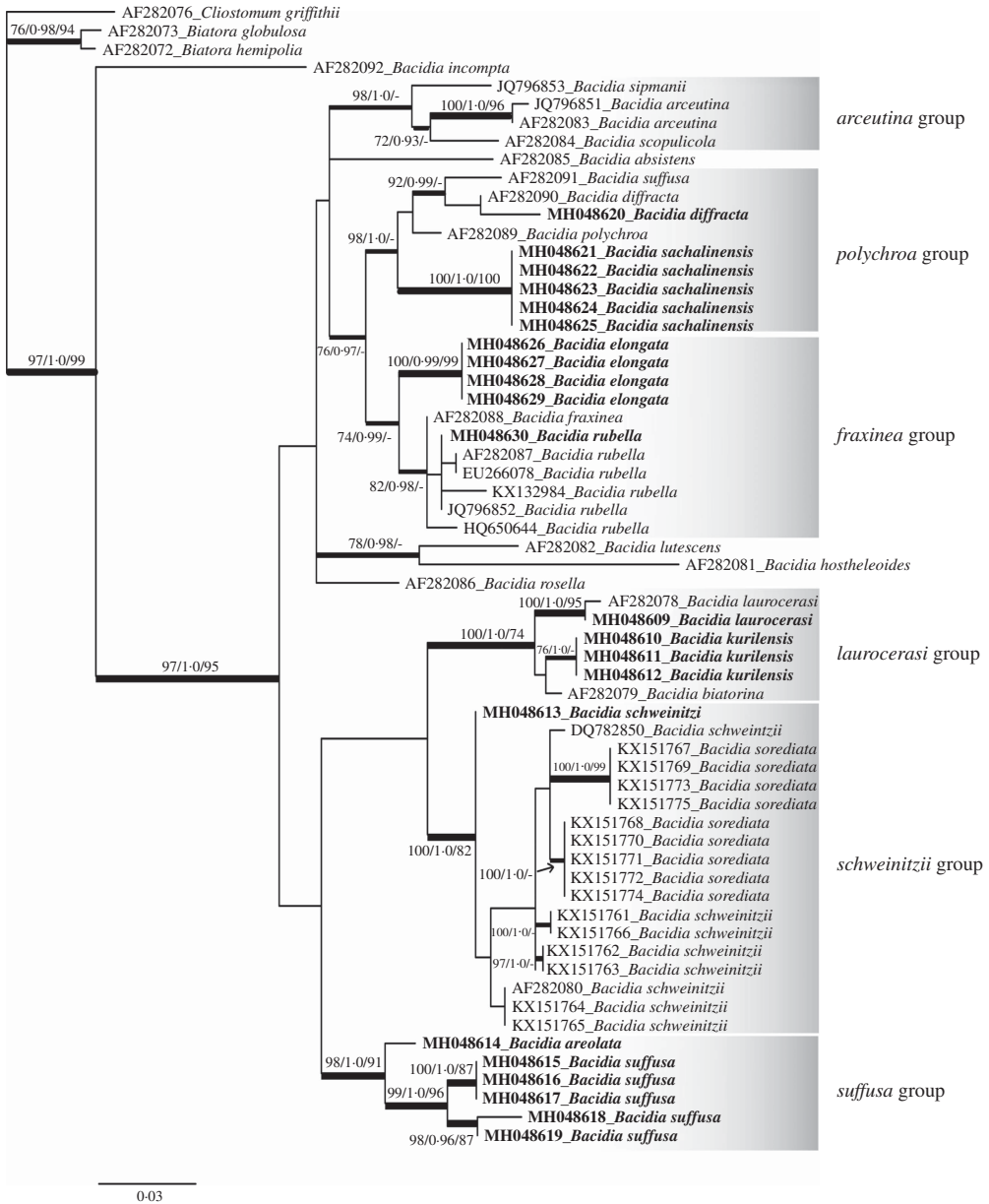
FIG. 1. The most likely tree generated by phyological analysis of ITS1 and ITS2 regions and 5.8S gene in PAUP★ ML analysis and representing the phylogenetic relationships of *Bacidia* s.s. Bootstrap support ≥70% in RAxML analysis (first value), posterior probability ≥0·95 (second value) and ≥65% bootstrap support in ML analysis by PAUP★ (third value) were considered as highly supported and denoted by very thick lines. Support values between 50 and 70% were considered as weakly supported and are indicated by lines of medium thickness. New sequences are in bold.
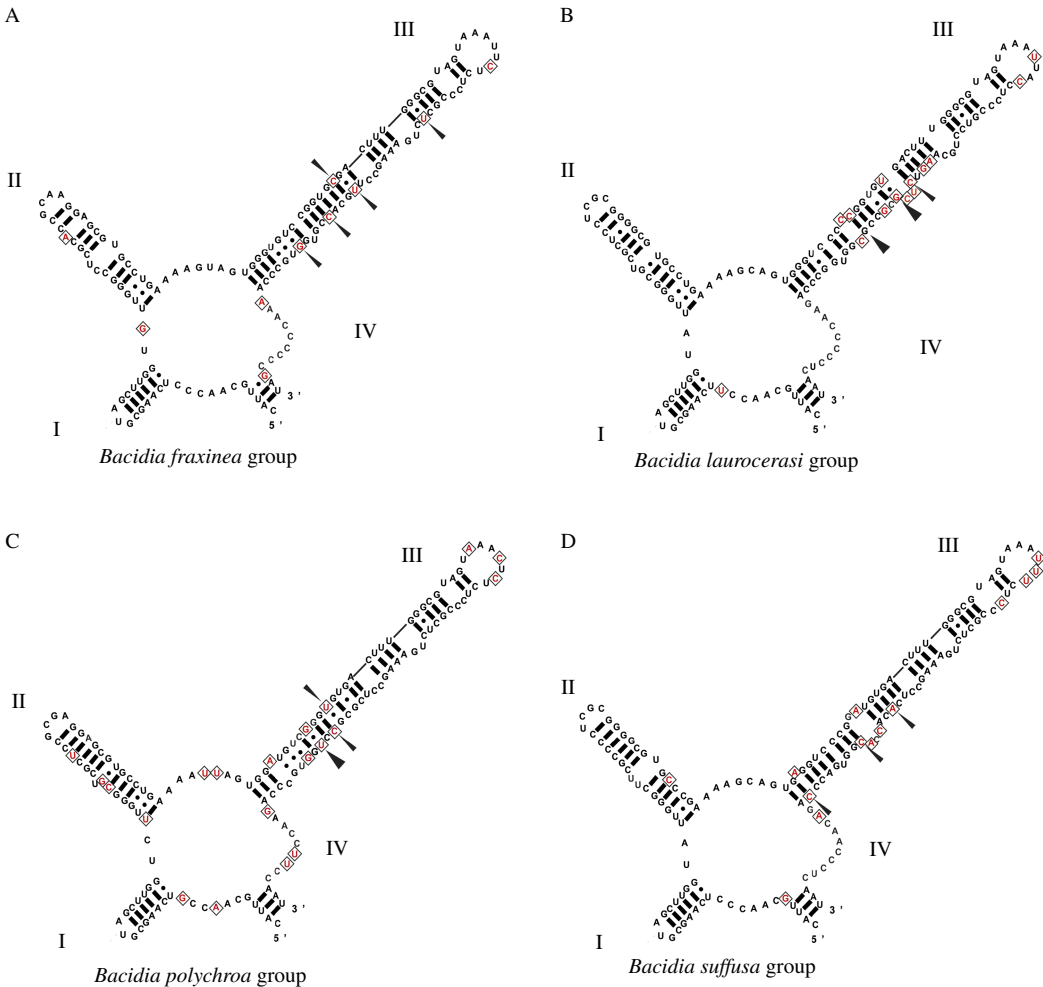
FIG. 2. Differences in secondary structure of ITS2 among groups within *Bacidia* s.s. Variable nucleotides among species within the groups are marked with diamonds, CBCs and hemi-CBCs are indicated by broad and narrow arrows, respectively.

supported *arceutina* group, including *B. sco-pulicola* (Nyl.) A.L. Sm. and *B. sipmanii* M. Brand *et al.*, are also not present in the Russian Far East. As mentioned above, the occurrence of *B. rosella* in the Russian Far East also remains questionable.

ITS secondary structure

Differences in the ITS2 secondary structure support all main groups of *Bacidia* s.s. and the

different lineages within the clades (Fig. 2), often involving CBCs and hemi-CBCs in the structurally conserved regions of helix III. By comparison, helices I, II and IV show only minor variation between groups and clades.

The four newly described species are supported by differences in their ITS2 secondary structure, mainly in hemi-CBCs. Thus, by comparison with the core (*Bacidia suffusa*, GenBank MH048616), *B. areolata* differs from *B. suffusa* and *B. elongata* by the

presence of three hemi-CBCs, and from *B. fraxinea* by five hemi-CBCs (Fig. 2D & A). *Bacidia sachalinensis* differs from *B. polychroa* by one CBC, G–U instead of C–G (Fig. 2).

Bacidia kurilensis differs from *B. laurocerasi* by two CBCs and one hemi-CBC in the conserved part of helix III (U–G instead of C–U, and C–G instead of G–U, respectively; Fig. 2C). *Bacidia biatorina* differs from *B. laurocerasi* by one CBC, where a U–A pairing was observed instead of G–C in the latter.

The ITS2 secondary structures in the *schweinitzii* group correspond to the clades in the trees. The two subclades of *B. sorediata* differ by one hemi-CBC, but in the case of the first group (including KX151767 etc.) there is an unpaired A–G that would reveal the presence of one CBC. Several *schweinitzii* subgroups form sister clades, but without support, while ITS2 secondary structure supports this grouping, based on three hemi-CBCs in helix III. These ITS secondary structure subgroups are comprised of: AF282080, KX151764 & KX151765; KX151761 & KX151766; DQ782850, KX151762 & KX151763, and a separate lineage of MH048613 from the Russian Far East.

The comparisons within the *lutescens-hostheleoides* "group" reveal one CBC and three hemi-CBCs in helix III as compared to the other groups. This "group" is very diverse with high nucleotide variation in the other helices and many specimens have not yet been sequenced.

Discussion

Since the first phylogenetic study, more than 50 additional ITS sequences of *Bacidia* s.s. have been added to GenBank, including the sequences obtained in this study. This has enabled the phylogeny of *Bacidia* s.s. to be refined and has made possible a better interpretation in the wider context. Phylogenetic relationships within *Bacidia* s.s. agree with the previous results presented by Ekman (2001), with the exception of the *lutescens-hostheleoides* "group" which is not considered to be a natural group. It has an uncertain

position with weak support. Both taxa have sequences that have evolved a great variety of nucleotides, which was demonstrated particularly in ITS2 secondary structure (see Results). This indicates that the grouping in this part of the phylogeny most likely results from incomplete species sampling rather than from a natural relationship. Thus long-branch attraction artefacts may occur and further sampling in this group is required to draw reliable conclusions.

Our study indicates that much of the diversity within *Bacidia* s.s. still needs to be investigated. Of the ten species found in the Russian Far East, four were not known from geographically close areas and thus are new to science. Table 2 provides a comparison of *Bacidia* species from Japan with those newly described species from the Russian Far East. The additional study of ITS2 has distinguished and supported all main groups of the genus. Despite a number of well-supported clades being recognized, the backbone within *Bacidia* s.s. remains poorly resolved. To overcome this problem and the relationships among the groups, sequences from additional loci are needed for follow-up studies.

Bacidia polychroa group

All species within the *polychroa* group share the K+ purplish/violet reaction in cross-sections of apothecia. The morphology of *B. polychroa* was first examined in a broad sense, including "typical" *B. polychroa*, granular *B. diffracta*, the specimen from GenBank first identified as *B. suffusa* (AF282091), and specimens from the Russian Far East initially identified as "*Bacidia polychroa* sp." The European specimen of *B. polychroa* from GenBank (AF282089), which was placed as a sister to *B. diffracta* (Fig. 1), was a typical morph and consequently corresponds to the type of *B. polychroa*. The *B. polychroa* typical morph is characterized by a wrinkled to warted thallus of scattered or contiguous areoles that become finally granular. It has orange-brown to dark red-brown apothecia with a distinct orange-brown hypothecium which is darker than the exciple below. *Bacidia sachalinensis*

has a mainly cracked to areolate thallus and lighter orange to orange-brown apothecia which is also characteristic of the North American morph of *B. polychroa* (see Table 3). The separation of *B. sachalinensis* from *B. polychroa* is also supported by hemi-CBCs in the ITS2 secondary structure and a low similarity of the sequences (94%).

Two species belonging to *B. diffracta* and a misidentified specimen of *B. suffusa* from North America (AF282091) present two distinct morphotypes. The specimen previously referred to *B. suffusa* is probably a separate species which is more closely related to *B. diffracta*. However, it represents an intermediate form between *B. diffracta* and *B. polychroa* and is characterized by a smooth, partly granular thallus and orange-brown to purplish brown apothecia as well as the typical K+ violet reaction (see Table 3). This could mean that either the European and North American specimens of *B. polychroa* are different species or simply that the lineage sorting is not complete between *B. diffracta* and *B. polychroa*. Both representatives of the granular forms of *B. diffracta*, AF282090 and MH048620, are similar to one another. The sequences reveal differences between them but, as only one specimen of each has been analyzed, they are treated here as a single species.

Bacidia sachalinensis exhibits substantial variation in thallus structure and apothecial colour, even in the same specimen, and this is also typical for both *B. diffracta* and *B. polychroa*. To study whether *B. polychroa* from the Far East was close to *B. polychroa* in a strict sense, we obtained several additional sequences from Far Eastern specimens, using as much variation in thallus and apothecial structure as possible with the intention of using these characters to delimit species. Despite this variation, all specimens examined in the phylogenetic analyses were found to belong to *B. polychroa* s.s. Only a single European specimen of *B. polychroa* (Sweden) and material from Sakhalin were included in the current analyses. Further study is required using collections from other parts of Europe, the Far East and North America to reveal the heterogeneity of this group.

Bacidia fraxinea group

Bacidia fraxinea and *B. rubella* represent two morphologically well-distinguished species, differing mainly in thallus structure (Ekman & Nordin 1993). Our dataset is not yet sufficient to make conclusions about the relationship between these morphospecies. Currently there is not enough evidence to challenge the recognition of *B. rubella* and *B. fraxinea* as distinct species because only one sequence of *B. fraxinea* is available. Further work is necessary here, so we recommend retaining the morphologically differentiated species.

Bacidia elongata represents a morphologically discrete, monophyletic entity, distinct from *B. fraxinea* mainly in its exciple structure. Consequently, it is here described as a new species. It falls close to the *fraxinea* group but the zone of enlarged cells (Fig. 3C) is characteristic for *B. elongata* and is rather exceptional. There are several species of *Bacidia* with a zone of enlarged cells such as *B. russeola* but it is closely related to *B. laurocerasi* (*laurocerasi* group) and *B. heterochroa*. We suggest that this zone of enlarged cells is a character which has evolved more than once and *B. elongata* is the first example known in the *fraxinea* group. These morphological differences are also supported by the low similarity of sequences (93–95%) and hemi-CBCs in the ITS2 secondary structure.

Bacidia laurocerasi group

Bacidia laurocerasi from the Russian Far East is placed as sister to the specimen for the USA on a zero-length branch, which confirms its identification (Fig. 1). Furthermore, morphological analysis has shown that *B. laurocerasi* from the Far East represents the "typical" form, corresponding to *B. laurocerasi* subsp. *laurocerasi* as detailed by Ekman (1996). This form is characterized by a poorly defined smooth thallus, black apothecia and brown epihymenium and exciple edge. In contrast, the four sequences of the new species *B. kurilensis*, sister to *B. laurocerasi*, reveal a morphologically discrete entity, characterized by a granular thallus and a greenish pigment in the epihymenium and

TABLE 3. *Main diagnostic features of the Russian Far Eastern species of* Bacidia s.s., *including several morphologically close species for comparison. Morphologically similar groups are indicated by grey or white banding.*

| Species of *Bacidia* | Thallus | Apothecium | | Exciple | | Hymenium (µm) | Epithecium | Hypothecium | Spores (µm) | *Pigments, K+/− |
		Colour	Pruina	Rim	Cell layer along rim					
diffracta	granular	brown-orange to dark purplish brown	+/−	brown-orange to orange-brown	absent	68–97	indistinctly coloured, colourless to orange-brown	pale brown-orange to orange-brown	32–69 × 1·9–4·1, with 3–11 septa	most pigmented parts K+ purple-red
suffusa (GenBank)	smooth to cracked to wrinkled	orange, orange-brown to purple-brown	+/−	laterally orange-brown	with 1–2 cell layers	62·5–67·5	pale orange to orange-brown	orange	32·5–51·0 × 1·7–3·0, with 3–7 septa	most parts K+ int. or brown part of K+ purplish
polychroa	cracked to areolate	brown-orange to dark purplish brown	+/−	brown-orange to orange-brown	without or with single cell layer up to 9 × 5 µm	56–102	colourless to orange-brown	±brown-orange to dark brown	31–74 × 1·9–5·0, with 2–15 septa	most pigmented parts K+ purple-red
sachalinensis	cracked to areolate to warted	pale orange to red-brown, rarely dark	+/−	pale brown to orange-brown	1–2 cell layers up to 8 × 7 µm	70·0–92·5	indistinctly coloured, colourless to orange-brown	pale brown-yellow to brown-orange	36·7–63·5 × 2·0–4·0, with 1–8 septa	most pigmented parts K+ purple-red
biatorina	granular	orange-brown to dark purplish brown	−	orange-brown to dark red-brown	1–2 cell layers up to 12 × 6 µm	83–87	brown-orange to red-brown	almost colourless	42–57 × 2·1–2·9, with 3–15 septa	pigmented parts exciple and epithecium K± int./K+ purplish
heterochroa	smooth, areolate, rimose	purple-brown to black	+/−	brown to red-brown	1 cell layer up to 6 µm wide	75–115	brown	colourless or pale yellow	32–73 × 2·5–4·3, with (3–)7–15 septa	pale yellow K+ int. or brown parts K+ purplish
kurilensis	granular to granular isidiose	reddish brown to almost black	−	dark brown with greenish hue	single cell layer up to 6 × 5 µm	80·0–107·5	dark brown with a dirty green hue	almost colourless to pale yellow	41–88 × 2·0–4·0, with 3–17 septa	pigmented parts K± int.

TABLE 3 (*continued*).

| Species of *Bacidia* | Thallus | Apothecium | | Exciple | | Hymenium (μm) | Epithecium | Hypothecium | Spores (μm) | *Pigments, K+/− |
		Colour	Pruina	Rim	Cell layer along rim					
laurocerasi	smooth to wrinkled to warted	purple-brown to purple-black	−	dark red-brown to black-brown	single cell layer up to 9 × 6 μm	71–131	dark brown	yellowish	50–108 × 1·9–3·7, with 7–28 septa	brown parts K+ purplish
salazarensis	crustose, ± rimose	black	+/−	red-brown sometimes with green in upper part	1 cell layer up to 6 μm wide	60–80	green	colourless to pale yellow	34–60 ×2·5–4·0, with 5–7 septa	pale yellow parts K+ int. or red-brown parts K+ purplish
areolata	smooth to areolate	pale pink to purple-brown	+/−	yellow to brown-orange	3–4 cell layers up to 12 × 6 μm	56·5–90	pale orange to orange-brown	pale yellow, almost colourless	40–82 × 2·5–4·5, with 6–15 septa	most pigmented parts K+ int.
elongata (dark morph)	wrinkled to granular	dark orange-brown to dark purple-brown	+/−	dark orange-brown	4 cell layers up to 20·0 × 5·5 μm	62·5–110·0	pale yellow, pale orange, rare brown-orange	pale yellow-brown to orange-brown	39–80 × 2·0–4·0, with 2–16 septa	brown parts K+ purplish, yellow K+ int.
suffusa	smooth, wrinkled to warted	yellow-brown to purplish to black	+	pale yellow to black-brown	4–6 cell layers up to 12 × 6 μm	77·5–137·5	yellowish	pale yellow to black-brown	40–95 × 2·5–5·0, with 6–17 septa	yellow to orange parts K+ int.
elongata (pale morph)	smooth to areolate	orange to orange-brown	+/−	pale orange-brown	4 cell layers up to 20·0 × 5·5 μm	62·5–110·0	colourless	pale yellow, almost colourless	39–80 × 2·0–4·0, with 2–16 septa	K −
fraxinea	smooth to areolate	orange-brown to darkbrown	+/−	straw to pale orange	without or with 1 cell layer up to 6 × 6 μm	76–103	colourless to straw	pale orange, straw	42–109 × 2·5–4·3, with 3–17 septa	pigmented parts K+ int.

*int. = intensifying
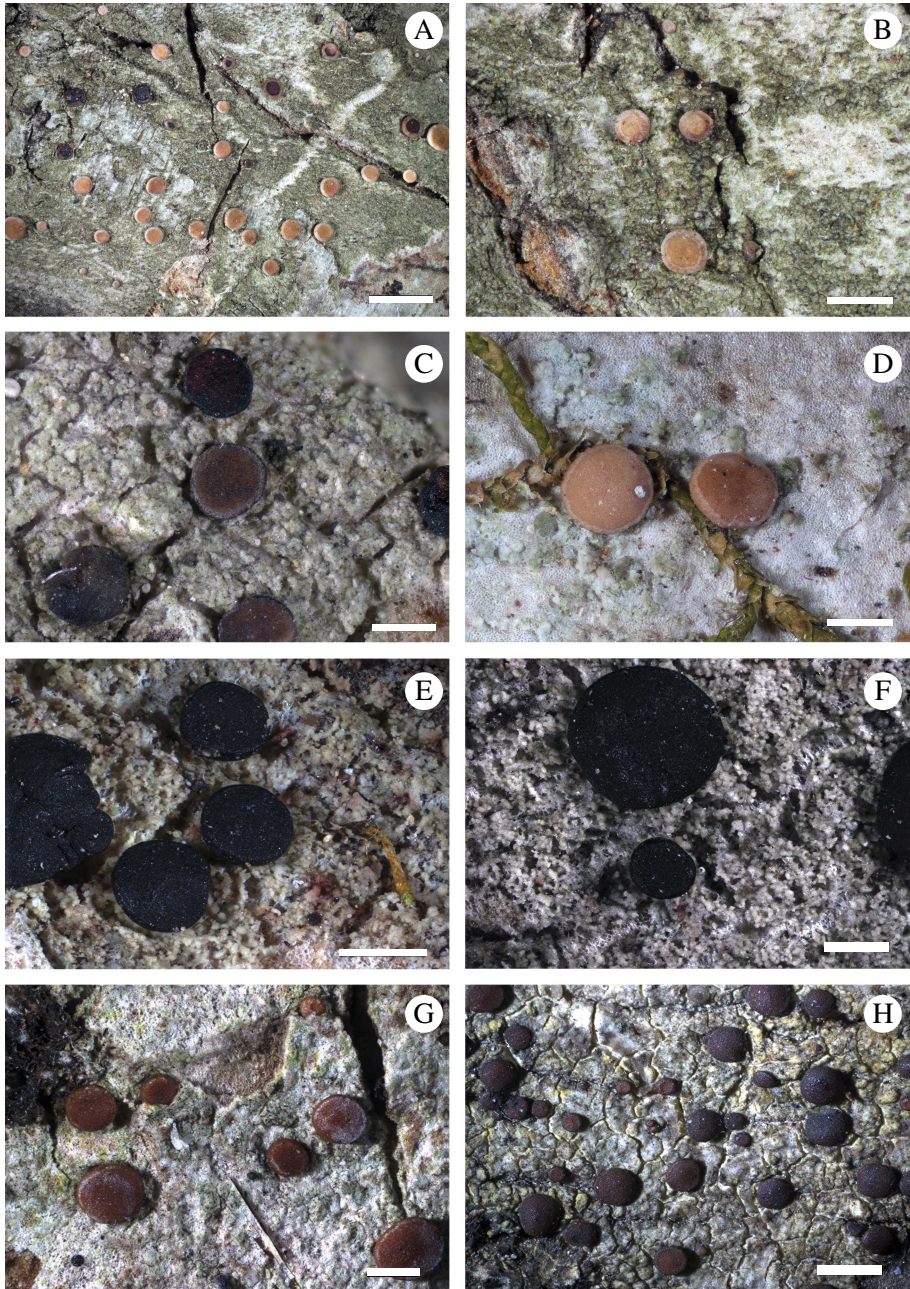
FIG. 3. New species of *Bacidia* from the Russian Far East. A & B, *Bacidia areolata*, holotype (M-0182592). C, *B. elongata*, dark morph, Primorskiy Krai (M-0182625). D, *B. elongata*, light morph, Khabarovskiy Krai, holotype (M-0182571). E & F, *B. kurilensis*, Kurile Island, holotype (M-0182620). G & H, *B. sachalinensis*, Sakhalin, holotype (M-0182619); G, smooth to warted thallus with light apothecia; H, cracked thallus with dark apothecia. Scales: A–G = 0·5 mm; H = 1·0 mm. In colour online.

upper part of the exciple (for details see Taxonomy). These morphological differences are also supported by the low similarity of the sequences (95%) and hemi-CBCs in the ITS2 secondary structure. The green pigmentation in the upper part of the hymenium in *B. kurilensis* is similar to that of *B. heterochroa* and *B. salazarensis* B. de Lesd., which also has a granular thallus. Neither *B. heterochroa* nor *B. salazarensis* were represented in this phylogenetic study.

Bacidia schweinitzii group

This group comprises *B. schweinitzii* and *B. sorediata* Lendemer & R.C. Harris. Specimens of the *schweinitzii* group were recovered in multiple clades within both *B. schweinitzii* s.s. (i.e. esorediate populations) and the sorediate morphotype (*Bacidia sorediata*), in accordance with the findings of Lendemer *et al.* (2016). The sequence from the Russian Far East specimen is placed basal to all other members of that group, but without significant support (59/0·93). In spite of this, according to Lendemer *et al.* (2016), *B. schweinitzii* from the Far East belongs to *B. schweinitzii* s.s. It is characterized by a granular thallus, black apothecia, blue-green pigmentation in the epihymenium and a dark reddish brown hypothecium. The specimen from GenBank (AF282080) was also obtained from a typical *B. schweinitzii* with a granular thallus and black apothecia. The internal branches in the *schweinitzii* s.l. part of the tree do not have significant support for the most part, leaving any relationships within this group unclear.

Bacidia suffusa group

The final group of the tree combines two morphologically indistinct lineages of *B. suffusa* from the Russian Far East and from North America. Both have characters which correspond with those of type material and can be referred to as the typical morph (Table 3). They probably represent different populations or cryptic species which can be separated geographically. Owing to the lack of good morphological characters, they are treated here on the population level. Although *B. areolata* is represented by only one sequence, there is quite strong morphological evidence for considering it to be a discrete species. Moreover, this is also supported by a low similarity of the sequences (92%) and hemi-CBCs in the ITS2 secondary structure. There are three hemi-CBCs between *B. suffusa* (Fig 2D) and *B. areolata* (not shown), and these are located in the most conserved region of helix III (Coleman 2009).

Taxonomy

Bacidia areolata J. Gerasimova & A. Beck sp. nov.

MycoBank No.: MB 821184

Similar to *Bacidia suffusa* but distinguished mainly by an areolate thallus and lighter-coloured apothecia.

Type: Russia, Khabarovskiy Krai, Khabarovskiy Rayon, Bolshekhekhtsirskiy State Natural Reserve, 48° 25′N, 134°77′E, 160 m, coniferous-broadleaf forest, on a terrace above the river, on bark of *Acer tegmentosum*, 6 September 2013, *J. V. Gerasimova* s. n. (M M-0182592—holotype; LE L-13014, UPS L-721140—isotypes). GenBank Accession no: MH048614

(Figs 3A & B, 4A & B)

Thallus poorly defined, either thin, partly smooth to areolate, of scattered, discrete or contiguous, flattened or ±convex areoles, or thick, continuous, wrinkled to warted; never with distinct granules; white, greyish green to deep green. *Prothallus* present between discrete areoles, white or rarely black along the border of the thallus. *Photobiont* chlorococcoid green alga, 6–15 × 8–18 µm.

Apothecia (0·3–)0·4–*0·5*–0·6(–0·9) mm, ±plane when young, remaining plane when mature or becoming slightly convex, epruinose, rarely with thin white pruina on the edge and disc of young and medium-aged apothecia. *Disc* pale pink, peach-coloured, pale beige to pale brown, rarely purple-brown when mature, often mottled. *Margin* pale pink, yellow-brown, raised above disc in young apothecia, later becoming ±plane. *Exciple* laterally 49·0–*60·4*–80·0 µm wide, without crystals or sometimes with radiating
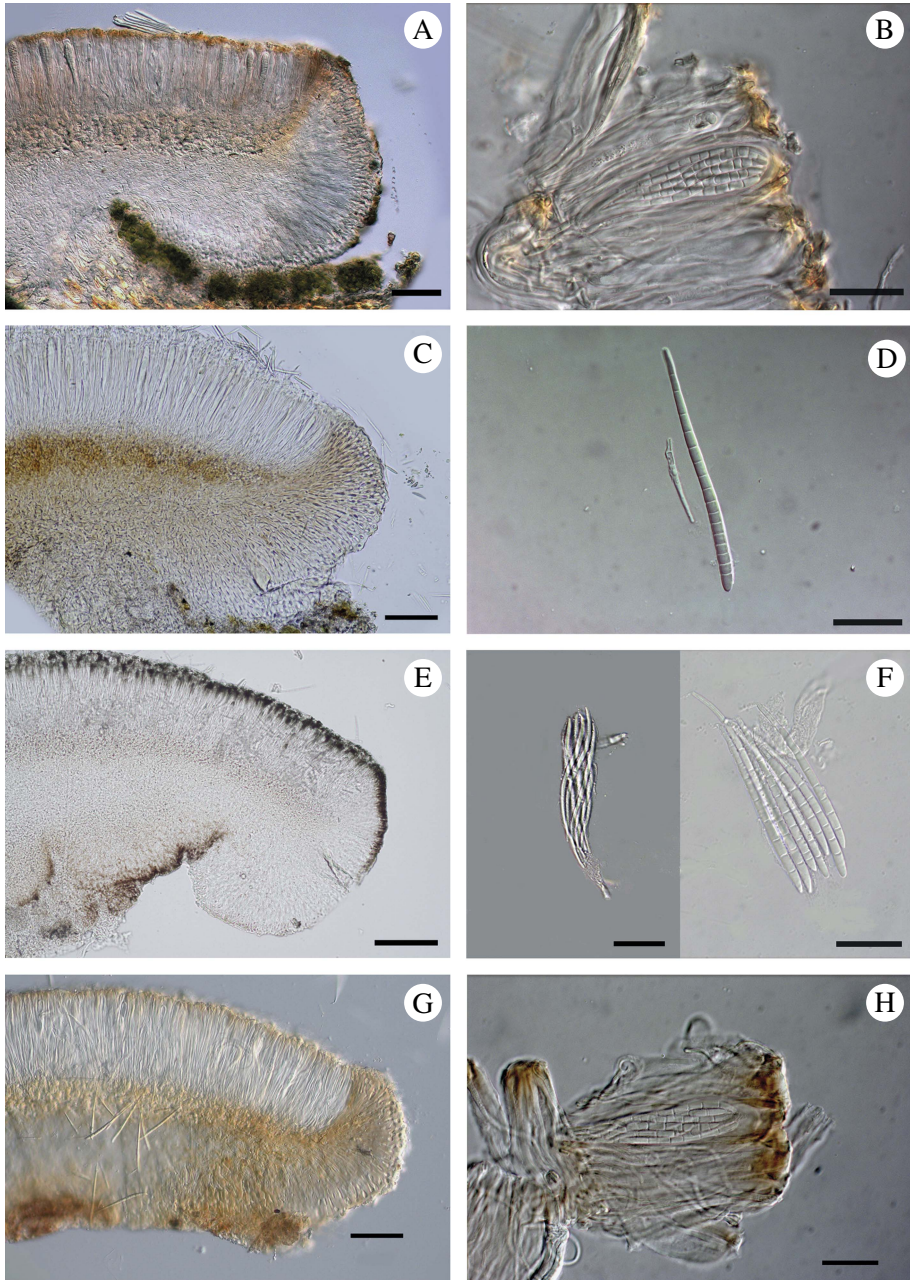
FIG. 4. New species of *Bacidia* from the Russian Far East. A & B, *Bacidia areolata*: A, TS apothecium; B, ascus with spores. C & D, *B. elongata*: C, TS apothecium; D, spore. E & F, *B. kurilensis*: E, TS apothecium; F, ascus with spores. G & H, *B. sachalinensis*: G, TS apothecium; H, ascus with spores. Scales: A, C & G = 50 µm; E = 100 µm; B, D, F & H = 20 µm. In colour online.

clusters of crystals dissolving in N. Rim yellow, yellow-brown, brown-orange, often darker in the upper part than in the lower part, 3–4 cell layers thick along the edge, distinct zone of enlarged cells with lumina that are 7–12 µm long and 4–6 µm wide; inner part paler than or ±concolorous with rim, downwards almost colourless to pale yellowish, K −. *Hymenium* 56·5–*76·2*–90·0 µm high, in lower part colourless; upper part pale orange to orange-brown, K+ yellow. *Hypothecium* pale yellow, almost colourless, K± yellow (reaction unclear). *Paraphyses* simple, thin, 1·0–1·5 µm wide in mid-hymenium, ±clavate or only slightly swollen in the apices, without internal pigment. *Asci* cylindrical or clavate, 50–68 µm long, 7–13 µm wide, I/KI + blue, with indistinct or sometimes tapering ocular chamber. *Ascospores* straight or slightly curved, (40·0–)47·2–*57·0*–66·9(–82·0) µm long, (2·50–)2·95–*3·45*–3·95(–4·50) µm wide (*n* = 66), with (6–)7–*9*–11(–15) septa (*n* = 43).

Pycnidia immersed in the thallus, black, 50–100 µm diam. *Conidia* curved, non-septate, 14–17 × 1·0 µm.

Etymology. The species is named with reference to the thallus structure.

Habitat and distribution. The species is known only from a single locality in Khabarovskiy Krai, in a coniferous-broadleaf forest with high humidity on a terrace above the river.

Comments. *Bacidia areolata* is very similar to *B. suffusa* but differs by its smooth, cracked to areolate thallus, lighter apothecia with less developed and often inconspicuous white pruina on the exciple edge, and shorter spores. It can also be separated by the thinner hymenium, which never exceeds 100 µm, but this feature alone is not enough to confirm the species. *Bacidia suffusa* from North America differs by having larger pycnidia, 100–125 µm diam., with filiform curved, non-septate conidia, 10–27 × 0·8 µm.

Additional specimens examined. Only type material seen.

Bacidia elongata J. Gerasimova & A. Beck sp. nov.

MycoBank No.: MB 821185

Similar to *Bacidia fraxinea* but differs in having a wide zone of enlarged cell lumina along the edge of the exciple.

Type: Russia, Khabarovskiy Krai, Khabarovskiy Rayon, Bolshekhekhtsirskiy State Natural Reserve, 48° 25′N, 134°77′E, 160 m, coniferous-broadleaf forest, on a terrace above the river, on bark of *Acer mono*, 5 September 2013, *J. V. Gerasimova* s. n. (M M-0182571—holotype; M M-0182572, LE L-13007—isotypes). GenBank Accession no: MH048626

(Figs 3C & D, 4C & D)

Thallus poorly defined, thin to rather thick, smooth to areolate, consisting of scattered or contiguous, ±flattened or convex areoles; or granular, consisting of ±globose, scattered or cluster-forming granules; rarely cracked. If the thallus forms a thick crust it is wrinkled to warted, consisting of layered irregularly-shaped warts; whitish when smooth, greyish, light green, greyish green, dark grey-green, with crystals in the upper cortex. *Prothallus* inconspicuous, sometimes present in between areoles, whitish. *Photobiont* chlorococcoid green alga, 6–15 × 8–18 µm.

Apothecia (0·25–)0·40–*0·55*–0·70(–0·95) mm, sessile, ±plane. Young apothecia occasionally barrel-shaped, when mature ±plane, to only slightly convex, rarely strongly convex or irregularly shaped. *Disc* almost white or pinkish in young apothecia, orange, orange-brown to dark orange-brown and dark purple-brown when mature. *Margin* concolourous or paler, light orange, rarely brown; persistent, often with thick layer of white pruina on the edge, especially in young apothecia. *Exciple* 49·0–*79·5*–110·0 µm wide, without crystals, but sometimes with clusters of crystals along the rim dissolving in N; colourless to orange-brown, with 4 layers of enlarged cells along the edge (1 layer of terminal cells ±globose, up to 5·0 × 5·0–7·0 µm, other 3 layers ±cylindrical with lumina that are 9–14(–20) × 4·0–5·5 µm). Exciple rim laterally almost colourless, yellowish, pale yellow-brown to orange-brown, consisting of radially arranged hyphae. Middle exciple orange-brown to colourless, consisting of periclinally arranged thin hyphae; K + yellow or brown, parts K+ purplish, N −. *Hymenium* 62·5–*92·0*–110·0 µm high, colourless in lower part; upper part diffusely

coloured, colourless to pale yellow, pale orange, rarely brown-orange. *Hypothecium* almost colourless to pale yellow, pale yellow-brown to orange-brown, usually darker than exciple below. *Paraphyses* simple, sometimes fork-branched, some with unclear septa, thin, 1·0–*1·5*–1·8 μm wide in mid-hymenium, ±clavate or only slightly swollen in the apices, 2·0–*2·5*–3·0 μm wide, without internal pigment. *Asci* cylindrical, 43–*72*–95 μm long, 7–*11*–19 μm wide, I/KI+ blue, ocular chamber inconspicuous. *Ascospores* acicular, straight or slightly curved, (39–)51–*59*–68(–80) μm long, (2·0–)2·5–*3·0*–3·5(–4·0) μm wide (*n* = 93), with (2–)5–*7*–12(–16) septa (*n* = 71).

Pycnidia not seen.

Etymology. The species is named with reference to the exciple structure, characterized by a wide zone of enlarged cell lumina along the edge.

Habitat and distribution. Corticolous species, occurring in mixed forests on the bark of hardwoods. Known phorophytes: *Acer mono*, *Fraxinus mandshurica* and *Ulmus glabra*.

Comments. There are some differences between specimens of this species collected in Khabarovskiy (holotype) and those from Primorskiy Krai. The type specimen from Khabarovskiy Krai differs partly in having apothecia mainly without pruina, hypothecium and exciple almost colourless or yellowish K± intensifying, and only the rim is coloured, brown-orange to orange-brown. By contrast, the specimens from Primorskiy Krai have a coloured hypothecium and exciple, and apothecia primarily with a thick layer of white pruina on the edge.

A pale specimen of *B. elongata* with a mostly smooth thallus appears to be close to *B. fraxinea*, but the wide zone of cells with enlarged lumina along the edge of the exciple clearly differentiates it from that species. In fact, the zone of cells with enlarged lumina in combination with its overall habit, places it morphologically close to *B. suffusa*, *B. millegrana*, *B. campalea* and related species. The dark morph of *B. elongata* is similar to *B. suffusa* but differs in lacking abundant

clusters of crystals in the exciple, a distinct pigment in the exciple rim and having different cell size along the edge of the exciple.

Additional specimens examined. **Russia:** *Primorskiy Krai*: Chuguyevskiy Rayon, Verkhneussuriyskiy Statsionar, in the valley of the Sokolovka River, conifer-broadleaf forest, on bark of *Ulmus glabra*, 1973, *L. N. Vasil'yeva* s. n. (PIG 29682); Krasnoarmeiskiy Rayon, forest close to the Mel'nichnoye settlement, birch forest (*Betula costata*), on bark of *Fraxinus mandshurica*, 21 viii 2013, *J. V. Gerasimova* s. n. (M M-0182626, LE L-13010); birch forest (*Betula costata*), on bark of *Ulmus glabra*, 21 viii 2013, *J. V. Gerasimova* s. n. (M M-0182627, LE L-13011); mixed forest with a predominance of *Pinus koraiensis*, with undergrowth of *Acer mono* and *Populus tremula*, on bark of *Acer mono*, 22 viii 2013, *J. V. Gerasimova* s. n. (M M-0182628, LE L-13012); mixed forest with a predominance of *Pinus koraiensis*, with undergrowth of *A. mono* and *Populus tremula*, on bark of *F. mandshurica*, 22 viii 2013, *J. V. Gerasimova* s. n. (M M-0182625, LE L-13013); the Sikhote-Alin' Nature Reserve, lowland forest, on bark of *A. mono*, 30 vi 1977, *I. F. Skirina* s. n. (PIG 28762); Partizanskiy Rayon, north-western slope of Mt. Lazovskaya, 43°39'12.9"N, 133°35'48.0"E, 1132 m, spruce-fir forest, on bark of *Picea* sp., 17 viii 2009, *I. F. Skirina* s. n. (PIG 26560); Mt. Ol'khovaya, 540 m, coniferous-broadleaf forest, on bark of *Acer mandshuricum*, 2010, *I. F. Skirina* s. n. (PIG 29468); valley of Postyshevka River, surroundings of the Krasnoarmeyskiy way station, 43°10'6.49"N, 133°00'9.35"E, 312 m, lowland forest, on bark of *Chosenia* sp., 26 viii 2012, *I. F. Skirina, F. V. Skirin* s. n. (PIG 32040).

Bacidia kurilensis J. Gerasimova, A. Ezhkin & A. Beck sp. nov.

MycoBank No.: MB 821186

Similar to *Bacidia laurocerasi* but differs by the presence of a green hue in the epihymenium and upper part of the excipulum edge, as well as by a distinctly granular thallus.

Type: Russia, Sakhalin Oblast, Kurile Islands, Kunashir Island, at the foot of the Mendeleev Volcano, 44°00'4.78"N, 145°42'26.85"E, 135 m, mixed conifer-broadleaf forest, on bark of *Salix udensis*, 26 July 2013, *A. K. Ezhkin* [B11/11.15] (M M-0182620—holotype; SAK 276—isotype).

GenBank Accession no: MH048610

(Figs 3E & F, 4E & F)

Thallus poorly defined, thin to thick, partly smooth, granular to granular isidiose; composed of discrete or more often contiguous, ±globose or extended, irregular

granules, forming a loose assemblage, sometimes slightly flattened to subsquamulose; light green-grey, grey-green, in the herbarium becoming partly brownish; lacking crystals in the upper cortex. *Prothallus* epiphloeodal, often present between granules or bordering the thallus, white or greyish. *Photobiont* chlorococcoid green alga, 6–15 × 8–18 μm and frequently with associated, free-living cyanobacteria.

Apothecia (0·5–)0·7–*0·9*–1·2(–1·4) mm diam., sessile, ±plane or very slightly convex, becoming moderately convex when mature, epruinose. *Disc* reddish brown, fuscous brown to almost black, rarely mottled and light brown in the middle. *Margin* concolorous with the disc, sometimes paler in the lower part of young apothecia or reddish brown. *Exciple* laterally 62·5–*78·0*–112·5 μm wide, without crystals. Rim dark brown in upper part with a greenish hue, lower down paler, brown to orange-brown; colourless in inner part and under hypothecium; brown pigment along the full length of the edge or rim with a single layer of enlarged cells up to 6 × 5 μm, without crystals, K+ intensifying. *Hymenium* 80·0–*95·0*–107·5 μm high, colourless in lower part, without crystals; upper part dark brown with a dirty green pigmentation, K+ intensifying. *Hypothecium* pale yellow, pale brown-yellow, almost colourless. *Paraphyses* simple, 1·5–2·0 μm in mid-hymenium, non-septate, slightly swollen at apices 2·5–4·0 μm, without internal pigment. *Asci* clavate to cylindrical, 54–70 × 9–11 mm; I/KI+ blue, ocular chamber inconspicuous. *Ascospores* acicular, straight or slightly curved, sometimes coiled in the ascus, (41–)55–65–74(–88) μm long (*n* = 85), (2·00–)2·30–*2·75*–3·15(–4·00) μm wide, with (3–)5–9–13(–17) septa (*n* = 85).

Pycnidia not seen.

Etymology. The epithet '*kurilensis*' refers to the group of islands where the species was first collected.

Distribution and habitat. Known from Kunashir Island at the foot of the Mendeleev Volcano. It grows on the bark of *Hydrangea paniculata*, *Kalopanax septemlobus* and *Salix udensis* in a sparse conifer-broadleaf forest with *Abies sachalinensis* and *Picea jezoensis* in a small river valley. The habitat is associated with high humidity and moderate insolation.

Comments. *Bacidia kurilensis* is closely related to *B. biatorina*, *B. heterochroa*, *B. laurocerasi* and *B. salazarensis*. *Bacidia biatorina* has a similar thallus structure and dark apothecia but differs in the shorter spores (42–57 μm) and lack of green pigmentation in the epihymenium and edge of the exciple. *Bacidia salazarensis* is characterized by spores having a lower length-width ratio, a rimose thallus and a different distribution (the only Asian specimen of *B. salazarensis* seen was from southern China). *Bacidia laurocerasi* has a similar exciple structure and long multiseptate spores but differs by having a smooth to areolate thallus and lacking the green pigmentation in the exciple and epihymenium. *Bacidia heterochroa* differs mainly by lacking the granular thallus.

Additional specimens examined. **Russia:** *Sakhalin:* Sakhalin Oblast, Kunashir Island, at the foot of the Mendeleev Volcano, 44°00'4·78"N, 145°42'26·85"E, 135 m, mixed conifer-broadleaf forest, on bark of *Kalopanax septemlobus*, 2013, *A. K. Ezhkin* B7/11.15 (M M-0182621, LE, SAK 272); 44°00'4·78"N, 145°42'26·85"E, 135 m, mixed conifer-broadleaf forest, on bark of *Hydrangea paniculata*, 2013, *A. K. Ezhkin* B17/11.15 (M M-0182622, LE, SAK 282).

Bacidia sachalinensis J. Gerasimova, A. Ezhkin & A. Beck sp. nov.

MycoBank No.: MB 821187

Similar to *Bacidia polychroa* but differing in thallus and exciple structure, and in its shorter spores with fewer septa (40–58 × 2–3 μm with 1–8 septa).

Type: Russia, Sakhalin, Sakhalin Oblast, Yuzhno-Sakhalinsk, Rogatka River, 46°58'5·70"N, 142°47'49·03"E, 163 m, floodplain forest, on bark of *Populus maximowiczii*, 19 May 2014, *A. K. Ezhkin* [B8/12.14] (M M-0182619—holotype; LE L-12961, SAK 145—isotypes).

GenBank Accession no: MH048621

(Figs 3G & H, 4G & H)

Thallus poorly defined, thin to thick, either discontinuous, smooth, indistinctly areolate, consisting of scattered, discrete to contiguous, ±flattened small areoles, or

continuous, warted to wrinkled, cracked; white, whitish green, pale grey to dirty grey, grey-green. *Prothallus* sometimes present, between areoles, white. *Photobiont* chlorococcoid green alga, 6–15 × 8–18 μm.

Apothecia (0·30–)0·45–0·65–0·85(–1·30) mm diam., ±plane when young, later becoming convex, epruinose or rarely with thin white pruina on the edge and the disc of young to medium-aged apothecia. *Disc* pale orange to intensely orange, brown-orange, yellow-brown, rusty brown to dark orange-brown and red-brown, rarely dark brown when mature. *Margin* concolorous with the disc or slightly darker, raised above disc in young apothecia, later level with the disc, and finally excluded in old and convex apothecia. *Exciple* laterally 46·0–63·8–75·0 μm wide, without crystals. Rim pale brown, yellow-brown, orange-brown, lower down almost colourless, along the margin edge with 2 layers of enlarged cells with lumina that are 2·3–3·8–7·8 × 2·6–5·4–7·7 μm (if ± globose then up to 8 × 8 μm), without crystals; inner part (the same as rim) pale brown, yellow-brown, orange-brown, sometimes almost colourless below; K+ purplish. *Hymenium* 70·0–78·8–92·5 μm high, in lower part colourless, in upper part indistinct and diffusely coloured, pale yellow-brown, pale orange-brown to orange-brown, sometimes olive, yellowish, almost colourless. *Hypothecium* pale brown-yellow to yellow-brown, brown-orange, darker than exciple, K+ purplish. *Paraphyses* simple, thin, 1·60–1·85–2·10 μm wide in mid-hymenium, ± clavate or only slightly swollen in the apices, 1·8–2·4–3·5 μm wide, without internal pigment. *Asci* cylindrical or clavate, 37·0–54·5–66·0 × 7·0–11·0–16·7 μm wide, I/KI + blue, with tapering ocular chamber. *Ascospores* acicular, straight or slightly curved, sometimes coiled in ascus (36·7–)43·5–49·1–54·7(–63·5) μm long (2·00–)2·40–2·70–3·00(–4·25) μm wide (*n* = 125), with (1–)3–5–7(–8) septa.

Etymology. The epithet '*sachalinensis*' refers to the locality where the species was collected.

Distribution and habitat. Known only from a single locality on Sakhalin. It was collected on the bark of mature trees, in an old floodplain poplar-willow forest with high understorey in a very humid habitat with a fair amount of sunlight. Known phorophytes include *Populus maximowiczii* and *Ulmus laciniata*.

Comments. Bacidia sachalinensis has a very variable thallus structure and apothecial colour and this is also typical for North American and European specimens of *B. polychroa*. It is morphologically and anatomically very similar to *B. polychroa* but differs in having 1–2 layers of cells with enlarged lumina along the edge of the exciple, shorter spores with fewer septa (40–58 × 2–3 μm with 1–8 septa) and a usually smooth and poorly defined thallus with light coloured apothecia. North American specimens of *B. polychroa* have longer and wider spores with more septa (31–74 × 1·9–5·0 μm with 2–15 septa (Ekman 1996)) while European specimens have spores that are intermediate in size (33–75 ×2·0–4·5 μm with 3–16 septa (Foucard 2001; Llop 2007; Coppins & Aptroot 2009; Wirth *et al.* 2013)). *Bacidia diffracta* differs mainly by having a granular thallus.

Additional specimens examined. **Russia:** *Sakhalin*: Sakhalin Oblast, Yuzhno-Sakhalinsk neighbourhood, Rogatka River, 46°58'4.789"N, 142°48'18.88"E, 161 m, floodplain forest, on bark of *Populus maximowiczii*, 2014, *A. K. Ezhkin* B7/12.14 (M M-0182621, LE L-12960, SAK 144); 46°58'5.707"N, 142°47'49.03"E, 163 m, floodplain forest, on bark of *Populus maximowiczii*, 2014, *A. K. Ezhkin* B9/12.14 (M M-0182623, LE L-12962, SAK 146); 46°58'2.118"N, 142°46'16.75"E, 108 m, floodplain forest, on bark of *Populus maximowiczii*, 2014, *A. K. Ezhkin* B10/12.14 (LE L-12963, SAK 147); 46°58'5.707"N, 142°47'49.03"E, 162 m, floodplain forest, on bark of *Ulmus laciniata*, 2014, *A. K. Ezhkin* B11/12.14 (LE L-12964, SAK 148); 46°58'4.789"N, 142°48'18.88"E, 161 m, floodplain forest, on bark of *Populus maximowiczii*, 2014, *A. K. Ezhkin* B12/12.14 (M M-0182624, LE L-12965, SAK 149).

Bacidia schweinitzii (Fr.) A. Schneid.

Bacidia schweinitzii occurs in the temperate forests of Canada around the Great Lakes and the Maritimes but it also occurs in eastern Asia and the eastern parts of the USA as far south as northern Florida (Ekman 1996; Lendemer *et al.* 2016). The species is

reported here from Russia for the first time. It was collected in the temperate region of the southern part of the Russian Far East, in Primorskiy and Khabarovskiy Krai, and also on Kunashir Island.

This species has been found on the bark and trunks of a wide variety of conifer and deciduous trees, often among or on top of the branches colonized by mosses in dense coniferous-broadleaf and spruce-fir forests. At the Russian sites, the understorey often has ferns, bryophytes and bamboo present. Specimens were collected on several occasions on the bark of fallen, well-decomposed trees in shaded, very humid sites. Known phorophytes in the Russian Far East include: *Abies nephrolepis*, *Acer ukurunduense*, *Betula costata*, *B. ermanii*, *Fraxinus mandshurica*, *Kalopanax septemlobus*, *Picea jezoensis*, *Picea* sp., *Pinus* sp., *Populus tremula*, *Prunus cerasus*, *Quercus mongolica*, *Quercus* sp., *Tilia amurensis* and *Ulmus laciniata*.

Specimens examined. **Russia:** *Khabarovskiy Krai*: Khabarovskiy Rayon, Bolshekhekhtsirskiy Nature Reserve, 48°25′N, 134°77′E, 157 m, coniferous-broadleaf forest, on a terrace above the river, on bark of *Picea jezoensis*, 5 ix 2013, *J. V. Gerasimova* s. n. (LE L-13004); 48°22′N, 134°77′E, 865 m, spruce-fir forest with *Betula ermanii*, on bark of *Picea jezoensis*, 3 ix 2013, *J. V. Gerasimova* s. n. (M M-0182635, LE L-13003); 48°21′N, 134°79′E, 845 m, thick spruce forest, on bark of *Picea jezoensis*, 4 ix 2013, *J. V. Gerasimova* s. n. (M M-0182634, LE L-12999); 48°23′N, 134°77′E, 451 m, coniferous-broadleaf forest near the cordon, on bark of *Fraxinus mandshurica*, 2 ix 2013, *J. V. Gerasimova* s. n. (M M-0182580, M M-0182629, LE L-13001, L-12998); 48°22′N, 134°77′E, 820 m, spruce forest with *Betula ermanii* on the edge of drying zone, on bark of *Picea jezoensis*, 3 ix 2013, *J. V. Gerasimova* s. n. (M M-0182629, LE L-12998); *ibid*, *J. V. Gerasimova* s. n. (M M-0182630, LE L-13000); 48°22′N, 134°77′E, 865 m, spruce-fir forest with *Betula ermanii*, on bark of *Abies nephrolepis*, 3 ix 2013, *J. V. Gerasimova* s. n. (M M-0182631, LE, UPS L-721214); 48°23′N, 134°77′E, 451 m, coniferous-broadleaf forest near the cordon, on bark of *Betula costata*, 2 ix 2013, *J. V. Gerasimova* s. n. (LE L-13002); Kukanskiy Range, 50°55′N, 134°26′E, 715 m, spruce-larch green moss forest, on bark of *Picea* sp., 23 viii 2012, *I. A. Galanina, L. S. Yakovchenko* s. n. (VBGI). *Primorskiy Krai*: Chuguyevskiy Rayon, Mt. Snezhnaya, south-west slope, old spruce-fir forest, on top of moss twigs on bark of *Picea* sp., 5 viii 2003, *I. F. Skirina, F. V. Skirin* s. n. (PIG 15673); Verkhneussuriyskiy Statsionar, in the valley of the Sokolovka River, conifer-broadleaf forest, on bark of *Acer ukurunduense*, 1973, *L. N. Vasil'yeva* s. n. (PIG 13267);

Verkhneussuriyskiy Statsionar, in the valley of the Sokolovka River, conifer-broadleaf forest, lowland forest, on bark of *Prunus cerasus*, 15 vii 1980, *L. N. Vasil'yeva* s. n. (PIG 13268); Khasanskiy Rayon, neighbourhood of Kravtsovka settlement, 42°38′N, 141°44′E, oak (*Quercus mongolica*) forest, on bark of *Quercus mongolica*, 6 v 2013, *I. A. Galanina* s. n. (VBGI); *ibid.*, on bark of *Q. mongolica*, 6 v 2013, *I. A. Galanina* s. n. (VBGI); Ryazanovka River, oak forest, on bark of *Quercus* sp., 1985, *I. F. Skirina* s. n. (PIG 5653); neighbourhood of Peschanyy Peninsula, oak forest, on bark of *Quercus* sp., 17 viii 2008, *I. F. Skirina* s. n. (PIG 23811); Krasnoarmeiskiy Rayon, western slope of the Sikhote-Alin', 46°13′N, 136°70′E, 1338 m, slope of the upper reaches of Valincu River, on bark of *Picea jezoensis*, 25 viii 2013, *J. V. Gerasimova* s. n. (M M-0182579, LE, UPS L-721217); 46°21′N, 136°66′E, 1010 m, thick spruce-fir forest with fir and mosses in the understorey, on bark of *Abies nephrolepis*, 29 viii 2013, *J. V. Gerasimova* s. n. (LE L-12997); 46°15′N, 136°70′E, 1180 m, spruce-fir forest with mosses in the understorey, on bark of *Picea jezoensis*, 26 viii 2013, *J. V. Gerasimova* s. n. (LE); 46°14′N, 136°70′E, 1275 m, thick spruce-fir forest, the southern slope, in the upper reaches of Valincu River, on bark of *Picea jezoensis*, 26 viii 2013, *J. V. Gerasimova* s. n. (LE); *ibid.*, on bark of *Betula costata*, 26 viii 2013, *J. V. Gerasimova* s. n. (LE L-12996); western slopes of the Sikhote-Alin', upper reaches of the Bol'shaya Ussurka, the northern slope, spruce-fir forest, on a fallen tree, 1981, *I. F. Skirina* s. n. (PIG 6653); *ibid.*, on bark of *Acer ukurunduense*, 1981, *I. F. Skirina* s. n. (PIG 6600); Sikhote-Alin' Nature Reserve, Sredniy Creek, birch (*Betula ermanii*) forest, on bark of *Betula ermanii*, 1980, *I. F. Skirina* s. n. (PIG 5578); Sikhote-Alin' Nature Reserve, neighbourhood of Mt. Kolumbe, spruce-fir forest, on bark of *Abies* sp. and *Picea* sp., 15 vii 1980, *I. F. Skirina* s. n. (PIG 3437); Lazovskiy Rayon, neighbourhood of Valentin settlement, the Mt. Koldun rise, coniferous-broadleaf forest, on bark of *Quercus* sp., 25 viii 2009, *I. F. Skirina* s. n. (PIG 24140); Partizanskiy Rayon, Alekseyevskiy Range, Mt. Olkhovaya, the southern slope, 700 m, conifer-broadleaf forest, on bark of *Quercus* sp., 4 vii 2007, *I. F. Skirina* s. n. (PIG 21200); Alekseyevskiy Range, Mt. Ol'khovaya, 540 m, lowland forest near the river on bark of *Populus tremula*, 7 viii 2007, *I. F. Skirina* s. n. (PIG 23804); the spur of Mt. Chantinza, 43°08′N, 132°58′E, 602 m, coniferous-broadleaf forest, on bark of *Tilia amurensis*, 25 viii 2012, *I. F. Skirina, F. V. Skirin* s. n. (PIG 32039); Pozharskiy Rayon, spurs of Strel'nikov Range, 1 km from the outpost, 263 m, oak forest, oak on the slope, on bark of *Quercus* sp., 20 vii 2007, *I. F. Skirina* s. n. (PIG 21850); Spasskiy Rayon, neighbourhood of Orlovka settlement, 45°20′46·5″N, 133°36′50·5″E, mixed forest, on bark of *Quercus* sp., 26 vi 2009, *I. F. Skirina, F. V. Skirin* s. n. (PIG 25692); Terneiskiy Rayon, Terneiskiy forestry, neighbourhood of Tayozhnyy settlement, Lagernaya River, 45°42′18·2″N, 136°17′40·3″E, 717 m, pine-spruce forest on the west-south-west slope, on bark of *Pinus* sp., 10 vii 2011, *I. A. Galanina* s. n. (VBGI); neighbourhood of Tayozhnyy settlement, Mrachnyy Creek, 45°44′38·9″N, 136°09′29·3″E, 745 m, pine-spruce forest, on bark of *Picea*

jezoensis, 9 vii 2011, *I. A. Galanina* s. n. (VBGI); neighbourhood of Tayozhnyy settlement, 45°41'07·4"N, 136° 10'26·5"E, 713 m, pine-spruce forest on a gentle slope, on the top of moss twigs on bark of *Picea* sp., 8 vii 2011, *I. A. Galanina* s. n. (VBGI); neighbourhood of Tayozhnyy settlement, Mrachnyy Creek, 45°44'13·6"N, 136° 09'31·9"E, 745 m, pine-spruce forest, on bark of *Picea jezoensis*, 2011, *I. A. Galanina* s. n. (VBGI); *ibid.*, on bark of *Picea jezoensis*, 2011, *I. A. Galanina* s. n. (VBGI). *The Jewish Autonomous Oblast*: Bastak Nature Reserve, "Dubovaya Sopka", near the cordon, oak forest, on bark of *Quercus* sp., 17 x 2005, *I. F. Skirina* s. n. (PIG 18012). *Sakhalin*: Sakhalin Oblast, Kunashir Island, at the foot of the Mendeleev Volcano, 43°59'37·07"N, 145°46'50·62"E, 105 m, old spruce-fir forest with *Abies sachalinensis*, *Picea glehnii* and *P. jezoensis*, on bark of fallen strongly decomposing tree, 2014, *A. K. Ezhkin* B20/11.15 (SAK 285); neighbourhood of Lagunnoye Lake, 44°02'50·2"N, 145° 46'01·6"E, 79 m, mixed conifer-broadleaf forest, on bark of *Kalopanax septemlobus*, 2015, *A. K. Ezhkin* B10/11.15 (SAK 275); neighbourhood of Lagunnoye Lake, 44° 02'50·2"N, 145°46'01·6"E, 79 m, mixed conifer-broadleaf forest, on bark of *Ulmus laciniata*, 2015, *A. K. Ezhkin* B21/ 11.15 (SAK 286).

SUPPLEMENTARY MATERIAL

For supplementary material accompanying this paper visit https://doi.org/10.1017/S0024282918000397

REFERENCES

Andersen, H. L. & Ekman, S. (2005) Disintegration of the *Micareaceae* (lichenized Ascomycota): a molecular phylogeny based on mitochondrial rDNA sequences. *Mycological Research* **109**: 21–30.

Beck, A. & Mayr, C. (2012) Nitrogen and carbon isotope variability in the green-algal lichen *Xanthoria parietina* and their implications on mycobiont-photobiont interactions. *Ecology and Evolution* **2**: 3132–3144.

Brotherus, V. P., Okamura, K. & Zahlbruckner, A. (1936) Materialien zu einer Flora der Kryptogamenspflanzen des fernen Ostens. *Acta Instituti Botanici Academiae Scientiarum URSS, Serie 2* **3**: 589–596.

Brummitt, R. K. (2001) *World Geographical Scheme for Recording Plant Distributions*, 2nd edn. Pittsburgh: Hunt Institute for Botanical Documentation, Carnegie Mellon University.

Coleman, A. W. (2003) ITS2 is a double-edged tool for eukaryote evolutionary comparisons. *Trends in Genetics* **19**: 370–375.

Coleman, A. W. (2009) Is there a molecular key to the level of "biological species" in eukaryotes? A DNA guide. *Molecular Phylogenetics and Evolution* **50**: 197–203.

Coppins, B. J. & Aptroot, A. (2009) *Bacidia* De Not. 1846. In *Lichens of Great Britain and Ireland* (C. W. Smith, A. Aptroot, B. J. Coppins, A. Fletcher, O. L. Gilbert, P. W. James & P. A. Wolseley, eds): 189–207. London: British Lichen Society.

Czarnota, P. & Guzow-Krzemińska, B. (2012) ITS rDNA data confirm a delimitation of *Bacidina arnoldiana* and *B. sulphurella* and support a description of a new species within the genus *Bacidina*. *Lichenologist* **44**: 743–755.

Darriba, D., Taboada, G. L., Doallo, R. & Posada, D. (2012) jModelTest 2: more models, new heuristics and parallel computing. *Nature Methods* **9**: 772.

Edgar, R. C. (2004) MUSCLE: multiple sequence alignment with high accuracy and high throughput. *Nucleic Acids Research* **32**: 1792–1797.

Ekman, S. (1996) The corticolous and lignicolous species of *Bacidia* and *Bacidina* in North America. *Opera Botanica* **127**: 1–148.

Ekman, S. (2001) Molecular phylogeny of the *Bacidiaceae* (*Lecanorales*, lichenized Ascomycota). *Mycological Research* **105**: 783–797.

Ekman, S. & Nordin, A. (1993) The taxonomy of *Bacidia fraxinea* and its relationship to *B. rubella*. *Annales Botanici Fennici* **30**: 77–82.

Foucard, T. (2001) *Svenska Skorplavar och Svampar som Växer på dem*. Stockholm: Interpublishing.

Galanina, I. A. (2008) *Sinuzii Epifitnykh Lishaynikov v Dubovykh Lesakh yuga Primorskogo Kraya* [*Synusiae of Epiphytic Lichens in Oak Forests of the Southern Primorskii Krai*]. Vladivostok: Dalnauka. [In Russian].

Gerasimova, J. V. (2016) *Bacidia absistens* (Nyl.) Arnold (*Ramalinaceae*, *Lecanorales*) v Rossii: nomenklatura, opisanie, ekologiya i rasprostraneniye [*Bacidia absistens* (Nyl.) Arnold (*Ramalinaceae*, *Lecanorales*) in Russia: nomenclature, description, ecology, and distribution]. *Turczaninowia* **19**: 88–93. [In Russian].

Groner, U. & LaGreca, S. (1997) The 'Mediterranean' *Ramalina panizzei* north of the Alps: morphological,

chemical and rDNA sequence data. *Lichenologist* **29:** 441–454.

Guindon, S. & Gascuel, O. (2003) A simple, fast and accurate method to estimate large phylogenies by maximum likelihood. *Systematic Biology* **52:** 696–704.

Hafellner, J. (1984) Studien in Richtung einer naturlicheren Gliederung der Sammelfamilien *Lecanoraceae* und *Lecideaceae. Nova Hedwigia* **79:** 241–371.

Harada, H., Okamoto, T. & Yoshimura, I. (2004) A checklist of lichens and lichen-allies of Japan. *Lichenology* **2:** 47–165.

Huelsenbeck, J. P. & Rannala, B. (2004) Frequentist properties of Bayesian posterior probabilities of phylogenetic trees under simple and complex substitution models. *Systematic Biology* **53:** 904–913.

Inoue, M. (1994) Phytogeography of lecideoid lichens in Japan. *Journal of the Hattori Botanical Laboratory* **76:** 183–195.

James, T. Y., Kauff, F., Schoch, C. L., Matheny, P. B., Hofstetter, V., Cox, C. J., Celio, G., Gueidan, C., Fraker, E., Miadlikowska, J., *et al.* (2006) Reconstructing the early evolution of Fungi using a six-gene phylogeny. *Nature* **443:** 818–822.

Jeon, H.-S., Lökös, L., Han, K.-S., Ryu, J.-A., Kim, J. A., Koh, Y. J. & Hur, J.-S. (2009) Isolation of lichen-forming fungi from Hungarian lichens and their antifungal activity against fungal pathogens of hot pepper anthracnose. *Plant Pathology Journal* **25:** 38–46.

Kashiwadani, H. & Inoue, M. (1993) The lichens of Kushiro Marsh, Hokkaido. *Memoirs of the National Science Museum Tokyo* **26:** 53–66.

Kashiwadani, H. & Sasaki, K. (1987) Lichens of Mt. Hakkoda, Northern Japan. *Memoirs of the National Science Museum Tokyo* **20:** 67–81.

Kuznetsova, E. S., Motiejūnaitė, J., Galanina, I. A. & Yakovchenko, L. S. (2013) *Bacidia suffusa* and *Taeniolella punctata* new to the Russian Far East. *Graphis Scripta* **25:** 51–55.

Lendemer, J. C., Harris, R. C. & Ladd, D. (2016) The faces of *Bacidia schweinitzii*: molecular and morphological data reveal three new species including a widespread sorediate morph. *Bryologist* **119:** 143–171.

Llop, E. (2007) *Lecanorales: Bacidiaceae: Bacidia* y *Bacidina. Flora Liquenológica Ibérica* **3:** 1–49.

Lücking, R. (1992) Foliicolous lichens – a contribution to the knowledge of the lichen flora of Costa Rica, Central America. *Beihefte zur Nova Hedwigia* **104:** 1–179.

Lücking, R. (2008) Foliicolous lichenized fungi. *Flora Neotropica* **103:** 1–867.

Malme, G. O. A. (1935) *Bacidiae* itineris Regnelliani primi. *Arkiv för Botanik* **27A:** 1–40.

Mark, K., Cornejo, C., Keller, C., Flück, D. & Scheidegger, C. (2016) Barcoding lichen-forming fungi using 454 pyrosequencing is challenged by artifactual and biological sequence variation. *Genome* **59:** 685–704.

Miadlikowska, J., Kauff, F., Högnabba, F., Oliver, J. C., Molnár, K., Fraker, E., Gaya, E., Hafellner, J., Hofstetter, V., Gueidan, C., *et al.* (2014) A multigene phylogenetic synthesis for the class Lecanoromycetes (Ascomycota): 1307 fungi representing 1139 infrageneric taxa, 317 genera and 66 families. *Molecular Phylogenetics and Evolution* **79:** 132–168.

Müller, J. (1892) Lichenes Yatabeani, in Japonia lecti et a cl. prof. Yatabe missi. *Nuovo Giornale Botanico Italiano* **24:** 189–202.

Neshataeva, V. Yu., Chernyagina, O. A., Czernyadjeva, I. V., Himelbrant, D. E., Kuznetsova, E. S. & Kirichenko, V. E. (2004) Korennyye starovozrastnyye yelovyye lesa basseyna reki Yelovka, Tsentral'naya Kamchatka (tsenoticheskiye, briofloristicheskiye i likhenobioticheskiye osobennosti). [Pristine old-growth spruce forests of the Yelovka River basin (Central Kamchatka): the species composition of vascular plants, mosses, and lichens and the community structure features]. In *Proceedings of the IV Scientific Conference "Conservation of Biodiversity of Kamchatka and Coastal Waters", 17–18 November, 2003, Petropavlovsk-Kamchatskiy, Russia*, p. 100–124. [In Russian].

Nylander, W. (1890) *Lichenes Japoniae. Accedunt Observationibus Lichenes Insulae Labuan.* Paris: P. Schmidt.

Nylander, W. (1900) Lichenes Ceylonenses et Additamentum ad Lichenes Japoniae. *Acta Societatis Scientiarum Fennicae* **26:** 1–33.

Printzen, C. (1995) Die Flechtengattung *Biatora* in Europa. *Bibliotheca Lichenologica* **60:** 1–275.

Printzen, C. (2014) A molecular phylogeny of the lichen genus *Biatora* including some morphologically similar species. *Lichenologist* **46:** 441–453.

Rambaut, A. (2009) *FigTree v1.3.1.* Available at: http://tree.bio.ed.ac.uk/software/figtree/

Reese Næsborg, R., Ekman, S. & Tibell, L. (2007) Molecular phylogeny of the genus *Lecania* (*Ramalinaceae*, lichenized Ascomycota). *Mycological Research* **111:** 581–591.

Ronquist, F., Teslenko, M., van der Mark, P., Ayres, D. L., Darling, A., Höhna, S., Larget, B., Liu, L., Suchard, M. A. & Huelsenbeck, J. P. (2012) MrBayes 3.2: efficient Bayesian phylogenetic inference and model choice across a large model space. *Systematic Biology* **61:** 539–542.

Santesson, R. (1952) Foliicolous lichens I. A revision of the taxonomy of the obligately foliicolous, lichenized fungi. *Symbolae Botanicae Upsalienses* **12:** 1–590.

Schmull, M., Miadlikowska, J., Pelzer, M., Stocker-Wörgötter, E., Hofstetter, V., Fraker, E., Hodkinson, B. P., Reeb, V., Kukwa, M., Lumbsch, H. T., *et al.* (2011) Phylogenetic affiliations of members of the heterogeneous lichen-forming fungi of the genus *Lecidea sensu* Zahlbruckner (Lecanoromycetes, Ascomycota). *Mycologia* **103:** 983–1003.

Sérusiaux, E. (1993) New taxa of foliicolous lichens from western Europe and Macaronesia. *Nordic Journal of Botany* **13:** 447–461.

Sérusiaux, E., van den Boom, P. P. G., Brand, M. A., Coppins, B. J. & Magain, N. (2012) *Lecania falcata*, a new species from Spain, the Canary Islands and

the Azores, close to *Lecania chlorotiza*. *Lichenologist* **44:** 577–590.

Skirina, I. F. (1995) *Lishayniki Sikhote-Alinskogo Biosfernogo Rayona.* [*Lichens of Sikhote-Alin Biosphere Area*] Vladivostok: Dalnauka [In Russian].

Skirina, I. F. (2015) Spisok lishaynikov Sikhote-Alinskogo zapovednika [List of lichens of the Sikhote-Alin Reserve]. *Biodiversity and Environment of Far East Reserves* **3:** 10–102 [In Russian].

Skirina, I. F. & Moiseyevskaya, E. B. (2004) *Lishayniki Primorskogo Kraya: Annotirovannyy Bibliograficheskiy Ukazatel' Literatury (1912–2004).* [*Lichens of Primorskiy Krai: Annotated Bibliographical List of Literature (1912–2004)*]. Vladivostok: Dalnauka [In Russian].

Stamatakis, A. (2014) RAxML version 8: a tool for phylogenetic analysis and post-analysis of large phylogenies. *Bioinformatics* **30:** 1312–1313.

Stamatakis, A., Hoover, P. & Rougemont, J. (2008) A rapid bootstrap algorithm for the RAxML Web servers. *Systematic Biology* **57:** 758–771.

Swofford, D. L. (2002) *PAUP*: Phylogenetic Analysis Using Parsimony (*and Other Methods)*. [Version 4]. Sunderland, Massachusetts: Sinauer Associates.

Tchabanenko, S. I. (2002) *Konspekt Flory Lishaynikov yuga Rossiyskogo dal'nego Vostoka* [*Conspectus of Lichen Flora of the Southern Russian Far East*]. Vladivostok: Dalnauka. [In Russian].

Tuckerman, E. (1864) Observations on North American and other lichens. *Proceedings of the American Academy of Arts and Sciences* **6:** 263–287.

Vainio, E. A. (1921) Lichenes ab A. Yasuda in Japonia collecti. Continuatio I. *Botanical Magazine* **35:** 45–79.

Vězda, A. (1978) Neue oder wenig bekannte Flechten in der Tschechoslowakei. II. *Folia Geobotanica et Phytotaxonomica* **13:** 397–420.

Vězda, A. (1986) Neue Gattungen der Familie *Lecideaceae* s. lat. (Lichenes). *Folia Geobotanica et Phytotaxonomica* **21:** 199–219.

Vězda, A. (1991) *Bacidina* genus novum familiae *Lecideaceae* s. lat. (Ascomycetes lichenisati). *Folia Geobotanica et Phytotaxonomica* **25:** 431–432.

White, T. J., Bruns, T., Lee, S. & Taylor, J. W. (1990) Amplification and direct sequencing of fungal ribosomal RNA genes for phylogenetics. In *PCR Protocols: a Guide to Methods and Applications* (M. A. Innis, D. H. Gelfand, J. J. Sninsky & T. J. White, eds): 315–322. New York: Academic Press.

Wirth, V., Hauck, M. & Schultz, M. (2013) *Die Flechten Deutschlands*. Stuttgart: Eugen Ulmer KG.

Yakovchenko, L. S., Galanina, I. A., Malashkina, E. V. & Bakalin, V. A. (2013) Mosses and lichens in the minimally disturbed forest communities of the Lower Amur River area (Russian Far East). *Komarovskiye Chteniya* **60:** 9–66.

Yasuda, A. (1925) *Flechten Japans*. Sendai.

Zahlbruckner, A. (1916) Neue Flechten – VIII. *Annales Mycologici* **14:** 45–61.

Zahlbruckner, A. (1921–1940) *Catalogus Lichenum Universalis*. Band I–X. Leipzig: Gebrüder Borntraeger.

Chapter 4

Multilocus-phylogeny of the lichen-forming genus *Bacidia* s. str. (Ramalinaceae, Lecanorales) with special emphasis on the Russian Far East

Julia V. Gerasimova, Aleksandr K. Ezhkin, Evgeny A. Davydov and Andreas Beck

Standard Paper

Multilocus-phylogeny of the lichen-forming genus *Bacidia* s. str. (*Ramalinaceae*, *Lecanorales*) with special emphasis on the Russian Far East

Julia V. Gerasimova[1,2] (ID), Aleksandr K. Ezhkin[3], Evgeny A. Davydov[4] (ID) and Andreas Beck[2,5]

[1]Ludwig-Maximilians-Universität München, Systematic Botany and Mycology, Menzinger Str. 67, 80638 Munich, Germany; [2]Botanische Staatssammlung München, Department of Lichenology and Bryology, SNSB-BSM, Menzinger Str. 67, 80638 Munich, Germany; [3]Institute of Marine Geology and Geophysics, Far East Branch of the Russian Academy of Sciences, Nauki St. 1B, 693022 Yuzhno-Sakhalinsk, Russia; [4]Altai State University, Lenina Avenue 61, 656049 Barnaul, Russian Federation and [5]GeoBio-Center, Ludwig-Maximilians-Universität München, 80333 Munich, Germany

Abstract

To clarify deep relationships among species lineages within *Bacidia* s. str., and to investigate the robustness of the deeper branches, we combined data from three traditionally used RNA-coding genes (nrITS, nrLSU and mtSSU) with two protein-coding genes (*RPB*1 and *RPB*2). The multigene phylogeny contained 48 newly generated sequences from the Russian Far East and all *Bacidia* s. str. sequences from GenBank (131 sequences). We subjected the alignments for the single and concatenated data sets to Bayesian inference (BI) and two maximum likelihood (ML) analyses (RAxML and IQ-TREE). The topologies of phylogenetic trees recovered from BI and ML analyses were highly concordant. The multilocus phylogeny of *Bacidia* s. str. was congruent with previous results based on nrITS sequences from the Russian Far East but with considerably higher support values for most of the deeper branches. A correlation between the recovered clades and apothecial pigments in the upper part of the hymenium and lateral exciple was observed. Based on morphological and molecular evidence, *Bacidia obtecta* is described as new to science. It was recovered as the sister lineage of *B. elongata*. The two species are alike in having up to four enlarged lumina cells along the exciple edge, but *B. obtecta* differs in the abundant crystals found in the upper hymenium and lateral exciple, and by having spores with fewer septa.

Key words: *Bacidia obtecta*, crustose lichen, diversity, multilocus alignments, nuclear genes, protein-coding genes

(Accepted 16 August 2021)

Introduction

Bacidia De Not. is an almost exclusively epiphytic crustose lichen genus, characterized by smooth or warted to granular thalli; acicular multiseptate spores with an average of 30–40, up to 100 μm in length and 2.0–4.0 μm in width; and a pronounced exciple, consisting of radiating hyphae, frequently with enlarged lumina cells at the tips (Ekman 1996; Llop 2007). Until recently, a large variety of lichens were included in the genus *Bacidia* in a broad sense. Zahlbruckner (1921–1940) used the name for crustose lichens with a chlorococcoid photobiont, biatorine apothecia, and ascospores with three or more transverse septa. This circumscription was unnatural and included numerous taxa not closely related to the type species, *Bacidia rosella* (Pers.) De Not. (Gerasimova & Ekman 2017).

The first extensive phylogenetic study of *Bacidia* was based on gene sequences of the nuclear ribosomal internal transcribed spacer (nrITS). It resulted in a re-evaluation of the generic delimitation,

suggesting the transfer of several species to genera such as *Biatora* Fr., *Toninia* A. Massal. and *Bacidina* Vězda (Ekman 2001). In more recent phylogenetic studies, several species have been transferred to further genera, such as *Bellicidia* Kistenich et al., *Bibbya* J. H. Willis, *Scutula* Tul. and *Toniniopsis* Frey (Kistenich et al. 2018). These phylogenetic studies narrowed the generic concept, although the relationship between species, and support for the species groups, remained unclear. Several additional studies, partially focusing on *Bacidia*, used two or multilocus data sets, combining sequences from nrITS with mitochondrial small subunit rDNA (mtSSU) (Andersen & Ekman 2005; Lendemer et al. 2016; Malíček et al. 2018), and nuclear ribosomal large subunit rDNA (nrLSU) with mtSSU (Lumbsch et al. 2004; Sérusiaux et al. 2012), but they covered only a small number of species of *Bacidia* s. str. Additional multilocus phylogenetic studies involving two genes encoding the largest and the second-largest subunit of RNA polymerase II (*RPB*1 and *RPB*2, respectively) also encompassed only six species, namely *B. absistens* (Nyl.) Arnold, *B. arceutina* (Ach.) Arnold, *B. squamulosula* (Nyl.) Zahlbr., *B. schweinitzii* (Fr. ex Tuck.) A. Schneid., *B. rosella* and *B. rubella* (Hoffm.) A. Massal. (James et al. 2006; Miadlikowska et al. 2006, 2014; Reese Næsborg et al. 2007; Ekman et al. 2008; Kistenich et al. 2018).

Author for correspondence: Julia V. Gerasimova. E-mail: jgerasimova.lich@yandex.ru

In the first molecular study on *Bacidia* s. str. from the Russian Far East (RFE), taxon sampling was expanded (Gerasimova *et al.* 2018). Four new species were described, and these are currently considered endemic. While well-supported groups within *Bacidia* s. str. were revealed, support in the nodes of basal clades was low and several polytomies remained.

The main goal of this study was to investigate whether a phylogeny of *Bacidia* s. str. inferred from a larger, multilocus data set with a broader taxon sampling would yield higher backbone support than the previous studies based on nrITS sequences. We address the phylogeny of *Bacidia* s. str. based on nrITS data together with newly obtained data from nrLSU, mtSSU and two protein-coding genes, *RPB*1 and *RPB*2, and 131 sequences of *Bacidia* currently available in GenBank.

Material and Methods

Specimens

This study was based on fresh collections of *Bacidia* gathered by the authors in the field from 2013 to 2015 in the southern part of the Russian Far East (Primorskiy and Khabarovskiy Krai), and on Sakhalin and the Kurile Islands (as indicated in Gerasimova *et al.* (2018)). The second author collected the *Bacidia obtecta* specimens on Sakhalin in 2017 (see details under Taxonomy). Voucher specimens are deposited in the herbaria of the Botanische Staatssammlung München (M), Institute of Marine Geology and Geophysics (SAK) and Altai State University (ALTB). The inclusion of *Bacidia squamulosula* was based on a specimen examined in M (M-0012326; K. Kalb, *Lichenes Neotropici* No. 405, *Bacidiopsora squamulosula* (Nyl.) Kalb. Detailed information on the newly obtained sequences, together with their respective voucher information and GenBank Accession numbers, is given in Table 1.

Morphology

Microscopic observations were made using a Zeiss Axioplan light microscope (Oberkochen, Germany) equipped with differential interference contrast. Cross-sections of apothecia were made on a Leica Jung Histoslide 2000 Mikrotom (Heidelberg, Germany), with a thickness of 8–10 μm. Micrographs of cross-sections were taken on a Zeiss Axioplan with an attached AxioCam 512 Color camera and processed with the Zeiss ZEN 2.3 (blue edition) image software. Macrographs of external characters were taken on a Leica Z6 Apo microscope (with a ×1.0 Planapo lens; Leica, Germany) with a Sony Alpha 6400 camera (Sony, Japan) attached and equipped with a StackShot Macro Rail (Cognisys, USA) as detailed in Gerasimova *et al.* (2021). A single image was mounted from 40–100 serial images using Helicon Focus v.7 software (Helicon, USA).

Measurements are given as (min–) average ± SD (–max) (SD = standard deviation, n_1 = number of all observations, n_2 = number of specimens observed). We provide a detailed description of specimens using standard microscopic techniques following Ekman (1996) and use the proper exciple subdivision scheme, differentiating the following structures: the rim, lateral part and medullary part. Pigment characterization follows Meyer & Printzen (2000) and Ekman (1996).

DNA extraction, PCR amplification and DNA sequencing

DNA extraction was carried out using the Stratec Invisorb Spin Plant Mini Kit (Stratec Molecular GmbH, Berlin, Germany)

following the manufacturer's instructions. Five to eight apothecia were used from fresh material not older than five years. Thallus fragments were removed to minimize the risk of contamination by, for example, lichenicolous fungi. PCR amplification, purification and sequencing were performed as described in Gerasimova *et al.* (2018). Cycling conditions included initial denaturation at 95 °C for 2 min, 5 cycles of 95 °C for 40 s, 54 °C for 60 s, 72 °C for 90 s, 33 cycles of 95 °C for 40 s, 54 °C for 60 s, 72 °C for 90 s, and a final extension step at 72 °C for 7 min. In those cases when PCR products were insufficient, a second PCR with a reduced number of cycles was conducted: denaturation at 95 °C for 2 min, 5 cycles of 95 °C for 40 s, 54 °C for 60 s and 72 °C for 90 s, 22 cycles of 95 °C for 40 s, 54 °C for 60 s and 72 °C for 90 s, with a final extension step at 72 °C for 7 min. We used five pairs of primers: ITS1F (White *et al.* 1990) and ITS4m (Beck & Mayr 2012), LR0R (Rehner & Samuels 1994) and LR5 (Vilgalys & Hester 1990), mtSSU1 and mtSSU3R (Zoller *et al.* 1999), fRPB2-5F and fRPB2-7cR (Liu *et al.* 1999), and newly designed primers for *Bacidia* gRPB1AFba (5′-GAG TGY CCG GGA CAT TTT GG-3′) and fRPB1cRba2 (5′-GSC CRG CAA TRT CGT TAT CCA-3′).

Alignment and phylogenetic analyses

Forty-eight new sequences of *Bacidia* s. str. from three ribosomal RNA-coding (nrITS, nrLSU, mtSSU) and two protein-coding genes (*RPB*1 and *RPB*2) were obtained and combined with 22 nrITS sequences from our previous study and 109 sequences of *Bacidia* s. str. from GenBank (Table 1). *Bacidia schweinitzii* (JG014), *B. areolata* Gerasimova & A. Beck (JG114) and *B. obtecta* sp. nov. (JG139-141) were newly sequenced.

Altogether 85 individuals from 24 OTUs of *Bacidia* s. str. were included. '*Phyllopsora*' *borbonica* Timdal & Krog and *Sporacestra pertexta* (Nyl.) Stapnes & Timdal were selected as the outgroup based on the results of Kistenich *et al.* (2018).

BLAST searches in GenBank were performed to detect and exclude accessory/lichenicolous fungi and potential contaminations. Alignments were carried out using standard settings in MUSCLE v.3.8.31 (Edgar 2004) as implemented in PhyDE-1 v.0.9971 and optimized manually. Positions where a gap had to be inserted in more than 95% of the sequences were excluded. The most variable ITS1 region was aligned using Gblocks v.0.91.1 (https://ngphylogeny.fr/tools/tool/276/form). The alignments are provided in Supplementary Material File S1 (available online).

Sequences of *Bacidia friesiana* (Hepp) Körb., *B. purpurans* R. C. Harris *et al.*, *B. hostheleoides* (Nyl.) Zahlbr. and *B. thiersiana* Lendemer (deposited as *Bacidia lutescens* Malme in GenBank) were revealed as separate lineages. *Bacidia purpurans* is more distantly related to *Bacidia* s. str. than the outgroup (Supplementary Material File S2, Figs S1–S3, available online). According to a BLAST search, *B. friesiana* (MH539765) is closest to *Bacidina* with more than 90% similarity. Given the high morphological variation and the necessity for further sequencing, we refrain from transferring this species to another genus.

We performed analyses for single-locus and concatenated data sets as follows: 1) single-locus data set for each locus separately (trees are included in Supplementary Material File S3, Figs S5–S19, available online); 2) concatenated multilocus data set including 26 taxa (including the outgroup) with sequences from three to all five genes available for each specimen (both newly obtained and GenBank sequences (Fig. 1; Supplementary Material File S3, Figs S1–S2, available online); 3) concatenated all-taxa data set including 87 taxa (including the outgroup) with a minimum

Table 1. DNA codes and specimen information used in this study for species of *Bacidia* and outgroup taxa, with their respective GenBank Accession numbers. New sequences are in bold.

DNA code (JG)	Name	Country	Specimen voucher/isolate	nrITS	nrLSU	mtSSU	*RPB*1	*RPB*2
	Bacidia absistens	Norway	*Ekman* 3223 (BG)	AF282085		MG925845	MG926139	MG926229
	B. albogranulosa	Czech Republic	*Vondrák* 17113 (PRA)	MK158339		MK158334		
	B. albogranulosa	Russia	*Malíček* 9622 (hb. Malíček)	MK158340		MK158335		
	B. albogranulosa	Czech Republic	*Vondrák* 11888 (PRA)	MK158342		MK158332		
	B. albogranulosa	Czech Republic	*Vondrák* 11889 (PRA)	MK158341		MK158333		
	B. albogranulosa	Czech Republic	*Malíček* 8013 (hb. Malíček)			MK158336		
	B. albogranulosa	Ukraine	*Vondrák* 12235 (PRA)			MK158337		
	B. albogranulosa	Czech Republic	*Vondrák* 12865 (PRA)			MK158338		
	B. arceutina	Sweden	*Ekman* 3110 (BG)	AF282083	MG926041	MG925846	MG926140	MG926230
	B. arceutina	Switzerland	*van den Boom* (LG DNA 579)	JQ796851	JQ796842	JQ796829		
	B. arceutina	United Kingdom	E:DNA:EDNA09-01505	FR799125				
	B. arceutina	United Kingdom	E:DNA:EDNA09-01507	FR799126				
	B. arceutina	United Kingdom	E:DNA:EDNA09-01587	FR799127				
JG037	*B. areolata*	Russia	*Gerasimova* M-0182592 (M)	MH048614		**MW506357**	**MW540434**	**MW522875**
JG114	*B. areolata*	Russia	*Davydov* 17428 & *Yakovchenko* (ALTB)	**MW491455**		**MW506358**		
	B. biatorina	Sweden	*Knutsson* 94-148 (hb. Knutsson)	AF282079				
JG083	*B. diffracta*	USA	*Wetmore* 46555-A (M)	MH048620				
	B. diffracta	USA	*Wetmore* 26401 (MIN)	AF282090				
	B. ekmaniana	USA	*Lendemer* 33836 (NY1538)			KX151741		
	B. ekmaniana	USA	*Lendemer* 33920 (NY1543)			KX151743		
	B. ekmaniana	USA	*Lendemer* 30488A (NY1454)			KX151746		
	B. ekmaniana	USA	*Lendemer* 31362 (NY1455)			KX151744		
	B. ekmaniana	USA	*Lendemer* 33783 (NY1537)			KX151745		
	B. ekmaniana	USA	*Lendemer* 34000 (NY1540)			KX151742		
JG007	*B. elongata*	Russia	*Ezhkin* M-0182571 (M)	MH048626				
JG101	*B. elongata*	Russia	*Ezhkin* M-0182625 (M)	MH048627	**MW493329**	**MW506351**	**MW540430**	**MW522870**
JG102	*B. elongata*	Russia	*Ezhkin* M-0182626 (M)	MH048628	**MW493330**	**MW506352**		**MW522871**
JG103	*B. elongata*	Russia	*Ezhkin* M-0182627 (M)	MH048629				
	B. fraxinea	Sweden	*Johansson* 1620 (BG)	AF282088				
	B. hostheleoides	United Kingdom	*Seaward* 108121 (priv. hb.)	AF282081				

(*Continued*)

Table 1. (*Continued*)

DNA code (JG)	Name	Country	Specimen voucher/isolate	GenBank Accession number				
				nrITS	nrLSU	mtSSU	*RPB*1	*RPB*2
JG092	*B. kurilensis*	Russia	*Ezhkin* M-0182620 (M)	MH048610	**MW493325**	**MW506348**	**MW540428**	**MW522868**
JG095	*B. kurilensis*	Russia	*Ezhkin* M-0182621 (M)	MH048611	**MW493326**			
JG096	*B. kurilensis*	Russia	*Ezhkin* M-0182622 (M)	MH048612				
JG091	*B. laurocerasi*	Russia	*Galanina* (424)	MH048609				
	B. laurocerasi subsp. *laurocerasi*	USA	*Wetmore* 74318 (MIN)	AF282078				
JG139	*B. obtecta*	Russia	*Ezhkin* M-0308498 (M)	**MW491457**	**MW493335**	**MW506362**		**MW522877**
JG140	*B. obtecta*	Russia	*Ezhkin* M-0308497 (M)	**MW491458**	**MW493336**	**MW506363**		**MW522878**
JG141	*B. obtecta*	Russia	*Ezhkin* M-0308496 (M)	**MW491459**				
	B. polychroa	Sweden	*Knutsson* 91-215 (hb. Knutsson)	AF282089				
	B. rosella	Sweden	*Ekman* 3117 (BG)	AF282086	AY300829	AY300877	AY756412	AM292755
JG085	*B. rubella*	Russia	*Gerasimova* M-0182581 (M)	MH048630	**MW493331**	**MW506353**	**MW540431**	
	B. rubella	Poland	AFTOL-ID 1793	HQ650644	DQ986793	DQ986808		DQ992422
	B. rubella	Switzerland	*van den Boom* (LG DNA 578)	JQ796852	JQ796843	JQ796830		
	B. rubella	Sweden	*Ekman* 3021 (BG)	AF282087		AY567723		
	B. rubella	Ukraine	*Vondrák* 12200 (PRA)	MK158343		MK158331		
	B. rubella	Switzerland	*van den Boom* (LG DNA 581)			JQ796831		
	B. rubella	Switzerland	LIFU076-16	KX132984				
	B. rubella	Hungary	*Hur* H06122	EU266078				
JG082	*B. sachalinensis*	Russia	*Ezhkin* M-0182619 (M)	MH048621				
JG097	*B. sachalinensis*	Russia	*Ezhkin* M-0182623 (M)	MH048622	**MW493333**	**MW506355**	**MW540433**	**MW522873**
JG098	*B. sachalinensis*	Russia	*Ezhkin* IMGIG 147	MH048623	**MW493334**	**MW506356**		**MW522874**
JG099	*B. sachalinensis*	Russia	*Ezhkin* IMGIG 148	MH048624				
JG100	*B. sachalinensis*	Russia	*Ezhkin* M-0182624 (M)	MH048625				
JG014	*B. schweinitzii*	Russia	*Gerasimova* M-0182579 (M)	**MW491454**	**MW493327**			
JG015	*B. schweinitzii*	Russia	*Gerasimova* M-0182580 (M)	MH048613	**MW493327**	**MW506350**	**MW540429**	**MW522869**
	B. schweinitzii	USA	*Wetmore* 72619 (MIN)	AF282080	MG926045		MG926146	MG926235
	B. schweinitzii	USA	AFTOL-ID 642	DQ782850	DQ782911	DQ972998	DQ782830	DQ782872
	B. schweinitzii	USA	AFTOL-ID 4969		KJ766527	KJ766354		
	B. schweinitzii	USA	*Shaheen* (NY1451)	MG461696				
	B. schweinitzii	USA	*Tripp* 2614 (NY1448)	KX151762		KX151750		

	B. schweinitzii	USA	*Lendemer* 29364 (NY1449)	KX151763		KX151751		
	B. schweinitzii	USA	*Lendemer* 31230A (NY1450)	KX151766				
	B. schweinitzii	USA	*Lendemer* 31238 (NY1451)	KX151764		KX151752		
	B. schweinitzii	USA	*Lendemer* 30548 (NY1452)	KX151761		KX151749		
	B. schweinitzii	USA	*Lendemer* 31855 (NY1453)	KX151765		KX151753		
	B. scopulicola	Sweden	*Ekman* 3106 (BG)	AF282084				
	B. sipmanii	Spain	*Sérusiaux* (LG DNA 361)	JQ796853	JQ796844	JQ796832		
	B. sorediata	USA	*Lendemer* 31692 (NY1389)	KX151768		KX151755		
	B. sorediata	USA	*Lendemer* 31527 (NY1397)	KX151771		KX151758		
	B. sorediata	USA	*Lendemer* 33702 (NY1539)	KX151767		KX151754		
	B. sorediata	USA	*Lendemer* 33787 (NY1544)	KX151772		KX151759		
	B. sorediata	USA	*Lendemer* 33869 (NY1546)	KX151773		KX151760		
	B. sorediata	USA	*Lendemer* 35031 (NY1747)	KX151769		KX151756		
	B. sorediata	USA	*Lendemer* 35386 (NY1748)	KX151770		KX151757		
	B. sorediata	USA	*Lendemer* 38909 (NY2294)	KX151774				
	B. sorediata	USA	*Barton* 658 (NY2496)	KX151775				
	B. squamulosula	Ecuador	*Kalb, Lich. Neotropici* No. 405 (SE-314)	MG925955	MG926051	MG925856	MG926152	
	B. suffusa	USA	*Wetmore* 74771 (MIN)	AF282091				
JG038	*B. suffusa*	Russia	*Gerasimova* M-0182593 (M)	MH048616		**MW506359**	**MW540435**	
JG039	*B. suffusa*	Russia	*Gerasimova* M-0182594 (M)	MH048617		**MW506360**		
JG051	*B. suffusa*	Russia	*Gerasimova* M-0182601 (M)	MH048615		**MW506361**		**MW522876**
JG080	*B. suffusa*	USA	*Tucker* 17000 (M)	MH048618				
JG081	*B. suffusa*	USA	*Wetmore* 40219 (M)	MH048619				
	B. suffusa	USA	*Lumbsch* 19190c (AFTOL-ID 5785)		KJ766528	KJ766355	KJ766836	
	B. thiersiana	USA	*Ekman* L1161 (LD)	AF282082				
	Sporacestra borbonica	Réunion	*Krog & Timdal* RE08,12 (isolate 1040)	MG925988	MG926086	MG925890	MG926184	
	S. pertexta	Cuba	*Pérez-Ortega* s. n. (isolate 511)	MG926000	MG926093	MG925903	MG926194	MG926268
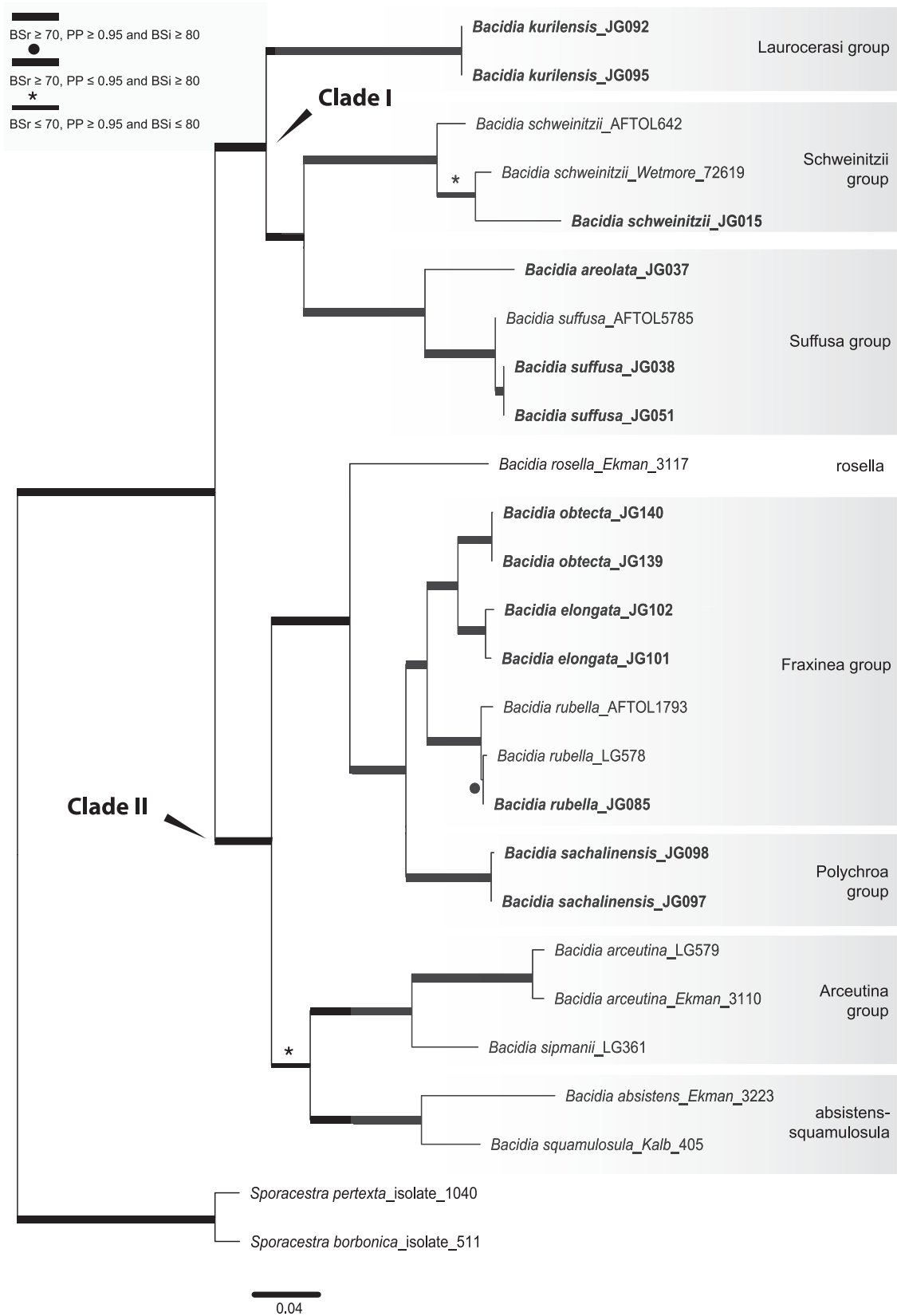
Fig. 1. Maximum likelihood (ML) tree of *Bacidia* s. str. resulting from the RAxML analysis of the concatenated multilocus data set with a minimum of three loci included (out of nrITS, nrLSU, mtSSU, *RPB*1 and *RPB*2). RAxML bootstrap values (BSr), Bayesian posterior probabilities (PP) and IQ-TREE bootstrap values (BSi) are indicated. Highly supported branches with BSr ≥ 70%, PP ≥ 0.95 and BSi ≥ 80% are marked in bold; strongly supported branches with BSr ≥ 70% and BSi ≥ 80% are also marked in bold with a black dot above the branch; branches with PP ≥ 0.95 are marked in narrower bold lines and a star above the branches. *Sporacestra* taxa are the outgroup. *Bacidia lutescens* is referred to as *B. thiersiana* in the text.

of one sequence available (both newly obtained and GenBank sequences) in order to include all specimens with sequences available (Fig. 2; Supplementary Material File S3, Figs S3–S4, available online).

Based on the support values of the phylogenetic analyses, no supported incongruence between the single-locus tree topologies was found; therefore, the concatenated alignment was analyzed. The number of taxa and alignment details for the single and concatenated data sets are summarized in Table 2. We used the multilocus alignment to produce a robust phylogeny, including the taxa with sequences from a minimum of three available loci. For comparison, we analyzed the all-taxa data set with all *Bacidia* s. str. specimens, even if only the sequence of a single locus was available.

The alignment with nrITS, nrLSU, mtSSU, *RPB*1 and *RPB*2 was subjected to Bayesian inference (BI) and maximum likelihood (RAxML and IQ-TREE) analyses for the single and concatenated data sets separately, as implemented in Gerasimova *et al.* (2021).

Substitution models for the entire (no-partitioned) concatenated and single-locus data sets were selected using jModelTest v.2 (Darriba *et al.* 2012) following the Akaike selection criterion (AIC). The best substitution model was selected in jModelTest with 1-, 2- and 6-model groups with additional options of independent state (nucleotide) frequencies, gamma-distributed rate variations across sites and a proportion of invariable sites (24 possible models).

Bayesian inference was carried out in MrBayes v.3.2.6 (Ronquist *et al.* 2012) using the Markov chain Monte Carlo method (MCMC) and GTR + I + G model. Two parallel runs were performed (two cold chains) with a single tree saved every 10th generation for a total of 1 000 000 generations. According to the trends in likelihood values, the convergence of the Markov chain was reached after 10 000 generations. As a result, the initial 10% was discarded as burn-in and the results summarized as a 50% majority-rule consensus tree.

Maximum likelihood (ML) analysis was performed with RAxML v.8.2.4 on the CIPRES web portal (Miller *et al.* 2010). The GTRGAMMA model with rapid bootstrap analysis searching for the best-scoring ML tree, using a majority-rule consensus tree and 1000 bootstrap iterations, was used for the entire data. The bipartition of the best-scoring tree was drawn onto the most likely tree topology following the recommendation of Stamatakis (2014).

Further tree reconstruction using ML analysis was performed in IQ-TREE v.1.6.12 using standard bootstrap approximation with 1000 bootstraps, specifying the GTR + I + G model as suggested by jModelTest (Nguyen *et al.* 2015).

The phylogenetic trees were visualized using FigTree v.1.4.2 (Rambaut 2009). The ML trees based on the different substitution models from single and concatenated data sets were congruent, therefore only the RAxML trees for the concatenated data sets are shown. Clades that received bootstrap support values (BSr) ≥ 70% in RAxML, posterior probabilities (PP) ≥ 0.95 in BI and bootstrap values (BSi) ≥ 80% in IQ-TREE were considered highly supported. The concatenated and individual gene trees obtained from RAxML, MrBayes and IQ-TREE are provided as Supplementary Material File S3 (Figs S1–S19).

Results

The BI and ML analyses for the single and concatenated data sets recovered highly concordant topologies of the phylogenetic trees. Both multilocus and all-taxa trees resulted in well-supported basal nodes (Figs 1 & 2).

Single-locus trees were congruent with the multilocus and all-taxa trees, but with high support in the terminal groups and low support in the backbone. All clades in the multilocus tree received strong support (i.e. with BSr ≥ 70%, PP ≥ 0.95 and BSi ≥ 80%) both in the terminal and deeper branches with only a small number of exceptions. The clade including *B. arceutina*, *B. absistens* and *B. squamulosula* was supported in BI (BSr/PP/BSi: 66/0.97/ 62); the subclade with two *B. rubella* from the RFE (JG085) and Switzerland (LG578) was supported in RAxML (BSr/PP/BSi: 87/ 0.75/71), and the subclade with *B. schweinitzii* from the RFE (JG015) and the USA (*Wetmore* 72619) was supported in BI only (BSr/PP/BSi: 56/0.99/61). The multilocus tree is congruent with the all-taxa phylogeny, forming the same groups with high support values (Fig. 2). The enlarged all-taxa phylogeny comprises all specimens with sequence data available; therefore, we discuss the groups in more detail based on this tree. According to phylogenetic results and morphological characters, six *Bacidia* s. str. groups are recognized: Laurocerasi, Schweinitzii, Suffusa, Fraxinea, Polychroa, and Arceutina. The separate lineages of 1) *B. ekmaniana* R. C. Harris *et al.*, *B. absistens* and *B. squamulosula*, and 2) *B. hostheleoides* and *B. thiersiana*, are discussed individually. Furthermore, a correlation between these phylogenetic groups and the apothecial pigments was observed (see Table 3 and Discussion).

The Laurocerasi group, consisting of the three lineages *B. biatorina* (Körb.) Vain., *B. kurilensis* Gerasimova *et al.* and *B. laurocerasi* (Delise ex Duby) Zahlbr., received strong support (BSr/ PP/BSi: 92/1.0/93).

Specimens of *B. schweinitzii* and *B. sorediata* Lendemer & R. C. Harris formed a paraphyletic clade (Schweinitzii group), comprising several separate clades with the highest support (BSr/PP/BSi: 99/1.0/100). Two subclades were present in *B. schweinitzii*, each containing an additional phylogenetic structure. One subclade, with high support (BSr/PP/BSi: 84/0.95/83), includes only GenBank sequences of *B. schweinitzii* from North America (AFTOL642 and NY). The second subclade contains both individuals from the RFE and North America and two subclades of *B. sorediata*, but without significant support (BSr/PP/ BSi: 40/0.8/46). Individuals of *B. schweinitzii* from the RFE (JG014 and JG015) were found in two groups in the ITS phylogeny (see Supplementary Material File S3, Figs S5–S7, available online). Given the differences in nrITS sequences (3% = 13 nucleotides), they probably belong to two independent species (see Discussion below). This is also supported by morphological observations which indicate differences in thallus and apothecial characters (details are summarized in Supplementary Material File S4, available online). The Schweinitzii group is sister to the Suffusa group; together, they form a well-supported clade (BSr/ PP/BSi: 78/1.0/79).

The clade containing *B. areolata* and *B. suffusa* (Fr.) A. Schneid. (Suffusa group) was highly supported (BSr/PP/BSi: 100/1.0/99). Two separate well-supported lineages in *B. suffusa* represent the North American and RFE populations. For two individuals from the USA, JG080 and JG081, only the nrITS2 sequences were available, most likely due to the age of the specimens (Gerasimova *et al.* 2018). However, compared to the RFE population, they already reveal variations in the relatively conserved nrITS2 region: four transitions at several positions, indicating a 2% difference. For another individual from the USA (AFTOL5785), the nrITS sequence is unavailable, but there are nrLSU, mtSSU and *RPB*1 sequences. In the mtSSU phylogeny, it also forms a separate lineage from the RFE individual, JG051,

Table 2. Overview of the numbers of taxa and newly produced sequences for each genetic marker and concatenated alignment for *Bacidia* in this study.

	nrITS	nrLSU	mtSSU	*RPB*1	*RPB*2	Multilocus data set	All-taxa data set
Number of taxa (including outgroup species)	75	24	55	17	17	26	87
Newly produced sequences	5	11	14	8	10	13	48
Length with gaps (bp)	434	850	783	639	1084	3786	3785
Parsimony informative sites	174	110	173	284	409	1111	1149

with a 3% (= three nucleotides) difference (Supplementary Material File S3, Figs S11–S13). The Suffusa group formed a strongly supported clade with the Schweinitzii and Laurocerasi groups (BSr/PP/BSi: 90/1.0/87).

The highly supported Fraxinea group (BSr/PP/BSi: 100/1.0/99) comprises sequences representing *B. fraxinea* Lönnr., *B. rubella*, *B. elongata* Gerasimova & A. Beck and a new lineage. Detailed morphological analysis showed that this lineage differs from recently known species in *Bacidia* s. str., forming the highly supported sister group to *B. elongata* (BSr/PP/BSi: 99/1.0/98). Consequently, *Bacidia obtecta* sp. nov. is described here.

The recently described *B. albogranulosa* Malíček et al. nested together with *B. polychroa* (Th. Fr.) Körb., *B. diffracta* S. Ekman and *B. sachalinensis* Gerasimova et al. (Polychroa group) with the highest support (BSr/PP/BSi: 100/1.0/99). The sister relationship with the *B. polychroa* lineage (Knutsson 91-215) received high support in the RAxML phylogeny (BSr/PP/BSi: 71/-/59) but recovered a polytomy in BI.

Bacidia ekmaniana is the sister group of *B. absistens* and *B. squamulosula*, but without significant support (BSr/PP/BSi: 56/0.77/63). Together with *B. arceutina*, *B. scopulicola* (Nyl.) A. L. Sm. and *B. sipmanii* M. Brand et al. (Arceutina group) they formed a well-supported clade in RAxML (BSr/PP/BSi: 71/0.77/68). In the multilocus phylogeny, the clade was highly supported in BI only (BSr/PP/BSi: 66/0.97/62). *Bacidia arceutina* from Switzerland (LG579) formed a separate lineage to individuals from the United Kingdom (FR799125–FR799127) and Sweden (*Ekman* 3110), with high support in the ML phylogenies (BSr/PP/BSi: 97/0.67/97). Compared to sequences from the United Kingdom, it contained a 1% (= five nucleotides) difference in nrITS and a 1% (= six nucleotides) difference in nrLSU. Likewise, the sequence from Sweden differed by 1% (= three nucleotides) in the mtSSU compared to one from Switzerland (LG579).

The basal clade with *B. thiersiana* and *B. hostheleoides* received high support but revealed long branches (BSr/PP/BSi: 85/0.96/85).

Three main clades were recovered in *Bacidia* s. str.: clade I comprises the Laurocerasi, Schweinitzii and Suffusa groups; clade II includes the Fraxinea, Polychroa, and Arceutina groups, and clades of *B. ekmaniana*, *B. absistens* and *B. squamulosula*; clade III, sister to the others, includes *B. thiersiana* and *B. hostheleoides*.

Discussion

The multilocus phylogeny resulted in groups congruent with previous results based on nrITS (Ekman 2001; Gerasimova et al.

2018), but significantly increased backbone support of the clades in both multilocus and all-taxa phylogenetic trees (Figs 1 & 2).

The phylogenetic trees group the taxa into two large clades: the first clade (I) includes the Laurocerasi, Schweinitzii and Suffusa groups, while the second clade (II) includes the Fraxinea, Polychroa, and Arceutina groups and clades of *B. ekmaniana*, *B. absistens* and *B. squamulosula*. In the phylogeny, they are represented by specimens from the temperate region and can be separated based on apothecial pigment (Table 3). The well-supported third clade (III) includes *B. thiersiana* and *B. hostheleoides*, which are widespread in south-eastern North America and the Neotropics, respectively (Malme 1935; Ekman 1996; Lendemer 2020).

Specimens in clade I have either dark brown, red-brown and green pigments (Laurocerasi-brown and Bagliettoa-green) or a combination of these in the upper part of the hymenium and lateral exciple (Table 3). In contrast, those in clade II have a mixture of yellow, orange and/or brown apothecial pigments (Arceutina-yellow, Polychroa-brown and Rubella-orange). An exception is a clade containing *B. absistens*, the pigmentation of which is highly variable (see groups below). Specimens in clade III are characterized by almost colourless or faintly and diffusely pigmented internal apothecial structures (Ekman 1996).

The taxon sampling in the phylogeny of *Bacidia* s. str. still needs to be completed; therefore, division of the clades based on the apothecial pigment is provisional. Given the available data, the main focus in this discussion is on representatives of *Bacidia* s. str. from the RFE. For convenience, the order of the groups corresponds to the position in the phylogenetic tree from top to bottom.

Laurocerasi group (including B. biatorina, B. kurilensis and B. laurocerasi clades)

Bacidia laurocerasi is one of the most widespread species of the group, occurring in Europe, Macaronesia, Africa, South and North America, Asia, Australia and New Zealand (Ekman 1996; Llop 2007; Coppins & Aptroot 2009). *Bacidia biatorina* is reported less frequently, and known collection localities include Europe, North America and Asia. In contrast, *B. kurilensis* is known only from the Kuril Islands and is considered endemic (Gerasimova et al. 2018). The phylogeny contains *B. biatorina* from Sweden, *B. laurocerasi* from North America and the RFE, and *B. kurilensis* from the RFE.

All three taxa share Laurocerasi-brown in the exciple and upper part of hymenium (Table 3). The mixture of Laurocerasi-brown and Bagliettoa-green found in the upper part of the

Fig. 2. Maximum likelihood (ML) tree of *Bacidia* s. str. resulting from the RAxML analysis of the concatenated all-taxa data set with a minimum of one sequence available (out of nrITS, nrLSU, mtSSU, *RPB*1 and *RPB*2). RAxML bootstrap values (BSr), Bayesian posterior probabilities (PP) and IQ-TREE bootstrap values (BSi) are indicated. Highly supported branches with BSr ≥ 70%, PP ≥ 0.95, and BSi ≥ 80% are marked in bold; strongly supported branches with BSr ≥ 70% and BSi ≥ 80% are also marked in bold with a black dot above the branch; branches with PP ≥ 0.95 are marked in narrower bold lines and a star above the branches; branches with PP ≥ 0.95, and/or BSr ≥ 70% and/or BSi ≥ 80% are marked with a white dot. *Sporacestra* taxa are the outgroup. *Bacidia lutescens* is referred to as *B. thiersiana* in the text.
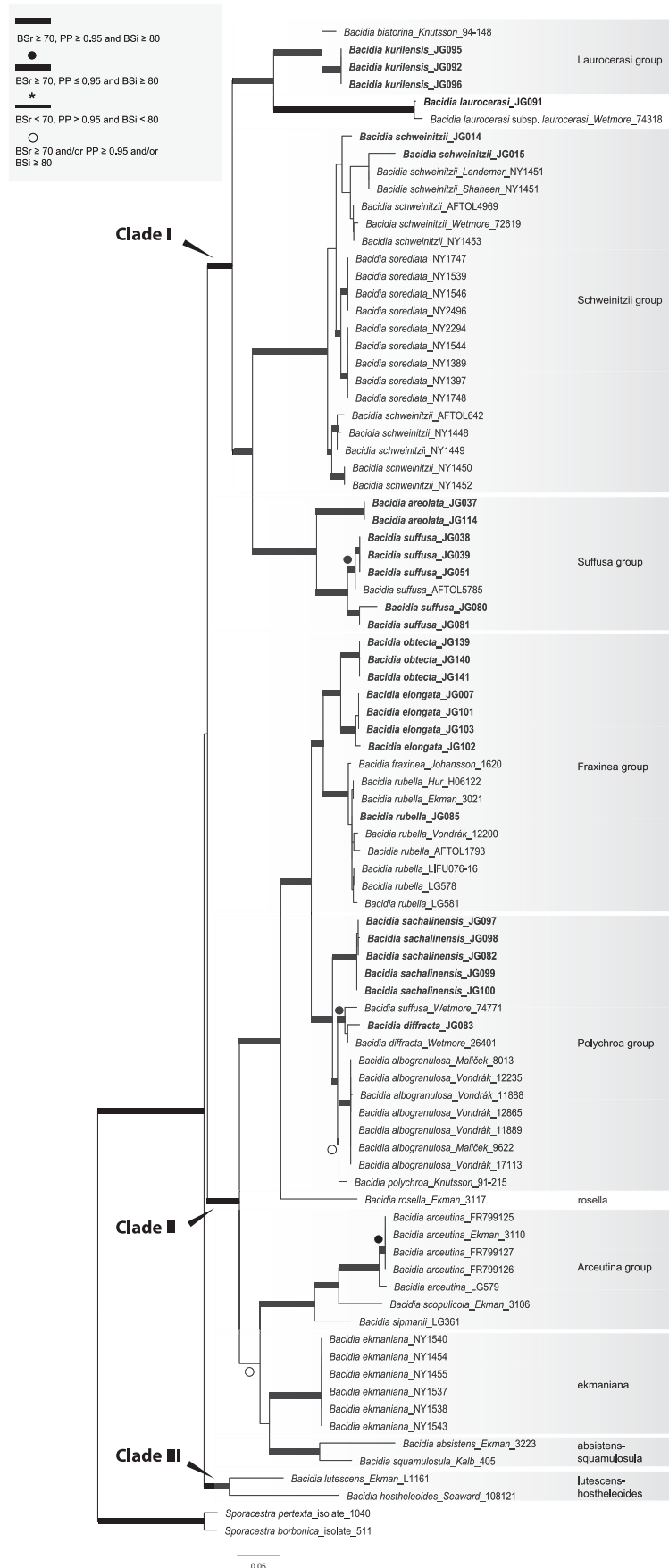
Table 3. Comparison of the pigmentation in the different phylogenetic groups in *Bacidia* s. str. as shown in Fig. 2. Pigment characterization follows Meyer & Printzen (2000) and Ekman (1996). The three parts of the table represent the pigmentation of the two major clades and separate lineages of *Bacidia* s. str.

Group	Upper hymenium	Exciple edge	Lateral exciple	Hypothecium
Laurocerasi	Laurocerasi-brown + Bagliettoa-green (in *B. kurilensis*)	Laurocerasi-brown	Laurocerasi-brown/ Rubella-orange	Arceutina-yellow
Schweinitzii	Bagliettoa-green	Bagliettoa-green	Schweinitzii-red	Schweinitzii-red
Suffusa	Laurocerasi-brown	Laurocerasi-brown	Rubella-orange	Rubella-orange
Fraxinea	Rubella-orange	Rubella-orange	Rubella-orange	Rubella-orange
Polychroa	Polychroa-brown	Rubella-orange	Rubella-orange	Rubella-orange
Arceutina	Arceutina-yellow	Arceutina-yellow	Arceutina-yellow	Arceutina-yellow
B. ekmaniana	Polychroa-brown	-	Rubella-orange	Rubella-orange
B. absistens	Bagliettoa-green/ Laurocerasi-brown	Bagliettoa-green	Laurocerasi-brown	Arceutina-yellow
B. squamulosula	Rubella-orange	-	Arceutina-yellow	Arceutina-yellow
B. gigantensis	Grey to grey-brown coloration	Arceutina-yellow	Arceutina-yellow	Arceutina-yellow
B. thiersiana	-	-	-	-
B. hostheleoides	No colour or small amounts of Rubella-orange	No colour or small amounts of Rubella-orange	No colour or small amounts of Rubella-orange	No colour or small amounts of Rubella-orange

hymenium in *B. kurilensis* remains unique in this group (Gerasimova *et al.* 2018).

All three lineages formed a strongly supported group that confirms our earlier results based on nrITS locus sequences. Two *B. laurocerasi* individuals formed a rather distant lineage from *B. biatorina* and *B. kurilensis*. However, as they all share the same pigment in the apothecia, we consider them to be one group.

Schweinitzii group (including B. schweinitzii and B. sorediata clades)

Bacidia schweinitzii occurs in the temperate forests of Canada around the Great Lakes and the Maritimes, in eastern Asia and the eastern parts of the USA, and the temperate region of the southern part of the RFE, in Primorskiy and Khabarovskiy Krai, and Kunashir Island (Ekman 1996; Lendemer *et al.* 2016; Gerasimova *et al.* 2018). *Bacidia sorediata* is so far known only from coastal south-eastern North America, particularly the Mid-Atlantic Coastal Plain (Lendemer *et al.* 2016).

The high variability in morphology of *B. schweinitzii* s. lat. has already been discussed in previous studies (Ekman 1996; Lendemer *et al.* 2016). Two morphotypes, sorediate and esorediate, were recognized based on morphology and were subsequently shown to be concordant with the molecular results, leading to the description of three new species (Lendemer *et al.* 2016). It has been shown that sequences within the *B. schweinitzii* group formed multiple clades within *B. schweinitzii* s. str. (esorediate populations) and *Bacidia sorediata* s. lat. (sorediate morphotype). Sequences derived from sorediate populations were grouped within two strongly supported clades, sister to each other but without support. Sequences derived from esorediate specimens were recovered in a series of clades whose relationships were poorly supported. Thus, data from the nrITS and mtSSU regions

appear to be insufficient to resolve the relationships between sorediate and esorediate populations with confidence.

The multilocus phylogeny presented here confirmed that *B. schweinitzii* is paraphyletic and contains lineages of several taxa. Nevertheless, not all branches within *B. schweinitzii* received high support values in both the multilocus and all-taxa phylogenies, maintaining unclear relationships within this group.

Two *B. schweinitzii* representatives, JG014 and JG015, form a grade and are not sister taxa in the ITS phylogeny (see Supplementary Material File S3, Figs S5–S7, available online). Instead JG015, having an abundantly granular thallus forming coral-like structures, was nested within the North American individuals. In addition, its apothecia are black, adpressed to the surface, with a brown to dark brown hypothecium merging into a darker brown exciple below and medullary part which does not form a distinct colourless zone. The spores are acicular and shorter with fewer septa, 37–46–50 × 2.5–3.5 µm, 5–7 septa (Fig. 3B & D; Supplementary Material File S4, available online). According to Lendemer *et al.* (2016), such specimens can be assigned to the 'typical' *B. schweinitzii* morph by the granular thallus and apothecial coloration.

In contrast, JG014 has morphological characters that do not clearly match any species currently recognized in the *B. schweinitzii* group. Morphological observation demonstrated that it differs in the ±smooth to warted thallus; black caliciform apothecia, which rise above the surface; dark brown hypothecium merging into the dark brown-red exciple (K+ purplish), which forms a distinct colourless zone in the lateral part and the base of the medulla; acicular spores, 56–69–80 × 2.5–3.0 µm, 7–15 septa (Fig. 3A & C; Supplementary Material File S4). *Bacidia ekmaniana* also forms a distinct colourless zone in the lateral and medullary parts, in a similar way to JG014, but differs by having orange-brown apothecia and a lighter orange-brown hypothecium and exciple (K+ darker brown). It is thus likely that JG014 belongs to a different species. However,
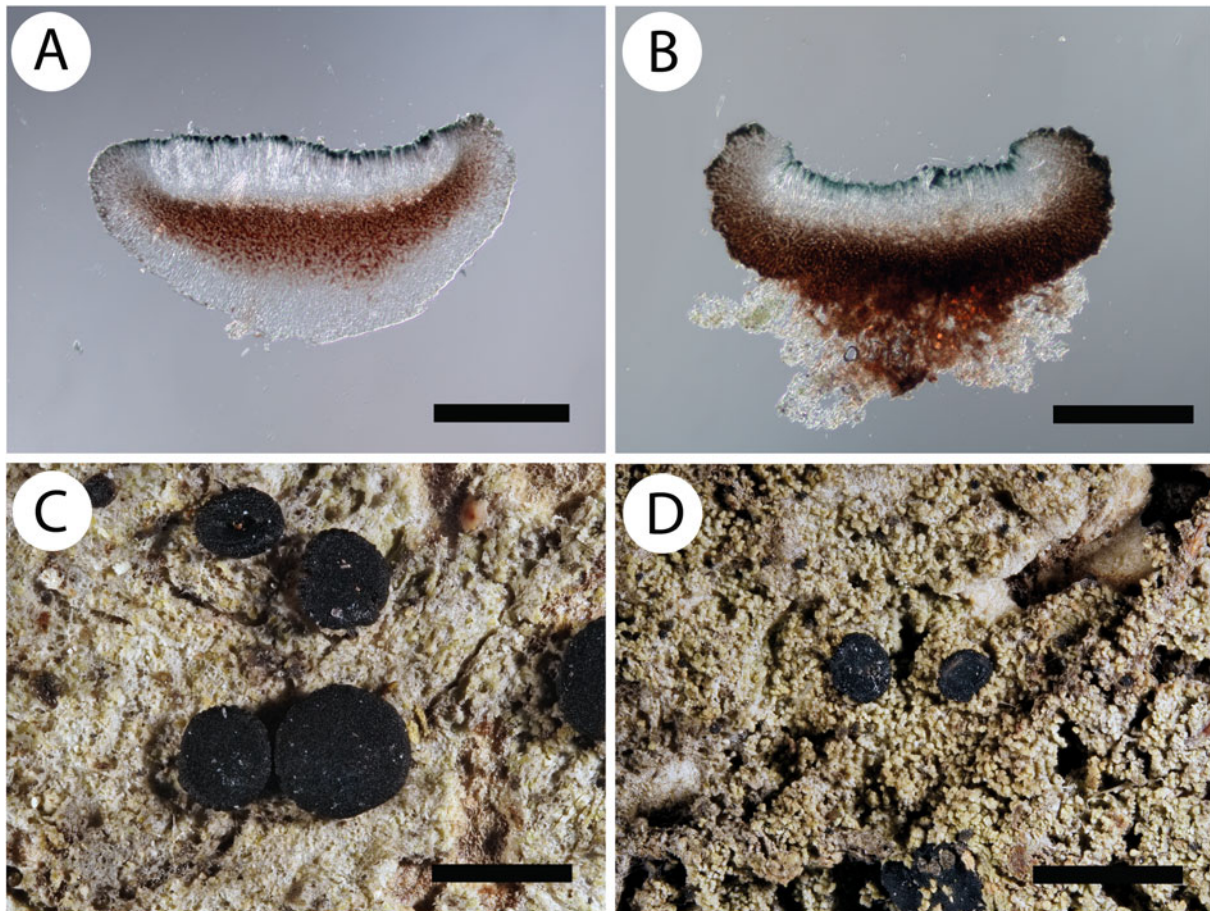
Fig. 3. Cross-sections of apothecia and thallus structure of two individuals of *Bacidia schweinitzii*. A & C, M-0182579 (JG014). B & D, M-0182580 (JG015). A, dark brown hypothecium, merging into the coloration of exciple below. Exciple forms a distinct colourless zone in the lateral and medullary part. B, brown hypothecium merging into the coloration of the exciple. Dark brown exciple not forming a distinct colourless zone. C, thallus smooth to warted, consisting of single or contiguous ±roundish warts. D, thallus granular, consisting of ±globose to subsquamulose granules. Scales: A & B = 200 μm; C & D = 1 mm. In colour online.

further details and careful investigation of all the type material and specimens from GenBank are necessary for making a comprehensive description and species delimitation; therefore, we currently refrain from describing new entities.

Suffusa group (including B. areolata and B. suffusa clades)

Bacidia suffusa s. lat. occurs in the eastern temperate region of North America, in the North Caucasus and the RFE (Ekman 1996; Gerasimova *et al.* 2018). *Bacidia areolata* is known from the RFE and considered endemic. The phylogeny contains the sequences from North America and the RFE.

The specimens of *B. areolata* and *B. suffusa* formed a strongly supported clade and share Laurocerasi-brown in the exciple edge and upper part of the hymenium. Since our first molecular study, additional sequences of *B. suffusa* from the USA have been submitted to GenBank (AFTOL5785), including nrLSU, mtSSU and *RPB*1 sequences (Table 1). As the two individuals from the USA, JG080 and JG081, are represented by short sequences of nrITS2 only, the relationship to the other *B. suffusa* from North America remains unclear. Nevertheless, *B. suffusa* from the RFE formed a separate lineage from the ones collected in North America in the combined and single-locus trees based on nrLSU, mtSSU and *RPB*1 sequences. We could not study the individual from GenBank and suggest including more specimens

from North America and other regions. Thus, we consider individuals of *B. suffusa* from the RFE and North America as different populations but belonging to the same species.

The newly sequenced specimen of *B. areolata* (JG114) represents the second occurrence of this species. Compared to the type specimen (JG037, M-0182592), it also has three layers of enlarged lumina cells along the edge of the exciple. The thallus structure, apothecial pigment and measurements are also in the range found in the type specimen. Nevertheless, JG114 differs from the type specimen by the lack of any pruina on the apothecial margin and the presence of abundant colourless crystals in the lateral exciple, dissolving in KOH with the following colour changes: green → yellow → colourless.

Fraxinea group (including B. obtecta, B. elongata, B. rubella and B. fraxinea clades)

The most widespread taxon of the group, *B. rubella*, has a Holarctic distribution and is known from Europe, Macaronesia, Africa, Asia and North America (Ekman 1996; Llop 2007; Coppins & Aptroot 2009). *Bacidia fraxinea* is less frequent and occurs in eastern parts of north and central Europe and the northern Mediterranean region (Ekman & Nordin 1993). In contrast, both *B. elongata* and *B. obtecta* are known only from Sakhalin and can be considered endemic (Gerasimova *et al.* 2018).

Table 4. Main characters separating *Bacidia obtecta* from the closely related *B. elongata* and *B. fraxinea*. Measurements for *B. fraxinea* are based on those from Ekman & Nordin (1993) and measurements of *B. elongata* from Gerasimova *et al.* (2018). Quantitative information of our measurements is given as (min–) average ± SD (–max), while that for *B. fraxinea* was taken from the original manuscript.

	B. obtecta	*B. elongata*	*B. fraxinea*
Thallus	Thick, wrinkled, warted; grey-green to yellowish green	Thin to thick, smooth to areolate, wrinkled and warted; grey to dark grey-green	Thin and almost smooth to thick and verrucose, areolate or irregularly cracked, grey
Apothecial colour	Beige to rusty brown	Orange to dark purple-brown	Orange-brown to dark brown
Margin	Paler than disc, beige to pale brown, distinct; with pruina	Concolorous with or paler than disc, light orange; with pruina	Concolourous with disc; with or without pruina
Apothecial size (mm)	(0.4–)0.85 ± 0.25(–1.5)	(0.25–)0.55 ± 0.15(–0.95)	0.6–1.1
Crystals in exciple	Throughout lateral part of exciple and upper hymenium; K+, N−	Without or with clusters of crystals in exciple; N+, K−	With or without radiating clusters of minute crystals in exciple rim; N+, K−
Hypothecium	Orange-brown	Colourless, pale yellow to orange-brown	Straw-coloured to pale orange
Number of enlarged lumina cells along exciple edge	Up to 4 layers	Up to 4 layers	Without or with single cell layer
Size (μm)	Up to 5 × 13	Up to 7 × 20	Up to 6 × 6
Ascospore length (μm)	(47–)61.2 ± 7.0(–79)	(39–)59 ± 8(–80)	(42–)50–67–85(–109)
Ascospore width (μm)	(2.0–)3.0 ± 0.36(–4.0)	(2.0–)2.5 ± 0.5(–4.0)	(2.5–)2.6–3.0–3.4(–4.3)
Number of septa	(1–)6 ± 2(–11)	(2–)5–7–12(–16)	5–17

The phylogeny contains specimens of *B. rubella* from Europe and the RFE, *B. fraxinea* from Europe, and *B. elongata* and *B. obtecta* from the RFE. The phylogeny recovered the whole clade with high support, but the relationship between *B. rubella* and *B. fraxinea* remains unclear. The only sequence of *B. fraxinea* (*Johansson* 1620) was nested together with other *B. rubella* included in the analysis. Therefore, more specimens of *B. fraxinea* need to be studied.

All four taxa share Rubella-orange in the upper part of the hymenium, hypothecium and exciple. Moreover, they all have a similar coloration of the apothecia (orange to orange-brown), often with white pruina along the margin. Three taxa, *B. obtecta*, *B. elongata* and *B. fraxinea*, are characterized by smooth, warted to wrinkled thalli. This contrasts with the granular thallus of *B. rubella*.

Recent studies showed that *B. elongata* forms a separate entity sister to *B. fraxinea*, differing in its exciple structure that usually has up to four layers of enlarged lumina cells (Gerasimova *et al.* 2018). This feature is also characteristic of the closely related and newly described *B. obtecta*, whereas *B. fraxinea* and *B. rubella* have only a single layer of enlarged lumina cells. Compared with *B. elongata*, *B. obtecta* has abundant colourless crystals in the upper part of the hymenium and lateral exciple, and spores with fewer septa (a detailed description is provided under Taxonomy and in Table 4).

Polychroa group (including B. albogranulosa, B. polychroa, B. diffracta and B. sachalinensis clades)

Bacidia polychroa represents the most widespread species of the group, occurring in Europe, North and South America, and Asia (Ekman 1996; Llop 2007; Coppins & Aptroot 2009). The known collection localities of *B. albogranulosa* include the Czech Republic, Poland, Russia (Caucasus) and Ukraine (Malíček *et al.* 2018). *Bacidia diffracta* and *B. sachalinensis* are endemics and are so far known from North America and the RFE, respectively

(Ekman 1996; Gerasimova *et al.* 2018). The phylogeny contains *B. polychroa* from Sweden, *B. albogranulosa* from Europe, *B. diffracta* from North America, and *B. sachalinensis* from the RFE.

The phylogeny recovered the whole clade with high support and is concordant with the previous results of Gerasimova *et al.* (2018), who provide a detailed discussion. All taxa within the clade share Polychroa-brown in the hypothecium, exciple and hymenium, the K+ purplish reaction in apothecial cross-sections. However, this reaction is unknown for the recently described *B. albogranulosa* since it is known only in its sterile form (Malíček *et al.* 2018).

Arceutina group (including B. arceutina, B. scopulicola and B. sipmanii clades)

Bacidia arceutina is the most widespread epiphytic species of the group. The known collection localities include Europe, Asia and North America (Coppins & Aptroot 2009). In contrast, *B. scopulicola* and *B. sipmanii* are almost exclusively epilithic, occurring in coastal Europe from Scandinavia to the Azores, and in North America (Coppins & Aptroot 2009). The phylogeny includes the specimens of all three taxa collected in Europe.

All three taxa share Arceutina-yellow in the apothecial structures. So far, none of the three species have been observed from the RFE. *Bacidia arceutina* from Switzerland formed separate lineages from those originating in the United Kingdom (FR799125-FR799127) and Sweden (*Ekman* 3110). However, given the low genetic differentiation in nrITS, nrLSU and mtSSU (1% in each), we regard them as conspecific.

Clades including B. ekmaniana, B. absistens and B. squamulosula

Bacidia ekmaniana is known from south-eastern North America, occurring from the Appalachian Mountains to the Coastal Plain
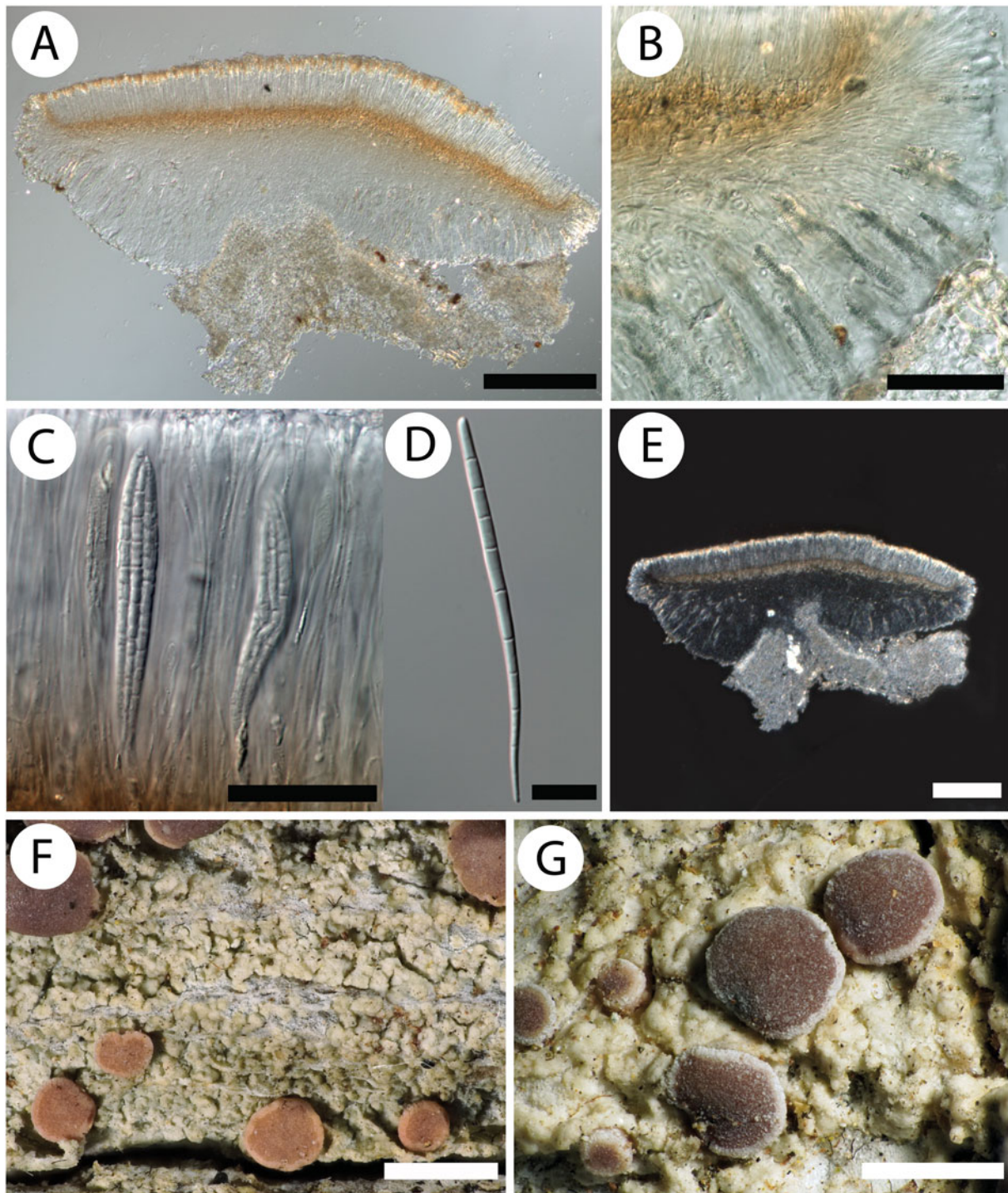
Fig. 4. Cross-section of apothecium and thallus structure of *Bacidia obtecta* (M-0308496, holotype). A, cross-section of apothecium. B, clusters of crystals radially arranged in the lateral part of the exciple. C, asci with ascospores. D, acicular multiseptate ascospore. E, crystals in the cross-section of apothecium visualized using polarized light. F, general overview of apothecia and thallus structure. G, detailed view of apothecia and thallus structure. Thallus wrinkled, irregularly shaped. Rusty brown apothecia with scurfy surface and white pruina along the margin. Scales: A, B & E = 200 μm; C = 50 μm; D = 20 μm; F & G = 1 mm. In colour online.

and southern Interior Highlands (Lendemer *et al.* 2016). The known distribution of *B. absistens* includes Europe, Macaronesia, Africa, Asia and North America (Ekman 1996; Coppins & Aptroot 2009; Gerasimova 2016), whereas *B. squamulosula* is known from South and North America (Dahl 2017; McMullin *et al.* 2020).

Bacidia ekmaniana and *B. squamulosula* share a mixture of Rubella-orange and Arceutina-yellow in the apothecia, a feature

they share with other taxa from clade II (Table 3). In contrast, the pigmentation in *B. absistens* is highly variable. It may contain a mixture of Bagliettoa-green, Laurocerasi-brown or grey coloration in the upper hymenium and exciple edge (Gerasimova 2016). Thus, the pigmentation of *B. absistens* is unique in this clade. The significant morphological variation in this species requires further study, involving more specimens.

The recently published *B. gigantensis* formed a sister clade to *B. absistens* and *B. squamulosula* in the original publication of McMullin *et al.* (2020) and the relationships of these taxa are discussed in detail there. *Bacidia gigantensis* has grey to grey-brown coloration in the upper hymenium and exciple, also observed in *B. absistens* (Gerasimova 2016). The three taxa, *B. absistens*, *B. gigantensis* and *B. squamulosula* contain secondary compounds, 4-O-methylcryptochlorophaeic and homosekikaic acids. This is unusual and is not known for any other *Bacidia* s. str., which contain atranorin as the main secondary compound (Ekman 1996). In addition, all three taxa are characterized as having minute colourless crystals in the exciple.

Clade including *B. thiersiana* and *B. hostheleoides*

Bacidia thiersiana (deposited as *Bacidia lutescens* in GenBank) is widespread in south-eastern North America, while *B. hostheleoides* is widely distributed in the Neotropics (Malme 1935; Ekman 1996; Lendemer 2020). *Bacidia thiersiana* is characterized by having some oil droplets in the hypothecium and by the production of lobaric acid, both unique characters in *Bacidia* s. str. phylogeny. Both taxa are characterized by almost colourless or faintly and diffusely pigmented internal apothecial structures (Ekman 1996; Lendemer 2020). However, *B. hostheleoides* has small amounts of Rubella-orange in the proper exciple, hypothecium and hymenium when pigmented (Ekman 1996).

These taxa belong to a well-supported clade with long branches, most likely resulting from incomplete species sampling rather than a genuine relationship. Therefore, further sampling in this group is still required to draw reliable conclusions.

Taxonomy

Bacidia obtecta Gerasimova, A. Ezhkin & A. Beck sp. nov.

MycoBank No.: MB 838949

Similar to *Bacidia elongata* but differs by abundant colourless crystals in the upper part of the hymenium and lateral exciple, dissolving in KOH, and by having spores with fewer septa.

Type: Russia, Sakhalin, Tymovskiy District, valley of the Tym River, Zonal'noye village surroundings, 51°04′42.6899″N, 142°44′25.8756″E, *c.* 100 m a.s.l, floodplain forest, on the bark of *Populus maximowiczii*, 4 June 2017, *A. K. Ezhkin* [B4/02.2018] (M M-0308496—holotype; UPS, SAK 1368—isotypes).

(Fig. 4)

Thallus indefinite, continuous or discrete, relatively thick, wrinkled, sinuous, consisting of scattered or continuous wrinkled, irregularly shaped or ±convex warts, grey, grey-green to yellowish green. *Prothallus* white. *Photobiont* chlorococcoid.

Apothecia (0.4–)0.85 ± 0.25(–1.5) mm, ±plane when young, soon becoming markedly convex, then margin is excluded; disc pruinose, with scurfy/incrusted surface; margin of young and medium-aged apothecia often with thick white pruina. *Disc* beige, pale orange, orange-brown to rusty brown. *Margin* distinct, always paler than disc, beige or pale brown. *Epithecium* colourless, interspersed with abundant colourless crystals between the paraphysis apices, less than 1 μm. *Exciple* laterally 86–94.3–98 μm high, with abundant colourless crystals, less than 1 μm. *Rim* pale to intense straw-coloured, along the edge with up to four

layers of enlarged lumina cells that are 3–5 μm wide and 5–13 μm long. *Lateral part* pale to intense straw-coloured or yellow. *Medullary part* of the same colour as lateral part, downwards almost colourless. *Hymenium* 73.5–108–135 μm high. *Hypothecium* pale to intense orange-brown (Rubella-orange). *Paraphyses* simple, thin, colourless, sometimes bifurcate, 1.0–1.5 μm wide, ±clavate or only slightly swollen at the apices, 1.5–3.0 μm, without internal pigment. *Ascospores* acicular, straight, $(47–)61.2 ± 7.0(–79)$ μm long $(n_1 = 88, n_2 = 3)$, $(2.0–)3.0 ± 0.36(–4.0)$ μm wide $(n_1 = 88, n_2 = 3)$, with $(1–)6 ± 2(–11)$ septa $(n_1 = 88, n_2 = 3)$.

Pycnidia not observed.

Pigments. Hypothecium K+ intensifying or yellowish, exciple C+ and N+ yellow, subsequently becoming colourless. Rubella-orange in hypothecium and exciple. Crystals dissolve in K, forming the following reaction: green → yellow → colourless; do not dissolve in N or C.

Etymology. Apothecial disc covered with pruina on top, which gives a 'powdery' appearance.

Habitat and distribution. The specimens were collected in the floodplain forest in river valleys on the bark of *Chosenia arbutifolia* and *Populus maximowiczii*. So far, known only from Sakhalin. Probably endemic to the island.

Comments. *Bacidia obtecta* is similar to *B. elongata* and *B. fraxinea* but differs in several distinct features, summarized in Table 4. Compared to *B. elongata* and *B. fraxinea*, it is distinguished by the apothecial colour, which is mainly brown to rusty brown, abundant colourless crystals in the upper part of the hymenium and lateral exciple, which dissolve in KOH but not in HNO₃, and spores with fewer septa. From *B. fraxinea* it can be additionally distinguished by the number of enlarged lumina cells along the exciple edge.

Additional specimens examined. **Russia:** *Sakhalin*: Tymovskiy District, valley of Pilenga River, Adotymovo village surroundings, 51°02′07.6236″N, 142°49′26.5692″E, *c.* 160 m a.s.l, floodplain forest, on bark of *Populus maximowiczii*, 5 vi 2017, *A. K. Ezhkin* [B2/02.2018; GPS 547] (M M-0308497, SAK 1365); *ibid.*, valley of Tym River, Zonal'noye village surroundings, 50°38′51.2951″N, 142°45′48.2868″E, *c.* 160 m a.s.l, floodplain forest, on bark of *Chosenia arbutifolia*, 6 vi 2017, *A. K. Ezhkin* [B1/02.2018; GPS 551] (M M-0308498, SAK 1362).

Author ORCIDs. Julia V. Gerasimova, 0000-0002-3212-3596; Aleksandr Ezhkin, 0000-0002-2242-2250; Andreas Beck, 0000-0003-2875-4464.

References

Andersen HL and Ekman S (2005) Disintegration of the *Micareaceae* (lichenised *Ascomycota*): a molecular phylogeny based on mitochondrial rDNA sequences. *Mycological Research* **109**, 21–30.

Beck A and Mayr C (2012) Nitrogen and carbon isotope variability in the green-algal lichen *Xanthoria parietina* and their implications on mycobiont-photobiont interactions. *Ecology and Evolution* **2**, 3132–3144.

Coppins BJ and Aptroot A (2009) *Bacidia* De Not. 1846. In Smith CW, Aptroot A, Coppins BJ, Fletcher A, Gilbert OL, James PW and Wolseley PA (eds), *Lichens of Great Britain and Ireland*. London: British Lichen Society, pp. 189–207.

Dahl MS (2017) *Molecular systematics and taxonomy of* Sporacestra *and relatives (*Ramalinaceae, Ascomycota*)*. Master's thesis, University of Oslo.

Darriba D, Taboada GL, Doallo R and Posada D (2012) jModelTest 2: more models, new heuristics and parallel computing. *Nature Methods* **9**, 772.

Edgar RC (2004) MUSCLE: multiple sequence alignment with high accuracy and high throughput. *Nucleic Acids Research* **32**, 1792–1797.

Ekman S (1996) The corticolous and lignicolous species of *Bacidia* and *Bacidina* in North America. *Opera Botanica* **127**, 1–148.

Ekman S (2001) Molecular phylogeny of the *Bacidiaceae* (*Lecanorales*, lichenized *Ascomycota*). *Mycological Research* **105**, 783–797.

Ekman S and Nordin A (1993) The taxonomy of *Bacidia fraxinea* and its relationship to *B. rubella*. *Annales Botanici Fennici* **30**, 77–82.

Ekman S, Andersen HL and Wedin M (2008) The limitations of ancestral state reconstruction and the evolution of the ascus in the *Lecanorales* (lichenized *Ascomycota*). *Systematic Biology* **57**, 141–156.

Gerasimova JV (2016) *Bacidia absistens* (Nyl.) Arnold (*Ramalinaceae*, *Lecanorales*) in Russia: nomenclature, description, ecology, and distribution. *Turczaninowia* **19**, 88–93. [In Russian].

Gerasimova JV and Ekman S (2017) Taxonomy and nomenclature of seven names in *Bacidia* (*Ramalinaceae*, *Lecanorales*) described from Russia. *Phytotaxa* **316**, 292–296.

Gerasimova JV, Ezhkin AK and Beck A (2018) Four new species of *Bacidia* s.s. (*Ramalinaceae*, *Lecanorales*) in the Russian Far East. *Lichenologist* **50**, 603–625.

Gerasimova JV, Urbanavichene IN, Urbanavichus GP and Beck A (2021) Morphological and phylogenetic analyses of *Toniniopsis subincompta* s. lat. (*Ramalinaceae*, *Lecanorales*) in Eurasia. *Lichenologist* **53**, 1–13.

James TY, Kauff F, Schoch CL, Matheny PB, Hofstetter V, Cox CJ, Celio G, Gueidan C, Fraker E, Miadlikowska J, *et al.* (2006) Reconstructing the early evolution of *Fungi* using a six-gene phylogeny. *Nature* **443**, 818–822.

Kistenich S, Timdal E, Bendiksby M and Ekman S (2018) Molecular systematics and character evolution in the lichen family *Ramalinaceae* (*Ascomycota*: *Lecanorales*). *Taxon* **67**, 871–904.

Lendemer JC (2020) *Bacidia thiersiana* (*Ramalinaceae*), a new species with lobaric acid widespread in southeastern North America. *Bryologist* **123**, 39–47.

Lendemer JC, Harris RC and Ladd D (2016) The faces of *Bacidia schweinitzii*: molecular and morphological data reveal three new species including a widespread sorediate morph. *Bryologist* **119**, 143–171.

Liu YJ, Whelen S and Hall BD (1999) Phylogenetic relationships among ascomycetes: evidence from an RNA polymerase II subunit. *Molecular Biology and Evolution* **16**, 1799–1808.

Llop E (2007) *Lecanorales*: *Bacidiaceae*: *Bacidia* y *Bacidina*. *Flora Liquenológica Ibérica* **3**, 1–49.

Lumbsch HT, Schmitt I, Palice Z, Wiklund E, Ekman S and Wedin M (2004) Supraordinal phylogenetic relationships of *Lecanoromycetes* based on a Bayesian analysis of combined nuclear and mitochondrial sequences. *Molecular Phylogenetics and Evolution* **31**, 822–832.

Malíček J, Palice Z, Vondrák J, Łubek A and Kukwa M (2018) *Bacidia albogranulosa* (*Ramalinaceae*, lichenized *Ascomycota*), a new sorediate lichen from European old-growth forests. *MycoKeys* **44**, 51–62.

Malme GOA (1935) *Bacidiae* itineris Regnelliani primi. *Arkiv för Botanik* **27A**, 1–40.

McMullin RT, McCune B and Lendemer JC (2020) *Bacidia gigantensis* (*Ramalinaceae*), a new species with homosekikaic acid from the north shore of Lake Superior in Ontario, Canada. *Bryologist* **123**, 215–224.

Meyer B and Printzen C (2000) Proposal for a standardized nomenclature and characterization of insoluble lichen pigments. *Lichenologist* **32**, 571–583.

Miadlikowska J, Kauff F, Hofstetter V, Fraker E, Grube M, Hafellner J, Reeb V, Hodkinson BP, Kukwa M, Lücking R, *et al.* (2006) New insights into classification and evolution of the *Lecanoromycetes* (*Pezizomycotina*, *Ascomycota*) from phylogenetic analyses of three ribosomal RNA- and two protein coding genes. *Mycologia* **98**, 1088–1103.

Miadlikowska J, Kauff F, Högnabba F, Oliver JC, Molnár K, Fraker E, Gaya E, Hafellner J, Hofstetter V, Gueidan C, *et al.* (2014) A multigene phylogenetic synthesis for the class *Lecanoromycetes* (*Ascomycota*): 1307 fungi representing 1139 infrageneric taxa, 317 genera and 66 families. *Molecular Phylogenetics and Evolution* **79**, 132–168.

Miller MA, Pfeiffer W and Schwartz T (2010) Creating the CIPRES Science Gateway for inference of large phylogenetic trees. In *Proceedings of the Gateway Computing Environments Workshop (GCE), 14 November 2010, New Orleans, Louisiana*, pp. 1–8.

Nguyen LT, Schmidt HA, von Haeseler A and Minh BQ (2015) IQ-TREE: a fast and effective stochastic algorithm for estimating maximum-likelihood phylogenies. *Molecular Biology and Evolution* **32**, 268–274.

Rambaut A (2009) FigTree v.1.3.1. [WWW resource] URL http://tree.bio.ed.ac.uk/software/figtree/.

Reese Næsborg R, Ekman S and Tibell L (2007) Molecular phylogeny of the genus *Lecania* (*Ramalinaceae*, lichenized *Ascomycota*). *Mycological Research* **111**, 581–591.

Rehner SA and Samuels GJ (1994) Taxonomy and phylogeny of *Gliocladium* analysed from nuclear large subunit ribosomal DNA sequences. *Mycological Research* **98**, 625–634.

Ronquist F, Teslenko M, van der Mark P, Ayres DL, Darling A, Höhna S, Larget B, Liu L, Suchard MA and Ronquist JP (2012) MrBayes 3.2: efficient Bayesian phylogenetic inference and model choice across a large model space. *Systematic Biology* **61**, 539–542.

Sérusiaux E, van den Boom PPG, Brand MA, Coppins BJ and Magain N (2012) *Lecania falcata*, a new species from Spain, the Canary Islands and the Azores, close to *Lecania chlorotiza*. *Lichenologist* **44**, 577–590.

Stamatakis A (2014) RAxML version 8: a tool for phylogenetic analysis and post-analysis of large phylogenies. *Bioinformatics* **30**, 1312–1313.

Vilgalys R and Hester M (1990) Rapid genetic identification and mapping of enzymatically amplified ribosomal DNA from several *Cryptococcus* species. *Journal of Bacteriology* **172**, 4238–4246.

White TJ, Bruns T, Lee S and Taylor JW (1990) Amplification and direct sequencing of fungal ribosomal RNA genes for phylogenetics. In Innis MA, Gelfand DH, Sninsky JJ and White TJ (eds), *PCR Protocols: a Guide to Methods and Applications*. New York: Academic Press, pp. 315–322.

Zahlbruckner A (1921–1940) *Catalogus Lichenum Universalis*. Band I–X. Leipzig: Gebrüder Borntraeger.

Zoller S, Scheidegger C and Sperisen C (1999) PCR primers for the amplification of mitochondrial small subunit ribosomal DNA of lichen-forming ascomycetes. *Lichenologist* **31**, 511–516.

Chapter 5

High diversity of Type I Polyketide Genes in *Bacidia rubella* as revealed by the comparative analysis of 23 lichen genomes

Julia V. Gerasimova, Andreas Beck, Silke Werth and Philipp Resl

High Diversity of Type I Polyketide Genes in *Bacidia rubella* as Revealed by the Comparative Analysis of 23 Lichen Genomes

Julia V. Gerasimova [1,2,*] **, Andreas Beck** [1,2] **, Silke Werth** [1,†] **and Philipp Resl** [1,3,†]

1   Systematics, Biodiversity and Evolution of Plants, LMU Munich, 80638 Munich, Germany; beck@snsb.de (A.B.); werth@bio.lmu.de (S.W.); philipp.resl@uni-graz.at (P.R.)

2   Botanische Staatssammlung München, SNSB-BSM, 80638 Munich, Germany

3   Institute of Biology, University of Graz, 8010 Graz, Austria

*   Correspondence: jgerasimova@lmu.de; Tel.: +49-89-17861-268

†   These authors contributed equally to this work.

Abstract: Fungi involved in lichen symbioses produce a large array of secondary metabolites that are often diagnostic in the taxonomic delimitation of lichens. The most common lichen secondary metabolites—polyketides—are synthesized by polyketide synthases, particularly by Type I PKS (TI-PKS). Here, we present a comparative genomic analysis of the TI-PKS gene content of 23 lichen-forming fungal genomes from Ascomycota, including the de novo sequenced genome of *Bacidia rubella*. Firstly, we identify a putative atranorin cluster in *B. rubella*. Secondly, we provide an overview of TI-PKS gene diversity in lichen-forming fungi, and the most comprehensive Type I PKS phylogeny of lichen-forming fungi to date, including 624 sequences. We reveal a high number of biosynthetic gene clusters and examine their domain composition in the context of previously characterized genes, confirming that PKS genes outnumber known secondary substances. Moreover, two novel groups of reducing PKSs were identified. Although many PKSs remain without functional assignments, our findings highlight that genes from lichen-forming fungi represent an untapped source of novel polyketide compounds.

Keywords: lichen; secondary compounds; comparative genomics; fungi; polyketide synthases (PKS); Type I PKS

1. Introduction

Fungi synthesize an extensive array of chemically and functionally diverse natural products, termed secondary metabolites, with roles in defense, self-protection and development [1,2]. Based on their properties and the core enzymes and precursors involved in their biosynthesis, four major groups of fungal secondary metabolites are distinguished: polyketides, non-ribosomal peptides (NRPS), terpenoids and tryptophan derivatives [3]. Most fungal secondary metabolites are encoded by genes located adjacent to each other (i.e., "clustered") in the genome [2,4].

In lichen-forming fungi, polyketides are the most common class of secondary metabolites [5,6]. Although lichen polyketides can be produced by mycobionts grown axenically under appropriate conditions [7–10], they are usually formed in intact symbioses [11,12]. Many lichen polyketides are synthesized by Type I polyketide synthases (TI-PKS) [13], the closest structural and functional analogue of which is the mammalian fatty acid synthase [14]. In the minimal configuration, the domain structure of TI-PKSs always includes a ketoacyl synthase (KS), an acyltransferase (AT), and an acyl carrier protein (ACP). These domains are essential for polyketide synthesis [3]. This configuration can be supplemented with domains such as starter unit-ACP transacylase (SAT), ketoreductase (KR), dehydratase (DH), enoyl reductase (ER), methyltransferase (CMeT), and thioesterase (TE) [3].

The presence of optional domains has led to the classification of fungal PKSs into three subgroups based on their ability to perform redox reactions. The first subgroup

comprises non-reducing (NR) PKSs, which lack reductive domains and mainly produce aromatic polyketides [13,15]. The second subgroup contains partially reducing (PR) PKSs, typically having a single KR or a KR and DH domain. Finally, reducing (R) PKSs contain a complete set of reductive domains, viz. KR, DH, and ER. All three subgroups can be found in lichen-forming fungi. Previous work suggests various ecological roles of polyketides in lichens ranging from light-screening and chemical weathering to allelopathic effects and herbivore defense [3,6,16,17]. More broadly, secondary metabolite profiles including polyketides are often characteristic of taxonomic groups and are thus extensively used to identify lichens.

The first PKS gene from a lichen-forming fungus was cloned and analyzed by Armaleo et al. in 2011 [18], and in recent years secondary metabolite research has benefited from genome mining approaches in bacteria, fungi, and plants, uncovering hidden diversity (e.g., [19–21]). The fact that genes encoding natural product biosynthetic pathways are often clustered in the genome [2] facilitates the identification of biosynthetic gene clusters (BGCs) in whole genome sequences. In many cases, the chemical structure of their products can be predicted from the biosynthetic logic of enzymes encoded in a BGC and their similarity to known counterparts [22–25]. Despite this progress, the biosynthetic genes for most secondary metabolites of lichen-forming fungi remain uncharacterized. Observations that lichen-forming fungi contain more biosynthetic genes than characterized chemical compounds also complicates clear gene assignments to particular metabolites. Consequently, previous studies have focused only on a few well-known compounds, e.g., usnic acid, grayanic acid, and atranorin (e.g., [18,25–29]). However, the increasing availability of lichen-forming fungal genomes provides a largely untapped resource for identifying additional biosynthetic genes [30].

Here, we investigate the diversity of BGCs in the de novo sequenced *Bacidia rubella* (Hoffm.) A. Massal. (Ramalinaceae) genome within a two-level comparative genomic framework. We aim to identify genes involved in the biosynthesis of atranorin, a secondary metabolite present in many lichens including *B. rubella.* To achieve this, we examine the secondary metabolite biosynthetic potential of *B. rubella* by comparing its genome to that of Ramalinaceae species: *Bacidia gigantensis*, *Ramalina intermedia* and *R. peruviana*. The secondary metabolites of these four closely-related species are known, and the chemical substance profiles overlap. This facilitates comparison of the presence, absence and structure of PKS genes, and enables the evaluation of BGCs for previously characterized genes, including those encoding for atranorin biosynthesis. We then extend this comparative approach to include an additional nineteen, publicly available fungal genomes from the Lecanoromycetes. Most of these genomes were obtained from pure cultures, with high genome completeness and little contamination. By employing an in-silico approach combined with phylogenetic reconstructions of previously characterized sequences, we gain insight into the putative functions of TI-PKS BGCs in lichen-forming fungi. Our comparative genomic results are congruent with previous work, indicating a high diversity of BGCs in lichen-forming fungi that extends beyond what can be observed from chemical profiles (e.g., [9,25]). This sheds new light on the potential of lichen–forming fungi to produce different secondary metabolites, with direct relevance for natural product research and production.

2. Materials and Methods

2.1. In Vitro Cultivation of the Bacidia rubella Mycobiont

The lichen-forming fungus *Bacidia rubella* was axenically cultivated from a specimen collected from Germany (Bavaria, Lkr. Neuburg-Schrobenhausen, Markt Rennertshofen, south-east of Bertoldsheim, Naturwaldreservat "Mooser Schütt"; mixed forest, on bark of the trunk of *Fraxinus* sp., ca. 1.0 m above the ground, ca. 400 m asl.; M-0307710) in April 2019. The mycobiont culture was obtained from a multispore discharge of a single apothecium of *B. rubella* following the method of Yoshimura et al. [31]. Briefly, young and middle-aged apothecia were detached from the thallus and soaked in sterile water for about

an hour. Then, they were fixed to the top of a Petri dish lid using petroleum jelly while keeping the lid slightly open to let the apothecia dry slowly. We used Bold's Basal Media (BBM) with doubled nitrate (25 g/L) as an initial substrate. Upon germination, the spores were transferred to a malt-yeast extract medium (Lichen medium) [32]. The mycobiont cultures were stored in a growth chamber (Wachstumsschrank Binder KBWF 720; Binder GmbH, Tuttlingen) at 16 °C and 60% relative humidity. They were subcultured every two to three months until a sufficient biomass for genomic analysis was obtained (ca. one year).

2.2. DNA Isolation and Sequencing

To obtain concentrated high-molecular-weight genomic DNA, about 1 cm^2 of mycelium was taken and ground in liquid nitrogen with a pre-cooled pistil. Genomic DNA was isolated using the MagAttract HMW DNA Kit following the manufacturer's protocol and subsequent purification steps with magnetic beads (HMW genomic DNA from fresh or frozen tissue protocol), resulting in a total yield of 1 µg. The final concentration was 9.53 ng/µL, measured with a NanoDrop 1000 spectrophotometer (Peqlab Biotechnologie, GmbH, Erlangen, Germany) and Qubit 4 Fluorometer (ThermoFisher Scientific, Waltham, MA, USA) using 1X dsDNA HS Assay Kits. DNA extraction, PCR amplification and Sanger sequencing (using nrITS primers) were performed to evaluate possible contamination and confirm the cultures' identities. First, a paired-end library was constructed using Illumina DNA Prep (earlier known as Nextera DNA Flex Library Prep) and sequenced on NovaSeq 6000 (NovaSeq SP 150 bp Paired-end Flow Cell, Illumina) at the Biomedical Sequencing Facility (BSF, Vienna, Austria). A total concentration of 0.2 µg was used for Illumina library preparation. To supplement the Illumina data, we prepared several Oxford Nanopore libraries using the SQK-LSK109 kit and sequenced them on a MinION sequencer using R9.4.1 flow cells (altogether, four runs were conducted). The total yield of DNA was in the range of 0.12–0.31 µg.

2.3. Data Generation and Initial Read-Quality Assessment

To obtain a high-quality genome, we used a hybrid assembly approach using Illumina short-reads and Oxford Nanopore long reads. In total, we produced 17 Gbp of raw paired-end Illumina reads with 500× coverage. Raw data inspection with FastQC v0.11.7 [33] indicated high-quality reads (quality score (Q) above 34) and no excessive adapter contamination or read duplication. Basecalling of Nanopore raw signals was performed using Flappie v2.1.3 (git commit 4de542f; https://github.com/nanoporetech/flappie) into a total of 22 Gbp of raw sequences up to 94.5 Kb of read length.

2.4. Genome Completeness and Quality Assessment

The paired-end Illumina reads and unpaired nanopore reads were assembled using hybridSPAdes [34] with k-mer sizes of 33, 55, 77 and 127. To examine the assembly for potential non-target contigs, de novo assembly was subjected to BLASTX using DIAMOND [35] against a custom database comprising the protein sets of the NCBI nr database (downloaded in July 2018). The results of this DIAMOND search were used as input for blobtools v1.1.1 [36]. The final results showed the absence of foreign contigs; therefore, further filtering was unnecessary. The quality of the assembly and genome statistics were assessed using QUAST v5.0.2 [37]. The completeness of the genomes was assessed using all single-copy BUSCO genes of the ascomycota_odb9 set (part of the phylociraptor pipeline; git commit 4cfd3c4; accessed on 2 July 2021; see below).

2.5. Dataset Construction

The dataset consists of the de novo sequenced genome of *B. rubella* and twenty-two additional representative genomes of Lecanoromycetes, the largest radiation of lichen-forming fungi. We included in our study twenty-three genomes obtained from pure fungal cultures with the exception of *B. gigantensis* and *R. intermedia*, which were obtained by sequencing the whole thallus (Table 1). The dataset aims to identify known and possible

unknown BGCs placing them together with previously characterized PKSs from other fungi and bacteria. The genomes were downloaded using phylociraptor, which automatically downloads genomes from NCBI and combines them with additionally specified genomes provided by the user [38]. We kept the original taxon names from NCBI for convenience, even though the current taxonomic status might differ.

Table 1. Starting material, sequencing strategy and genome quality statistics of Ramalinaceae genomes analyzed in this study.

Nuclear Genome	*Bacidia rubella*	*Bacidia gigantensis*	*Ramalina intermedia*	*Ramalina peruviana*
Substrate	bark	bark	rock	twig
Growth form	crustose	crustose	fruticose	fruticose
Source	Axenic culture	Whole thallus	Whole thallus	Axenic culture
Sequencing method	Illumina NovaSeq SP; MinION	PromethION 24	Illumina MiSeq	Illumina MiSeq
Raw reads produced	17 Gbp; 22 Gbp (roughly)	32 Gbp	13.33 Gbp	-
Coverage	500×	500×	290×	2.0×
Assembly size (Mb)	33.52	33.11	26.19	25.53
Largest scaffold (bp)	2,353,056	3,530,911	898,913	694,821
Average scaffold (bp)	657,358	1,379,912	148,821	25,764
Number of scaffolds	51	24	176	991
N50	1,771,855	1,807,239	282,362	43,940
GC (%)	45.28	44.67	51.90	50.58
Num of predicted genes	8773	8451	7405	6756
Num of predicted proteins	8728	8400	7355	6706
Number of unique proteins	2514	2343	1099	1088
tRNAs	45	51	50	50
Proteins with at least one ortholog	5860	5711	6111	5467
Single-copy orthologs	2345	2345	2345	2345
Secreted proteins (SignalP)	678	612	464	384

2.6. Genome Annotation

The publicly available genomes were sequenced with different sequencing technologies at different times and are thus of varying quality. To make annotations comparable, we performed ab initio gene calling and functional annotations for all of them. The downloaded genomes were analyzed using the smsi-funannotate (https://github.com/reslp/smsi-funannotate; git commit 398a144; accessed on 4 June 2021) pipeline based on funannotate v.1.8.7 [39]. First, we removed duplicated identical contigs (funannotate clean) in each assembly. To avoid long contig/scaffold names, we sorted our assembly by contig length and then renamed the fasta headers (funannotate sort). Afterwards, we made a soft repeat masking of the assembly using tantan (funannotate mask) [40]. The following steps included gene prediction using the gene-callers Augustus v3.3.2 [41], snap [42], GlimmerHMM v3.0.4 [43] and Genemark ES v4.68 [44]. For Augustus, we used *Aspergillus nidulans* as a pre-trained species. All the pipelines were run on the cluster of the University of Graz and our in-house Linux Server at LMU Munich. The genome statistics are summarized in Table 4 (See Section 3.2. Biosynthetic Gene Composition in Twenty-Three Annotated Fungal Genomes). The output files of the newly annotated genomes from NCBI and JGI used in this study are available on figshare (http://doi.org/10.6084/m9.figshare.19487837).

2.7. Annotation of Biosynthetic Gene Clusters

The identification, annotation and analysis of secondary metabolite BGCs in the studied fungal genome sequences were performed with antiSMASH v6.0 as a part of the smsi-funannotate pipeline and thus all BGC numbers are referred to antiSMASH prediction. We chose all BGCs from the annotation results that contained orthologous core TI-PKSs for our comparative genomic and phylogenetic analyses. The GBK output files with annotated BGCs and predicted genes were visualized on the antiSMASH webserver (fungal version; accessed: November 2021) [45].

2.8. Identification of Atranorin Biosynthetic Gene Cluster and Phylogeny

To identify atranorin candidate genes, we downloaded sequences from PKS16 of *Cladonia grayi* (GenBank: ADM79459; 2089 aa) and PKS23 of *Stereocaulon alpinum* (GenBank: QXF68953; 2500 aa). Both PKSs were previously reported as possible candidates involved in the biosynthesis of atranorin (see Section 3.1.1 Atranorin in Section 3 Results and Discussion for details). As atranorin synthesis involves an oxidation, the cluster must contain a cytochrome P450 as well as additional genes, *O*-methyltransferase (OMT), and transporter gene [29]. The presence of these genes was verified by our annotation results, showing OMT (PF08241), cytochrome P450 (PF00067), and transporter gene (PF00400) present in the putative atranorin BGC in *B. rubella*. The gene arrows plot, comparing two atranorin clusters in *Bacidia rubella* and *Cladonia rangiferina*, was drawn using the gggenes v0.4.1 R package (https://github.com/wilkox/gggenes/; accessed on 20 April 2022).

We used BLASTP v2.9.0+ [46] to detect the orthologs of those characterized sequences in all PKS sequences we identified on the twenty-three studied genomes. We filtered BLAST output to retain sequences with a minimum identity of 30% over the alignment length and a minimum query coverage of 50%, sorted for the highest bit score and lowest e-value. Additionally, we used the best blast subject hits with the highest percent similarity to the query gene. The best hits from the blast results (>30%) were selected for the PKS23 alignment. The taxon selection was confirmed with the clade from the large TI-PKS phylogenetic tree.

We aligned the 29 identified amino acid sequences using MAFFT v7.480 [47] and calculated the maximum likelihood using IQ-TREE v2.1.4 [48] with 1000 ultrafast bootstrap replicates, after selecting the best-fitting substitution model (LG+G8+F) with ModelFinder [49]. The final alignment comprised 29 sequences from 16 taxa, with 2320 amino acid sites, 2071 distinct patterns, 1756 parsimony-informative, 221 singleton sites, and 343 constant sites.

2.9. Topology Test to Confirm Atranorin Biosynthetic Genes

Our maximum-likelihood phylogeny recovered the *B. rubella* (Ramalinaceae) atranorin gene (bacrubpred_000804) as sister to a clade comprised of *Cladonia rangiferina* and *S. alpinum* (claranpred_005882 and QXF68953, respectively), which both belong to Cladoniaceae. Miadlikowska et al. [50] recovered Parmeliaceae as the closest relative of Cladoniaceae, with a clade of these two families being sister to Ramalinaceae. Thus, we tested if the monophyly of a clade comprising *Bacidia* + Cladoniaceae is significantly supported against the expected phylogenetic relationship comprising Parmeliaceae + Cladoniaceae. For this, we compared (1) an unconstrained ML tree to recover *Bacidia* + Cladoniaceae as monophyletic, and (2) a constrained tree with *Bacidia* sister to Cladoniaceae + Parmeliaceae (Figure 1).
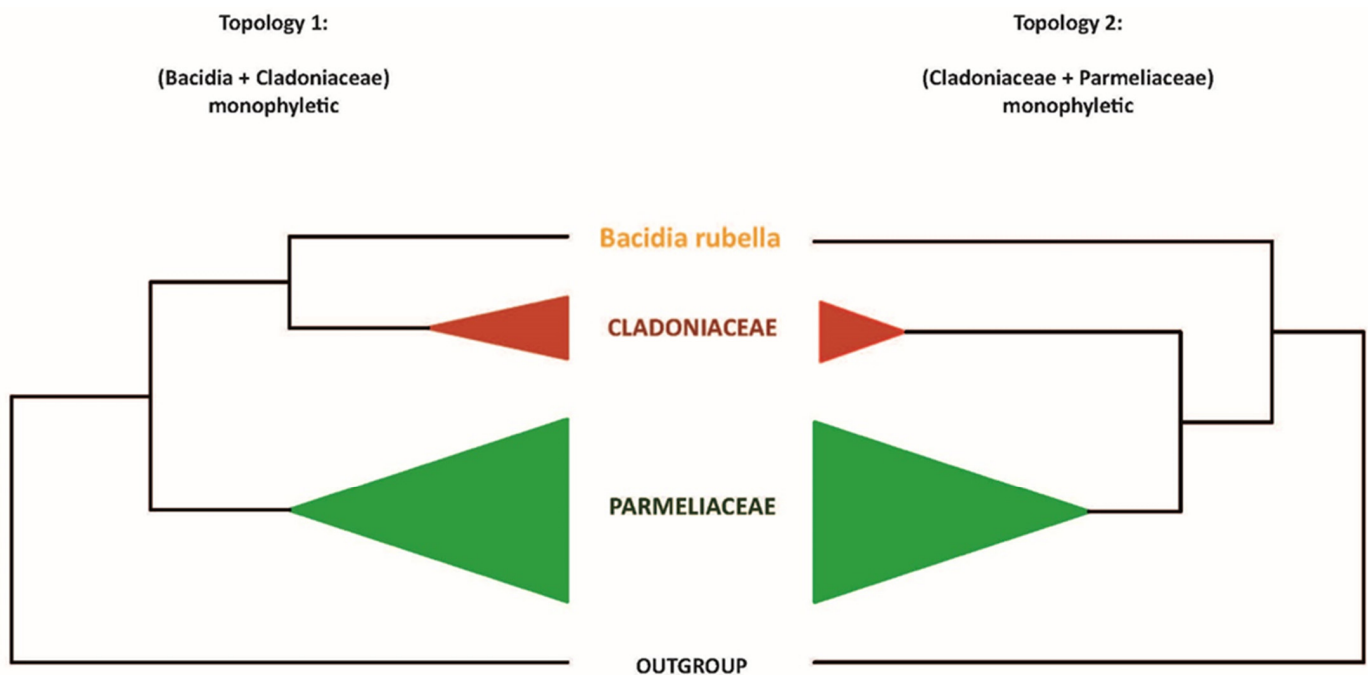
Figure 1. Two alternative topologies used for comparison in the topology test. Topology 1, recovering *Bacidia* + Cladoniaceae as monophyletic; Topology 2, recovering Cladoniaceae + Parmeliaceae as monophyletic.

For the topology test, we used PKS23 sequences in the strict sense, i.e., from the species known as atranorin produces with *Gyalolechia flavorubescens* and *Xanthoria elegans* as outgroups. The constrained tree can be multifurcating and need not contain all species; therefore, finally, we shortened our tree to the taxa we wanted to test. First, we performed a constrained search for both topologies using the LG model for the amino acid dataset. Then, we concatenated both trees and implemented tree topology tests, based on the Kishino-Hasegawa test [51], Shimodaira–Hasegawa test [52], Expected Likelihood Weight [53], and approximately unbiased (AU) test [54] using IQ-TREE (-m LG -z concatenated_trees.treels -n 0 -zb 10,000 -au). We considered tree topology to be unlikely if its test *p*-value was <0.05 (marked with a "-" sign). The trees were visualized and examined using FigTree 1.3.1 [55].

2.10. Identification of Orthologues and Orthogroups with BUSCO and OrthoFinder

Orthofinder uses a hybrid approach based on sequence similarity estimated by a BLAST all-vs-all search with DIAMOND and subsequent reconstruction of gene trees and a species tree to identify (single copy) orthologs and paralogs. To identify orthologues of extracted PKSs, we inferred orthogroups with Orthofinder v2.5.4 [56] for (1) all predicted proteins and (2) all extracted TI-PKSs, independently. The independent runs for two datasets were conducted to check for the concordance of the final results. As the results were not contradictory, we discussed the result of TI-PKS only. The Markov Cluster (MCL) inflation parameter was set up by default (1.5). The trees utilized by Orthofinder were reconstructed using Fasttree v2.1.10 (-m msa, -A muscle, and -S diamond (default)) [57].

2.11. Type I Iterative PKS Alignment

We performed a phylogenetic analysis of all TI-PKSs identified in twenty-three studied genomes of Lecanoromycetes, to assess the relationship of non-reducing PKSs (NR-PKS) and reducing PKSs (R-PKS) (including partly reducing PKSs). First, we prepared a list of all identified TI-PKS based on our functional annotations. We retrieved the sequences based on the corresponding gene ID numbers included in the gff3 file of each genome using a custom python script (select_transcript.py: https://github.com/reslp/genomics/blob/master/select_transcripts.py; accessed on 13 October 2021). We included predicted

ketoacyl synthase (KS) amino acid alignment reported by Kroken et al. [14] to enhance our dataset. The inclusion of reference PKSs enables us to compare the tree topology proposed in Kroken et al. [14] to our larger sampling of putative PKS genes.

All TI-PKS sequences were combined into a single file and aligned using MAFFT v7.480 [47]. We chose the E-INS-i alignment strategy because it performs better when aligning sequences with several conserved motifs interspersed in long, unalignable regions. We trimmed the alignment using trimAl v.1.4.rev15 [58]. Initial testing of different trimming settings (e.g., -gappyout, -strict, and -automated), showed that parameter combination (-gt 0.70 -resoverlap 0.70 -seqoverlap 60) is a good trade-off between removing ambiguously aligned sites and keeping phylogenetically informative sites of the PKS sequences. The final data matrix consisted of 624 amino acid sequences with 1049 amino acid sites, 1049 distinct patterns, and 1043 parsimony-informative sites from 61 taxa (23 studied genomes and 38 other fungal and bacterial taxa from Kroken et al. [14]). In addition, PKS23 from *Stereocaulon alpinum* (QXF68953) and PKS16 from *Cladonia grayi* (ADM79459) from NCBI were included. The alignment is available on figshare (http://doi.org/10.6084/m9.figshare.19487837).

We selected the best-fitting substitution model (LG+F+G4) according to the Akaike and Bayesian Information Criteria using the ModelFinder implemented in IQ-TREE [49] on our TI-PKS alignment. We calculated a phylogenetic tree using maximum-likelihood (ML) analysis implemented in IQ-TREE v2.1.4 [48], with 1000 ultrafast bootstrap replicates [59]. We also calculated a tree using RAxML-NG v1.0.3 [60] with parameters –all –bs-trees 100 –model LG+F+G4 –threads 16 –data-type AA. The inferred phylogenetic tree was then rooted with Bacterial Type II polyketide sequences using phyx [61].

To compare the congruence of the trees, we utilized Dendroscope v3.7.6 [62] using Tanglegram (Algorithms). The resulting tree was visualized using FigTree 1.3.1 [55] and a custom R script, with additional annotations added in Adobe Illustrator v24.0.3.

3. Results and Discussion

3.1. General Characteristics of De Novo Bacidia rubella Genome

We report the de novo assembled genome of the lichen-forming fungus *Bacidia rubella* obtained from an axenic fungal culture. Our hybrid approach to sequencing, using Illumina short-read with Oxford Nanopore long-read, resulted in a high-quality genome assembly of *B. rubella*. The final assembly had a size of 33.52 Mb in 51 scaffolds, an N50 of 1.77 Mb (Table 1), and was 98% BUSCO complete (fungi_odb9). Using multiple ab-initio gene-calling methods, 8773 genes were identified (Table 1). The similarity of standard genome metrics between *B. rubella* and *B. gigantensis* [63] suggests a high-quality *B. rubella* genome (Table 1).

The genome of *B. rubella* contains 31 BGCs (Table 2), including six non-reducing and four reducing TI-PKS sequences. This TI-PKS biosynthetic arsenal is similar to that of *B. gigantensis*, containing 11 identified TI-PKS genes (seven NR-PKSs and four R-PKSs, respectively; Table 2). Despite the overall similarity of TI-PKS gene numbers in *B. rubella* and *B. gigantensis*, our BLAST-based comparison of these biosynthetic clusters showed only two significant hits between the two species: one for R-PKS (bacgigpred_003963 and bacrubpred_000636), and one for NR-PKS (bacgigpred_008278 and bacrubpred_000202), with 62.8 and 63% similarity in amino-acid sequences, respectively. This result is not surprising, given that both fungal species differ in their secondary metabolite profiles. The only secondary compound of *B. rubella* is atranorin, which is the most widespread secondary metabolite found in the genus *Bacidia* s. lat. (Ekman 1996) [64]. In contrast, *B. gigantensis* is currently the only known *Bacidia* species to produce homosekikaic acid [65].

Table 2. Overview of biosynthetic gene clusters and polyketide synthase families found in the twenty-three studied fungal genomes. The occurrence of the major secondary substance of *B. rubella*, atranorin, is highlighted. All sequences except the de novo sequenced *B. rubella* genome are from NCBI, if not otherwise specified in the first column.

| Species (NCBI)	Species Tag	Genome Size (Mb)	No of Clusters	Type I PKS (Total)	Type I NR-PKS	Type I R-PKS	PR-PKS	Hybrid PKS-NRPS	NRPS/ Putative NRPS	Metabolites Reported
Alectoria sarmentosa (ASM973377v1)	alesarpred	39.5	36	12	5	7	0	1	2/12	Usnic acid, alectoronic acid (major), thamnolic, squamatic and barbatic acids
Bacidia gigantensis (ASM1945646v1)	bacgigpred	33.1	31	11	7	4	0	1	5/10	Homosekikaic acid
Bacidia rubella (this study)	bacrubpred	33.5	31	10	6	4	0	0	3/7	**Atranorin**
Cladonia grayi (JGI: Cgr/DA2myc/ ss v2.0)	clagrapred	34.4	48	21	8	12	1	0	2/11	4-O-demethylgrayanic acid, colensoic acid, confumarprotoce-traric acid, divaronic acid, fumarprotocetraric acid, grayanic acid, protocetraric acid, stenosporonic acid
Cladonia macilenta (Clmac_v1)	clamacpred	36.8	55	25	15	10	0	2	3/9	Thamnolic acid, barbatic acid, didymic acid, squamatic acid, usnic acid, rhodocladonic acid
Cladonia metacorallifera (KoLRI002260_v2)	clametpred	36.6	51	24	10	14	0	1	1/11	Usnic acid, didymic acid, squamatic acid, rhodocladonic acid
Cladonia rangiferina (ASM614605v1)	claranpred	34.5	68	34	14	20	0	2	3/12	**Atranorin**, protocetraric acid, fumarprotocetraric acid
Cladonia uncialis (ASM292778v1)	clauncpred	30.7	61	30	15	14	1	2	1/11	Usnic acid, squamatic acid
Cyanodermella asteris (Astra)	cyaastpred	28.6	35	11	5	5	1	1	3/10	Astin, skyrin
Dibaeis baeomyces (JGI)	dibbaepred	34.2	55	27	11	15	1	0	4/14	Baeomycic acid, squamatic acid
Endocarpon pusillum (Z07020)	endpuspred	36.2	32	14	4	9	1	1	3/4	Not reported
Evernia prunastri (ASM318436v1)	eveprupred	40.2	86	36	16	19	1	4	3/20	Usnic acid, **atranorin**, and chloroatranorin, evernic acid
Graphis scripta (JGI: CBS 132367)	grascrpred	34.8	54	21	6	15	0	1	6/14	Not reported
Gyalolechia flavorubescens (KoLRI002931)	gyaflapred	34.4	41	16	8	8	0	1	3/8	Parietin, emodin, fallacinal, fragilin
Lasallia hispanica (ASM325442v1)	lashispred	39.7	28	15	8	6	1	1	0/3	Gyrophoric acid, lecanoric acid, umbilicaric acid, skyrin
Lasallia pustulata (ASM863619v1)	laspuspred	32.9	26	17	9	7	1	0	0/4	Gyrophoric acid, lecanoric acid, hiascinic acid, skyrin
Letharia columbiana (Lecol_v1.0)	letcolpred	52.2	43	14	7	7	0	2	3/6	Vulpinic acid and **atranorin**

Table 2. *Cont.*

Species (NCBI)	Species Tag	Genome Size (Mb)	No of Clusters	Type I PKS (Total)	Type I NR-PKS	Type I R-PKS	PR-PKS	Hybrid PKS-NRPS	NRPS/ Putative NRPS	Metabolites Reported
Letharia lupina (Lelup_v1.1)	letluppred	49.2	48	18	11	7	0	2	3/11	Vulpinic acid and **atranorin** in the cortex, with norstictic acid in the hymenium of the apothecia
Pseudevernia furfuracea (Pfur_oli_TBG_2151)	psefurpred	37.8	48	26	8	18	0	3	3/11	**Atranorin**, physodic acid and oxyphysodic acid
Ramalina intermedia (RamPxa02_v1.0)	ramintpred	26.2	54	31	13	17	1	3	5/9	Usnic acid (major); medulla with homosekikaic acid (major), sekikaic acid (major), 4′-O-methylnorhomosekikaic acid (minor)
Ramalina peruviana (RamPxa01_v1)	ramperpred	25.5	43	17	9	7	1	1	4/10	Usnic acid, homosekikaic acid (major), sekikaic acid (major), and 4′-O-methylnorhomosekikaic acid and 4′-O-methylnorsekikaic acid (minor)
Usnea hakonensis (Uhk_1.0)	usnhakpred	40.4	70	23	10	12	1	3	5/22	Usnic and norstictic acids
Xanthoria elegans (ASM1131630v1)	xanelepred	44.2	63	25	7	18	0	1	7/17	Parietin (major), fallacinal, emodin, teloschistin and parietinic acid

The two species *Ramalina intermedia* and *R. peruviana* belong to the same family as the genus *Bacidia* but differ in having many more BGCs compared to *B. gigantensis* and *B. rubella*. In detail, *R. intermedia* contains 54 BGCs, including thirteen non-reducing, seventeen reducing and one partially reducing TI-PKS sequences. *Ramalina peruviana*, on the other hand, contains 43 BGCs including nine non-reducing and seven reducing genes, and one partially reducing gene (Table 2).

3.1.1. Atranorin

Atranorin is the main secondary compound known in *B. rubella* [64], and its biosynthetic pathway has received attention in previous studies on lichen-forming fungi [26,29]. Our phylogenetic results—which included previously identified sequences of genes involved in atranorin production from *Cladonia* species and *Stereocaulon alpinum*—revealed a putative PKS23 homolog in *B. rubella*. This is consistent with the phylogenetic investigation of Kim et al. [29], where PKS23 sequences were reported to group together with sequences from atranorin-producing lichen-forming fungi (see Section 3.3 Type I PKS phylogeny). The domain configuration of *B. rubella* PKS23 also supports our phylogenetic results, showing the same organization of putative atranorin BGC in *B. rubella* as has been reported for *Cladonia rangiferina* (Figure 2). The *B. rubella* PKS23 cluster contains a cytochrome P450 domain (*atr2*) required for oxidation, as well as an *O*-methyltransferase (OMT) domain (*atr3*) and transporter gene (*atr4*), which are involved in atranorin biosynthesis [29]. A BLASTp search of the OMT domain (*atr3*) in *B. rubella* PKS23 resulted in 36% protein sequence identity to Trt5 (UniProtKB accession no. Q0C8A3). This level of similarity is consistent with previous findings by Kim et al. [29] for *C. rangiferina* PKS23.
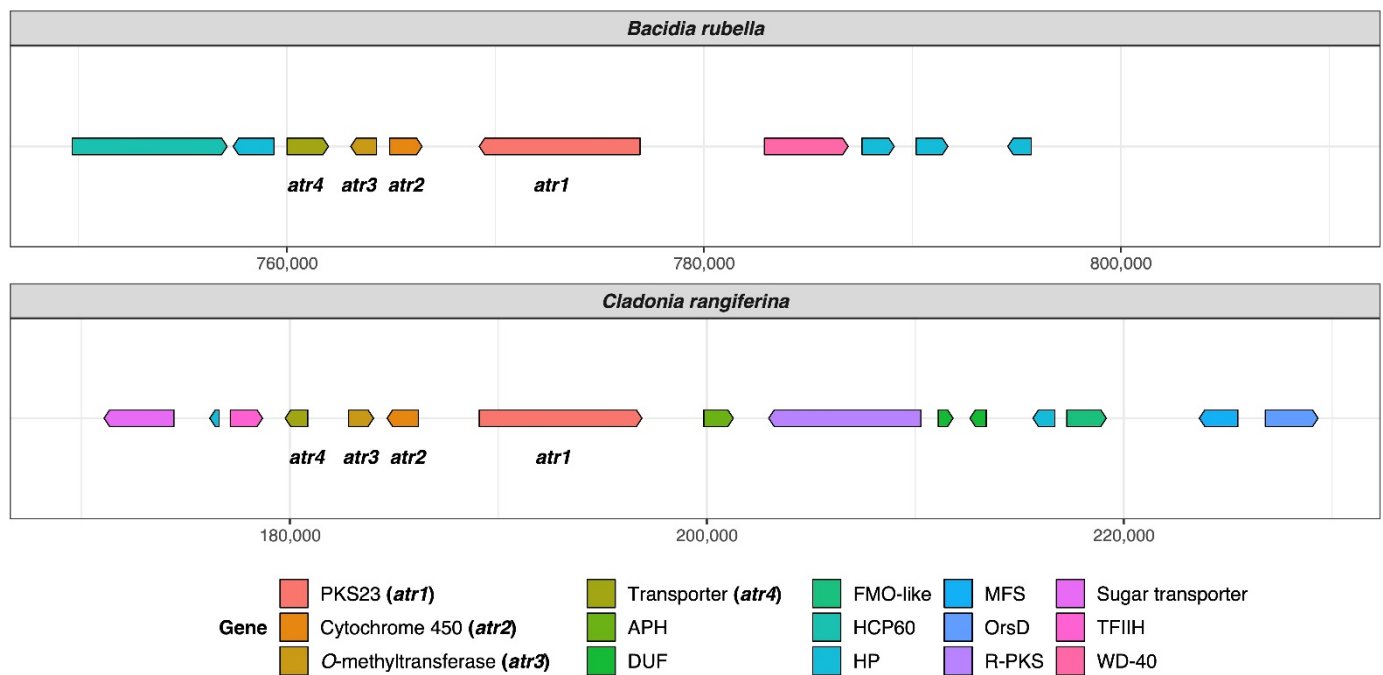
Figure 2. Organization of putative atranorin BGCs in *Bacidia rubella* and *Cladonia rangiferina*. The genes PKS23 (*atr1*), Cytochrome 450 (*atr2*), *O*-methyltransferase (*atr3*), and transporter gene (*atr4*) are present on the left side of the gene arrow plot. The BLAST percent similarity between two genes is 73% for *atr1*, 74% for *atr2*, 78% for *atr3*, and 91.5% for *atr4*. APH, phosphotransferase enzyme family (PF01636); DUF, domain of unknown function; FMO-like, flavin-containing monooxygenase family (PF00743); HCP60, HSP60 chaperone family (PF00118); HP, hypothetical protein; MFS, Major Facilitator Superfamily, transporter gene (PF07690); R-PKS, reducing PKS (in this case from R-VIII group); OrsD, Orsellinic acid/F9775 biosynthesis cluster protein D family (PF12013); TFIIH, Ssl1-like protein, subunit of the transcription factor II H complex (PF04056); Sugar_tr, Sugar transporter family (PF00083); WD-40, WD40 repeat (PF00400).

The newly identified, putative PKS23 sequence of *B. rubella* was recovered as a sister to PKS23 sequences from *C. rangiferina* and *S. alpinum*, suggesting a sister-group relationship of *Bacidia* with Cladoniaceae (See Figure 3 in Section 3.3: Type I PKS Phylogeny), whereby this clade formed a sister-group to the PKS23 sequences from Parmeliaceae (schematically shown in Figure 1).

This is in contrast to the family-level taxonomy previously established, e.g., by Peršoh et al. [66] and Miadlikowska et al. [50], where Cladoniaceae is more closely related to Parmeliaceae than to Ramalinaceae. To test the monophyly of the clade comprising *Bacidia* + Cladoniaceae compared to a group comprised of Parmeliaceae and Cladoniaceae, we performed a phylogenetic tree topology test on the PKS23 dataset. Specifically, we compared the unconstrained ML tree recovering *Bacidia* + Cladoniaceae as monophyletic (Topology 1) versus the constrained tree recovering Cladoniaceae + Parmeliaceae as monophyletic and *Bacidia* sister to that branch (Topology 2; Figure 1).

Our results showed that the topology constraining Cladoniaceae + Parmeliaceae as monophyletic is significantly less likely (0.8%, Figure 1, Table 3). Possible explanations are that the ancestor of *Bacidia* may have acquired the PKS23 gene from an ancestor of Cladoniaceae via horizontal gene transfer or that the PKS23 genes were generated by convergent evolution. It is obvious that these hypotheses require additional testing with augmented sampling of PKS23 sequences from Cladoniaceae, Parmeliaceae, and Ramalinaceae. Both scenarios may also explain the scattered occurrence of atranorin in Ramalinaceae.

Table 3. Parameters for the topology test. Topology 1, recovering *Bacidia* + Cladoniaceae as monophyletic; Topology 2, recovering Cladoniaceae + Parmeliaceae as monophyletic. Value for the Kishino–Hasegawa test (Kishino and Hasegawa, 1989), Shimodaira and Hasegawa, 1989), expected likelihood weights (Strimmer and Rambaut, 2002) and approximately unbiased (AU) test (Shimodaira, 2002) are given.

Tree	logL	Delta	p-KH	p-SH	c-ELW	p-AU
Bacidia + Cladoniaceae	−28,054.52811	2.062×10^{-8}	0.495+	0.814+	0.496+	0.566+
Cladoniaceae + Parmeliaceae	−28,108.54142	54.013	0.0126−	0.0126−	0.00853−	0.0081−

deltaL: logL difference from the maximal logl in the set. p-KH: *p*-value of one-sided Kishino–Hasegawa test (1989). p-SH: *p*-value of Shimodaira–Hasegawa test (2000). c-ELW: Expected Likelihood Weight (Strimmer and Rambaut 2002). p-AU: *p*-value of approximately unbiased (AU) test (Shimodaira, 2002).

Even though a PKS16 gene from *Cladonia grayi* was first shown to be involved in grayanic acid production by Armaleo et al. [18], a homolog of this gene from *C. rangiferina* was later suggested to be involved in atranorin production by Elshobary et al. [26]. In our phylogeny, these genes group together with genes from several other *Cladonia* and lichen-forming fungi (PKS16 clade, See Figure 3 in Section 3.3: Type I PKS Phylogeny), but not all of them are known as atranorin producers (Table 2). Moreover, atranorin is a B-orcinol depside, and a corresponding biosynthetic gene would require a CMeT domain to add a methyl group to the depside ring. This is not the case for PKS16, which is thought to be involved in the synthesis of orcinol depsides [25]. Our comparison of known metabolites in lichen-forming fungi containing PKS16 does not reveal a clear pattern either (See Figure 3 in section: Type I PKS Phylogeny, Group NR-I, PKS16 clade; Table 2). As such, the biosynthetic role of PKS16 genes remains elusive.

3.1.2. Homosekikaic Acid

Homosekikaic acid is a major secondary metabolite in *Bacidia gigantensis* as well as in both *Ramalina intermedia* and *R. peruviana*. However, it has not been found in *B. rubella*. To our knowledge, there was no putative PKS reported as being involved in the biosynthesis of homosekikaic acid, and its biosynthesis has not been characterized using gene expression or heterologous expression experiments. To identify candidate genes involved in the biosynthesis of homosekikaic acid in these three species, we used BLASTp on all predicted BGC sequences from the two *Bacidia* and *Ramalina* species. We identified three BGC candidates with BLAST similarity ranging from 53 to 93%, but none of them were a TI-PKS. Instead, we recovered Type 3-PKS homologs from *B. gigantensis* (BGC 1.2), *R. intermedia* (BGC 6.1) and *R. peruviana* (BGC 223.1) as potential homosekikaic biosynthetic genes; however, none of *B. rubella* BGCs showed a high similarity to them. Furthermore, our TI-PKS phylogeny did not reveal any clade with both *Ramalina* species and *B. gigantensis* that excluded *B. rubella*. A possible explanation for the observed pattern is that the BGC responsible for synthesizing homosekikaic acid is present in the genome of *B. rubella*, but not expressed, and therefore homosekikaic acid is not produced in detectable amount. This hypothesis requires testing with gene expression experiments and analyses of substance profiles.

3.1.3. Other Biosynthetic Genes Identified In Silico in the Two *Bacidia* Species

Using further in silico analyses with antiSMASH, we were able to identify genes encoding enzymes to synthesize secondary metabolites such as clavaric acid (100% similarity) and squalestatin S1 (40% similarity). These terpenes have been identified in both *Bacidia*. Moreover, we identified a monascorubrin biosynthetic gene in *B. rubella* confirmed by 100% BLAST identity to the monascorubrin biosynthetic gene from *Talaromyces* (*Penicillium*) *marneffei* (PKS3: HM070047) [67]. Apart from monascorubrin biosynthesis, PKS3 genes were suggested to be involved in the production of the well-known toxin citrinin, as well as a yellow pigment, ankaflavin [67]. Monascorubrin and its related compounds are polyketides used as natural red colorants for food [68]. In *B. rubella*, monascorubrin could be

responsible for the characteristic orange to the orange-brown coloration of the apothecia. However, these substances have not yet been reported from *B. rubella*.

In the genome of *B. gigantensis*, we identified genes possessing high sequence similarity with genes involved in the production of pyranonigrin E (100% similarity to BGC0001124), naphthopyrone (100% similarity to BGC0000107), and melanin (100% similarity to BGC0001265). However, in most cases, only a part of the sequences showed a high percentage of similarity; therefore, our in-silico based report is provisional. Additional detailed studies are necessary to confirm these first functional assignments.

3.2. Biosynthetic Gene Composition in Twenty-Three Annotated Fungal Genomes

The basic statistics for all twenty-three studied genomes are provided in Table 4. According to BUSCO homology searches against the fungal dataset (fungi_odb9), most genomes were highly gene complete. We included only two genomes with completeness below 90%, namely *Alectoria sarmentosa* (75.8%) and *Graphis scripta* (88.6%). The number of predicted genes was in the range of 6756 to 11,072. The lowest number of predicted genes was observed for *Ramalina peruviana* (most likely due to issues in the quality of the assembly given the lower sequencing depth of 2×), and the highest number was observed for *Evernia prunastri* (Table 4).

Table 4. Genome basics for twenty-three studied fungal genomes.

Assembly	No. of Contigs	Largest Contig (bp)	Total Length (Mb)	GC (%)	N50 (bp)	N75 (bp)	BUSCO Completeness (%)	Genes Predicted	Proteins Predicted
Alectoria sarmentosa	915	400,628	39.9	40.22	93,085	44,808	75.8	8440	8406
Bacidia gigantensis	24	3,530,911	33.1	44.67	**1,807,239**	**1,552,797**	**95.8**	8451	8400
Bacidia rubella	246	2,353,056	33.7	45.25	**1,771,855**	**1,480,693**	**97.9**	8773	8728
Cladonia grayi	414	958,967	34.6	44.44	243,412	104,892	**96.8**	9215	9168
Cladonia macilenta	240	2,265,542	37.1	44.68	**1,469,036**	**1,071,353**	**96.8**	8183	8135
Cladonia metacorallifera	30	2,400,105	36.6	44.91	**1,591,850**	**1,304,658**	**97.5**	8357	8313
Cladonia rangiferina	1008	751,829	35.6	45.46	273,041	142,056	**98.2**	9264	9218
Cladonia uncialis	2124	143,175	32.8	46.38	34,871	18,367	**91.7**	8706	8645
Cyanodermella asteris	37	3,440,352	28.6	53.29	**1,790,936**	**1,105,189**	**97.2**	7946	7851
Dibaeis baeomyces	1369	352,342	35.2	47.02	70,496	37,098	**97.9**	9799	9756
Endocarpon pusillum	908	803,103	37.1	46.00	178,225	78,254	**93.1**	8446	8392
Evernia prunastri	277	732,541	40.3	48.97	264,454	154,311	**97.9**	11,072	10,979
Graphis scripta	1453	383,549	36.2	46.66	78,723	38,837	88.6	9808	9744
Gyalolechia flavorubescens	36	2,816,824	34.4	41.89	**1,693,300**	**1,515,355**	**97.5**	8062	8008
Lasallia hispanica	1619	615,827	41.2	51.28	145,035	51,438	**97.9**	8218	8162
Lasallia pustulata	43	3,307,933	32.9	51.67	**1,808,250**	**1,551,388**	**98.2**	6973	6936
Letharia columbiana	161	2,188,364	52.2	39.57	666,803	377,091	**92.0**	9966	9890
Letharia lupina	31	3,031,725	49.2	38.73	**2,098,233**	**1,574,492**	**96.2**	9266	9206
Pseudevernia furfuracea	46	3,053,396	37.7	47.86	**1,178,799**	859,355	**97.2**	9148	9082

Table 4. *Cont.*

Assembly	No. of Contigs	Largest Contig (bp)	Total Length (Mb)	GC (%)	N50 (bp)	N75 (bp)	BUSCO Completeness (%)	Genes Predicted	Proteins Predicted
Ramalina intermedia	196	898,913	26.2	51.89	273,318	142,876	**97.5**	7405	7355
Ramalina peruviana	1657	694,821	26.9	50.75	40,431	15,829	90.0	6756	6706
Usnea hakonensis	879	624,317	41.1	45.57	166,123	71,534	**96.5**	10,700	10,641
Xanthoria elegans	261	990,773	44.3	40.70	385,707	188,494	**98.2**	9033	8911

We investigated the BGCs predicted in all twenty-three studied genomes that belong to different taxonomic groups and synthesize a plethora of secondary metabolites (Table 2; Table 4). Our results revealed a high number of BGCs, with an average of 48 clusters per genome. The smallest number was recovered in the genome of *Lasallia pustulata* (26 BGCs), and the highest in *Evernia prunastri* (86 BGCs), which agrees with the results reported by Calchera et al. based on 15 lichenized genomes [6]. In nearly half the genomes, NR-PKSs are more common than R-PKS (Table 2). This evidence is in contrast to previous results reporting that R-PKS gene numbers exceed the number of NR-PKS genes [6]. As such, a larger data set is necessary to confirm whether R-PKS or NR-PKSs are more numerous in the genomes of lichen-forming fungi. The total number of TI-PKSs identified across all studied genomes was 478. Of those, 44.35% were of the non-reducing (NR), 53.35% of reducing (R), and 2.3% of partly reducing (PR) PKSs. The highest number of PKS genes was found in *E. prunastri* (36 TI-PKS clusters) and *C. rangiferina* (34 clusters) and the lowest numbers were in *B. rubella* (10 TI-PKS clusters), *B. gigantensis* (11 clusters), and *Cyanodermella asteris* (10 clusters) (Table 2).

Our broad genomic sampling provides phylogenetic context for the NR-PKS genes of *B. rubella* and *B. gigantensis*. The six TI-PKS genes from *B. rubella* are NR-PKSs (three in Subclade I and three in Subclade II), while for *B. gigantensis* seven TI-PKS genes are NR-PKSs (all are in Subclade I).

The discrepancy between the large number of recovered TI-PKS sequences and the few experimentally verified secondary metabolites (Table 2) raises questions about the role these genes play in the secondary metabolism, and about the products they produce (e.g., [9,24,25,29]. However, results linking PKS genes to lichen secondary metabolites beyond in silico methods are still scarce.

3.3. Type I PKS Phylogeny

Our maximum-likelihood phylogeny of TI-PKS with a total of 624 sequences recovered from twenty-three fungal genomes and supplemented with previously published sequences is the largest analysis of biosynthetic gene content of various TI-PKS genes in lichen-forming fungi to date.

The TI-PKSs phylogenetic tree is divided into six main subgroups (Figure 3): Bacterial Type II PKS (including bacterial and mitochondrial ketoacyl-ACP-synthetases; used as outgroup), Bacterial Type I PKS (also including some fungal sequences), animal fatty acid synthase (FAS), PR-PKS, NR-PKS, and R-PKS. Lichen PKS genes are distributed across the three of these main subgroups, viz. PR-PKS, NR-PKS, and R-PKS. These groups were also recognized by Kroken et al. [14] and Calchera et al. [6], but both used the single KS domain for tree reconstruction, and the latter subsumed PR-PKS and R-PKS.
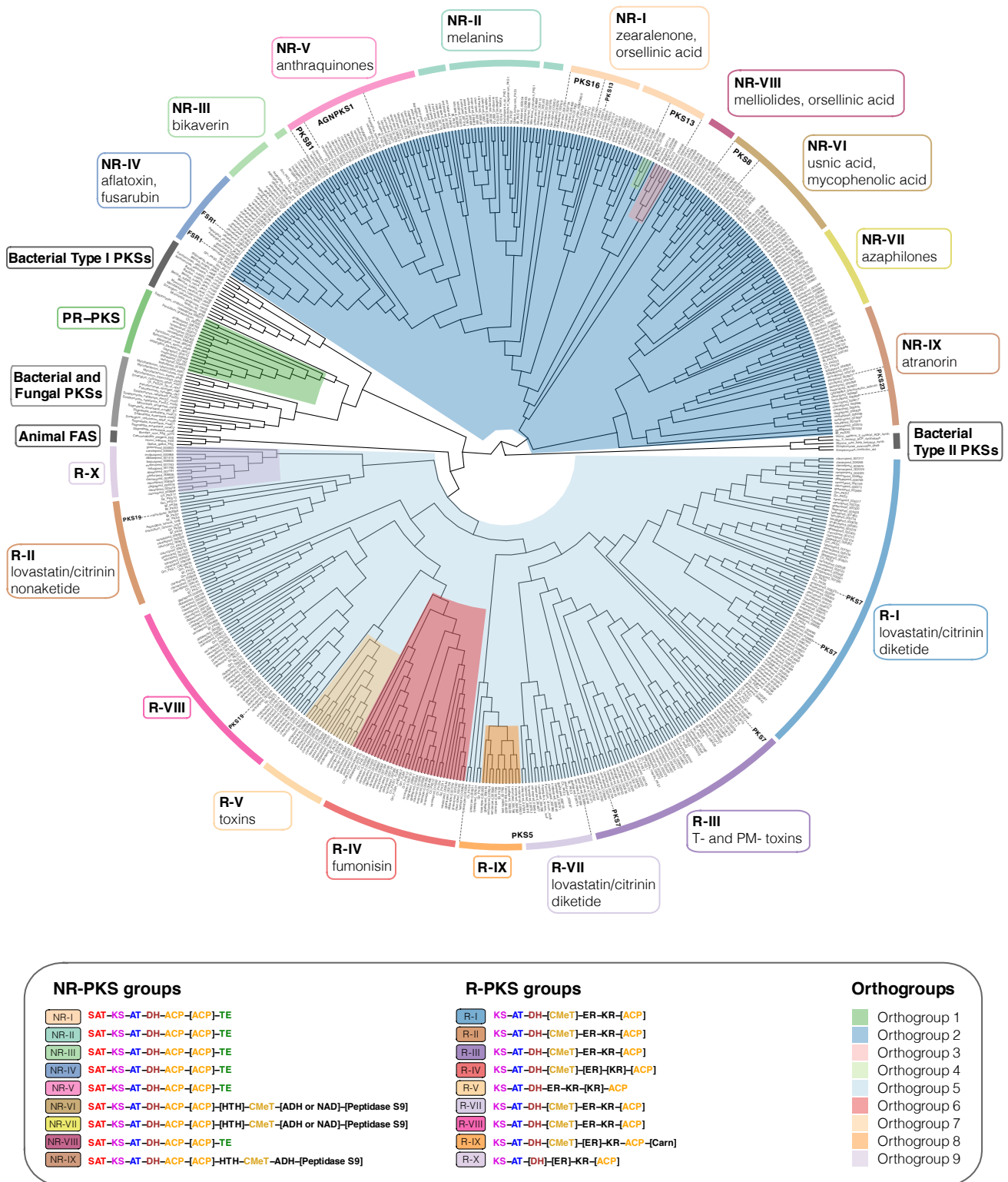
Figure 3. Maximum-likelihood phylogeny of Type I PKS genes inferred by IQ-TREE using Type II Bacterial PKSs as outgroup. Clades containing lichen-forming fungi are highlighted and the corresponding Orthogroups (1 to 9, respectively) are indicated by different colors. PR-PKS corresponds

to Orthogroup 1 (green); the nine NR-PKS groups (NR-I to NR-IX) belong to Orthogroups 2, 3 and 4 (dark blue, pink and light green, respectively); the ten R-PKS groups (R-I to R-X) belong to Orthogroups 5, 6, 7, 8, and 9 (light blue, red, peach, orange, and lilac, respectively). Characteristic secondary substances for the groupings are given in the corresponding colored boxes. Groups not containing lichen-forming fungal genes are indicated by grey boxes. For each group, the domain arrangement of PKS is highlighted with distinct colors: SAT—starter unit-ACP transacylase; KS—ketoacyl synthase; AT—acyltransferase; ACP—acyl carrier protein; KR—ketoreductase; DH—dehydratase; ER—enoyl reductase; CMeT—methyltransferase; TE—thioesterase; HTH—helix-to-helix; ADH—adhydrolase; NAD—NAD-binding; Carn—Choline/Carnitine O-acyltransferase domain.

- *TI-PKS domain content mostly corresponds to phylogeny*

TI-PKS genes encode for multi-domain enzymes, with each domain executing a specific function. The order and domain content of the PKSs thus defines the class of polyketides produced by the corresponding BGC. The presence or absence of individual domains has led to the classification of fungal PKSs into three main subgroups. The first subgroup comprises NR-PKSs, which lack reductive domains. The generalized domain content of NR-PKS in fungi studied here is SAT-KS-AT-DH-ACP-[ACP]-HTH-CMeT-[TE or ADH or NAD]-[Peptidase S9] (NR-I to NR-IX; Figure 3).

The second subgroup comprises PR-PKSs containing a single KR domain or KR and DH domains. The generalized domain content in PR-PKS according to our phylogeny is KS-AT-[DH]-KR-ACP (PR-PKS; Figure 3).

Finally, the third subgroup—R-PKSs—contains a complete set of reductive domains, viz. KR, DH, and ER and thus exhibit the following domain structure: KS-AT-DH-CMeT-ER-KR-ACP-[Carn] (R-I to R-X; Figure 3). Additional domains, such as helix-to-helix (HTH), adhydrolase (ADH), NAD-binding (NAD), Peptidase S9, and Choline/Carnitine O-acyltransferase domain (Carn) were not shown in the previous studies of TI-PKS in lichen-forming fungi. We discuss them in detail below in the corresponding sections.

- *The discrepancy of grouping PKS genes*

Assigning PKS genes to different groups in fungi on the account of gene domain composition and their synthesized products was introduced by Kroken et al. [14] and later refined based on DH-domain pocket sizes by Ahuja et al. [69] and Liu et al. [70]. This classification was used in several studies investigating PKS gene diversity in lichen-forming fungi, e.g., [29,71]. Despite this existing classification, it remains unclear if all groups indeed form monophyletic clades and if all genes from one group synthesize the same (or at least chemically similar) substances. In our phylogeny, previously proposed groups were not always monophyletic (e.g., NR-II; Figure 3), and experimentally characterized genes from one group have been shown to produce different substances (e.g., PKS81 and AGNPKS1 in NR-V; Figure 3). Additionally, we performed an ortholog clustering using Orthofinder on all TI-PKS sequences to provide an objective way of identifying groups of sequences. This resulted in nine orthogroups (Figure 3: colored clades), named Orthogroup 1 to Orthogroup 9, respectively. Orthogroup 1 corresponds to the PR-PKSs (Figure 3). NR-PKSs are spread across Orthogroups 2, 3, and 4 but none of them correspond explicitly to any of the nine groups identified before by Pizarro et al. [71] and Kim et al. [29]. Orthogroups 5, 6, 7, 8, and 9 contain R-PKSs, where only Orthogroup 6 (R-IV) and 7 (R-V) agree with groups defined in Kroken et al. [14] and Punya et al. [72]. However, all Orthogroups identified here form well supported clades in the PKS phylogeny (Figure 3). The discrepancy between our results and previous studies needs to be investigated in subsequent studies. In our phylogeny, several groups of the NR-PKS and R-PKS showed differences in the PKS domains present corresponding to the supported clades; these groups do contain support from different sources and thus merit discussion (see below).

3.3.1. Lichen-Forming Fungi Contain Only a Few Partially Reducing PKSs in the Phylogenetic Neighbourhood to Bacterial PKSs

The PR-PKS sequences formed a well-supported clade sister to bacterial Type I PKS sequences with other fungal PKSs (PR-PKS; Figure 3). Their domain configuration is KS-AT-[DH]-KR-ACP, including only a single reductase domain (KR). In contrast to the large NR- and R-PKS groups, PR-PKS contains genes mainly from *Aspergillus* and *Penicillium*, and only a few genes from lichen-forming fungi. Genes from the studied fungal genomes have the typical PR-PKS domain composition, but in two genes from two *Ramalina* (ramintpred_001715 and ramperpred_002012), the DH domain was missing. PR-PKS genes form a sister clade to Bacterial Type I PKSs (Figure 2). Bacterial T1-PKSs often possess a KR domain catalyzing the first step in the reductive modification of beta-carbonyl centers in the growing polyketide chain. This domain requires NADPH to reduce the keto- to a hydroxy group [73].

The "simple" domain configuration of Bacterial and PR-PKS genes compared to NR- and R-PKSs has not escaped our attention. Our study was not designed to specifically test how PKS genes in Ascomycetes were acquired and how they diversified. However, the placement of Bacterial and NR-PKS sequences as the earliest branches in our phylogeny supports the hypothesis suggested by Kroken et al. [14] that fungal TI-PKS genes could have been acquired by an ancient horizontal gene transfer event between bacteria and fungi. Additionally, our results suggest that ancestral TI-PKS genes may have been partially reducing. Under this scenario, NR- and R-PKS evolution could have been connected to domain structure modification (such as gaining SAT in NR-PKS) and subsequent functional diversification. However, this cannot be concluded with certainty without a greatly expanded sample of genomes from other fungal groups, including genomes from early branching fungal lineages and comprehensive ancestral state reconstructions.

3.3.2. Fungal PKSs Producing Non-Reduced Polyketides

The Diversity of NR-PKS Sequences

In previous studies, NR-PKSs were divided into nine major groups based on protein sequence similarity and PKS domain content [14,29,69,71]. Similar to previous studies, we observed characteristic domain configurations for the different clades in our phylogeny. The domain structure of NR-PKSs in the studied fungi can be generalized as SAT-KS-AT-DH-ACP-[ACP]-HTH-CMeT-[TE or ADH or NAD]-[Peptidase S9]; however, some PKS genes may deviate from this structure. The observed domain content variations are not random but rather occur in two main patterns: either through the duplication of the ACP domain, or through the addition of an N-terminal TE domain. PKS genes possessing an additional ACP domain are scattered throughout different NR-PKS clades, suggesting multiple independent gains. However, the functional significance of ACP domain duplications is still unknown [14].

Most of the NR-PKS sequences belong to a large clade containing groups NR-I to NR-V and NR-VIII, with domain configuration containing a TE domain at the N-terminal end.

The irregularly present additional TE domain is involved in a thioesterase-mediated product release, which is the most common release mechanism in TI-PKS [74]. It regularly extends to a C-C Claisen cyclization domain (TE/CLC domain), e.g., in *Aspergillus parasiticus* PksA [75]. Although CYC domains have previously been reported from various fungi [14,69,70], we could not identify them in our analyses and thus did not indicate them in the phylogeny.

Subclade I of NR-PKSs (Including Groups NR-I to NR-V, and NR-VIII)

Group NR-I

The paraphyletic group NR-I contains several clades with previously characterized sequences involved in the biosynthesis of aromatic compounds derived from orsellinic acid, such as grayanic acid (PKS16), physodic acid and olivetoric acid [24,25], lecanoric acid [76],

xanthones, aflatoxin, and naphthoquinones [14]. In addition, the clade also comprises PKS13 sequences from several lichen-forming fungi and *Gibberella zeae* as well as a PKS15 sequence from *Botryotinia fuckeliana* with unknown functions.

Group NR-II

Our results show that NR-II is a diverse group, comprised of several clades containing sequences from lichen-forming fungi interspersed with characterized PKS genes proposed to be involved in the biosynthesis of various substances. The earliest branching clade contains genes involved in the 6-hydroxymellein biosynthesis (NR-II; Figure 3), a key intermediate in terrein biosynthesis [77]. Terrein, produced in large quantities by *Aspergillus terreus*, has phytotoxic activity and has the potential to serve as a novel antibiotic [78]. Our phylogeny revealed sequences of four lichen-forming fungi (clagrapred_001463, clauncpred_002890, psefurpred_002946, and grascrpred_004317) clustering together with *terA* gene in *A. terreus*. A BLAST search of *terA* (GenBank: EAU38791) against these sequences revealed 58 to 67% similarity at the amino acid level, indicating a high degree of conservation despite an approximate 350-million-year split of Eurotiomycetes (*Aspergillus*) and Lecanoromycetes [79]. Terrein has not been reported from lichen-forming fungi; therefore, without further experiments and detailed substance characterization, terrein production in lichen-forming fungi remains hypothetical.

Another important pattern is the occurrence of characterized melanin genes and melanin precursors in different clades. Melanins are a diverse group of substances that play a role in virulence, morphogenesis or the response to environmental stress, and can be synthesized via different pathways [80]. PKSs produce two forms of melanin: either 1,8-dihydroxynaphtalene (DHN) melanin or Deoxybostrycoidein-melanin [81]. Melanins are insoluble and thus cannot be studied by standard biochemical methods [80]. In the PKS gene survey by Kroken et al. [14], all melanin synthesizing genes were grouped together in a single monophyletic clade. In our analysis, they are recovered in at least three clades containing sequences from several Lecanoromycetes and *Endocarpon pusillum*. Sister to NR-II is a clade containing sequences from *Colletotrichum lagenarium* (PKS1), *Glarea* sp., *Nodulisporium* sp., and *C. heterostrophus* (PKS18), which were also characterized as producers of melanin [14]. The high number of genes from lichen-forming fungi close to characterized melanin biosynthetic genes suggests an essential role of melanins in lichens.

Groups NR-III and NR-IV

The sister groups NR-III and NR-IV contain sequences of proteins producing large polyketide chains, such as conidial yellow pigment Alb1 (NR-III) or aflatoxin/ sterigmatocystin of *A. nidulans* (NR-IV) [14,71,82].

NR-III additionally contains characterized PKSs producing duclauxin (35–71% similarity) and naphthopyrone (100% similarity). Duclauxins are dimeric, heptacyclic fungal polyketides with various activities [83], while bis-naphthopyrones act in herbivore defense in filamentous ascomycetes [84].

Several genes recovered in the NR-IV group are potentially involved in producing different fungal pigments. The genes from *Ramalina intermedia* (ramintpred_005964) and *Cladonia grayi* (clagrapred_006320) were assigned to an FSR1 gene, which is involved in producing highly pigmented naphthoquinones fusarubins responsible for fruiting body coloration of *Fusarium fujikuroi* [85]. A BLAST search of the *R. intermedia* gene (ramintpred_005964) revealed 72.3% similarity to a PKS of *Cladonia metacorallifera* (GenBank: QIX11499) that is involved in the biosynthesis of the red compound cristazarin, characterized by antibacterial and antitumor activity [86]. Sequences of *Bacidia rubella* and several *Cladonia* species producing red pigments were recovered sister to the putative *Ramalina intermedia* FSR1 gene. Interestingly, *R. intermedia*, at the same time, lacks red pigments [87]. This close phylogenetic proximity raises the possibility that combinations of substances synthesized by different PKS genes could be responsible for red-colored pigments (see also discussion on monascorubin above), particularly for the red fruiting bodies in *B. rubella*.

Group NR-V

According to the previous studies, NR-V contains PKSs without the TE domain [71]; however, in the characterized PKSs in our phylogeny, the TE or R domains were present in all clades. The genes in the NR-V group are suggested to be involved in the production of different mycotoxins, such as desertorin (*Aspergillus nidulans*) and atrochrysone (*Aspergillus fumigatus*) [71,88,89].

The crown clades in the NR-V group include the annotated PKS81 orthologs from *Cladonia metacorallifera*, *C. macilenta*, *Lasallia pustulata* and *L. hispanica* as sister to a PKS19 sequence from *Cochliobolus heterostrophus* and two clades with characterized Agnpks1 also from several lichen-forming fungi. Agnpks1 (Atrochrysone carboxylic acid synthase) was originally described from *Penicillium divaricatum* and is involved in the biosynthesis of agnestins and dihydroxy-xanthone metabolites [90]. Xanthones and related benzophenones are produced by various filamentous fungi. They exhibit insecticide, antioxidant, antibacterial, anti-inflammatory, and anticancer activities [91]. Examples include desmethyl-sterigmatocystin, a key intermediate of the aflatoxin group of mycotoxins produced by *Aspergillus flavus*, and a norlichexanthone from the lichen-forming *Lecanora straminea* [90]. An additional BLAST search of norlichexanthone synthase from *L. straminea* (GenBank: D7PI15) against our annotated fungal sequences showed at least 37% similarity to sequences from the clade containing PKS81 and Agnpks1. The relationship between these two genes remains unclear, but given our results, PKS81 might belong to or have evolved from Agnpks1. Additional closer investigations will be necessary to show the role of PKS81 and Agnpks1 orthologs in lichen-forming fungi and their possible role in xanthone biosynthesis.

Subclade II of NR-PKSs (Including Groups NR-VI, NR-VII, and NR-IX)

The second largest clade of NR-PKSs includes the previously recovered groups NR-VI, NR-VII, and the recently defined group NR-IX [29] (Figure 3). The generalized domain arrangement in these groups is SAT-KS-AT-DH-ACP-[ACP]-[HTH]-CMeT-[ADH/NAD]-[Peptidase S9], deviating from the generalized arrangement for other NR-PKS (see above). Although previously reported from all NR-PKS groups except group NR-V [69,71], we did not observe TE domains in groups NR-VI, NR-VII, and NR-IX. Instead, we observed NAD and ADH domains—in some cases followed by a Peptidase S9 (PFAM: PF00326) domain. Peptidase S9 belongs to proteolytic enzymes that consume serine in their catalytic activity, and they are ubiquitously found in viruses, bacteria, and eukaryotes [92]. We also observed a helix-turn-helix domain (HTH) being inserted after one or two ACP domains in several groups. The HTH domain was previously found in PKSs in fungi but it has not been shown in the arrangement of the NR-PKSs of lichen-forming fungi before. Proteins with an HTH motif are, for example, involved in DNA repair, RNA metabolism, and protein–protein interaction [93], and could thus be involved in developmental or morphogenic processes.

Group NR-VI

Characterized PKSs in this group include PKS18 and PKS19 genes from *Botryotinia fuckeliana*. Genes from this group were suggested to be involved in usnic acid biosynthesis [71], and according to Kim et al. [29] they belong to PKS8. Our results show that this group is divided into two clades. The first clade contains genes of known usnic acid producers such as *Ramalina intermedia*, *R. peruviana*, *Cladonia metacorallifera*, *C. macilenta*, *C. uncialis*, *Evernia prunastri*, *Alectoria sarmentosa*, *Letharia columbiana*, and *Usnea hakonensis*, interspersed with genes from lichen-forming fungi known not to produce usnic acid. The second clade includes genes mostly from lichen-forming fungi not producing usnic acid, including a gene from *B. rubella* (bacrubpred_000551). However, sequences from *Cladonia macilenta*, *C. uncialis*, and *Evernia prunastri* were also recovered in this clade.

Group NR-VII

The only genes characterized in this group are PKS17 from *Botryotinia fuckeliana* and PKS21 from *Cochliobolus heterostrophus*. These genes have been proposed to produce citrinin or lovastatin [14,94,95]. The other identified genes from the lichen-forming fungi in this group had 50 to 70% BLAST similarity to genes involved in the biosynthesis of monascorubrin, citrinin, conidial yellow, azanigerone A, and stipitatic acid (see also discussion on monascorubrin above). As mentioned above, the biosynthetic gene from *B. rubella* (bacrubpred_007642) has a 100% identity to the monascorubrin biosynthetic gene.

Group NR-IX

The recently recognized group NR-IX [29] contains several predicted PKS23 sequences, involved in the biosynthesis of atranorin (see sections on 3.1.1 Atranorin and 3.1.2 Homosekikaic acid above) and methylated orsellinic acid derivatives. In contrast to the groups NR-VI and NR-VII, NR-IX sequences always contain an ADH and lack a NAD domain after CMeT, while Peptidase S9 is only sporadically present. It is necessary to note that only one ACP domain was present in the PKS23, including atranorin producers. In addition, other characterized PKSs of this group are from *Cochliobolus heterostrophus* (PKS22 and PKS23) and *Botryotinia fuckeliana* (PKS16 and PKS20).

3.3.3. Fungal PKSs Producing Reduced Polyketides

The Diversity of R-PKS Sequences

R-PKS genes are involved in synthesizing various reduced, usually linear polyketides. Many are precursors of toxins that are active in animals (e.g., lovastatin, citrinin, and fumonisin) or plants (e.g., T-toxin and PM-toxin) [96–99]. We follow this classification in our discussion whenever possible, while also highlighting deviations. Compared to NR-PKSs, less is known about the possible roles of R-PKSs. In our phylogeny, R-PKSs formed a large clade sister to NR-PKSs with many well-supported subclades. Unlike what has been shown in previous studies, all studied R-PKSs here lacked a second ACP domain, and in some cases, ACP was missing. According to Kroken et al. [14], four major groups (R-I to R-IV) of R-PKS genes can be distinguished based on their overall domain structure and produced compounds. This classification was later extended to groups R-V to R-VIII by Punya et al. [72]. Over 70% of the studied fungal sequences could be assigned to groups designated by Kroken et al. [14] and Punya et al. [72] with the general domain content: KS-AT-DH-[CMeT]-ER-KR-[ACP]. Two clades recovered by Punya et al. [72] are missing from our tree, namely R-VI and R-VIII. Clade VI contained uncommon PKS-NRPS hybrids with four additional domains after ACP, viz. condensation (C), adenylation (A), thiolation (T), and reductase (R) [72]. As our study focused on the TI-PKSs, it did not include hybrid NRPS-PKS genes. The sequences from R-VIII were not present in our phylogeny, and are thus not feasible to identify with confidence.

Based on our phylogenetic results, we identified two R-PKS clades that did not match any of the R-PKS groups reported in previous studies. Sequences in those two clades had characteristic domain structures and were recovered as distinct orthogroups in our Orthofinder analysis. This leads us to propose these clades as new reducing PKS groups, R-IX and R-X, following the numbering scheme by Kroken et al. [14] and Punya et al. [72].

Groups of R-PKSs

Group R-I

Group R-I is the largest group of R-PKSs in our tree. It contains one of the R-PKS genes synthesizing the diketide portion of lovastatin and citrinin, T-toxin, and PM-toxin [14]. Our results show that the genes of this group, recovered in a monophyletic clade by Kroken et al. [14], were nested in different clades in our analysis; therefore, R-I assignment is not complete.

Group R-II

Group R-II forms a well-supported clade and it was previously characterized by the absence of an ER domain [14]. In our phylogeny, however, ER domain was present in all lichen-forming fungi. The group includes many previously published sequences and orthologs from *Cladonia* and *Letharia* species, *Xanthoria elegans*, *Pseudevernia furfuracea*, and *Ramalina intermedia*. The *R. intermedia* ortholog was assigned to PKS19. It was predicted to be involved in the production of heptaketides with a role in a lesion of rice leaves formation in *Magnaporthe oryzae* [100]. Two characterized proteins from *A. terreus* lovB and *P. citrinum* mlcA synthesize the cyclic nonaketide portion of lovastatin and citrinin.

Group R-III

Group R-III forms a clade comprised of four sequences previously assigned to this group by Kroken et al. [14], and a sequence from *Cyanodermella asteris*. PKSs from this clade do not possess a CMeT domain. The experimentally characterized gene in group R-III is *C. heterostrophus* PKS2, which, along with PKS1, is required for the synthesis of T-toxin [14]. This group contains several sequences from Kroken et al. [14] interspersed with sequences from various lichen-forming fungi.

Group R-IV

Genes belonging to R-IV may contain a conserved CMeT domain. Thus, their domain configuration somewhat resembles that of groups R-I and R-II. However, N-terminal domains ER, KR, and ACP can be present or absent in R-IV. The only characterized PKS in this group is *G. moniliformis* FUM1 (Gm_FUM1_AAD43562), which makes the linear polyketide precursor of the toxin fumonisin [98]. This group contains several sequences from Kroken et al. [14] interspersed with sequences from various lichen-forming fungi.

Group R-V

Sequences in group R-V have similar domain composition like sequences from Orthogroup 7: KS-AT-DH-ER-KR-[KR]-ACP. However, a second KR domain is only present in *Dibaeis baeomyces* (dibbaepred_000831). We recovered genes from several lichen-forming fungi in this group. Again, experimentally characterized genes from *Gibberella moniliformis* (Gm_PKS13) and *Botryotinia fuckeliana* (Bf_PKS10) also recovered here indicate a possible role in toxin biosynthesis (Figure 3) [14].

Group R-VII

This group contains several previously characterized sequences as well as sequences from *R. intermedia*, *P. furfuracea*, *G. furfuracea,* and *C. macilenta* where we could assign PKS5 annotations. Additional sequences from lichen-forming fungi also recovered here had no functional annotations; as such the role of these genes remains unclear. The characterized sequences of *Aspergillus* (*Aspergillus_terreus_lovF*) and *Penicillium* (*Penicillium_citrinum_mlcB*) indicate a role in the production of the diketide portion of lovastatin and citrinin, but they were assigned to group R-I by Kroken et al. [14].

Novel group R-IX

A new group of reducing PKSs can be delineated based on a specific domain composition and our orthogroup assignment. We tentatively call this group R-IX following the naming scheme of Kroken et al. [14] and Punya et al. [72]. R-IX is sister to group R-VII and differs from all other groups by having a facultative Choline/Carnitine O-acyltransferase domain (Carn) following the ACP domain: KS-AT-DH-[CMeT]-ER-KR-[ACP]-[Carn] (Figure 3). The Carn domain can be found in several eukaryotic acetyltransferases and also at the C terminus of a highly reducing polyketide synthase (SdnO), where it is part of a gene cluster mediating the biosynthesis of glycoside antibiotics sordarin and hypoxysordarin [101].

Novel group R-X

Similar to R-IX, a second group of reducing PKSs can be identified based on a specific domain composition and orthogroup assignment. This group R-X, recovered as Orthogroup 9, contains only genes from lichen-forming fungi. Together with Group R-II, they share a sister-group relationship to all other R-PKSs in our phylogeny (Figure 3). Genes from this group may not have DH, ER and ACP domains, resulting in the following domain content: KS-AT-[DH]-[ER]-KR-[ACP]. Most fungal genes recovered here are missing the DH and ER domain. However, the genes from *Lasallia hispanica* (lashispred_001760) and *Evernia prunastri* (eveprupred_001763) contain a complete domain configuration: KS-AT-DH-ER-KR-ACP.

4. Conclusions and Limitations

This study presents a comprehensive analysis of the PKS gene content of the de novo sequenced genome of *B. rubella* and twenty-two publicly available genomes of mainly lichen-forming fungi. Our results reveal that a BGC including PKS23 is likely involved in biosynthesis of atranorin in *B. rubella*. Similar to previous studies (e.g., [6,23,24,29]), we observed a large diversity of PKS genes in lichen-forming fungi as well as *B. rubella*, much larger than expected based on their recorded secondary metabolite profiles. This highlights the potential of lichen-forming fungi to produce a much higher number of substances than previously assumed, as mentioned by Calchera et al. [6] focusing on foliose lichens. Our in silico approach provides first insights into the possible roles of PKS genes in crustose *B. rubella*; however, we are aware that this comes with limitations. Only detailed studies of individual BGCs combining gene expression analyses with analytical chemistry and metabolomics will allow thorough testing of the hypotheses proposed here. The prospects for this are promising as an increasing number of studies succeeded in the heterologous expression of lichen-forming fungal genes, (e.g., [29,76,86,102,103]). Subsequent in vivo studies of metabolite profiles in lichen-forming fungi supplemented by high-resolution MS/MS spectra [104] or metabolic profiling based on stable isotope analysis [105] will contribute to our knowledge on how secondary metabolites in lichen-forming fungi are produced and what roles they play. Combined with the growing number of available lichen-forming fungal genomes, we will be able to refine our understanding and formulate novel hypotheses about the biosynthetic potential of lichens.

References

1. Keller, N.P. Fungal Secondary Metabolism: Regulation, Function and Drug Discovery. *Nat. Rev. Microbiol.* **2019**, *17*, 167–180. [CrossRef] [PubMed]
2. Rokas, A.; Mead, M.E.; Steenwyk, J.L.; Raja, H.A.; Oberlies, N.H. Biosynthetic Gene Clusters and the Evolution of Fungal Chemodiversity. *Nat. Prod. Rep.* **2020**, *37*, 868–878. [CrossRef] [PubMed]
3. Keller, N.P.; Turner, G.; Bennett, J.W. Fungal Secondary Metabolism—from Biochemistry to Genomics. *Nat. Rev. Microbiol.* **2005**, *3*, 937–947. [CrossRef] [PubMed]
4. Keller, N.P.; Hohn, T.M. Metabolic Pathway Gene Clusters in Filamentous Fungi. *Fungal Genet. Biol.* **1997**, *21*, 17–29. [CrossRef] [PubMed]
5. Huneck, S.; Yoshimura, I. Identification of Lichen Substances. In *Identification of Lichen Substances*; Huneck, S., Yoshimura, I., Eds.; Springer: Berlin/Heidelberg, Germany, 1996; pp. 11–123. ISBN 978-3-642-85243-5.
6. Calchera, A.; Dal Grande, F.; Bode, H.B.; Schmitt, I. Biosynthetic Gene Content of the 'Perfume Lichens' *Evernia prunastri* and *Pseudevernia furfuracea*. *Molecules* **2019**, *24*, 203. [CrossRef] [PubMed]
7. Culberson, C.F.; Armaleo, D. Induction of a Complete Secondary-Product Pathway in a Cultured Lichen Fungus. *Exp. Mycol.* **1992**, *16*, 52–63. [CrossRef]
8. Culberson, C.F.; Culberson, W.L.; Johnson, A. Characteristic Lichen Products in Cultures of Chemotypes of the *Ramalina siliquosa* Complex. *Mycologia* **1992**, *84*, 705–714. [CrossRef]
9. Hamada, N. The Effect of Various Culture Conditions on Depside Production by an Isolated Lichen Mycobiont. *Bryologist* **1989**, *92*, 310–313. [CrossRef]
10. Stocker-Wörgötter, E.; Elix, J.A. Secondary Chemistry of Cultured Mycobionts: Formation of a Complete Chemosyndrome by the Lichen Fungus of *Lobaria spathulata*. *Lichenologist* **2002**, *34*, 351–359. [CrossRef]
11. Hamada, N.; Tanahashi, T.; Miyagawa, H.; Miyawaki, H. Characteristics of Secondary Metabolites from Isolated Lichen Mycobionts. *Symbiosis* **2001**, *31*, 23–33.
12. Molina, M.C.; Crespo, A.; Vicente, C.; Elix, J.A. Differences in the Composition of Phenolics and Fatty Acids of Cultured Mycobiont and Thallus of *Physconia distorta*. *Plant Physiol. Biochem.* **2003**, *41*, 175–180. [CrossRef]
13. Cox, R.J. Polyketides, Proteins and Genes in Fungi: Programmed Nano-Machines Begin to Reveal Their Secrets. *Org. Biomol. Chem.* **2007**, *5*, 2010–2026. [CrossRef] [PubMed]
14. Kroken, S.; Glass, N.L.; Taylor, J.W.; Yoder, O.C.; Turgeon, B.G. Phylogenomic Analysis of Type I Polyketide Synthase Genes in Pathogenic and Saprobic Ascomycetes. *Proc. Natl. Acad. Sci. USA* **2003**, *100*, 15670. [CrossRef] [PubMed]
15. Nicholson, T.P.; Rudd, B.A.M.; Dawson, M.; Lazarus, C.M.; Simpson, T.J.; Cox, R.J. Design and Utility of Oligonucleotide Gene Probes for Fungal Polyketide Synthases. *Chem. Biol.* **2001**, *8*, 157–178. [CrossRef]
16. Lawrey, J.D. Biological Role of Lichen Substances. *Bryologist* **1986**, *89*, 111–122. [CrossRef]
17. Rundel, P.W. The Ecological Role of Secondary Lichen Substances. *Biochem. Syst. Ecol.* **1978**, *6*, 157–170. [CrossRef]
18. Armaleo, D.; Sun, X.; Culberson, C. Insights from the First Putative Biosynthetic Gene Cluster for a Lichen Depside and Depsidone. *Mycologia* **2011**, *103*, 741–754. [CrossRef]
19. Mullins, A.J.; Murray, J.A.H.; Bull, M.J.; Jenner, M.; Jones, C.; Webster, G.; Green, A.E.; Neill, D.R.; Connor, T.R.; Parkhill, J.; et al. Genome Mining Identifies Cepacin as a Plant-Protective Metabolite of the Biopesticidal Bacterium *Burkholderia ambifaria*. *Nat. Microbiol.* **2019**, *4*, 996–1005. [CrossRef]
20. Nielsen, J.C.; Grijseels, S.; Prigent, S.; Ji, B.; Dainat, J.; Nielsen, K.F.; Frisvad, J.C.; Workman, M.; Nielsen, J. Global Analysis of Biosynthetic Gene Clusters Reveals Vast Potential of Secondary Metabolite Production in *Penicillium* Species. *Nat. Microbiol.* **2017**, *2*, 17044. [CrossRef]
21. Lichman, B.R.; Godden, G.T.; Buell, C.R. Gene and Genome Duplications in the Evolution of Chemodiversity: Perspectives from Studies of Lamiaceae. *Physiol. Metab.* **2020**, *55*, 74–83. [CrossRef]
22. Medema, M.H.; Fischbach, M.A. Computational Approaches to Natural Product Discovery. *Nat. Chem. Biol.* **2015**, *11*, 639–648. [CrossRef] [PubMed]
23. Navarro-Muñoz, J.C.; Selem-Mojica, N.; Mullowney, M.W.; Kautsar, S.A.; Tryon, J.H.; Parkinson, E.I.; De Los Santos, E.L.C.; Yeong, M.; Cruz-Morales, P.; Abubucker, S.; et al. A Computational Framework to Explore Large-Scale Biosynthetic Diversity. *Nat. Chem. Biol.* **2020**, *16*, 60–68. [CrossRef] [PubMed]
24. Singh, G.; Armaleo, D.; Dal Grande, F.; Schmitt, I. Depside and Depsidone Synthesis in Lichenized Fungi Comes into Focus through a Genome-Wide Comparison of the Olivetoric Acid and Physodic Acid Chemotypes of *Pseudevernia furfuracea*. *Biomolecules* **2021**, *11*, 1445. [CrossRef] [PubMed]
25. Singh, G.; Calchera, A.; Merges, D.; Otte, J.; Schmitt, I.; Grande, F.D. A Candidate Gene Cluster for the Bioactive Natural Product Gyrophoric Acid in Lichen-Forming Fungi. *bioRxiv* **2022**. [CrossRef]
26. Elshobary, M.E.; Becker, M.G.; Kalichuk, J.L.; Chan, A.C.; Belmonte, M.F.; Piercey-Normore, M.D. Tissue-Specific Localization of Polyketide Synthase and Other Associated Genes in the Lichen, *Cladonia rangiferina*, Using Laser Microdissection. *Phytochemistry* **2018**, *156*, 142–150. [CrossRef]
27. Abdel-Hameed, M.; Bertrand, R.L.; Piercey-Normore, M.D.; Sorensen, J.L. Identification of 6-Hydroxymellein Synthase and Accessory Genes in the Lichen *Cladonia uncialis*. *J. Nat. Prod.* **2016**, *79*, 1645–1650. [CrossRef]

28. Abdel-Hameed, M.; Bertrand, R.L.; Piercey-Normore, M.D.; Sorensen, J.L. Putative Identification of the Usnic Acid Biosynthetic Gene Cluster by de novo Whole-Genome Sequencing of a Lichen-Forming Fungus. *Fungal Biol.* **2016**, *120*, 306–316. [CrossRef]

29. Kim, W.; Liu, R.; Woo, S.; Bin Kang, K.; Park, H.; Yu, Y.H.; Ha, H.-H.; Oh, S.-Y.; Yang, J.H.; Kim, H.; et al. Linking a Gene Cluster to Atranorin, a Major Cortical Substance of Lichens, through Genetic Dereplication and Heterologous Expression. *mBio* **2021**, *12*, e01111-21. [CrossRef]

30. Boustie, J.; Tomasi, S.; Grube, M. Bioactive Lichen Metabolites: Alpine Habitats as an Untapped Source. *Phytochem. Rev.* **2011**, *10*, 287–307. [CrossRef]

31. Yoshimura, I.; Yamamoto, Y.; Nakano, T.; Finnie, J. Isolation and Culture of Lichen Photobionts and Mycobionts. In *Protocols in Lichenology: Culturing, Biochemistry, Ecophysiology and Use in Biomonitoring*; Kranner, I.C., Beckett, R.P., Varma, A.K., Eds.; Springer: Berlin/Heidelberg, Germany, 2002; pp. 3–33. ISBN 978-3-642-56359-1.

32. Honegger, R.; Zippler, U.; Gansner, H.; Scherrer, S. Mating Systems in the Genus *Xanthoria* (Lichen-Forming Ascomycetes). *Mycol. Res.* **2004**, *108*, 480–488. [CrossRef]

33. Andrews, S. FastQC: A Quality Control Tool for High Throughput Sequence Data. 2010. Available online: https://www.bioinformatics.babraham.ac.uk/projects/fastqc/ (accessed on 20 April 2022).

34. Antipov, D.; Korobeynikov, A.; McLean, J.S.; Pevzner, P.A. HybridSPAdes: An Algorithm for Hybrid Assembly of Short and Long Reads. *Bioinformatics* **2016**, *32*, 1009–1015. [CrossRef] [PubMed]

35. Buchfink, B.; Reuter, K.; Drost, H.-G. Sensitive Protein Alignments at Tree-of-Life Scale Using DIAMOND. *Nat. Methods* **2021**, *18*, 366–368. [CrossRef]

36. Laetsch, D.; Blaxter, M. BlobTools: Interrogation of Genome Assemblies [Version 1; Peer Review: 2 Approved with Reservations]. *F1000Research* **2017**, *6*, 1287. [CrossRef]

37. Gurevich, A.; Saveliev, V.; Vyahhi, N.; Tesler, G. QUAST: Quality Assessment Tool for Genome Assemblies. *Bioinformatics* **2013**, *29*, 1072–1075. [CrossRef] [PubMed]

38. Resl, P.; Hahn, C. Phylociraptor—Rapid Phylogenomic Tree Calculator. 2021. Available online: https://github.com/reslp/phylociraptor (accessed on 20 April 2022).

39. Palmer, J.M.; Stajich, J. Funannotate: Eukaryotic Genome Annotation; Zenodo. Available online: https://zenodo.org/record/4054262#.YmeT83ZBxPY (accessed on 15 April 2022).

40. Frith, M.C. A New Repeat-Masking Method Enables Specific Detection of Homologous Sequences. *Nucleic Acids Res.* **2011**, *39*, e23. [CrossRef] [PubMed]

41. Stanke, M.; Schöffmann, O.; Morgenstern, B.; Waack, S. Gene Prediction in Eukaryotes with a Generalized Hidden Markov Model That Uses Hints from External Sources. *BMC Bioinform.* **2006**, *7*, 62. [CrossRef]

42. Korf, I. Gene Finding in Novel Genomes. *BMC Bioinform.* **2004**, *5*, 59. [CrossRef]

43. Majoros, W.H.; Pertea, M.; Salzberg, S.L. TigrScan and GlimmerHMM: Two Open Source Ab Initio Eukaryotic Gene-Finders. *Bioinformatics* **2004**, *20*, 2878–2879. [CrossRef]

44. Ter-Hovhannisyan, V.; Lomsadze, A.; Chernoff, Y.O.; Borodovsky, M. Gene Prediction in Novel Fungal Genomes Using an Ab Initio Algorithm with Unsupervised Training. *Genome Res.* **2008**, *18*, 1979–1990. [CrossRef]

45. Blin, K.; Shaw, S.; Kloosterman, A.M.; Charlop-Powers, Z.; van Wezel, G.P.; Medema, M.H.; Weber, T. AntiSMASH 6.0: Improving Cluster Detection and Comparison Capabilities. *Nucleic Acids Res.* **2021**, *49*, W29–W35. [CrossRef]

46. Camacho, C.; Coulouris, G.; Avagyan, V.; Ma, N.; Papadopoulos, J.; Bealer, K.; Madden, T.L. BLAST+: Architecture and Applications. *BMC Bioinform.* **2009**, *10*, 421. [CrossRef] [PubMed]

47. Katoh, K.; Standley, D.M. MAFFT Multiple Sequence Alignment Software Version 7: Improvements in Performance and Usability. *Mol. Biol. Evol.* **2013**, *30*, 772–780. [CrossRef] [PubMed]

48. Nguyen, L.-T.; Schmidt, H.A.; von Haeseler, A.; Minh, B.Q. IQ-TREE: A Fast and Effective Stochastic Algorithm for Estimating Maximum-Likelihood Phylogenies. *Mol. Biol. Evol.* **2015**, *32*, 268–274. [CrossRef] [PubMed]

49. Kalyaanamoorthy, S.; Minh, B.Q.; Wong, T.K.F.; von Haeseler, A.; Jermiin, L.S. ModelFinder: Fast Model Selection for Accurate Phylogenetic Estimates. *Nat. Methods* **2017**, *14*, 587–589. [CrossRef]

50. Miadlikowska, J.; Kauff, F.; Högnabba, F.; Oliver, J.C.; Molnár, K.; Fraker, E.; Gaya, E.; Hafellner, J.; Hofstetter, V.; Gueidan, C.; et al. A Multigene Phylogenetic Synthesis for the Class Lecanoromycetes (Ascomycota): 1307 Fungi Representing 1139 Infrageneric Taxa, 317 Genera and 66 Families. *Mol. Phylogenet. Evol.* **2014**, *79*, 132–168. [CrossRef]

51. Kishino, H.; Hasegawa, M. Evaluation of the Maximum Likelihood Estimate of the Evolutionary Tree Topologies from DNA Sequence Data, and the Branching Order in Hominoidea. *J. Mol. Evol.* **1989**, *29*, 170–179. [CrossRef]

52. Shimodaira, H.; Hasegawa, M. Multiple Comparisons of Log-Likelihoods with Applications to Phylogenetic Inference. *Mol. Biol. Evol.* **1999**, *16*, 1114. [CrossRef]

53. Strimmer, K.; Rambaut, A. Inferring Confidence Sets of Possibly Misspecified Gene Trees. *Proc. R. Soc. Lond. B Biol. Sci.* **2002**, *269*, 137–142. [CrossRef]

54. Shimodaira, H. An Approximately Unbiased Test of Phylogenetic Tree Selection. *Syst. Biol.* **2002**, *51*, 492–508. [CrossRef]

55. Rambaut, A. FigTree: Tree Figure Drawing Tool. 2009. Available online: http://tree.bio.ed.ac.uk/software/figtree/ (accessed on 21 February 2022).

56. Emms, D.M.; Kelly, S. OrthoFinder: Phylogenetic Orthology Inference for Comparative Genomics. *Genome Biol.* **2019**, *20*, 238. [CrossRef]

57. Price, M.N.; Dehal, P.S.; Arkin, A.P. FastTree 2—Approximately Maximum-Likelihood Trees for Large Alignments. *PLoS ONE* **2010**, *5*, e9490. [CrossRef] [PubMed]

58. Capella-Gutiérrez, S.; Silla-Martínez, J.M.; Gabaldón, T. TrimAl: A Tool for Automated Alignment Trimming in Large-Scale Phylogenetic Analyses. *Bioinformatics* **2009**, *25*, 1972–1973. [CrossRef] [PubMed]

59. Minh, B.Q.; Nguyen, M.A.T.; von Haeseler, A. Ultrafast Approximation for Phylogenetic Bootstrap. *Mol. Biol. Evol.* **2013**, *30*, 1188–1195. [CrossRef] [PubMed]

60. Kozlov, A.M.; Darriba, D.; Flouri, T.; Morel, B.; Stamatakis, A. RAxML-NG: A Fast, Scalable and User-Friendly Tool for Maximum Likelihood Phylogenetic Inference. *Bioinformatics* **2019**, *35*, 4453–4455. [CrossRef] [PubMed]

61. Brown, J.W.; Walker, J.F.; Smith, S.A. Phyx: Phylogenetic Tools for Unix. *Bioinformatics* **2017**, *33*, 1886–1888. [CrossRef] [PubMed]

62. Huson, D.H.; Scornavacca, C. Dendroscope 3: An Interactive Tool for Rooted Phylogenetic Trees and Networks. *Syst. Biol.* **2012**, *61*, 1061–1067. [CrossRef]

63. Allen, J.L.; Jones, S.J.M.; McMullin, R.T.; Rokas, A. Draft Genome Sequence of the Lichenized Fungus *Bacidia gigantensis. Microbiol. Resour. Announc.* **2021**, *10*, e00686-21. [CrossRef]

64. Ekman, S. The Corticolous and Lignicolous Species of Bacidia and Bacidina in North America. *Opera Bot.* **1996**, *127*, 1–148.

65. McMullin, R.T.; McCune, B.; Lendemer, J.C. *Bacidia gigantensis* (Ramalinaceae), a New Species with Homosekikaic Acid from the North Shore of Lake Superior in Ontario, Canada. *Bryologist* **2020**, *123*, 215–224. [CrossRef]

66. Peršoh, D.; Beck, A.; Rambold, G. The Distribution of Ascus Types and Photobiontal Selection in Lecanoromycetes (Ascomycota) against the Background of a Revised SSU NrDNA Phylogeny. *Mycol. Prog.* **2006**, *3*, 103–121. [CrossRef]

67. Woo, P.C.Y.; Lam, C.-W.; Tam, E.W.T.; Lee, K.-C.; Yung, K.K.Y.; Leung, C.K.F.; Sze, K.-H.; Lau, S.K.P.; Yuen, K.-Y. The Biosynthetic Pathway for a Thousand-Year-Old Natural Food Colorant and Citrinin in *Penicillium marneffei. Sci. Rep.* **2014**, *4*, 6728. [CrossRef] [PubMed]

68. Chen, W.; Chen, R.; Liu, Q.; He, Y.; He, K.; Ding, X.; Kang, L.; Guo, X.; Xie, N.; Zhou, Y.; et al. Orange, Red, Yellow: Biosynthesis of Azaphilone Pigments in *Monascus* Fungi. *Chem. Sci.* **2017**, *8*, 4917–4925. [CrossRef] [PubMed]

69. Ahuja, M.; Chiang, Y.-M.; Chang, S.-L.; Praseuth, M.B.; Entwistle, R.; Sanchez, J.F.; Lo, H.-C.; Yeh, H.-H.; Oakley, B.R.; Wang, C.C.C. Illuminating the Diversity of Aromatic Polyketide Synthases in *Aspergillus nidulans. J. Am. Chem. Soc.* **2012**, *134*, 8212–8221. [CrossRef] [PubMed]

70. Liu, L.; Zhang, Z.; Shao, C.-L.; Wang, J.-L.; Bai, H.; Wang, C.-Y. Bioinformatical Analysis of the Sequences, Structures and Functions of Fungal Polyketide Synthase Product Template Domains. *Sci. Rep.* **2015**, *5*, 10463. [CrossRef]

71. Pizarro, D.; Divakar, P.K.; Grewe, F.; Crespo, A.; Dal Grande, F.; Lumbsch, H.T. Genome-Wide Analysis of Biosynthetic Gene Cluster Reveals Correlated Gene Loss with Absence of Usnic Acid in Lichen-Forming Fungi. *Genome Biol. Evol.* **2020**, *12*, 1858–1868. [CrossRef]

72. Punya, J.; Swangmaneecharern, P.; Pinsupa, S.; Nitistaporn, P.; Phonghanpot, S.; Kunathigan, V.; Cheevadhanarak, S.; Tanticharoen, M.; Amnuaykanjanasin, A. Phylogeny of Type I Polyketide Synthases (PKSs) in Fungal Entomopathogens and Expression Analysis of PKS Genes in *Beauveria bassiana* BCC 2660. *Fungal Biol.* **2015**, *119*, 538–550. [CrossRef]

73. Bonnett, S.A.; Whicher, J.R.; Papireddy, K.; Florova, G.; Smith, J.L.; Reynolds, K.A. Structural and Stereochemical Analysis of a Modular Polyketide Synthase Ketoreductase Domain Required for the Generation of a Cis-Alkene. *Chem. Biol.* **2013**, *20*, 772–783. [CrossRef]

74. Du, L.; Lou, L. PKS and NRPS Release Mechanisms. *Nat. Prod. Rep.* **2010**, *27*, 255–278. [CrossRef]

75. Korman, T.P.; Crawford, J.M.; Labonte, J.W.; Newman, A.G.; Wong, J.; Townsend, C.A.; Tsai, S.-C. Structure and Function of an Iterative Polyketide Synthase Thioesterase Domain Catalyzing Claisen Cyclization in Aflatoxin Biosynthesis. *Proc. Natl. Acad. Sci. USA* **2010**, *107*, 6246–6251. [CrossRef]

76. Kealey, J.T.; Craig, J.P.; Barr, P.J. Identification of a Lichen Depside Polyketide Synthase Gene by Heterologous Expression in *Saccharomyces cerevisiae. Metab. Eng. Commun.* **2021**, *13*, e00172. [CrossRef]

77. Zaehle, C.; Gressler, M.; Shelest, E.; Geib, E.; Hertweck, C.; Brock, M. Terrein biosynthesis in *Aspergillus terreus* and its impact on phytotoxicity. *Chem. Biol.* **2014**, *21*, 719–731. [CrossRef] [PubMed]

78. Asfour, H.Z.; Awan, Z.A.; Bagalagel, A.A.; Elfaky, M.A.; Abdelhameed, R.F.A.; Elhady, S.S. Large-Scale Production of Bioactive Terrein by *Aspergillus terreus* Strain S020 Isolated from the Saudi Coast of the Red Sea. *Biomolecules* **2019**, *9*, 480. [CrossRef]

79. Beimforde, C.; Feldberg, K.; Nylinder, S.; Rikkinen, J.; Tuovila, H.; Dörfelt, H.; Gube, M.; Jackson, D.J.; Reitner, J.; Seyfullah, L.J.; et al. Estimating the Phanerozoic History of the Ascomycota Lineages: Combining Fossil and Molecular Data. *Mol. Phylogenet. Evol.* **2014**, *78*, 386–398. [CrossRef] [PubMed]

80. Eisenman, H.C.; Casadevall, A. Synthesis and Assembly of Fungal Melanin. *Appl. Microbiol. Biotechnol.* **2012**, *93*, 931–940. [CrossRef] [PubMed]

81. Toledo, A.V.; Franco, M.E.E.; Yanil Lopez, S.M.; Troncozo, M.I.; Saparrat, M.C.N.; Balatti, P.A. Melanins in Fungi: Types, Localization and Putative Biological Roles. *Physiol. Mol. Plant Pathol.* **2017**, *99*, 2–6. [CrossRef]

82. Yu, J.H.; Leonard, T.J. Sterigmatocystin Biosynthesis in *Aspergillus nidulans* Requires a Novel Type I Polyketide Synthase. *J. Bacteriol.* **1995**, *177*, 4792–4800. [CrossRef]

83. Gao, S.-S.; Zhang, T.; Garcia-Borràs, M.; Hung, Y.-S.; Billingsley, J.M.; Houk, K.N.; Hu, Y.; Tang, Y. Biosynthesis of Heptacyclic Duclauxins Requires Extensive Redox Modifications of the Phenalenone Aromatic Polyketide. *J. Am. Chem. Soc.* **2018**, *140*, 6991–6997. [CrossRef]

84. Xu, Y.; Vinas, M.; Alsarrag, A.; Su, L.; Pfohl, K.; Rohlfs, M.; Schäfer, W.; Chen, W.; Karlovsky, P. Bis-Naphthopyrone Pigments Protect Filamentous Ascomycetes from a Wide Range of Predators. *Nat. Commun.* **2019**, *10*, 3579. [CrossRef]

85. Studt, L.; Wiemann, P.; Kleigrewe, K.; Humpf, H.-U.; Tudzynski, B. Tudzynski Bettina Biosynthesis of Fusarubins Accounts for Pigmentation of *Fusarium fujikuroi* Perithecia. *Appl. Environ. Microbiol.* **2012**, *78*, 4468–4480. [CrossRef]

86. Jeong, M.-H.; Park, C.-H.; Kim, J.A.; Choi, E.D.; Kim, S.; Hur, J.-S.; Park, S.-Y. Production and Activity of Cristazarin in the Lichen-Forming Fungus *Cladonia metacorallifera*. *J. Fungi* **2021**, *7*, 601. [CrossRef]

87. Bowler, P.A.; Rundel, P.W. The *Ramalina intermedia* Complex in North America. *Bryologist* **1974**, *77*, 617–623. [CrossRef]

88. Galagan, J.E.; Calvo, S.E.; Cuomo, C.; Ma, L.-J.; Wortman, J.R.; Batzoglou, S.; Lee, S.-I.; Baştürkmen, M.; Spevak, C.C.; Clutterbuck, J.; et al. Sequencing of *Aspergillus nidulans* and Comparative Analysis with *A. fumigatus* and *A. oryzae*. *Nature* **2005**, *438*, 1105–1115. [CrossRef] [PubMed]

89. Lim, F.Y.; Hou, Y.; Chen, Y.; Oh, J.-H.; Lee, I.; Bugni, T.S.; Keller, N.P. Genome-Based Cluster Deletion Reveals an Endocrocin Biosynthetic Pathway in *Aspergillus fumigatus*. *Appl. Environ. Microbiol.* **2012**, *78*, 4117–4125. [CrossRef] [PubMed]

90. Szwalbe, A.J.; Williams, K.; Song, Z.; de Mattos-Shipley, K.; Vincent, J.L.; Bailey, A.M.; Willis, C.L.; Cox, R.J.; Simpson, T.J. Characterisation of the Biosynthetic Pathway to Agnestins A and B Reveals the Reductive Route to Chrysophanol in Fungi. *Chem. Sci.* **2019**, *10*, 233–238. [CrossRef]

91. Jung, H.-A.; Su, B.-N.; Keller, W.J.; Mehta, R.G.; Kinghorn, A.D. Antioxidant Xanthones from the Pericarp of *Garcinia mangostana* (Mangosteen). *J. Agric. Food Chem.* **2006**, *54*, 2077–2082. [CrossRef]

92. Rawlings, N.D.; Barrett, A.J. Families of Serine Peptidases. In *Methods in Enzymology*; Academic Press: Cambridge, MA, USA, 1994; Volume 244, pp. 19–61, ISBN 0076-6879.

93. Roy, S.; Kundu, T.K. V-Chemical Principles of DNA Sequence Recognition and Gene Regulation. In *Chemical Biology of the Genome*; Roy, S., Kundu, T.K., Eds.; Academic Press: Cambridge, MA, USA, 2021; pp. 171–223. ISBN 978-0-12-817644-3.

94. Chiang, Y.-M.; Szewczyk, E.; Davidson, A.D.; Keller, N.; Oakley, B.R.; Wang, C.C.C. A Gene Cluster Containing Two Fungal Polyketide Synthases Encodes the Biosynthetic Pathway for a Polyketide, Asperfuranone, in *Aspergillus nidulans*. *J. Am. Chem. Soc.* **2009**, *131*, 2965–2970. [CrossRef]

95. Gallo, A.; Ferrara, M.; Perrone, G. Phylogenetic Study of Polyketide Synthases and Nonribosomal Peptide Synthetases Involved in the Biosynthesis of Mycotoxins. *Toxins* **2013**, *5*, 717–742. [CrossRef]

96. Hendrickson, L.; Davis, C.R.; Roach, C.; Nguyen, D.K.; Aldrich, T.; McAda, P.C.; Reeves, C.D. Lovastatin Biosynthesis in *Aspergillus terreus*: Characterization of Blocked Mutants, Enzyme Activities and a Multifunctional Polyketide Synthase Gene. *Chem. Biol.* **1999**, *6*, 429–439. [CrossRef]

97. He, Y.; Cox, R.J. The Molecular Steps of Citrinin Biosynthesis in Fungi. *Chem. Sci.* **2016**, *7*, 2119–2127. [CrossRef]

98. Proctor, R.H.; Brown, D.W.; Plattner, R.D.; Desjardins, A.E. Co-Expression of 15 Contiguous Genes Delineates a Fumonisin Biosynthetic Gene Cluster in *Gibberella moniliformis*. *Fungal Genet. Biol.* **2003**, *38*, 237–249. [CrossRef]

99. Yang, G.; Rose, M.S.; Turgeon, B.G.; Yoder, O.C. A Polyketide Synthase Is Required for Fungal Virulence and Production of the Polyketide T-Toxin. *Plant Cell* **1996**, *8*, 2139–2150. [CrossRef] [PubMed]

100. Jacob, S.; Grötsch, T.; Foster, A.J.; Schüffler, A.; Rieger, P.H.; Sandjo, L.P.; Liermann, J.C.; Opatz, T.; Thines, E. Unravelling the Biosynthesis of Pyriculol in the Rice Blast Fungus *Magnaporthe oryzae*. *Microbiology* **2017**, *163*, 541–553. [CrossRef] [PubMed]

101. Kudo, F.; Matsuura, Y.; Hayashi, T.; Fukushima, M.; Eguchi, T. Genome Mining of the Sordarin Biosynthetic Gene Cluster from *Sordaria araneosa* Cain ATCC 36386: Characterization of Cycloaraneosene Synthase and GDP-6-Deoxyaltrose Transferase. *J. Antibiot.* **2016**, *69*, 541–548. [CrossRef] [PubMed]

102. Sinnemann, S.J.; Andrésson, Ó.S.; Brown, D.W.; Miao, V.P.W. Cloning and Heterologous Expression of *Solorina crocea* PyrG. *Curr. Genet.* **2000**, *37*, 333–338. [CrossRef] [PubMed]

103. Bertrand, R.L.; Sorensen, J.L. Transcriptional Heterologous Expression of Two Type III PKS from the Lichen *Cladonia uncialis*. *Mycol. Prog.* **2019**, *18*, 1437–1447. [CrossRef]

104. Olivier-Jimenez, D.; Chollet-Krugler, M.; Rondeau, D.; Beniddir, M.A.; Ferron, S.; Delhaye, T.; Allard, P.-M.; Wolfender, J.-L.; Sipman, H.J.M.; Lücking, R.; et al. A Database of High-Resolution MS/MS Spectra for Lichen Metabolites. *Sci. Data* **2019**, *6*, 294. [CrossRef]

105. Kuhn, V.; Geisberger, T.; Huber, C.; Beck, A.; Eisenreich, W. A Facile in Vivo Procedure to Analyze Metabolic Pathways in Intact Lichens. *New Phytol.* **2019**, *224*, 1657–1667. [CrossRef]

Chapter 6

6.1. Discussion

6.1.1. Bacidia s. str. and Bacidia s. lat.: Narrowing down the list of Bacidia in Russia

One of the aims of this dissertation was to provide a correct taxonomic placement for the names treated under *Bacidia* that were described from the Russian territory. Particularly, seven type specimens representing seven species were collected during 19th-century expeditions that were known only from a single locality. Given that herbarium specimens represented the only available material, and that and all specimens were collected on stones, easily crumbling substrate of sand or plant debris, a careful microscopical examination was necessary.

Bacidia alborussula (Nyl.) Zahlbr. and *Bacidia graminum* (Vain.) Zahlbr. were described from the Chukotka Peninsula (easternmost peninsula of Asia), where they were collected on siliceous rock and on decaying plant debris, respectively. Another two specimens, *Bacidia indigens* (Vain.) Zahlbr. and *Bacidia subabbrevians* (Nyl.) Zahlbr. were also collected on the Chukotka Peninsula, where they inhabited sandy soil and decaying plant or bryophyte parts, respectively. The type material of *Bacidia primigenia* Vain. was collected on sandy soil covering pine roots along Konda River, a tributary to the Irtysh River in western Siberia. *Bacidia freshfieldii* (Vain.) Zahlbr. was described from Northern Caucasus, where it was collected on siliceous rock. Finally, the lectotype of *Bacidia xylophila* Malme was collected on wood on Preobrazhenia Island in the Khatanga Gulf of the Laptev Sea (Arctic Ocean).

Characteristic to all species was that most of them were characterized by rod- or spindle-shaped ascospores, except *Bacidia indigens* with needle-shaped ascospores. The latter, however, was characterized by a proper apothecial exciple consisting of radiating isodiametric cells (a so-called paraplectenchymatic exciple), while most of the *Bacidia* species are characterized by a mixture of narrow and wide cell lumina in the proper exciple (i.e., prosoplectenchymatic). These results indicate that none of these seven species belonged to *Bacidia* s. str. In the end, five of the names represent distinct species, one is of uncertain status but clearly belonged to another genus, and the seventh is a synonym (Gerasimova & Ekman, 2017). Thus, *B. alborussula*, *B. graminum*, and *B. indigens* were transferred to *Haematomma*, *Lecania*, and *Bacidina*, respectively. *Bacidia freshfieldii* and *B. subabbrevians* were provisionally kept in *Bacidia* even though none of them was congeneric with the type of that genus. *Bacidia primigenia* belonged in *Arthrorhaphis*,

107

while *B. xylophila* turned to be a younger synonym of *Lecania subfuscula* (Gerasimova & Ekman, 2017).

Assessment of all types, and herbarium and freshly collected material showed that the main distribution of *Bacidia* s. str. is constrained to warm temperate and cold temperate regions according to the map by Sayre *et al.* (2020). Moreover, nearly all *Bacidia* s. str. species in Russia are known as inhabitants of bark of various broad-leaved and coniferous trees, indicating a certain specialization on a woody substrate and epiphytic lifestyle. The only known exception is *Bacidia herbarum* which belongs to the genus in a strict sense, growing on plant debris, moss twigs and occasionally on soil.

6.1.2. Distribution and altitudinal differences of Bacidia s. lat. in the mountains

As discussed above, several species that have long been considered to belong in *Bacidia* s. lat. have been transferred to other genera in recent years. One of those species is *Bacidia subincompta*, which was recently transferred to *Toniniopsis subincompta* (Chapter 2). According to previous observations, *Toniniopsis subincompta* s. lat. has been reported from Europe, Asia, Macaronesia, Africa, and North America in a range of woodlands from sea level to an altitude of c. 3000 m (Ekman, 1996; Smith *et al.*, 2009). The species is also used as an indicator for old-growth forest and is included in indices for defining the conservation value of forest areas (Rücker and Wittmann, 1995; Rose and Coppins, 2002; Smith *et al.*, 2009; Brackel, 2019).

A set of specimens of the *T. subincompta* complex from the mountain regions of the North Caucasus (Russia) as well as Allgäu (Bavaria) was sequenced, showing phylogenetic support for the delimitation of species and correlation with the variability of the examined characters (Chapter 2). The microscopical observations and phylogenetic results clearly demonstrated the presence of two distinct species, *Toniniopsis separabilis* and *T. dissimilis* (the name used for these taxa so far, *T. subincompta,* turned out to be a synonym). Based on the material examined, *T. separabilis* seems to be the more common taxon (76.4%) and has a broader distribution range (Russia, Canada, Norway, Sweden, Estonia, Germany, Austria, Czech Republic, Slovakia, Romania, and Turkey). *Toniniopsis dissimilis* is less frequent (23.6%), with a known distribution in Russia, Norway, Sweden, Finland, Germany, Slovakia, Austria, and Turkey. According to the results, the latter species seems to be better adapted to colder conditions as we have only seen specimens

collected above 1000 m or in high latitudes. This evidence shows a great potential of these two species for investigating cold and altitudinal adaptations (Chapter 2).

Based on observations of specimens from North America by Ekman (1996), *T. subincompta* has the same variation in thallus structure as we observed in specimens from Eurasia. We found only bacilliform ascospores in all specimens except two but looked mainly at middle-aged apothecia (Chapter 2). Our observations correspond with those on *T. subincompta* from Great Britain and Spain with short bacilliform ascospores (Llop, 2007; Smith *et al.*, 2009). However, a single herbarium specimen observed from Canada was determined to be *T. separabilis*, with characters corresponding to our description (Chapter 2). Based on this observation, it is most likely that *T. subincompta* s. lat. from North America represents a separate taxonomic unit, distinct from the specimens from Eurasia. Further detailed studies of herbarium and newly collected material from North America is necessary for verification.

6.1.3. Albinism and cyanotrophy and in Toniniopsis subincompta s. lat.

Interesting cases of albinism and cyanotrophic associations were observed in *Toniniopsis separabilis*, which are unusual for *Toniniopsis* and have not yet been observed in *Bacidia*.

Albinism is an inherited genetic condition that reduces the amount of melanin pigment formed in the body (Manga, 2018), and particularly in lichen fruiting bodies (Gilbert, 1996). The dark color of apothecia and thallus is due to the presence of melanin compounds which serve as a sunscreen from high ultraviolet light (UV) and solar radiation and may also serve as an antioxidant by scavenging reactive oxygen species (Solhaug *et al.*, 2003). At the same time, melanins increase the absorbance of solar energy resulting in a thallus and apothecia temperature increase, opposite to yellow secondary compound atranorin which acts as a light shield and thus having less effect on the heat balance of lichens (McEvoy *et al.*, 2007; Armaleo *et al.*, 2008; Solhaug *et al.*, 2010; Mafole *et al.*, 2017). In the specimens of *Toniniopsis subincompta* s. lat., the observed case of albinism is represented by the presence of a very bright form instead of the more commonly black fruiting bodies (Fig. 6.1). Remarkably, albino morphs have been found in ca 6% of *T. separabilis* specimens but were not observed in specimens of *T. dissimilis* (Chapter 2). To test if albino and dark morphs represented different species, both morphs were sequenced using specimens collected from the same tree. The result showed that the two isolates had 99% identity in their nrITS sequence and thus belong to the same species, but they differ

from each other in all three analyzed genes (Chapter 2). This interesting aspect of lichen biology deserves further study to ascertain if all albino morphs form a separate lineage or are formed independently, for example, by spontaneous mutation (Chapter 2). As both morphs were collected in the same habitat and side of the tree, the necessity of the effect of the affected compounds on the defence of *Toniniopsis* is still in need to be demonstrated.
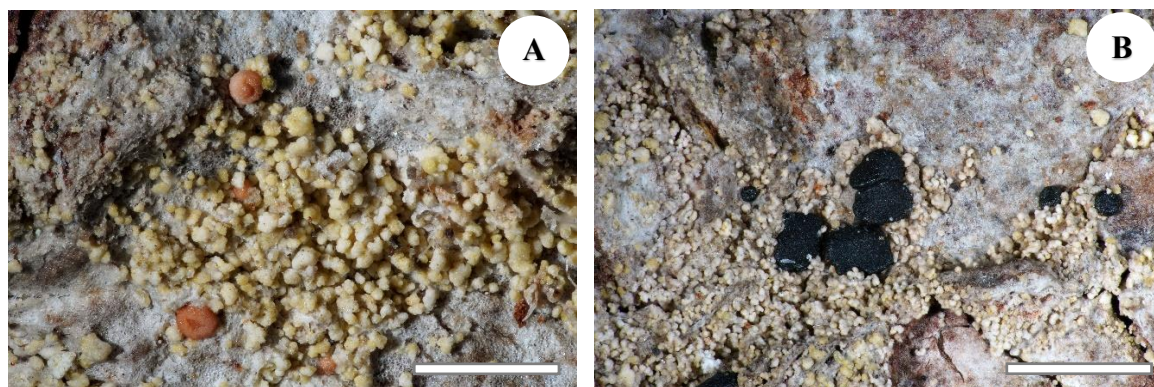
6.1. Detail of *Toniniopsis separabilis* (M-0182613) thallus and apothecia morphs. A, thallus thick, wrinkled, forming isidium-like bulges with albino morph apothecia. B, thallus the same with dark morph apothecia. Scales: 1 mm.

The presence of one or two photosynthetic partners is, per definition, obligate for a lichen symbiosis. However, in case of a facultative or obligate additional association of lichens to free-living or ± lichenized cyanobacteria, this association is called **cyanotrophy** (Poelt and Mayrhofer, 1988). The strong cyanotrophic association in some of the observed specimens sometimes leads to a modification of the thallus, resulting in black-coloured patches. The most diverse composition of associated cyanobacteria was observed in a specimen from Oberallgäu, with algal species from three different genera: *Gloeocapsa*, *Nostoc,* and *Scytonema* (Chapter 2).

Before, it was already known that immature stages of some lichens containing green algae might establish loose cyanotrophic associations with free-living cyanobacteria and/or cyanolichens (Rikkinen, 2003). Such associations in Ramalinaceae were observed in *Thalloidima* A. Massal., which comprises primarily parasitic species on cyanolichens when young or remain parasitic (Kistenich *et al.*, 2018). However, the analyzed specimens were undoubtedly associated with free-living cyanobacteria, substantiating this association as facultative (Fig. 6.2).

Earlier reports on cyanotrophy in crustose lichens have mainly been referring to saxicolous, or epilithic species, indicating a possible influence of low nutrient levels of the

substratum (Poelt and Mayrhofer, 1988). In this study, all specimens with cyanobacteria of *T. separabilis* were exclusively epiphytic growing on bark of *Picea* spp., *Populus* spp., *Salix* spp., *Thuja* spp., and *Ulmus* spp. Remarkably, cyanotrophy was observed only in *T. separabilis* and is considered facultative as ca 16% of the observed specimens associated with cyanobacteria (Chapter 2).
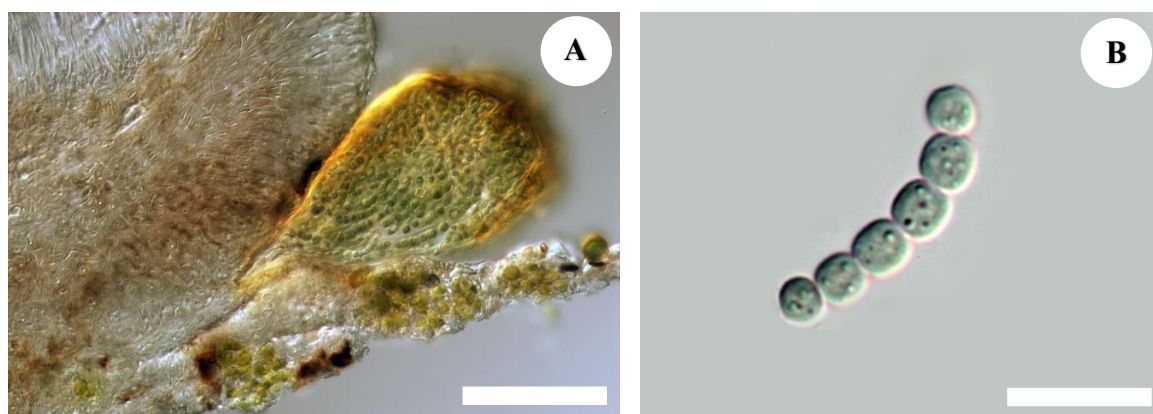
Figure 6.2. Cyanotrophic association in *Toniniopsis separabilis* (M-0289891). A, cross-section of apothecium with associated cyanobacterium cells. B, Separate *Nostoc* sp. cell. A = 50 μm; B = 15 μm.

6.2. Phylogeny

6.2.1. Phylogenetic studies of Bacidia s. str. in Russia

The first phylogenetic study in *Bacidia* was based on nrITS sequences and narrowed the species concept, resulting in a reassessment of the genus, and transferring several species to other genera such as *Biatora* Fr., *Toninia* A. Massal., and *Bacidina* Vězda (Ekman, 2001). The results of this study also indicated that many species with blue-green pigmentation in the epithecium and/or with rod-shaped or spindle-shaped ascospores considered as *Bacidia*, were more closely related to *Toninia* s. lat., and as is also discussed earlier in the Chapter 2, to *Toniniopsis*.

Subsequent phylogenetic studies on *Bacidia* using sequences from several phylogenetic markers, namely nrITS with mtSSU (Andersen and Ekman, 2005; Lendemer *et al.*, 2016; Malíček *et al.*, 2018), and nrLSU and mtSSU (Lutzoni *et al.*, 2004; Sérusiaux *et al.*, 2012), included only few species of *Bacidia* s. str. Additional multilocus phylogenetic studies involving RPB1 and RPB2 also covered six species, only (James *et al.*, 2006; Miadlikowska *et al.*, 2006, 2014; Reese Næsborg *et al.*, 2007; Ekman *et al.*, 2008;

111

Kistenich *et al.*, 2018). Even with a range of phylogenetic methods employed, the relationships between species and support of the groups remained unclear.

In a first molecular study on *Bacidia* s. str. in Russia, the taxon sampling was expanded to include twenty-two newly obtained nrITS sequences from specimens collected in the Russian Far East (Gerasimova *et al.*, 2018; Chapter 3). As *Bacidia* species are abundant in habitats with high humidity and moderate insolation, the specimens were collected in swamps, riverbanks and valleys, as well as in open forests, on forest edges, and hill and mountain slopes close to the sea or near lakes or swamps, where their abundance was expected to be especially rich (Chapter 3 and 4). The sequences obtained were combined with all nrITS sequences publically available at that time. The main goal of this broader sampling was to clarify species boundaries in members of *Bacidia* s. str. from the Russian territory in relation to species from North America and Europe. Phylogenetic relationships within *Bacidia* s. str. agreed with the previous results presented by Ekman (2001) but additionally revealed well-supported groups within *Bacidia* s. str., nevertheless still with low support in basal nodes of the clades and several polytomies. To overcome this problem and clarify the relationships among the groups, sequences from additional loci were needed for follow-up studies.

6.2.2. Multilocus phylogeny of Bacidia

Since the first phylogenetic studies by Ekman (2001), over a hundred additional sequences of *Bacidia* s. str. have been added to GenBank, including the sequences obtained in this study. This has enabled the phylogeny of *Bacidia* s. str. to be refined and made possible a better interpretation of species complexes in a broader context and clarify deep relationships of the species. Thus, data from three widely used ribosomal RNA-encoding genes (nrITS, nrLSU and mtSSU) were sequenced and combined with two protein-coding genes (RPB1 and RPB2). The final multigene phylogeny contained 179 sequences: 48 newly generated sequences from the Russian Far East and all *Bacidia* s. str. sequences from GenBank (131 sequences) representing different localities in Eurasia and North America.

This first large multilocus phylogeny resulted in significantly increased backbone support (Chapter 4), including the groups congruent with previous results based on nrITS only (Ekman 2001; Gerasimova *et al.* 2018).

6.2.3 Phylogenetic grouping correlates with colouration of apothecia

Already in the first phylogenetic study on *Bacidia* in Russia, the correlation between inner coloration of apothecia and phylogenetic groups was observed and discussed (Chapter 3). However, the multilocus phylogeny revealed high support of the clades grouping the taxa into two large clades based on apothecial pigmentation, represented by specimens collected in the temperate region (Table 1). A well-supported third clade included *B. thiersiana* and *B. hostheleoides*, which are widespread in south-eastern North America and the Neotropics (Chapter 4).

The first clade (I) comprised the Laurocerasi, Schweinitzii and Suffusa groups, represented by specimens with either dark brown, red-brown, and green pigments (Laurocerasi-brown and Bagliettoa-green) or a combination of these in the upper part of the hymenium and lateral exciple (Table 1). The second clade (II) contained the Fraxinea, Polychroa, and Arceutina groups having a mixture of yellow, orange and/or brown apothecial pigments (Arceutina-yellow, Polychroa-brown and Rubella-orange). In contrast, specimens in clade III were characterized by almost colourless or faintly and diffusely pigmented internal apothecial structures. While atranorin is the most common secondary compound in *Bacidia*, several species showed a unique secondary metabolite composition in the apothecia of *Bacidia* (Table 1; Chapter 4), proving the untapped potential of *Bacidia* for secondary metabolite biosynthesis.

Table 1. Overview of apothecial coloration in *Bacidia* s. str. Colour is given according to Meyer and Printzen (2000) and Ekman (1996).

Group	Upper hymenium	Exciple edge	Lateral exciple	Hypothecium
Laurocerasi	Laurocerasi-brown + Bagliettoa-green (in *B. kurilensis*)	Laurocerasi-brown	Laurocerasi-brown/Rubella-orange	Arceutina-yellow
Schweinitzii	Bagliettoa-green	Bagliettoa-green	Schweinitzii-red	Schweinitzii-red
Suffusa	Laurocerasi-brown	Laurocerasi-brown	Rubella-orange	Rubella-orange
Fraxinea	Rubella-orange	Rubella-orange	Rubella-orange	Rubella-orange
Polychroa	Polychroa-brown	Rubella-orange	Rubella-orange	Rubella-orange
Arceutina	Arceutina-yellow	Arceutina-yellow	Arceutina-yellow	Arceutina-yellow
B. ekmaniana	Polychroa-brown	-	Rubella-orange	Rubella-orange
B. absistens (**4-O-methylcryptoc-hlorophaeic acid**)	Bagliettoa-green/ Laurocerasi-brown	Bagliettoa-green	Laurocerasi-brown	Arceutina-yellow
B. squamulosula (**homosekikaic acid**)	Rubella-orange		Arceutina-yellow	Arceutina-yellow
B. gigantensis (**homosekikaic acid**)	Grey to grey-brown pigment	Arceutina-yellow	Arceutina-yellow	Arceutina-yellow

B. thiersiana	-	-	-	-
B. hostheleoides	No colour or small amounts of Rubella-orange	No colour or small amounts of Rubella-orange	No colour or small amounts of Rubella-orange	No colour or small amounts of Rubella-orange

6.2.4. ITS2 structure

As additional support for species delimitation, the ITS2 secondary structure of morphologically close species of *Bacidia* s. str. was analyzed, emphasizing on compensatory base changes (CBCs) and hemi-CBCs (hCBC) in the structurally conserved regions of helix III (Fig. 6.3). CBCs are mutations that occur in the primary RNA transcript, whereby both nucleotides are paired in the secondary structure of the ITS transcript and mutate in a way that their bond is retained (e.g., G-C mutates to A-U) (Coleman, 2009).
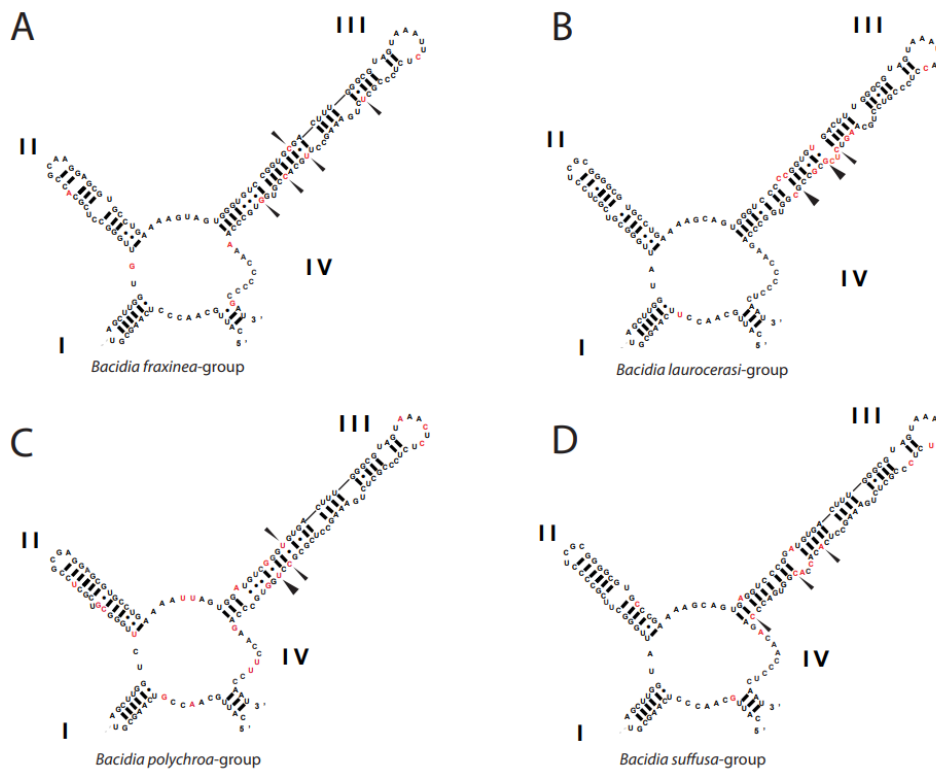
Figure 6.3. Differences in secondary structure of ITS2 among groups within *Bacidia* s. str. Variable nucleotides among species within the groups are marked with diamonds, CBCs and hemi-CBCs are indicated by broad and narrow arrows, respectively.

A hemi-CBC is a mutation in one of the two nucleotides while keeping the nucleotide bond (Coleman, 2009). Selected species corresponded to the supported clades as indicated on the phylogenetic tree. The additional study of ITS2 secondary structure

distinguished and supported all main clades of the genus, serving as additional evidence for species delimitation (Chapter 3).

6.2.5. New species to science endemic for the Far East of Russia

Based on morphological and phylogenetic data, five species new to science were described from the Russian territory in the course of this work. The type material of *Bacidia areolata* was collected in Khabarovskiy Krai, Bolshekhekhtsirskiy State Natural Reserve in coniferous-broadleaf forest, on a terrace above the river on the bark of *Acer tegmentosum*. It is closely related to *B. suffusa* but differs in having a smooth, cracked to areolate thallus and shorter ascospores. The type specimen of *Bacidia elongata* was discovered at the same locality on the bark of *Acer mono*. It is similar to *B. fraxinea* but differs in having a wide zone of cells with enlarged lumina along the edge of the exciple.

The type specimen of *Bacidia kurilensis* was collected in the Kunashir Island, at the foot of the Mendeleev Volcano in the mixed conifer broadleaf forest on bark of *Salix udensis*. It is closely related to *B. biatorina*, *B. heterochroa*, *B. laurocerasi* and *B. salazarensis*, but differs by the combination of a granular thallus, large black apothecia and a green hue in the upper part of the exciple edge as well as in the epihymenium.

Bacidia sachalinensis was described from Yuzhno-Sakhalinsk where it was collected in floodplain forest on bark of *Populus maximowiczii*. Its thallus structure and apothecium colour are variable, which is also typical for *Bacidia polychroa*, but it differs from the latter by having shorter ascospores with fewer septa and a mainly smooth to areolate thallus.

The last species, *Bacidia obtecta* was described from Sakhalin, where it was collected in floodplain forest in valley of the Tym' River, on the bark of *Populus maximowiczii*. Compared to *B. elongata* and *B. fraxinea*, it is distinguished by the apothecial colour, which is mainly brown to rusty brown, abundant colourless crystals in the upper part of the hymenium and lateral exciple, which dissolve in KOH but not in HNO_3, and ascospores with fewer septa. From *B. fraxinea* it can be additionally distinguished by the number of enlarged lumina cells along the exciple edge. To sum up, all five species are so far known only from the Russian Far East and thus can be considered endemics of the territory from where they were described (Chapter 3 and 4).

Due to its territorial proximity and as a substantially large list of species are known only from Japan, the species of *Bacidia* recorded in checklists of the lichens of Japan were

included in this study as well (Kashiwadani and Inoue, 1993; Inoue, 1994; Harada *et al.*, 2004). In those checklists, six species of *Bacidia* s. str. have been recorded from various studies but not specifically from Japan and were therefore not included in the subsequent discussion (Chapter 3). In summary, out of 19 *Bacidia* species reported in Japan, three turned to be synonyms of known *Bacidia* species, and only one species from Japan potentially belongs to *Bacidia* s. str. However, according to the description in the protologue, it did not match to any specimen from the Far East of Russia, and thus supported the difference to the newly described species.

6.3. Genomics

Genomics—dealing with information obtained from whole genomes—moves the field forward by generating extraordinary amounts of data. that can be combined with other data types (e.g., physiology or metabolomics) to yield highly interesting insights. The ever-growing volume of data plays a significant role in progressing biological research and helps addressing various important questions related to the evolution of organisms and mechanisms of adaptation to the environment. Many lichens have developed numerous adaptations to optimize their survival under various, often severe, environmental stresses and thus inhabit different substrates, taking benefit of the symbiotic lifestyle, e.g., by producing unique chemical compounds. Detailed knowledge of habitat requirements of lichens is also essential for their use as bioindicators (e.g., determining the conservation value of woodland areas) and for understanding how lichens might be affected by a changing climate.

Thus, one interesting case is *Bacidia rubella*, a relatively widespread species frequently found in habitats with a fair amount of humidity and sunlight similar to other *Bacidia* species, but also being capable of growing in forest edges and even in more extreme sun-exposed environments. Given its habitat range, this species was selected for in-detailed genomic studies. A newly produced and well-annotated *B. rubella* genome will form a basis for future investigations of genomic changes associated with ecological adaptations in the genus *Bacidia*.

6.3.1. Discovering BGC diversity in Bacidia

The genes encoding most fungal secondary metabolites are located adjacent to each other (i.e., "clustered") in the genome, and thus can be readily identified in a genome sequence

(Rokas *et al.*, 2020; Robey *et al.*, 2021). Moreover, in many cases, the chemical structure of their products can be predicted to a certain extent, based on the analysis and the biosynthetic logic of the enzymes encoded in a BGC and their similarity to known counterparts (Medema and Fischbach, 2015; Navarro-Muñoz *et al.*, 2020; Singh *et al.*, 2021, 2022).

The reliability of gene predictions is highly dependent on quality and completeness of a genome. Therefore, growing axenic cultures from individual lichen symbionts is an essential prerequisite for generating high-quality genomic data because it reduces possibility from chimeric contigs from algae, bacteria, and other fungi. For this reason, high accuracy and time-consuming techniques were necessary to obtain an axenic culture of the *Bacidia rubella* fungal symbiont for further genomic study (Stages of culture preparation are shown in Fig. 6.4).
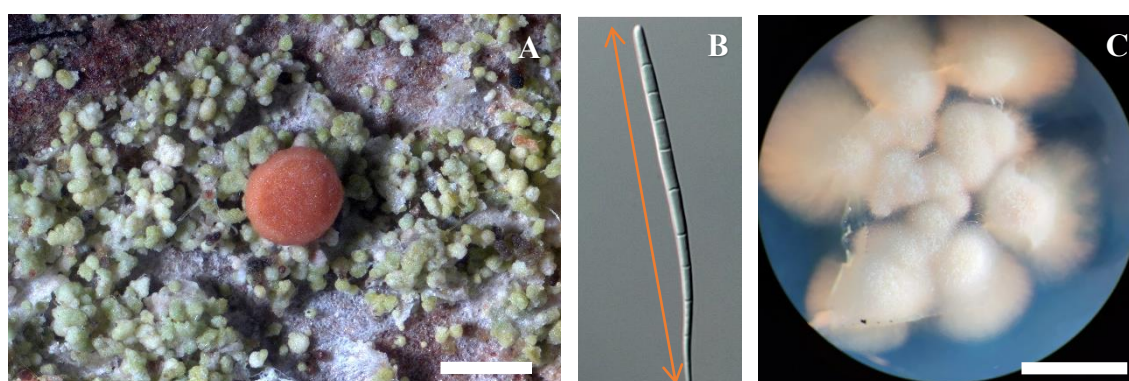
Figure 6.4. Stages of culture preparation of *Bacidia rubella*. A, Apothecia and thallus structure. B, acicular, or needle-shaped ascospore. C, six-months-old fungal culture. Scales: A & C = 0.5 mm, B = 50 μm.

The hybrid approach using Illumina short-read combined with Oxford Nanopore long-read technology enabled the generation of a high-quality genome assembly of *B. rubella* with a size of 33.52 Mb and 98% completeness according to BUSCO (Benchmarking Universal Single-Copy Orthologs: http://busco.ezlab.org/). BUSCO quantifies the completeness of genomic data sets in terms of the expected single copy orthologue content in comparison to those of model organisms (Simão *et al.*, 2015).

To study biosynthetic content, it is necessary to provide context for the putative biosynthetic genes identified in *B. rubella*; therefore, 22 publicly available genomes were added to for comprehensive comparative analyses (Chapter 5). These additional genomes included other publically available genomes of the family Ramalinaceae (*Bacidia gigantensis*, *Ramalina intermedia* and *R. peruviana*). The BUSCO completeness was 90%

or above for all studied genomes, except for *Alectoria* and *Graphis* (with 75.8% and 88.6%, respectively), indicating reliable BGC prediction. Based on the results obtained, a high diversity of BGCs in *Bacidia rubella* – way beyond what was reported from the species chemical profiles, known as a producer of atranorin (Table 2) – indicating its high potential to produce different secondary metabolites, with possible direct relevance for natural product research and production.

In the genome of *B. rubella,* 31 BGCs were found, including six non-reducing and four reducing TI-PKS sequences (Table 2). This TI-PKS biosynthetic content is similar to that of *B. gigantensis,* which contains 11 identified TI-PKS genes (seven NR-PKSs and four R-PKSs, respectively; Table 2). Despite the overall similarity of TI-PKS gene numbers between *B. rubella* and *B. gigantensis*, comparison of these biosynthetic clusters showed only two significant hits between the two species, one R-PKS and one NR-PKS, with ca 63% BLAST similarity of the amino-acid sequences, but function of those clusters is still to be discovered. This result indicates that both fungal species most likely do not only differ in their major secondary metabolite. To date, atranorin, the most widespread secondary metabolite found in the genus *Bacidia* s. lat., is known for *B. rubella* (Ekman 1996). On the other hand, *B. gigantensis* synthesizes homosekikaic (McMullin *et al.*, 2020), unique to this species and unknown in other *Bacidia* species.

Compared to *Bacidia* species, the two species *Ramalina intermedia* and *R. peruviana* differed in having even more BGCs. In detail, *R. intermedia* contains 54 BGCs, including 13 non-reducing, 17 reducing and one partially reducing TI-PKS sequences. *Ramalina peruviana*, on the other hand, contains 43 BGCs, including nine non-reducing, seven reducing and one partially reducing genes, respectively (Table 2). Similarly, to the two *Bacidia* species, the known secondary metabolites in the two *Ramalina* are also largely unknown. This fact makes this genomic study an important puzzle piece and a starting point for future research, where experiments can be designed to broaden the knowledge of secondary compound production in *Bacidia* and other lichen-forming fungi.

Table 2. Comparison of BGCs in Ramalinaceae

Species	Genome Size (Mb)	Number of Clusters	Type I PKS (total)	Type I NR-PKS	Type I R-PKS	PR-PKS	Hybrid PKS-NRPS	NRPS/ putative NRPS	Metabolites reported
Bacidia gigantensis	33.1	31	11	7	4	0	1	5/10	Homosekikaic acid
Bacidia rubella	33.5	31	10	6	4	0	0	3/7	Atranorin

Ramalina intermedia	26.2	54	31	13	17	1	3	5/9	Usnic acid, sekikaic acid, homosekikaic acid
Ramalina peruviana	25.5	43	17	9	7	1	1	4/10	Usnic acid, sekikaic acid, homosekikaic acid

6.4. Interesting findings of secondary compounds in *Bacidia rubella*

6.4.1. Atranorin

Over the years, various biological properties of atranorin have been examined (Studzinska-Sroka *et al.*, 2017 and reference therein), showing wide application in the pharmaceutical industry, e.g., in cancer treatment. Atranorin is one of the most common lichen secondary metabolites, characteristic for numerous lichen families but rarely found in some mosses and higher plants (Studzinska-Sroka *et al.*, 2017). It is the major secondary compound known in *Bacidia,* and particularly in *B. rubella* (Ekman 1996).

At the beginning of this research, there were two main hypotheses, suggesting two different PKS genes involved in the atranorin biosynthesis, namely PKS16 gene in *Cladonia rangiferina* (Elshobary *et al.*, 2018) and PKS23 gene in four *Cladonia* species (including *C. rangiferina*) as well as *Stereocaulon alpinum* (Kim *et al.*, 2021). Based on the similarity and phylogenetic results obtained in this study, a putative PKS23 gene involved in atranorin production was identified in *B. rubella*. A PKS16 homolog was not found. These results were consistent with the latter theory of Kim *et al.* (2021) grouping PKS23 sequences from atranorin-producing lichen-forming fungi together with *B. rubella* (Chapter 5). The newly identified, putative PKS23 sequence of *B. rubella* was recovered as sister to PKS23 sequences from *Cladonia rangiferina* and *Stereocaulon alpinum*, suggesting a sister-group relationship of *Bacidia* with Cladoniaceae, whereby the PKS23 sequences from Parmeliaceae formed a sister-group to that clade (Chapter 5, Fig. 1). One possible explanation is that the ancestor of *Bacidia* may have acquired the PKS23 gene from an ancestor of Cladoniaceae via horizontal gene transfer, which may also explain the scattered occurrence of atranorin in Ramalinaceae.

6.4.2. Further interesting findings. Monascorubrin: A compound which is possibly involved in red color of Bacidia rubella

Monascorubrin is one of the two classical orange *Monascus* pigments, which serves as the necessary precursor in the formation of the food colorant *Monascus* red pigments by

amination with primary amines (Jia *et al.*, 2019). A putative monascorubrin biosynthetic PKS gene has been identified in *B. rubella,* showing 48% BLAST identity with the putative PKS3 involved in the biosynthesis of monascorubrin in *Talaromyces* (*Penicillium*) *marneffei* (Woo *et al.*, 2014). Besides monascorubrin biosynthesis, it has been shown that PKS3 is also involved in the production of a well-known toxin, citrinin, as well as a yellow pigment, ankaflavin. Although, none of these substances have been reported for *B. rubella* yet, monascorubrin and its related compounds are polyketides used as natural red colourants for a wide range of food (Chen *et al.*, 2017). In *B. rubella*, however, monascorubrin might be responsible for the characteristic orange to the orange-brown colouration of the fruiting bodies.

6.5. General conclusion and perspectives

This dissertation resulted in an updated taxonomy and nomenclature of the genus *Bacidia* in Russia. Based on multiple lines of evidence (i.e., morphological, anatomical, and phylogenetic analyses), from the 35 initially reported species 19 remained under *Bacidia*, which is about 33% from the worldwide species diversity of *Bacidia* s. str. (according to the estimate by Ekman 1996). Almost half of the names from the initial checklist were removed by transferring species to other genera and six species were synonymized. However, three species were reported as new to Russia and five species we described as new to science. Despite the detailed study on *Bacidia*, further collecting and phylogenetic studies may show even higher diversity of *Bacidia* in Russia, as large parts could not be sampled.

My pioneering comparative genomic studies on *Bacidia* showed a high biochemical potential of the genus and raised further questions. The generation of experimental biochemical data, genome-mining, combined with phylogenetic analyses, remains an important way to gain insights into the biochemical potential of non-model organisms, including lichens. The *in-silico* approach provided first insights into the possible roles of these genes in *B. rubella*. However, future detailed studies of individual BGCs combining gene expression analyses with analytical chemistry and metabolomics will allow rigorous testing of the hypotheses proposed in this first genomic study in *Bacidia*. Prospects for this are promising as an increasing number of studies succeeded in the heterologous expression of lichen-forming fungal genes (e.g., Sinnemann *et al.*, 2000; Bertrand and Sorensen, 2019; Jeong *et al.*, 2021; Kealey *et al.*, 2021; Kim *et al.*, 2021). Subsequent *in vivo* studies of

metabolite profiles in lichen-forming fungi supplemented by high-resolution MS/MS spectra (Olivier-Jimenez *et al.*, 2019) or metabolic profiling based on stable isotope analysis (Kuhn *et al.*, 2019) will contribute to the knowledge on how secondary metabolites in lichen-forming fungi are produced.

References

Abdel-Hameed, M., Bertrand, R.L., Piercey-Normore, M.D., and Sorensen, J.L., 2016a. Identification of 6-hydroxymellein synthase and accessory genes in the lichen *Cladonia uncialis*. *Journal of Natural Products*, 79(6), pp.1645–1650.

Abdel-Hameed, M., Bertrand, R.L., Piercey-Normore, M.D., and Sorensen, J.L., 2016b. Putative identification of the usnic acid biosynthetic gene cluster by *de novo* whole-genome sequencing of a lichen-forming fungus. *Fungal Biology*, 120(3), pp.306–316.

Albarano, L., Esposito, R., Ruocco, N., and Costantini, M., 2020. Genome mining as new challenge in natural products discovery. *Marine drugs*, 18(4), p.199.

Allen, J.L., Jones, S.J., and McMullin, R.T., 2021. Draft genome sequence of the lichenized fungus *Bacidia gigantensis*. *Microbiology Resource Announcements*, 10(44), e00686-21.

Andersen, H.L., and Ekman, S., 2005. Disintegration of the Micareaceae (lichenized Ascomycota): a molecular phylogeny based on mitochondrial rDNA sequences. *Mycological Research*, 109(1), pp.21–30.

Aptroot, A., and da Silva Caceres, M.E., 2014. New lichen species from termite nests in rainforest in Brazilian Rondônia and adjacent Amazonas. *The Lichenologist*, 46(3), pp.365–372.

Armaleo, D., *et al.*, 2019. The lichen symbiosis re-viewed through the genomes of *Cladonia grayi* and its algal partner *Asterochloris glomerata*. *BMC Genomics*, 20(1), p.605.

Armaleo, D., Sun, X., and Culberson, C., 2011. Insights from the first putative biosynthetic gene cluster for a lichen depside and depsidone. *Mycologia*, 103(4), pp.741–754.

Armaleo, D., Zhang, Y., and Cheung, S., 2008. Light might regulate divergently depside and depsidone accumulation in the lichen *Parmotrema hypotropum* by affecting thallus temperature and water potential. *Mycologia*, 100(4), pp.565–576.

Armstrong, E.E., *et al.*, 2018. Draft genome sequence and annotation of the lichen-forming fungus *Arthonia radiata*. *Genome Announcements*, 6(14), e00281-18.

Banchi, E., *et al.*, 2018. ITS2 metabarcoding analysis complements lichen mycobiome diversity data. *Mycological Progress*, 17(9), pp.1049–1066.

Bates, S.T., *et al.*, 2011. Bacterial communities associated with the lichen symbiosis. *Applied and environmental microbiology*, 77(4), pp.1309–1314.

Begerow, D., Nilsson, H., Unterseher, M., and Maier, W., 2010. Current state and perspectives of fungal DNA barcoding and rapid identification procedures. *Applied Microbiology and Biotechnology*, 87(1), pp.99–108.

Bemm, F., Weiß, C.L., Schultz, J., and Förster, F., 2016. Genome of a tardigrade: Horizontal gene transfer or bacterial contamination? *Proceedings of the National Academy of Sciences*, 113(22), pp.E3054–E3056.

Bertrand, R.L., and Sorensen, J.L., 2019. Transcriptional heterologous expression of two type III PKS from the lichen *Cladonia uncialis*. *Mycological Progress*, 18(12), pp.1437–1447.

Blackwell, M., 2011. The Fungi: 1, 2, 3 … 5.1 million species? *American Journal of Botany*, 98(3), pp.426–438.

Boustie, J., Tomasi, S., and Grube, M., 2011. Bioactive lichen metabolites: alpine habitats as an untapped source. *Phytochemistry Reviews*, 10(3), pp.287–307.

Brackel, W. v, 2019. Rote Liste und Gesamtartenliste der Flechten (Lichenes), flechtenbewohnenden und flechtenähnlichen Pilze Bayerns. *Augsburg: Bayerisches Landesamt für Umwelt*.

Büdel, B., and Scheidegger, C., 2008. Thallus morphology and anatomy. In: I. Nash Thomas H., ed., *Lichen Biology*, 2nd ed. Cambridge: Cambridge University Press, pp.40–68.

Calchera, A., Dal Grande, F., Bode, H.B., and Schmitt, I., 2019. Biosynthetic gene content of the 'Perfume Lichens' *Evernia prunastri* and *Pseudevernia furfuracea*. *Molecules*, 24(1), p.203.

Cannon, P., *et al.*, 2021. Lecanorales: Ramalinaceae, including the genera *Bacidia*, *Bacidina*, *Bellicidia*, *Biatora*, *Bibbya*, *Bilimbia*, *Cliostomum*, *Kiliasia*, *Lecania*, *Megalaria*, *Mycobilimbia*, *Phyllopsora*, *Ramalina*, *Scutula*, *Thalloidima*, *Toninia*, *Toniniopsis* and *Tylothallia*. *Revisions of British and Irish Lichens*, 11, pp.1–82.

Cao, M.D., *et al.*, 2017. Scaffolding and completing genome assemblies in real-time with nanopore sequencing. *Nature Communications*, 8(1), 14515.

Cardarelli, M., *et al.*, 1997. Antimitotic effects of usnic acid on different biological systems. *Cellular and Molecular Life Sciences CMLS*, 53(8), pp.667–672.

Cardinale, M., *et al.*, 2012. Bacterial taxa associated with the lung lichen *Lobaria pulmonaria* are differentially shaped by geography and habitat. *FEMS Microbiology Letters*, 329(2), pp.111–115.

123

Cernava, T., *et al.*, 2015. Analyzing the antagonistic potential of the lichen microbiome against pathogens by bridging metagenomic with culture studies. *Frontiers in microbiology*, 6, pp.620–620.

Cernava, T., *et al.*, 2017. Deciphering functional diversification within the lichen microbiota by meta-omics. *Microbiome*, 5(1), p.82.

Chakraborty, P., 2018. Herbal genomics as tools for dissecting new metabolic pathways of unexplored medicinal plants and drug discovery. *Biochimie Open*, 6, pp.9–16.

Chapman, A., 2006. *Numbers of Living Species in Australia and the World, 1st edn.*

Chen, W., *et al.*, 2017. Orange, red, yellow: biosynthesis of azaphilone pigments in Monascus fungi. *Chemical Science*, 8(7), pp.4917–4925.

Coleman, A.W., 2009. Is there a molecular key to the level of "biological species" in eukaryotes? A DNA guide. *Molecular Phylogenetics and Evolution*, 50(1), pp.197–203.

Crawford, S.D., 2019. Lichens used in traditional medicine. In: *Lichen secondary metabolites*. Springer, pp.31–97.

Cui, J., *et al.*, 2020. Analysis and comprehensive comparison of PacBio and nanopore-based RNA sequencing of the *Arabidopsis* transcriptome. *Plant Methods*, 16(1), p.85.

Dal Grande, F., *et al.*, 2017. Adaptive differentiation coincides with local bioclimatic conditions along an elevational cline in populations of a lichen-forming fungus. *BMC Evolutionary Biology*, 17(1), p.93.

Dal Grande, F., *et al.*, 2018. The draft genome of the lichen-forming fungus *Lasallia hispanica* (Frey) Sancho & A. Crespo. *The Lichenologist*, 50(3), pp.329–340.

De Notaris, G., 1846. Frammenti lichenografici di un lavoro inedito. *Giornale Botanico Italiano*, 2, pp.174–224.

Demmig-Adams, B., *et al.*, 1990. Effect of high light on the efficiency of photochemical energy conversion in a variety of lichen species with green and blue-green phycobionts. *Planta*, 180(3), pp.400–409.

Devkota, S., Chaudhary, R.P., Werth, S., and Scheidegger, C., 2017. Indigenous knowledge and use of lichens by the lichenophilic communities of the Nepal Himalaya. *Journal of Ethnobiology and Ethnomedicine*, 13(1), p.15.

Divakar, P.K., *et al.*, 2015. Evolution of complex symbiotic relationships in a morphologically derived family of lichen-forming fungi. *New Phytologist*, 208(4), pp.1217–1226.

Divakar, P.K., *et al.*, 2016. A DNA barcoding approach for identification of hidden diversity in Parmeliaceae (Ascomycota): *Parmelia* sensu stricto as a case study. *Botanical Journal of the Linnean Society*, 180(1), pp.21–29.

Douglas, A.E., 1994. *Symbiotic interactions*. Oxon, GB: Oxford University Press, 1994.

Ekman, S., 1996. The corticolous and lignicolous species of *Bacidia* and *Bacidina* in North America. *Opera Botanica*, 127, pp.1–148.

Ekman, S., 2001. Molecular phylogeny of the Bacidiaceae (Lecanorales, lichenized Ascomycota). *Mycological Research*, 105(7), pp.783–797.

Ekman, S., Andersen, H.L., and Wedin, M., 2008. The limitations of ancestral state reconstruction and the evolution of the ascus in the Lecanorales (Lichenized Ascomycota). *Systematic Biology*, 57(1), pp.141–156.

Elix, J.A., and Stocker-Wörgötter, E., 2008. Biochemistry and secondary metabolites. In: I. Nash Thomas H., ed., *Lichen Biology*, 2nd ed. Cambridge: Cambridge University Press, pp.104–133.

Elshobary, M.E., *et al.*, 2018. Tissue-specific localization of polyketide synthase and other associated genes in the lichen, *Cladonia rangiferina*, using laser microdissection. *Phytochemistry*, 156, pp.142–150.

Färber, L., *et al.*, 2014. Sunscreening fungal pigments influence the vertical gradient of pendulous lichens in boreal forest canopies. *Ecology*, 95(6), pp.1464–1471.

Farrar, J.F., 1976. Lichen as an ecosystem: Observation and experiment. In: *Lichenology: Progress and Problems; Proceedings of an international Symposium*.

Fryday, A.M., 2019. Eleven new species of crustose lichenized fungi from the Falkland Islands (Islas Malvinas). *The Lichenologist*, 51(3), pp.235–267.

Gadd, G.M., 2013. Fungi and their role in the Biosphere. In: *Reference Module in Earth Systems and Environmental Sciences*. Elsevier.

Gauslaa, Y., and Solhaug, K.A., 2001. Fungal melanins as a sun screen for symbiotic green algae in the lichen *Lobaria pulmonaria*. *Oecologia*, 126(4), pp.462–471.

Gerasimova, J.V., and Ekman, S., 2017. Taxonomy and nomenclature of seven names in *Bacidia* (Ramalinaceae, Lecanorales) described from Russia. *Phytotaxa*, 316(3), pp.292-296-292–296.

Gerasimova, J.V., Ezhkin, A.K., and Beck, A., 2018. Four new species of *Bacidia* s.s. (Ramalinaceae, Lecanorales) in the Russian Far East. *The Lichenologist*, 50(6), pp.603–625.

Gerasimova, J.V., Urbanavichene, I.N., Urbanavichus, G.P., and Beck, A., 2021. Morphological and phylogenetic analyses of *Toniniopsis subincompta* s. lat. (Ramalinaceae, Lecanorales) in Eurasia. *The Lichenologist*, 53(2), pp.171–183.

Gilbert, O.L., 1996. The occurrence of lichens with albino fruit bodies (Ascomata) and their taxonomic significance. *The Lichenologist*, 28(1), pp.94–97.

Golubkova, N.S., 2003. *Bacidia* De Not. In: *Handbook of the lichens of Russia.* Bacidiaceae, Catillariaceae, Lecanoraceae, Megalariaceae, Mycobilimbiaceae, Rhizocarpaceae, Trapeliaceae. St. Petersburg: Nauka, pp.12–39.

Grigoriev, I.V., *et al.*, 2014. MycoCosm portal: gearing up for 1000 fungal genomes. *Nucleic Acids Research*, 42(D1), pp.D699–D704.

Grimm, M., *et al.*, 2021. The Lichens' Microbiota, Still a Mystery? *Frontiers in Microbiology*, 12.

Grube, M., *et al.*, 2015. Exploring functional contexts of symbiotic sustain within lichen-associated bacteria by comparative omics. *The ISME Journal*, 9(2), pp.412–424.

Grube, M., and Berg, G., 2009. Microbial consortia of bacteria and fungi with focus on the lichen symbiosis. *Fungal Biology Reviews*, 23(3), pp.72–85.

Harada, H., Okamoto, T., and Yoshimura, I., 2004. *A checklist of lichens and lichen-allies of Japan*. Japanese Society for Lichenology.

Haridas, S., *et al.*, 2020. 101 Dothideomycetes genomes: A test case for predicting lifestyles and emergence of pathogens. *Studies in Mycology*, 96, pp.141–153.

Hibbett, D., *et al.*, 2016. Sequence-based classification and identification of Fungi. *Mycologia*, 108(6), pp.1049–1068.

Hofstetter, V., Miadlikowska, J., Kauff, F., and Lutzoni, F., 2007. Phylogenetic comparison of protein-coding versus ribosomal RNA-coding sequence data: A case study of the Lecanoromycetes (Ascomycota). *Molecular Phylogenetics and Evolution*, 44(1), pp.412–426.

Honegger, R., 2009. *Plant relationships*. Springer-Verlag Berlin.

Inoue, M., 1994. Phytogeography of lecideoid lichens in Japan. *The Journal of the Hattori Botanical Laboratory*, 76, pp.183–195.

James, T.Y., *et al.*, 2006. Reconstructing the early evolution of Fungi using a six-gene phylogeny. *Nature*, 443(7113), pp.818–822.

Jeong, M.-H., *et al.*, 2021. Production and activity of cristazarin in the lichen-forming fungus *Cladonia metacorallifera*. *Journal of Fungi*, 7(8).

Jia, L., *et al.*, 2019. Monascorubrin and rubropunctatin: Preparation and reaction characteristics with amines. *Dyes and Pigments*, 170, p.107629.

John, V., and Breuss, O., 2004. Flechten der östlichen Schwarzmeer-Region in der Türkei (BLAM-Exkursion 1997). *Herzogia*, 17, pp.137–156.

Junttila, S., and Rudd, S., 2012. Characterization of a transcriptome from a non-model organism, *Cladonia rangiferina*, the grey reindeer lichen, using high-throughput next generation sequencing and EST sequence data. *BMC Genomics*, 13(1), p.575.

Kantivilas, G., 2018. Studies on *Bacidia* (lichenized Ascomycota, Ramalinaceae) in temperate Australia, including Tasmania: saxicolous and terricolous species. *The Lichenologist*, 50(4), pp.451–466.

Kashiwadani, H., and Inoue, M., 1993. The lichens of Kusiro Marsh, Hokkaido, Japan. *Memoirs of the National Science Museum Tokyo*, 26, pp.53–66.

Kealey, J.T., Craig, J.P., and Barr, P.J., 2021. Identification of a lichen depside polyketide synthase gene by heterologous expression in *Saccharomyces cerevisiae*. *Metabolic Engineering Communications*, 13, e00172.

Kim, W., *et al.*, 2021. Linking a gene cluster to atranorin, a major cortical substance of lichens, through genetic dereplication and heterologous expression. *mBio*, 12(3), e01111-21.

Kirk, P., Cannon, P., Stalpers, J., and Minter, D.W., 2008. Dictionary of the Fungi.10th ed. *CABI Publishing. Great Britain*.

Kistenich, S., Timdal, E., Bendiksby, M., and Ekman, S., 2018. Molecular systematics and character evolution in the lichen family Ramalinaceae (Ascomycota: Lecanorales). *TAXON*, 67(5), pp.871–904.

Kolawole, O., Meneely, J., Petchkongkaew, A., and Elliott, C., 2021. A review of mycotoxin biosynthetic pathways: associated genes and their expressions under the influence of climatic factors. *Fungal Biology Reviews*, 37, pp.8–26.

Kono, M., *et al.*, 2017. Physical contact and carbon transfer between a lichen-forming *Trebouxia* alga and a novel Alphaproteobacterium. *Microbiology*, 163(5), pp.678–691.

Kono, M., *et al.*, 2020. In vitro resynthesis of lichenization reveals the genetic background of symbiosis-specific fungal-algal interaction in *Usnea hakonensis*. *BMC Genomics*, 21(1), p.671.

Kuhn, V., *et al.*, 2019. A facile in vivo procedure to analyze metabolic pathways in intact lichens. *New Phytologist*, 224(4), pp.1657–1667.

127

Lawrey, J.D., 1989. Lichen secondary compounds: evidence for a correspondence between antiherbivore and antimicrobial function. *The Bryologist*, 92(3), pp.326–328.

Lendemer, J.C., Harris, R.C., and Ladd, D., 2016. The faces of *Bacidia schweinitzii*: molecular and morphological data reveal three new species including a widespread sorediate morph. *The Bryologist*, 119(2), pp.143–171.

Lichman, B.R., Godden, G.T., and Buell, C.R., 2020. Gene and genome duplications in the evolution of chemodiversity: perspectives from studies of Lamiaceae. *Physiology and Metabolism*, 55, pp.74–83.

Liu, L., *et al.*, 2015. Bioinformatical analysis of the sequences, structures and functions of fungal polyketide synthase product template domains. *Scientific Reports*, 5(1), p.10463.

Llop, E., 2007. *'Lecanorales': 'Bacidiaceae' I : 'Bacidia' y 'Bacidina'*. Sociedad Española de Liquenología.

Lücking, R., 2008. Foliicolous lichenized Fungi. *Flora Neotropica*, 103, pp.1–866.

Lücking, R., Hodkinson, B.P., and Leavitt, S.D., 2017. The 2016 classification of lichenized fungi in the Ascomycota and Basidiomycota – Approaching one thousand genera. *The Bryologist*, 119(4), pp.361–416.

Lumbsch, H.T., 2000. Phylogeny of filamentous ascomycetes. *Naturwissenschaften*, 87(8), pp.335–342.

Lutzoni, F., *et al.*, 2004. Assembling the fungal tree of life: progress, classification, and evolution of subcellular traits. *American Journal of Botany*, 91(10), pp.1446–1480.

Mafole, T.C., Chiang, C., Solhaug, K.A., and Beckett, R.P., 2017. Melanisation in the old forest lichen *Lobaria pulmonaria* reduces the efficiency of photosynthesis. *Fungal Ecology*, 29, pp.103–110.

Malíček, J., *et al.*, 2018. *Bacidia albogranulosa* (Ramalinaceae, lichenized Ascomycota), a new sorediate lichen from European old-growth forests. *MycoKeys*, 44, pp.51–62.

Manga, P., 2018. Chapter 4 - Molecular biology of albinism. In: J. Kromberg and P. Manga, eds., *Albinism in Africa*. Academic Press, pp.99–119.

Mark, K., *et al.*, 2020. Contrasting co-occurrence patterns of photobiont and cystobasidiomycete yeast associated with common epiphytic lichen species. *New Phytologist*, 227(5), pp.1362–1375.

Matheny, P.B., Liu, Y.J., Ammirati, J.F., and Hall, B.D., 2002. Using RPB1 sequences to improve phylogenetic inference among mushrooms (Inocybe, Agaricales). *American Journal of Botany*, 89(4), pp.688–698.

McEvoy, M., Gauslaa, Y., and Solhaug, K.A., 2007. Changes in pools of depsidones and melanins, and their function, during growth and acclimation under contrasting natural light in the lichen *Lobaria pulmonaria*. *New Phytologist*, 175(2), pp.271–282.

McLaughlin, D.J., *et al.*, 2009. The search for the fungal tree of life. *Trends in Microbiology*, 17(11), pp.488–497.

McMullin, R.T., McCune, B., and Lendemer, 2020. *Bacidia gigantensis* (Ramalinaceae), a new species with homosekikaic acid from the north shore of Lake Superior in Ontario, Canada. *The Bryologist*, 123(2), pp.215–224.

Medema, M.H., and Fischbach, M.A., 2015. Computational approaches to natural product discovery. *Nature Chemical Biology*, 11(9), pp.639–648.

Merinero, S., Bidussi, M., and Gauslaa, Y., 2015. Do lichen secondary compounds play a role in highly specific fungal parasitism? *Fungal Ecology*, 14, pp.125–129.

Meyer, B., and Printzen, C., 2000. Proposal for a standardized nomenclature and characterization of insoluble lichen pigments. *The Lichenologist*, 32(6), pp.571–583.

Miadlikowska, J., *et al.*, 2006. New insights into classification and evolution of the Lecanoromycetes (Pezizomycotina, Ascomycota) from phylogenetic analyses of three ribosomal RNA- and two protein-coding genes. *Mycologia*, 98(6), pp.1088–1103.

Miadlikowska, J., *et al.*, 2014. A multigene phylogenetic synthesis for the class Lecanoromycetes (Ascomycota): 1307 fungi representing 1139 infrageneric taxa, 317 genera and 66 families. *Molecular Phylogenetics and Evolution*, 79, pp.132–168.

Morabito, C., *et al.*, 2020. Illumina and PacBio DNA sequencing data, *de novo* assembly and annotation of the genome of *Aurantiochytrium limacinum* strain CCAP_4062/1. *Data in Brief*, 31, p.105729.

Muggia, L., Ametrano, C.G., Sterflinger, K., and Tesei, D., 2020. An overview of genomics, phylogenomics and proteomics approaches in Ascomycota. *Life*, 10(12), p.356.

Mullins, A.J., *et al.*, 2019. Genome mining identifies cepacin as a plant-protective metabolite of the biopesticidal bacterium *Burkholderia ambifaria*. *Nature Microbiology*, 4(6), pp.996–1005.

Nash, I., Thomas H. ed., 2008. *Lichen Biology*. 2nd ed. Cambridge: Cambridge University Press.

Navarro-Muñoz, J.C., *et al.*, 2020. A computational framework to explore large-scale biosynthetic diversity. *Nature Chemical Biology*, 16(1), pp.60–68.

Nielsen, H., 2017. Predicting secretory proteins with SignalP. In: D. Kihara, ed., *Protein Function Prediction: Methods and Protocols*. New York, NY: Springer New York, pp.59–73.

Olech, M., and Czarnota, P., 2009. Two new *Bacidia* (Ramalinaceae, lichenized Ascomycota) from Antarctica. *Polish Polar Research*, pp.339-346-339–346.

Olivier-Jimenez, D., *et al.*, 2019. A database of high-resolution MS/MS spectra for lichen metabolites. *Scientific Data*, 6(1), p.294.

Onofri, S., *et al.*, 2007. Evolution and adaptation of fungi at boundaries of life. *Advances in Space Research*, 40(11), pp.1657–1664.

Parks, D.H., *et al.*, 2017. Recovery of nearly 8,000 metagenome-assembled genomes substantially expands the tree of life. *Nature Microbiology*, 2(11), pp.1533–1542.

Poelt, J., and Mayrhofer, H., 1988. Über Cyanotrophie bei Flechten. *Plant Systematics and Evolution*, 158(2/4), pp.265–281.

Printzen, C., and Tønsberg, T., 2007. *Bacidia lobarica* (Bacidiaceae, Lecanorales) sp. nov., a sorediate lichen from the southeastern USA. *The Bryologist*, 110(3), pp.487–489.

Punya, J., *et al.*, 2015. Phylogeny of type I polyketide synthases (PKSs) in fungal entomopathogens and expression analysis of PKS genes in *Beauveria bassiana* BCC 2660. *Fungal Biology*, 119(6), pp.538–550.

Puvar, A.C., *et al.*, 2020. Bacterial line of defense in *Dirinaria* lichen from two different ecosystems: First genomic insights of its mycobiont *Dirinaria* sp. GBRC AP01. *Microbiological Research*, 233, p.126407.

Reeb, V., Lutzoni, F., and Roux, C., 2004. Contribution of RPB2 to multilocus phylogenetic studies of the euascomycetes (Pezizomycotina, Fungi) with special emphasis on the lichen-forming Acarosporaceae and evolution of polyspory. *Molecular Phylogenetics and Evolution*, 32(3), pp.1036–1060.

Reese Næsborg, R., Ekman, S., and Tibell, L., 2007. Molecular phylogeny of the genus *Lecania* (Ramalinaceae, lichenized Ascomycota). *Mycological Research*, 111(5), pp.581–591.

Resl, P., Fernández-Mendoza, F., Mayrhofer, H., and Spribille, T., 2018. The evolution of fungal substrate specificity in a widespread group of crustose lichens. *Proceedings of the Royal Society B*, 285(1889), p.20180640.

Resl, P., and Hahn, C., 2021. *phylociraptor - Rapid phylogenomic tree calculator*.

Rikkinen, J., 2003. Ecological and evolutionary role of photobiont-mediated guilds in lichens. *Symbiosis*, 34, pp.99–110.

Robey, M.T., *et al.*, 2021. An interpreted atlas of biosynthetic gene clusters from 1,000 fungal genomes. *Proceedings of the National Academy of Sciences*, 118(19), e2020230118.

Rokas, A., *et al.*, 2020. Biosynthetic gene clusters and the evolution of fungal chemodiversity. *Natural Product Reports*, 37(7), pp.868–878.

Rokas, A., Williams, B.L., King, N., and Carroll, S.B., 2003. Genome-scale approaches to resolving incongruence in molecular phylogenies. *Nature*, 425(6960), pp.798–804.

Rose, F., and Coppins, S., 2002. Site assessment of epiphytic habitats using lichen indices. In: *Monitoring with Lichens—Monitoring Lichens*. Springer, pp.343–348.

Roux, C., *et al.*, 2014. *Catalogue des lichens et champignons lichénicoles de France métropolitaine*.

Rücker, T., and Wittmann, H., 1995. *Mykologisch-lichenologische Untersuchungen im Naturwaldreservat Kesselfall (Salzburg, Österreich) als Diskussionsbeitrag für Kryptogamenschutzkonzepte in Waldökosystemen*. na.

Santesson, R., *et al.*, 2004. *Lichen-forming and lichenicolous fungi of Fennoscandia*. Museum of Evolution, Uppsala University.

Sayre, R., *et al.*, 2020. An assessment of the representation of ecosystems in global protected areas using new maps of World Climate Regions and World Ecosystems. *Global Ecology and Conservation*, 21, e00860.

Schneider, T., *et al.*, 2011. Structure and function of the symbiosis partners of the lung lichen (*Lobaria pulmonaria* L. Hoffm.) analyzed by metaproteomics. *Proteomics*, 11(13), pp.2752–2756.

Schoch, C.L., *et al.*, 2012. Nuclear ribosomal internal transcribed spacer (ITS) region as a universal DNA barcode marker for Fungi. *Proceedings of the National Academy of Sciences*, 109(16), pp.6241–6246.

Sérusiaux, E., *et al.*, 2012. *Lecania falcata*, a new species from Spain, the Canary Islands and the Azores, close to *Lecania chlorotiza*. *The Lichenologist*, 44(5), pp.577–590.

Simão, F.A., *et al.*, 2015. BUSCO: assessing genome assembly and annotation completeness with single-copy orthologs. *Bioinformatics*, 31(19), pp.3210–3212.

Singh, G., *et al.*, 2022. A candidate gene cluster for the bioactive natural product gyrophoric acid in lichen-forming fungi. *bioRxiv*, p.2022.01.14.475839.

Singh, G., Armaleo, D., Dal Grande, F., and Schmitt, I., 2021. Depside and depsidone synthesis in lichenized fungi comes into focus through a genome-wide comparison of the olivetoric acid and physodic acid chemotypes of *Pseudevernia furfuracea*. *Biomolecules*, 11(10).

Sinnemann, S.J., Andrésson, Ó.S., Brown, D.W., and Miao, V.P.W., 2000. Cloning and heterologous expression of *Solorina crocea* pyrG. *Current Genetics*, 37(5), pp.333–338.

Smith, C., *et al.*, 2009. *The Lichens of Great Britain and Ireland*. London: British Lichen Society.

Solhaug, K.A., Gauslaa, Y., Nybakken, L., and Bilger, W., 2003. UV-induction of sun-screening pigments in lichens. *New Phytologist*, 158(1), pp.91–100.

Solhaug, K.A., Larsson, P., and Gauslaa, Y., 2010. Light screening in lichen cortices can be quantified by chlorophyll fluorescence techniques for both reflecting and absorbing pigments. *Planta*, 231(5), pp.1003–1011.

Spribille, T., *et al.*, 2016. Basidiomycete yeasts in the cortex of ascomycete macrolichens. *Science*, 353(6298), pp.488–492.

Studzinska-Sroka, E., Galanty, A., and Bylka, W., 2017. Atranorin – an interesting lichen secondary metabolite. *Mini-Reviews in Medicinal Chemistry*, 17(17), pp.1633–1645.

Torzilli, A.P., Mikelson, P.A., and Lawrey, J.D., 1999. Physiological effect of lichen secondary metabolites on the lichen parasite *Marchandiomyces corallinus*. *The Lichenologist*, 31(3), pp.307–314.

Urbanavichus, G.P., 2010. *A checklist of the lichen flora of Russia*. St. Petersburg: Nauka.

Wang, Y.-Y., *et al.*, 2014. Genome characteristics reveal the impact of lichenization on lichen-forming fungus *Endocarpon pusillum* Hedwig (Verrucariales, Ascomycota). *BMC Genomics*, 15(1), p.34.

Wijayawardene, N., *et al.*, 2022. Outline of Fungi and fungus-like taxa – 2021. 13, pp.53–453.

Wilken, P.M., *et al.*, 2020. IMA Genome - F13. *IMA Fungus*, 11(1), p.19.

Wirth, V., Hauck, M., and Schultz, M., 2013. *Die Flechten Deutschlands*. Ulmer.

Woo, P.C.Y., *et al.*, 2014. The biosynthetic pathway for a thousand-year-old natural food colorant and citrinin in *Penicillium marneffei*. *Scientific Reports*, 4(1), 6728.

Xu, J., 2017. Fungal DNA barcoding. *The 6th International Barcode of Life Conference*, 01(01), pp.913–932.

Yang, M.-X., Devkota, S., Wang, L.-S., and Scheidegger, C., 2021. Ethnolichenology— the use of lichens in the Himalayas and southwestern parts of China. *Diversity*, 13(7), p.330.

Yoshimura, I., Yamamoto, Y., Nakano, T., and Finnie, J., 2002. Isolation and culture of lichen photobionts and mycobionts. In: I.C. Kranner, R.P. Beckett and A.K. Varma, eds., *Protocols in Lichenology: Culturing, Biochemistry, Ecophysiology and Use in Biomonitoring*, Springer Lab Manuals. Berlin, Heidelberg: Springer, pp.3–33.

Zahlbruckner, A., 1905. Ascolichenes. Lieferung 3. In: A. Engler and K. Prantl, eds., *Die natürlichen Pflanzenfamilien nebst ihren Gattungen und wichtigeren Arten insbesonderen den Nutzpflanzen*. pp.97–144.

Acknowledgements

Foremost, I would like to express my deepest gratitude to my advisor, Silke Werth, for allowing me to conduct my dissertation in her research group.

My special thank is to Andreas Beck for his patience, motivation, enthusiasm, continuing support, and valuable and helpful discussions that helped me become a scientist. His guidance and advice helped me in all the time of research and writing of this dissertation.

I would like to express my gratitude to Stefan Ekman, for the extensive two weeks of herbarium work on the identification of *Bacidia* specimens and for sharing his morphological expertise. Our joint work helped me establish myself as a specialist in this exciting group of lichens.

Many thanks go to Philipp Resl, who accompanied my first learning steps in genomics, for his extraordinary patience and excellent explanatory skills. Our genomic project would not be possible without his great and valuable contribution.

I would also like to acknowledge my committee members who have helped and encouraged me through my graduate studies.

Special thanks go to my parents, who always supported my decisions no matter how adventurous they were. I am very thankful to all my close friends, especially Eugen, who was happy when I selected a peaceful profession of a lichenologist, and Margaret for her belief in me throughout my life and whole scientific career, starting from school. I thank my friends and colleagues at the Munich Botanical Institute for their help, sharing their knowledge, and friendship. My special thanks are to Andreas Gröger, Seraina Rodewald, Diego Morales-Briones, Elizabeth Joyce, and other great postdocs and graduate students for creating excellent research and life atmosphere, which helped me a lot during the last months of my PhD study.

This dissertation was possible thanks to the funding support from the Bayerisches Hochschulzentrum für Mittel-, Ost- und Südosteuropa (BAYHOST yearly scholarship: 2018–2022).

CURRICULUM VITAE

Julia V. Gerasimova

Ludwig Maximilian University Munich
Systematics, Biodiversity & Evolution of Plants
Menzinger Str. 67 · 80638 Munich · Germany
Tel. +49 89 17861-268 · E-Mail: jgerasimova@lmu.de

KEY SKILLS AND EXPERIENCE

- Bioinformatics skills (confident level) and fieldwork experience.
- Strong organisational, communication, and English writing skills.
- Languages: English (fluent), German (basic knowledge).

EDUCATION

PhD student, Biology
Ludwig Maximilian University Munich
Advisor: Prof. Dr. Silke Werth
Dissertation: Lichen-forming fungal genus *Bacidia*: From taxonomy to genomics Supported by the Free State of Bavaria (BAYHOST fellowship)

10/2018 –05/2022

Research sojourn
Botanical State Collection Munich
Advisor: PD Dr. Andreas Beck
Project: A reconstruction of the phylogenetic relationships in *Bacidia* s. str. from the Russian Far East, using five markers: nrITS, nrLSU, mtSSU, RPB1, and RPB2.
Supported by the BAYHOST Mobility Grant (MB-2017-1/35)

2017

University degree
I. N. Ulyanov State Pedagogical University of Ulyanovsk
Advisor: Dr. Andrej V. Maslennikov
Diploma: Cenopopulation research of the *Globularia punctata* Layer. in Ulyanovsk region (excellent).

09/2005 –06/2012

EXPERIENCE

Research assistant (as a part-time job)
Ludwig Maximilian University Munich
Advisor: Prof. Dr. Silke Werth
Lichen-determination within a project on air-pollution in Munich; helping students with computer analyses on lichen genomics.

2019–2022

Research assistant (as a part-time job)
Botanical State Collection Munich
Advisor: PD Dr. Andreas Beck

August– November 2019

CT-analysis of lichens, analysing three-dimensional microstructures of lichens in 3D non-destructive imaging.

Associated researcher
Botanical State Collection, working jointly with PD Dr. Andreas Beck (Senior curator of lichens and bryophytes). **2018–2022**

Teacher (as a part-time job)
Regional State Institution of Additional Education **2017**
Giving lectures and practical lessons on biology and lichenology to children and students at the university.
Supervision of two bachelor theses on lichen diversity of selected area.
Laboratory assistant and trainee
Komarov Botanical Institute of the Russian Academy of Sciences at the Laboratory of Lichenology and Bryology. **2012–2017**
Field and herbarium work on lichens.

WORK IN THE HERBARIA

- Botanische Staatssammlung München, München, Germany (M);
- Senckenberg Museum für Naturkunde Görlitz (GLM);
- Centre of Natural History, Graz, Austria (GZU);
- Finnish Museum of Natural History, University of Helsinki, Finland (H);
- Herbarium at Natural History Museum and Botanical Garden, University of Tartu, Estonia (TU);
- Botany Museum of Evolution, Uppsala University, Sweden (UPS);
- Swedish Museum of Natural History, Stockholm, Sweden (S);
- Komarov Botanical Institute, St. Petersburg, Russia (LE).

CONFERENCES, WORKSHOPS, AND SEMINARS

- Invited speaker at the laboratory seminar of Imke Schmitt's group, 25.1.2022. Title: Genomic studies on *Bacidia*, small but characteristic old-growth forest dwellers;
- The 9th International Symposium in Lichenology (IAL9). 1-6 August 2021, Bonito, Brazil (Poster presentation). Title: Comparative genomics of free-living and lichen algae;
- RepeatExplorer Workshop on the Application of Next Generation Sequencing to Repetitive DNA Analysis. 21-23 May 2019, Budweis, Czech Republic;
- The 8th International Symposium in Lichenology (IAL8). 1-5 August, 2016, Helsinki, Finland (Poster presentation). Title: *Bacidia* s. str. (Lecanorales, Ascomycota) in Russian Far East.

AWARDS AND FELLOWSHIPS

- BAYHOST mobility grant (MB-2017-1/35). Project on the reconstruction of the phylogenetic relationships in *Bacidia* s. str. from the Russian Far East, using five markers: nrITS, nrLSU, mtSSU, RPB1, and RPB2.

- Three one-year scholarships program provided by the Free State of Bavaria (2018–2022). PhD study.
- LMU Travel Grant. Research stay at the Institute of Biology at the University of Graz (22.04.–21.05.2021); joint work with Dr. Philipp Resl on the genomic analyses.

PEER-REVIEWED PAPERS PUBLISHED OR IN REVIEW

(Google Scholar: https://scholar.google.com/citations?user=KfS9TeEAAAAJ&hl=de&oi=ao)

1. **Gerasimova JV**, Beck A, Werth S & Resl P (2022) High diversity of type I polyketide genes in *Bacidia rubella* as revealed by the comparative analysis of 23 lichen fungal genomes. *Journal of Fungi* 8(5): 449; https://doi.org/10.3390/jof8050449

2. Sebald V, Goss A, Ramm E, **Gerasimova JV** & Werth S (in review) NO2 air pollution drives species composition, but tree traits drive species diversity of urban epiphytic lichen communities. *Environmental Pollution*

3. Muchnik EE, Otte V, Tsurykau A, Breuss O, **Gerasimova JV** & Cherepenina DA (in review) New and noteworthy records of lichens and lichenicolous fungi of central European Russia. *Herzogia*.

4. **Gerasimova JV**, Urbanavichene IN, Urbanavichus GP & Beck A (2021) Morphological and phylogenetic analyses of *Toniniopsis subincompta* s. lat. (Ramalinaceae, Lecanorales) in Eurasia. *Lichenologist* 53: 1–13. https://doi:10.1017/S0024282921000013

5. **Gerasimova JV**, Ezhkin AK, Davydov EA & Beck A (2021) Multilocus-phylogeny of the lichen-forming genus *Bacidia* s. str. (Ramalinaceae, Lecanorales) with special emphasis on the Russian Far East. *Lichenologist* 53: 441–455. https://doi:10.1017/S0024282921000396

6. **Gerasimova JV**, Ruthensteiner B & Beck A (2021) MicroCT as a useful tool for analysing the 3D structure of lichens and quantifying internal cephalodia in *Lobaria pulmonaria*. *Applied Microbiology* 1(2): 189–200. https://doi.org/10.3390/applmicrobiol1020015

7. Suija A, **Gerasimova JV**, Jüriado I, Lõhmus P, Marmor-Ohtla L, Martin L, Randlane T & Zhdanov IS (2021) Updates to the list of Estonian lichenized, lichenicolous and allied fungi. *Folia Cryptogamica Estonica* 58: 243–250. https://doi.org/10.12697/fce.2021.58.23

8. Muchnik EE, Konoreva LA, Chesnokov SV, Paukov AG, Tsurykau A & **Gerasimova JV** (2019) New and otherwise noteworthy records of lichenized and lichenicolous fungi from Central European Russia. *Herzogia* 32(1): 111–126. doi:10.13158/heia.32.1.2019.111

9. **Gerasimova JV**, Ezhkin AK & Beck A (2018) Four new species of *Bacidia* s. str. (Ramalinaceae, Lecanorales) in Russian Far East. *Lichenologist* 50(6): 603–625. https://doi:10.1017/S0024282918000397

10. **Gerasimova JV** & Ekman S (2017) Taxonomy and nomenclature of seven names in *Bacidia* (Ramalinaceae, Lecanorales) described from Russia. *Phytotaxa* 316 (3): 292–296. DOI: https://doi.org/10.11646/phytotaxa.316.3.9

11. Himelbrant DE, Stepanchikova IS, Motiejūnaitė J, **Gerasimova JV**, Kuznetsova ES, Dyomina AV & Tsurykau AG (2017) New records of lichens and allied fungi from the Leningrad Region, Russia. VIII. *Folia Cryptogamica Estonica* 54: 63–70. https://doi:10.12697/fce.2017.54.11